MSU GEOLOGY FIELD CAMP MANUAL

DEPARTMENT OF EARTH SCIENCES

MONTANA STATE UNIVERSITY
Mountains & Minds

SUMMER 2016

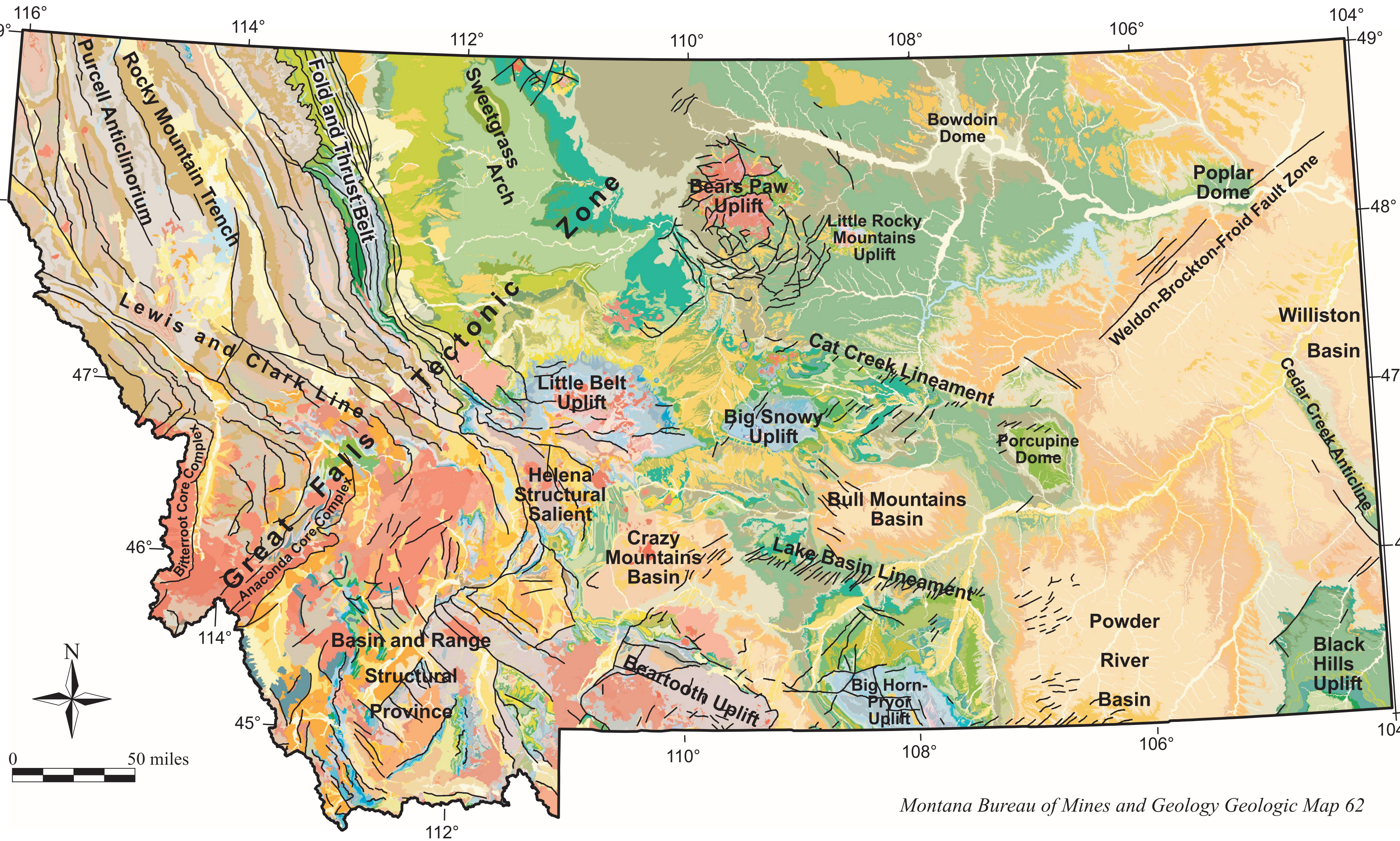

Montana Bureau of Mines and Geology Geologic Map 62

TABLE OF CONTENTS

CONTACT INFORMATION: FIELD COURSE FACULTY & DEPARTMENT

Dept. of Earth Sciences Office	Amanda Thompson Patrick Mulhill	406-994-3331
Earth Sciences Dept. Head:	Dr. Mary Hubbard	406-994-3331 (office)
Field Course Director:	Dr. Colin A. Shaw	406-994-6760 (office); 406-548-1987 (mobile)
Field Course Faculty:	Dr. David Bowen	406-581-5448 (mobile)
	Dr. Karen Williams	406-498-6994 (mobile)
	Dr. David Lageson	406-994-6913 (office); 406-581-3990 (mobile)
	Dr. David Mogk	406-994-6916 (office); 406-600-4071 (mobile)

STUDENT CONTACTS (DIY)

American Geosciences Institute Guidelines for Ethical Professional Conduct

These guidelines address common ethical topics across the geoscience community; the ethics statements of individual societies may expand beyond these guidelines.

Geoscientists play a critical role in ethical decision making about stewardship of the Earth, the use of its resources, and the interactions between humankind and the planet on which we live. Geoscientists must earn the public's trust and maintain confidence in the work of individual geoscientists and the geosciences as a profession. The American Geosciences Institute (AGI) expects those in the profession to adhere to the highest ethical standards in all professional activities. Geoscientists should engage responsibly in the conduct and reporting of their work, acknowledging the uncertainties and limits of current understanding inherent in studies of natural systems. Geoscientists should respect the work of colleagues and those who use and rely upon the products of their work.

In day-to-day activities geoscientists should:

- Be honest.
- Act responsibly and with integrity, acknowledge limitations to knowledge and understanding, and be accountable for their errors.
- Present professional work and reports without falsification or fabrication of data, misleading statements, or omission of relevant facts.
- Distinguish facts and observations from interpretations.
- Accurately cite authorship, acknowledge the contributions of others, and not plagiarize.
- Disclose and act appropriately on real or perceived conflicts of interest.
- Continue professional development and growth.
- Encourage and assist in the development of a safe, diverse, and inclusive workforce.
- Treat colleagues, students, employees, and the public with respect.
- Keep privileged information confidential, except when doing so constitutes a threat to public health, safety, or welfare.

As a member of a professional and scientific community, geoscientists should:

- Promote greater understanding of the geosciences by other technical groups, students, the general public, news media, and policy makers through effective communication and education.
- Conduct their work recognizing the complexities and uncertainties of the Earth system.
- Sample responsibly so that materials and sites are preserved for future study.
- Document and archive data and data products using best practices in data management, and share data promptly for use by the geoscience community.
- Use their technical knowledge and skills to protect public health, safety, and welfare, and enhance the sustainability of society.
- Responsibly inform the public about natural resources, hazards, and other geoscience phenomena with clarity and accuracy.
- Support responsible stewardship through an improved understanding and interpretation of the Earth, and by communicating known and potential impacts of human activities and natural processes.

2016 MSU Field Camp Schedule

Start Date: Tuesday, May 31, 2016 **Meeting Place:** Gaines Hall Parking, Grant Street,
End Date: Monday, July 04, 2016 **Meeting Time**: 8:00 am or as instructed

	Date	Day	Exercise	Location	Instr. 1	Instr. 2	Lodging
1	5/31	Tue	Intro - Field Methods	Bozeman area	*Staff*	*Staff*	KOA Dillon
2	6/1	Wed	Basic Structural Mapping - Sed	Dillon area	Shaw	Bowen	KOA Dillon
3	6/2	Thu	Basic Structural Mapping - Sed	Dillon area	Shaw		KOA Dillon
4	6/3	Fri	Basic Structural Mapping - Sed	Dillon area	Shaw		KOA Dillon
5	6/4	Sat	Basic Structural Mapping - Sed	Dillon area	Shaw		KOA Dillon
6	6/5	Sun	Basic Structural Mapping - Sed	Dillon area	Shaw		KOA Dillon
7	6/6	Mon	***Day off***	Dillon area			KOA Dillon
8	6/7	Tue	Fold & Thurst structure & strat	Dillon area	Lageson	Bowen	KOA Dillon
9	6/8	Wed	Fold & Thurst structure & strat	Dillon area	Lageson	Bowen	KOA Dillon
10	6/9	Thu	Fold & Thurst structure & strat	Dillon area	Lageson	Bowen	KOA Dillon
11	6/10	Fri	Fold & Thurst structure & strat	Dillon area	Lageson	Bowen	KOA Dillon
12	6/11	Sat	Fold & Thurst structure & strat	Dillon area	Lageson	Bowen	KOA Dillon
13	6/12	Sun	***Day off***	Dillon area			KOA Dillon
14	6/13	Mon	Fold-Thrust Structure & Strat	Dillon area	Lageson		KOA Dillon
15	6/14	Tue	Fold-Thrust Structure & Strat	Dillon area	Lageson		KOA Dillon
16	6/15	Wed	Fold-Thrust Structure & Strat	Dillon area	Lageson		KOA Dillon
17	6/16	Thu	Fold-Thrust Structure & Strat	Dillon area	Lageson		KOA Dillon
18	6/17	Fri	Fold-Thrust Structure & Strat	Dillon area	Lageson		KOA Dillon
19	6/18	Sat	Fold-Thrust Structure & Strat	>> Bozeman	Lageson		MSU
20	6/19	Sun	***Day off***	Bozeman			MSU
21	6/20	Mon	Geomorphology	TBD	Williams	Shaw	Camping
22	6/21	Tue	Geomorphology	TBD	Williams	Shaw	Camping
23	6/22	Wed	Geomorphology	TBD	Williams	Shaw	Camping
24	6/23	Thu	Geomorphology	TBD	Williams	Shaw	Camping
25	6/24	Fri	Geomorphology	TBD	Williams	Shaw	Camping
26	6/25	Sat	Geomorphology	TBD	Williams	Shaw	Camping
27	6/26	Sun	***Day off***				MSU
28	6/27	Mon	Hard Rock	SW-Montana	Mogk		Camping
29	6/28	Tue	Hard Rock	SW-Montana	Mogk		Camping
30	6/29	Wed	Hard Rock	SW-Montana	Mogk		Camping
31	6/30	Thu	Hard Rock	SW-Montana	Mogk		Camping
32	7/1	Fri	Hard Rock	SW-Montana	Mogk		Camping
33	7/2	Sat	Hard Rock	SW-Montana	Mogk		Camping
34	7/3	Sun	***Hard Rock - clean-up (pm)***	>> Bozeman	Mogk		MSU
35	7/4	Mon					

MSU Field Camp Campus Locations

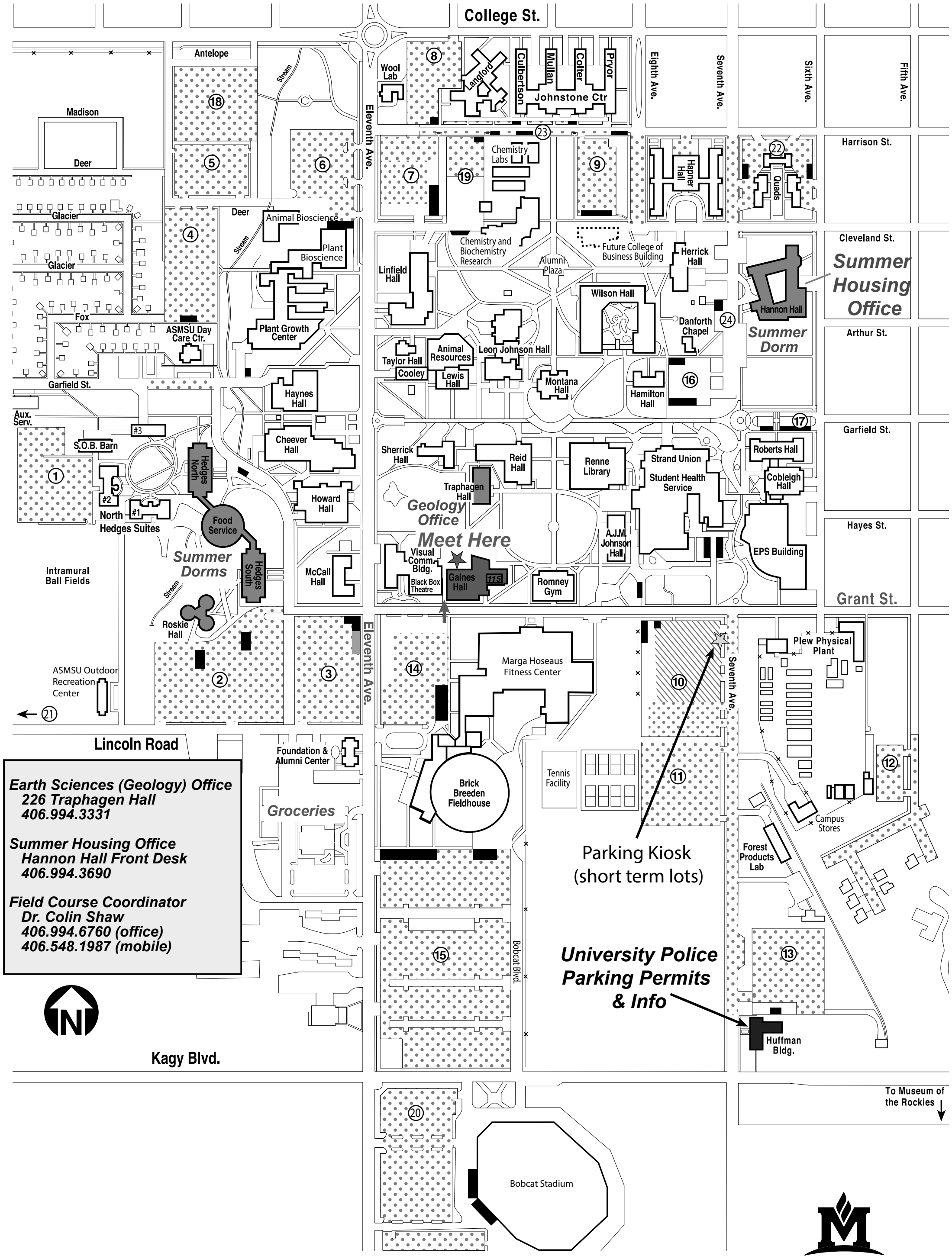

MONTANA STATE UNIVERSITY

Campus Parking

LOT NAME BY NUMBER

1 North Hedges	7 **West Linfield**	13 Huffman	19 **East Linfield**
2 Roskie	8 Langford	14 North Fieldhouse	20 West Stadium
3 South Hedges	9 Lewis & Clark	15 South Fieldhouse	21 Lincoln
4 South 12th St.	10 North Gatton (pay)	16 Hamilton Reserved	22 Quad
5 Deer Street	11 South Gatton	17 Roberts Reserved	23 Harrison
6 Greenhouse	12 Faculty Court	18 Antelope	24 S. 7th Reserved

VISITOR PARKING KEY

- Fee Parking
- $3.00 Hangtag
- A.D.A./Handicapped
- Construction Area

FIELD GEOLOGY EQUIPMENT CHECKLIST

Essential Field Gear

	Field text book as assigned (see p. 2)
	10x hand lens (best: Hastings Triplet)
	Rock hammer (~22 oz.)
	Two (2) field notebooks (see p. 2)
	Two technical pens (widths: 0.25mm, 0.5mm)
	Two-mechanical pencils (0.5mm)
	Replacement pencil lead (0.5mm)
	Stick-style eraser
	Two Plastic ruler-protractors (bookstore)
	Sharpee/permanent marker
	Set of colored pencils (at least 12)
	Safety pin (for marking maps/photos)
	Pocket knife (2-4” blade)
	Small first-aid kit
	Sturdy field boots (see note above)
	Two liter canteens or water bottles
	Waterproof-breathable parka
	Sun hat
	Sun glasses
	Sun screen (SPF 30 or greater)
	Wrist/pocket watch/phone
	Field back-pack
	Field belt – w/non-magnetic buckle (to carry compass/pouch/etc.)

Recommended Field Gear

	Wind/rain pants
	Large garbage bag for pack
	Leather work gloves
	Hammer holder for belt
	Small binoculars
	Camera (or phone)
	Photo scale
	Field pouch (for notebook/pencils)

** Customized Plateau Designs field pouches with the MSU Field Camp logo will be available for purchase at the beginning of field camp.*

Expendables to Bring

Quality drafting vellum 8.5”x11” (50 sheets)

Essential Personal Gear

	Duffel/backpack
	Field clothing
	Underclothing & work socks
	Cold-weather clothing layers (sweaters etc.)
	Warm hat
	Warm winter coat
	Warm gloves or mittens
	Personal toilet kit
	Prescription medicines, contact lenses, personal health needs
	Sleeping bag
	Tent (share w/1-2 friends if possible)
	Towel/washcloth

Recommended Personal Gear

	Camp/town clothing
	Camp shoes or sandals
	Reading book, stationary, stamps
	Travel alarm clock
	D-cell headlamp/flashlight & batteries
	Laundry bag & detergent
	Camp chair
	Radio/iPod/phone/personal stereo

Equipment Supplied by MSU

These items will be signed out to you and must be returned in good condition.	
	Brunton or Silva compass
	GPS or altimeter (as needed)
	Tablet computer/iPad (as needed)
	Acid dropper bottle
These items are yours to keep	
	Field Course Manual – spiral bound
	Plexiglas map board

Expendables Supplied by MSU

	Base maps, air photos, etc.
	Stereonet/equal area template/thumbtack
	Cross-section paper
	10% HCl

** **DO NOT** bring large coolers, camp stoves or cooking gear. Meals and all cooking gear and dishes will be provided You may bring a <u>small</u> personal cooler and/or <u>small</u> backpacking stove that fits in your duffle/backpack.*

Recommended Textbooks

1. **Geological Field Techniques (2012) Coe, Angela, Wiley-Blackwell, 336 pages.**

   Publisher: http://www.wiley.com/WileyCDA/WileyTitle/productCd-1118445082.html
   Amazon: http://www.amazon.com/Geological-Field-Techniques-Angela-Coe/dp/1444330624 MSU Bookstore: http://www.msubookstore.org/home.aspx

2. **MSU Geology Field Manual** (distributed at start of field course – no charge)

Equipment Recommendations

- **Field Notebooks.** Need two (2) copies, at least 100 pages each. Should have ruled pages on right for notes and cross-section gridded pages on left for sketches. Good choices include: *Rite-in-the-Rain Geological Field Book* (No. 540F) – special water-resistant paper, includes geologic reference material in back, expensive. *Sokkia Engineer's Field Book* (N. 8152-30) – trig, math and slope reference in back. *Forestry Suppliers Transit Field Book* (# 49361) – Good value.
- **Hand lenses (10x).** Hastings Triplet provides has best optics, but doublet lenses are acceptable.
- **Drafting pencils & pens.** High-quality mechanical pencils and drafting pens are the best choice to draw consistent, precise lines. Re-fillable *Rapidograph*-type pens (*Rotring*, *Koh-i-Noor*) make the best lines, but are expensive and difficult to maintain. Good felt-tip drafting pens by *Micron*, *Pentel*, and *Prismacolor* are good options.
- **Colored pencils.** *Prismacolor* and *Verithin* pencils are the best for precise and consistent color. *Verithin* are easiest to use in the field.
- **Drafting Vellum.** Get good quality translucent drafting vellum with 100% cotton fiber like *Clearprint Design Vellum.* Cheap 'onion-skin' tracing paper is OK for some uses, but is unacceptable for stereonets and final work of any kind.
- **Field Pouches.** Highly recommended to keep your notebook and pens/pencils close at hand. Light-weight nylon pouches (e.g. *Plateau Designs*) are the most versatile, although some prefer leather cases (e.g. *Gfeller Casemakers)*. We will haveteh outstanding *Plateau Designs* field pouches with the MSU field camp logo for sale at the start of field camp.

Equipment Suppliers

Bozeman

- MSU Bookstore: Text, drafting equipment & supplies, field notebooks (Rite in the Rain), etc.
- Selby's: Wide selection of drafting supplies, field equipment, field notebooks, GPS receivers, topo maps etc. 525 Professional Drive, 587-9597.
- REI: Outdoor gear. 2220 Tschache Street (N. 19th), 587-1938.
- Sportsman's Warehouse, 2220 Tschache Street (N. 19th)
- Northern Lights: Outdoor gear. 1716 W. Babcock, 586-7544.
- Bob Ward's Outdoor gear. 3011 max Avenue (N. 19th – Target shopping center). 586-4381.

Online

- Miners Supply: Good variety of geology-specific gear http://www.minerox.com/.
- Forestry Suppliers: Field gear, field notebooks, drafting supplies, compasses, GPS receivers, etc. http://www.forestry-suppliers.com/.
- Ben Meadows: Field gear field notebooks, drafting supplies, compasses http://www.benmeadows.com/.
- Dick Blick: Drafting supplies (good prices) http://www.dickblick.com/.

GUIDE TO EMERGENCY & MEDICAL PREPARATION

Before You Arrive:

- ***Check Insurance:*** *Students are required to carry medical insurance.*
- ***Bring Insurance Card:*** *Carry insurance cards and/or policy numbers with you.*
- ***Fill out Emergency Medical Information Form.***
- ***Check Records:*** Have you had a tetanus shot within the last five years?
- ***Inform instructors:*** Do you have medical issues that we need to know about? Do you have potentially life threatening allergies (bee-stings, food, plants, etc.)?

NOTE: If you are a certified First Responder, WFR, or EMT, let your instructors know and bring additional equipment appropriate to your medical rating.

Personal First Aid/Emergency Kit

Students are required to carry their own personal first aid kit while in the field (in your pack at all times). Be sure to stock it with any items that have been prescribed by a doctor for you, such as inhalers, glucose, or an "epi-pen" for allergic reactions (epinephrine for anaphylactic shock from insect bites, food, plant allergies, etc.). Carry these supplies in a waterproof bag or pouch.

Supplies for trauma care:

- Assorted sizes of adhesive strips (band aids), including some large ones
- One or more large 'trauma pad' or Quik-clot pads for bleeding
- One or more rolled ace bandage (elastic wrap)
- Water-proof medical tape (1- and 2-inch rolls)
- Assorted sizes of non-stick sterile dressings
- Alcohol wipes
- Triple antibiotic ointment (over-the-counter)
- Small bottle of sterile saline eye wash
- Tweezers (good for pulling cactus needles, etc.) & extra safety pins
- One pair rubber gloves

Recommended miscellaneous supplies:

- Pain and/or anti-inflammatory medication (your choice – some people have allergies that dictate what they can take or tolerate, so follow whatever your doctor recommends for you)
- Small flashlight or head lamp (don't left in your tent)
- Insect repellent (not recommended unless it is extremely buggy)
- Moleskin or molefoam or other pads and bandages for blisters on your feet

- ✧ Other prescription or non-prescription medications (decongestant for hay fever, antacid, throat lozenges, etc.)?
- ✧ Something for upset stomach and/or diarrhea
- ✧ Pocket mask for CPR (optional)
- ✧ Formable C-splint or air splint (optional)

Each field vehicle carries a comprehensive first aid kit for trauma care and a comprehensive medical kit will be available in camp.

What to Do…

In case of minor injury in the field. If you or your partner is injured and still able to walk, proceed to one of the field vehicles. Summon an instructor if possible or wait in the vehicle until an instructor or other students return. If the patient needs medical care you may drive the vehicles to the nearest hospital or clinic. Keys are always left with the vehicle for emergency situations. Do not take a vehicle unless the need for care is urgent.

In case of serious injury in the field. If you or your partner is seriously injured in the field do your best to provide first aid to stabilize the injury. ***Summon help.*** There will almost always be other students or instructors within earshot, especially if you climb to a highpoint. ***Stay with the patient unless it is absolutely necessary to leave to get help.*** If you *must* leave be sure the patient is stable, protected from the elements and has plenty of water.

- ***Snake bite.*** Remain calm and summon help or walk to vehicles. Get the patient to a hospital as quickly as possible. Antivenin is the only effective treatment and must be administered as soon as possible. Do not try to suck out venom and ***never*** cut the skin near the bite. Do not apply a tourniquet.
- ***Broken bone.*** Stabilize the limb with a splint and/or an elastic (Ace) bandage. Get to a vehicle and take the patient to a hospital. If the patient has a broken leg, summon help. To carry the patient to a vehicle. The field course has a backboard for transport of injured and immobile patients.
- ***Bleeding.*** If you or a partner has an injury that causes serious bleeding use a trauma pad or Quik-clot pack to stop the bleeding. Summon help. Carry the patient to a vehicle and drive to a hospital.

In case of injury in camp. Use your first aid kit or one of the group first aid kits to treat the injury. Inform an instructor or seek help from other students. If you or another student need to be transported to a hospital or clinic find an instructor or student driver. If the patient needs urgent care and you cannot find an instructor, you may take a vehicle. Do not take a vehicle without asking unless the need is urgent.

In case of illness. Inform an instructor and discuss treatment options. Accommodations will be made for serious illness at the discretion of the instructor and my include rest in camp, visit to the doctor, hospitalization etc.

Montana State University
Department of Earth Sciences
Field Geoscience Education Programs

Personal Conduct & Safety Policies

Revised 2015

Montana State University
Department of Earth Sciences

Table of Contents

This Handbook contains important policies and procedures that govern the Montana State University Field Programs. Please read these carefully before leaving for your summer field course or project. If you have any questions, contact Dr. Colin A. Shaw (colin.shaw1@montana.edu, 406-994-6760). This policy document is based on the Keck Geology Consortium Student Conduct Policy Manual, 2009-2010 with substantial modifications to comply with MSU policy and accommodate the unique circumstances of the MSU field course.

What You Are About to Do

Field courses at Montana State University bring together students from MSU and from colleges and universities across the country. Once the summer course starts, you will live together, often in close quarters, around the clock. You may spend time in isolated natural settings where there are significant natural dangers and where emergency responders may be hours away. The unique physical demands, social circumstances and objective hazards associated with field courses require constant attention to safety and high degree of cooperation, mutual respect and tolerance from all students, faculty and staff. These policies are designed to set a high standard of behavior that will help to secure the safety and well-being of all participants. Please read the field course policies carefully; you will be asked to sign a contact agreeing to abide by these policies for the duration of the course.

- In many ways, field camp is the gateway to your career as a professional geoscientist. Faculty and staff will treat you as the young professional that you are. In return we expect you to behave as a professional. A few common-sense rules will help us all stay safe, get along and learn.
- Safety First! Never behave in a way that puts yourself or others at risk. Keep an eye out for dangerous situations and alert other students and field camp staff.
- Treat your colleagues, field camp staff and other people you encounter as you would want to be treated. Be respectful of cultural and personal differences.
- Respect the land, plants, animals and private property. You will be a guest on Federal and private land, but others live here. Do not damage, deface, litter or otherwise disturb the landscape inhabitants.
- Pitch in with group tasks. Each student is responsible for contributing to day-to-day chores. Take the time to learn the field camp systems around camp and in the field. Learn how to help and keep an eye out for things that need doing. Be helpful; don’t wait to be asked.
- Report violations of field camp policy. Ensuring that we all follow the rules is the best way to stay safe and enjoy a memorable learning experience. Report violations to field camp staff or appropriate authorities.

Course Expectations & General Conduct

The Montana State University summer field course is a challenging five-week course involving strenuous outdoor activity. Although instructors strive to make the experience as safe and comfortable as possible field work does involve inherent risks. Students bear primary responsibility for their own safety and the safety of others during field camp. You must read this **MSU Field Course Manual** carefully and understand and agree to abide by the rules, and standards of conduct in the manual as well as to follow instructions given by instructors, graduate teaching assistants and field course staff.

Participating in the course implies that you understand your obligation to follow the rules, behave in a responsible and safe manner at all times. You assume full responsibility for personal injury to yourself and/or to members of your family, or for loss or damage to your personal property and expenses as a result of your own negligence or the negligence of other students. MSU reserves the right to refuse enrollment to any person it judges to be incapable of meeting the rigors and requirements of participating in the field program.

Physical Demands & Equipment

Some exercises may require moderate to strenuous exertion at altitudes between 4000 and 10,000 feet (1200-3000m). Students routinely hike for hours in remote areas over rough terrain. Thus, good to excellent physical conditioning and suitable equipment is essential. All weather conditions are possible during summer in the mountains of Montana including rain, snow, hail, lightning, freezing temperatures and dangerous winds. It is especially important to bring sturdy, comfortable boots (break them in before field camp!) and waterproof/water-resistant outerwear. Sunscreen and a broad-brimmed sunhat are required for protection from the high-altitude summer sun during long days in the field. Rattlesnakes are abundant, but students can minimize the risk of being bitten by exercising caution and wearing long trousers (no student or faculty member has ever been bitten on an MSU field course). Always look carefully before placing a hand on a rock outcrop. Rattlesnakes are effectively camouflaged. Most people that are bitten were harassing or provoking the snake. Don’t tempt fate. Leave snakes alone.

Stewardship

You will be working on both public and private land and will encounter local residents – human, animals and plants. This is their home. You are a guest here and it is imperative that you treat the land and its inhabitants with respect at all times – Many local people make their living on the land, including leased state and federal public land. Please take care not to damage property, disturb livestock, interfere with ranch or mining operations or otherwise cause problems for locals. *All gates should be left as you find them* (if closed – leave closed, if open – leave open). NEVER leave a gate open assuming that someone in the next vehicle will close it. Make sure that the last vehicle in your caravan closes the gate before driving on.

Do not harass wildlife (including snakes). The animals you will see are not aggressive, but can be dangerous when cornered or provoked. Keep your distance, watch, take photographs and enjoy, but don’t bother animals. Do not mutilate, damage or destroy plants.

Only take rock samples when necessary and avoid excessive damage to outcrops. Do not damage, destroy or remove unique features or fossils that you find in the rock. Leave them there for the benefit of future students. **Do not** write or scratch on rock outcrops. **NO GRAFFITI!** You will receive a grade of ‘F’ for a project if you are caught writing any form of graffiti.

Alcohol and Illegal Drug Policy

Alcohol

The MSU field camp is ‘dry’. No alcohol or alcohol consumption is permitted during instructional time, in field camp vehicles or in camp. Students who chose to consume alcohol on their own time, away from camp must abide by the following restrictions.

- All participants are expected to obey local laws including those that regulate the use of alcohol and drugs. Illegal drug use and underage drinking are strictly prohibited.
- Absolutely no drinking is allowed where driving might be a possibility within 8 hours.

- No alcohol is permitted in university vehicles, including closed containers.
- Any excessive consumption of alcohol leading to unacceptable behavior or inability to fully participate in field camp activities is strictly prohibited.
- No university funds can be spent on alcohol for students, faculty or guests under any circumstances.
- The minimum penalty for violation of the alcohol and drug policy is a warning and full letter grade reduction on the current project for the first offence followed by expulsion from the course with a grade of ‘F’ for the second offence. Instructors may impose harsher penalties for serious violations.

Illegal Drugs

The possession, use, or sale of illegal drugs will not be tolerated and will result in immediate termination of the student's participation in the program. The student's college and parents will be notified, and arrangements made for the return of the student to her/his home at the student’s expense.

Additional Rules, Expectations & Reminders

- Absolutely ***no*** smoking in the field (fire hazard).
- ***No*** firearms allowed in the field, in field camp vehicles, or in camp.
- Tread lightly. ***Do not*** damage or degrade the environment. No littering, digging, collecting of plant specimens, etc.
- ***Do not*** dispose of food wastes (even 'biodegradable' wastes like apple cores and orange peels) on the ground. Some of the areas we work are heavily used and rotting food is unsightly, offensive to local recreationists and bad for wildlife. In the dry climate of southwest Montana it can take years for an apple core or orange peel to ‘biodegrade’.
- Dig ***deep*** holes (at least 6 inches) for “personal disposal” needs including human solid waste and biodegradable food waste. Fill in and cover with a rock.
- ***No*** trundling (rock rolling).
- ***Never*** harass or haze livestock or wildlife.
- ***Don’t*** mess with snakes – it’s their home... not yours! Be safe and considerate and leave them alone.
- Be courteous to landowners and local residents. Honor all requests. Remember, this is their neighborhood.
- ***Be on-time*** at pick-up points – wear a watch or be sure to keep your phone charged. Plan your daily traverses to arrive before the scheduled departure.
- If you are going to succeed in this course, it is imperative that you work diligently in the evenings on your map, cross-sections, explanations, write-ups, etc. You will certainly not succeed if you procrastinate till the last day on each exercise.
- Assignment turn-in deadlines are **hard** deadlines.
- **Reminder: *If a gate is open, leave it open; if it is closed, then be sure to re-close it.***

- **Reminder**: Be careful crossing fences so as not to break them down. Use wire gates when available. Crawl under wires or climb where there is an in-line brace (horizontal bar). Don't stretch the wire by climbing on it or pulling it excessively.
- **Reminder**: The MSU Field camp is 'dry'. No alcoholic beverages are permitted in camp, in the field or in field camp vehicles. Drinking age in Montana is 21 years. Underage drinking is not permitted even on your own time or on days off.
- **Reminder*: No*** graffiti on rocks (personal initials, etc.)

<u>Policy Prohibiting Sexual Assault and Sexual Harassment</u>

Because of the unique setting of a geology field course, students and faculty must rely on each other and watch out for one another's safety. Trust and respect among all participants – students and faculty – are essential for the success of field course projects and the program in general. Respect and success are incompatible with sexual violence or sexual harassment. Sexual assault and sexual harassment are prohibited on all Montana State University programs, by the policies of your home college and by the policies of this field course. Sexual assault is also a serious crime.

Sexual harassment or abuse of any kind will not be tolerated. Students are strongly encouraged to report any incident of sexual harassment or sexual violence to the instructor or directly to the *Office of Institutional Equity* online reporting system http://www.montana.edu/equity/. Every effort will be made to ensure confidentiality and protect the privacy of all victims and witnesses. ***Sexual harassment is any unwelcome conduct of a sexual nature.*** Sexual harassment can include unwelcome sexual advances, requests for sexual favors, and other verbal, nonverbal, or physical conduct of a sexual nature, including rape, sexual assault, sexual battery and sexual coercion or other sexual misconduct. ***Sexual violence is any contact of a sexual nature perpetrated against a person's will or where a person is incapable of giving consent*** due to drugs, alcohol, or disability. Sexual violence includes sexual assault (rape), sexual misconduct and sexual coercion (definitions from MSU Sexual harassment Policy).

It's ***<u>not</u>*** OK…

It is OK to rely on each other, to become close and trusted friends and to become intellectual colleagues. It's *<u>not</u>* OK to confuse this with consent for sex or for sexualized innuendo.

Sexual assault is intentional sexual contact with another person without that person's unambiguous, expressed consent. The sexual contact can be intercourse, penetration of an orifice, touching of the genitals or other private body parts. Without consent, it's *<u>not</u>* OK. Ever!

Sexual harassment is unwelcome sexual advances, physical contact or sexual innuendo that substantially interferes with the educational environment. Sexualized banter and jokes can be considered sexual harassment. Sexual slurs, jibes or persistent 'hitting on' another for sex are *<u>not</u>* OK.

Abuse of drugs or alcohol is prohibited on Montana State University programs. Both alcohol and drugs impair the ability to knowingly consent to sexual activity as well as judgment about appropriate sexual boundaries. Violations of this policy are not excused by the inebriation of one or both of the participants.

Non-Fraternization Policy

Montana State University is committed to maintaining a learning and research environment in which faculty and students are safe and respected, with a central philosophy of focusing on interactions that contribute positively to the students' academic development. To avoid conflict of interest and potential exploitation of students arising from the inherent power differential between faculty and student participants, the MSU prohibits faculty from entering into any personal relationship that extends beyond a normal, traditionally acceptable faculty/student collegial or professional interaction. Unacceptable relationships may include, but are not necessarily limited to, romantic or amorous relationships, exclusive fraternization, quid-pro-quo, or favoritism. Even if such relationships are consensual, the potential impairment of faculty objectivity detracts from student development and impacts the dynamics of the research group. Such dual-role relationships can become problematic, with the possibility of charges of sexual harassment, or physical or psychological abuse.

If Sexual Abuse or Harassment Happens

Talk with a faculty member on your program, the field camp director, the MSU office of institutional equity, a responsible official at your home university, or the police or other civil authority where you are. Any one of these contacts can begin the process of getting help. Keep the attached list of names and telephone numbers of these people.

As hard as it is to raise an issue of sexual assault or sexual harassment when you are in a small community in an isolated area, please do it to protect yourself and other students. Talk with a faculty member on site or call home to one of the other resources. Don't keep it to yourself. If you need medical care or counselling a field camp faculty can help locate local medical, legal and safety resources.

It is your decision whether to report an incident to local authorities, to Montana State University or to your home college. If reported to the field course faculty, the Field Course Director or Earth Sciences Department Head, we will work with you to get help and to inform you of your options for reporting within our collegiate programs or to the police. We will also work with authorities from your home institution to investigate the incident, determine if it violated our Montana State University policies and/or the policies of your home institution, and take appropriate action to correct the situation.

You may make a report of sexual assault or sexual harassment any time, including after the field course is concluded. In addition to the other options identified in this policy, you may make a formal written complaint to ***Montana State University Office of Institutional Equity*** or to the responsible official on your home campus within 12 months of the incident.

You Have Options

If the living arrangements on your field course do not feel safe, the staff will work with you to find acceptable options. We need to know your concerns to help you find an appropriate arrangement. Do not put up with a bad feeling about your living arrangements. Tell a faculty member on your program. If you need separate living arrangements during your stay, speak to your faculty research advisor or to the project director and suitable arrangements will be made.

Think of Others

Mutual respect is the best guarantee of a good experience for everyone on a program. Field camp provides outstanding opportunities to make really close friendships with people in an intellectually exciting endeavor. Don't let anyone ruin this experience for you and don't ruin it for yourself or others. Be a good friend and intervene to help stop behavior that has no place in field camp.

Consensual intimate relationships may develop between students during a field course. Intimate relations between two people in a small residential group will likely change the dynamics within the group. Please don't flaunt an intimate relationship.

Contact Information Related to Sexual Harassment or Assault

At the end of this policy document there is a table listing resources that students can contact to get help, answer questions or to make a report. If you need help following any incident of sexual violence, harassment, or misconduct please reach out to field camp staff, one of the resources listed or to another student. There is no need to suffer in silence.

You are strongly encouraged to make a report if you believe that an incident of sexual harassment or misconduct has occurred involving you or another student. You may choose the most appropriate contact depending on the situation and the people involved. In an emergency contact local police by calling 911.

Health and Safety Policy

Field research and instruction presents some special challenges for the faculty. Students must take responsibility for their own health and wellness; however, project directors have a responsibility to inform all project participants of any unusual risks and living conditions, including such things as local health or environmental hazards, physical and climatic conditions. Additionally, directors must develop and coordinate an appropriate and effective response and support program in the case of an emergency.

When preparing students for the program, the colleges are held to the **"standard of foreseeability,"** which means we must anticipate (within "reason") the conditions and events that could impact the physical and emotional health of the students, and provide adequate information and advice.

Students must provide proof of medical insurance such as a copy of an insurance card. This will be kept on file in the Earth Sciences office. Students must also provide an emergency medical directive. These forms may contain confidential information and will be kept in a sealed envelope to be opened only in the event of an emergency when medical information is required and the student is incapacitated. Students are strongly encouraged to discuss any pertinent medical conditions or special considerations that may help faculty respond to medical situations more effectively including medication, allergies, diabetes, seizures, injuries, disabilities, etc.

Special Health Considerations

Preparation is essential. Students are responsible for arriving at field camp with the proper equipment, medications, clothing, tent and sleeping bag to liver safely and comfortably in the outdoors for the duration of the course. Field course staff will provide information on camping/lodging arrangements, expected field conditions, and accessibility of health care. You will receive general guidelines to help you select proper equipment, but – ultimately – you are responsible for your own kit.

1. Students may encounter poisonous snakes, bears, or other animals. Student may be required to work at altitude and/or in rugged terrain. Students will be living in tents for much of the field course and may lodge in dormitory-style or shared rooms. Students should guard against dehydration, sunburn, cold and damp conditions, hypothermia, ticks, biting insects, and other risks of outdoor life.
2. Summer weather in Montana can include a wide range of conditions ranging from extreme heat to winter-like cold. Rain is virtually guaranteed and significant accumulation of snow in the field area and/or camp is not uncommon. Students must bring appropriate clothing, tents and sleeping bags to ensure their health and comfort during the course.
3. Students and faculty who take prescription drugs should take enough to last the duration of the project. These meds should be in the original container, with the relevant prescription information. Participants with allergies should wear medical alert bracelets or carry an emergency medical ID card and notify faculty of procedures to follow in an emergency. ***Field course faculty are prohibited from distributing medicine to students.*** Participants should carry their own supply of common remedies such as pain relievers and antihistamine.
4. All participants should carry a basic first-aid kit. Students are responsible for providing their own first aid kit. The field course will provide group first aid kits in base camp and field vehicles.
5. Students and faculty will obtain their own hospitalization insurance before going into the field. Faculty members will be covered by their own college hospitalization policy. Students will be covered under their family policy, or if necessary, they will need to take out a short-term hospitalization policy. The field course requires that all students provide proof of insurance before the beginning of the course.
6. Students and faculty will be responsible for obtaining insurance that covers their travel to and from the field sites by air, train, or private vehicle.
7. MSU will cover travel and liability insurance in college-owned or rented vehicles.

Accommodations for Students with Disabilities

Students with disabilities that qualify under the Americans with Disabilities Act and Section 504 of the Rehabilitation Act and require accommodations should contact the MSU Office of Services for Students with Disabilities (406-836-4542) as early as possible and before the start of the program to ensure that they get the assistance that they need to be successful in this course. Please work with the MSU Disability Office, field camp director and instructors before the beginning of the program to address and discuss any special needs or special accommodations.

Because of the rigorous physical nature of field camp, the course may be unsuited to students with some types of physical disability. Reasonable accommodations will be made for disabilities that do allow students to participate in standard field course activities including hiking over rough terrain. In compliance with university, state, and federal policies and equal access laws, MSU and the field course will make reasonable efforts to develop a plan of appropriate academic accommodations for students with disabilities that affect learning.

Non-Discrimination Policy

MSU strives to provide a safe and welcoming environment for all students to live and learn regardless of race, ethnicity, national origin, gender, sexual orientation, disability or any other personal attribute. Students are encouraged to report any verbal, physical or implied intimidation or harassment to the instructor or directly to the *Office of Institutional Equity* (http://www.montana.edu/equity/). The university's commitment to diversity is embodied in the *MSU Statement on Diversity* http://www.montana.edu/president/communications/diversity.html).

Academic Integrity

Violations of academic integrity will not be tolerated. Each student in this course is expected to abide by the University Code of Academic Integrity (See MSU Student Handbook). Any work submitted by a student in this course for academic credit will be the student's own work. Collaboration is an important part of field camp, but collaboration does not mean plagiarizing the work of others. If you are not sure what the limits of collaboration are it is your responsibility to ask! You are encouraged to work together in the field and to discuss information and problems encountered in the field. However, this permissible cooperation should never involve one student having possession of a copy of all or part of work done by someone else. At the discretion of the instructor, penalties for violation of academic integrity can also be extended to include failure of the course and/or referral to the dean for university disciplinary action. For more information: http://www2.montana.edu/policy/student_conduct/student_conduct_code.htm.

Publication and Authorship Policy

Much work goes into a publication, including, but not limited to: Ideas, hypotheses, literature search, field work, lab work, testing hypotheses, drawing conclusions, writing, preparing illustrations, maps, and posters.

Any student or faculty member who has a significant role in any of this work should be an author. The term "significant" must be defined, ideally in advance. Certainly 30% of the work would result in co-authorship if only two geologists are involved, but would 10%? Similarly, 15% of the work would result in co-authorship if four geologists are involved, but would 5%?

"Publications" include published abstracts for oral presentations and poster sessions, geologic maps, and published papers. Students should not submit an abstract to the Geological Society of America or any other professional organization without discussing authorship with the project director, the other project faculty, and the student's on-campus research advisor. Similarly, professors should include students, or other faculty on the project, as co-authors if they have contributed significantly to the research. The researchers must also determine the order in which the authors will be listed.

Course Evaluations

Students will have the opportunity to complete anonymous evaluations of the course and instructors. The field course faculty will read all evaluations. Verbatim, anonymous copies of the project evaluations will be returned to the project faculty and field course director. If the field course director feels that evaluations contain information that may justify or require further action, he will contact the Earth Sciences Department Head. The Head will determine if further investigation is required and the scope of that investigation. If further investigation is undertaken, it will include an opportunity for the faculty member to respond to any charges. The Earth Sciences Department Head will review the results of the investigation and a judgment rendered as to appropriate action.

Dismissal, Withdrawal and Contract Obligation

If the course director feels that a student's conduct might bring the program into disrepute or threatens the health or safety of the participants, the field camp faculty, director or Earth Sciences Department Head can take action to dismiss the student from the project. The students have acknowledged this right in their contract. If the student is posing an imminent threat to the program or to the health and safety of the participants, this is a serious health and safety issue and should be handled as such. The faculty should take all action needed to stabilize the situation including removal of the student if necessary. The field course director and/or Earth Sciences Department Head should be contacted, and the appropriate procedure followed. If there is not an imminent threat, the project faculty will confer with field course director and a representative from the student's school, if applicable. The project director will take appropriate action. During the academic year, a complaint to the field course office should be made if a student's actions are believed to warrant removal from the program.

Complaints, Dismissal and Withdrawal Procedures

Complaints of violation of field course policies, including policies prohibiting sexual harassment and sexual assault, should be made in the following way:

- Complaints may be made to the project directors or faculty on site at a project, to the home campus official responsible for similar policies at the campus of either the complainant or the respondent, or to the field course Director.
- The person receiving the complaint will work with the complainant to reduce the complaint to writing. The field course Director and the Earth Sciences Department Head will be informed of the complaint.
- The complaint will be investigated promptly using a process that is appropriate to the circumstances and guided by principles of fundamental fairness to all persons involved. Investigations will seek to respect the privacy of all involved.
- Based on the information resulting from the investigation, the Earth Sciences Department Head will make a prompt determination regarding whether field course policies were violated and appropriate steps to respond to the complaint. Appropriate responses may include disciplinary action such as removal from a project and notification of a policy violation to the home campus.
- Both the complainant and the respondent will be informed of the Earth Sciences Department Head’s decision.

Field Course Contract (Student Copy)

By signing below I agree to the following.

- I have read the Montana State University Field Course Policy Handbook and I agree to conduct myself according to the standards of conduct described therein.
- I am familiar with the procedures for filing reports of misconduct or discrimination and for addressing grievances.
- I am covered by a valid medical insurance policy and have provided proof of insurance to field camp staff.
- I have completed the confidential medical information form (to be used only in case of emergency).

Name ____

Address ______________________________________

____

____

Signature ____

Date ________________________

APPENDIX:
Sexual Harrasment/Violence & Emergency – Crisis Lines and Reporting Contacts

Local Emergency/Police: Dial 911

MSU VOICE Crisis Line – call from anywhere

MSU VOICE Center – 24-hour Crisis Line

VOICE Center
24-Hour Crisis Line: (406) 994-7069

Office: (406) 994-7662
www.montana.edu/voice

Field Course & Department Staff

MSU – Department of Earth Sciences Field Course

Field Course Director:	Dr. Colin Shaw	406-994-6760 (office); 406-548-1987 (mobile)
Earth Sciences Dept. Head:	Dr. Mary Hubbard	406-994-3331 (office)
Field Course Faculty:	Dr. David Bowen	406-581-5448 (mobile)
	Dr. Jean Dixon	406-994-3342 (office); 805-722-2838 (mobile)
	Dr. David Lageson	406-994-6913 (office); 406-581-3990 (mobile)
	Dr. David Mogk	406-994-6916 (office); 406-600-4071 (mobile)

Sexual Harassment or Discrimination Reports/Complaints

MSU Office of Institutional Equity

Phone: (406) 994-2042
Online Reporting System: (anonymous option):
http://www.montana.edu/equity/
Director: Kate Grimes, J.D.
Equity Specialist: Janelle Barber

Mailing Address:
Montana State University
P.O. Box 172430
Bozeman, MT 59717-2430

Local Resources

Bozeman Area

HAVEN
Office: (406) 586-7689
24-Hour Crisis: (406) 586-4111
www.havenmt.org

Help Center
Office: (406) 587-7511
24-Hour Crisis: (406) 586-3333
www.bozemanhelpcenter.com

Dillon Area

Women's Resource Center/Community Support Center
24-Hour Crisis Line: (800) 253-9811
Office: (406) 683-6106 www.cscofswmt.org

Ennis/Virgina City Area (Madison/Beaverhead Counties)

Victim/Witness Advocacy Program
Office: (406) 843-4232

Livingston/Paradise Valley Area

Park County Victim Witness Assistance Program
Crisis Line: (406) 222-2050

Red Lodge Area

Domestic and Sexual Violence Services
24-Hour Crisis Line : (406) 425-2222
www.dsvsmontana.org

INTRODUCTION TO FIELD MAPPING OF GEOLOGIC STRUCTURES

GEOL 429 – Field Geology
Department of Earth Sciences
Montana State University

Dr. David R. Lageson
Professor of Structural Geology

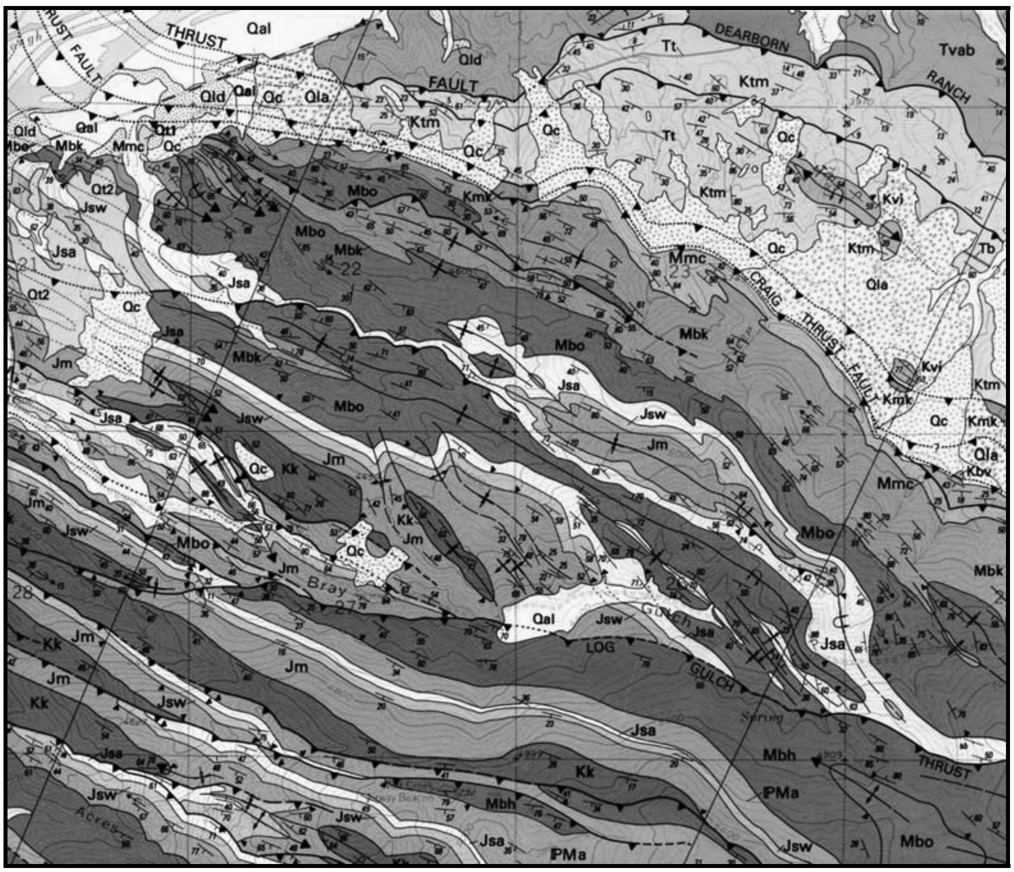

Source: Schmidt, R.G., 1977, Geologic map of the Craig quadrangle, Lewis and Clark and Cascade Counties, Montana: U.S. Geological Survey GQ-1411, 1:24,000.

CONTENTS

The author respectfully acknowledges Professor Gray Thompson's unpublished paper entitled "Geologic Mapping" (University of Montana), which was revised and used extensively in the compilation of this handout.

INTRODUCTION

Structural analysis proceeds through three linear stages: 1) **description** of the structural geometry of a deformed field area (bedding attitudes, planar fabrics, linear fabrics, folds, faults, joints, etc.); 2) **kinematic** analysis (movements responsible for the development of structures [translation, rotation, distortion, and dilation] and relative timing); and 3) **dynamic** analysis (interpretation of forces and stresses responsible for the deformation). Stage 1, descriptive structural analysis, is the product of careful field mapping.

Although maps are two-dimensional sheets of paper, they portray the geology in three-dimensions. This is because most structures tend to dip or plunge and, therefore, one can infer the direction and degree of dip or plunge through outcrop patterns. Also, we use special geologic symbols to indicate 3-dimensionality on our maps. Therefore, a geologic map is nothing more than the representation of 3-d structures on an arbitrary 2-d horizontal plane. Put another way, a geologic map is a cross-section of dipping and plunging structures projected on a horizontal plane. Clearly, it is necessary to carefully map out this 2-d view before one can visualize the 3-d geometry of deformed rocks. A well-done geologic map can provide a powerful *down-plunge view* of the 3-d structural geometry in a "true" cross-section view that is $\perp$ to plunge.

Field mapping can be physically and mentally challenging. Hundreds of questions arise, dictating that hundreds of decisions must be made during the course of a single day. Where should I go? What unit is this? Why does this bed abruptly end? Thus, field mapping is the ultimate application of the scientific method – a good field mapper is constantly testing predictions about the next outcrop and evaluating multiple hypotheses about the structure. In the midst of this mental workout, it is important to maintain your focus and purpose by remembering the goals of your project or research. Try to maintain a good sense of humor and enjoy the day. After all, didn't most of us decide to go into geology because we like being outdoors and we like thinking about the Earth?

To get started with structural field mapping, here are some tips:

- Eat a good breakfast
- Drink plenty of water throughout the day
- It is humanly impossible to take "too many" strike-and-dips
- In structural geology, accuracy and neatness count heavily!
- Force your mind to think in 3-d; with time and experience, this will come naturally
- Use your time in the field efficiently - always <u>have a plan</u> in the field!

DELIVERABLES

Each mapping/structural field project in GEOL 423 requires the following deliverables (i.e., products to be turned in), typically at a designated time/place on the evening of the last day of the project:

- Geologic map – lightly colored and burnished
- Structural cross-section(s) – lightly colored and burnished
- Key or explanation that describes all rock units and explains structural symbols, etc.
- Written report, usually based on a set of questions posed at the onset of the project; some reports may require accompanying stereonets
- Field notebook

In order to accomplish this (on time), it is essential to work during each and every evening during the course of a multi-day project. An evening work plan might be the following:

- Evening 1 – construct your topo-profiles and "boxes" for your cross-section(s) lines; begin work on the key; start to ink your field map; plan your next day (perhaps following a cross-section line)
- Evening 2 – continue to ink your field map; start to make cross-section sketches; continue work on the key; plan your next day
- Evening 3 – continue to ink your field map; finish one of your cross-sections (assuming you have more than one cross-section); make an initial outline of your report; plan your next day
- Evening 4 – continue to ink your field map; finish your second cross-section; spend some more time thinking about your report, particularly how you are going to answer the questions (compile strike-dip data on stereonets); plan your final day to maximize in-filling of your map in critical areas
- Evening 5 – finish inking and coloring your map and key; finalize your report (deadline = mid-evening)

This suggested work schedule would obviously be compressed with mapping projects that span less than five days, so plan accordingly.

CONSTRUCTING A GEOLOGIC MAP IN THE FIELD

The art and science of geologic mapping involves the accurate depiction of contacts between rock units on a base map of some sort. This is what it's all about – being able to draw a contact on a topo-map or air photo! Obviously, this task is best done in the field where you can visually verify the location of contacts (don't try to "dry lab" a geo-map back in camp). Your ability to construct a reasonable geologic map in the field fundamentally depends on two things. **First**, you must know exactly where you are on a topo-sheet or aerial photo at all times – being lost is simply not an option! **Second**, you must know where you are in the stratigraphic section, which sometimes requires a little scrambling around (this obviously becomes easier with experience in an area). Unless you know where you are and what you're standing on, it is impossible to draw a contact. Therefore, the overriding goal is accurate mapping of contacts and related geologic features (faults, etc.); it is not good enough to depict the "general idea" – we insist on accurately mapped contacts.

Procedure:

1. Keep track of your location on the map or aerial photo continuously as you traverse an area; typically, you will want to plan your traverses perpendicular to strike, thus crossing as many units as possible.
2. Orient the map in the direction that you are traversing: if you are walking east, then you should be looking eastward on the map. Always look ahead to where you want to go next on the topographic map, so when you get there you have already anticipated the topography - *have a plan!*
3. When you encounter a contact between two mappable units, stick a pin through the map at your location, turn the map over, circle the pinhole, and assign a station number to it; then, enter the station number in your field notebook as the heading for entries relating to that map station.
4. A typical station number might be abbreviated in the following manner:

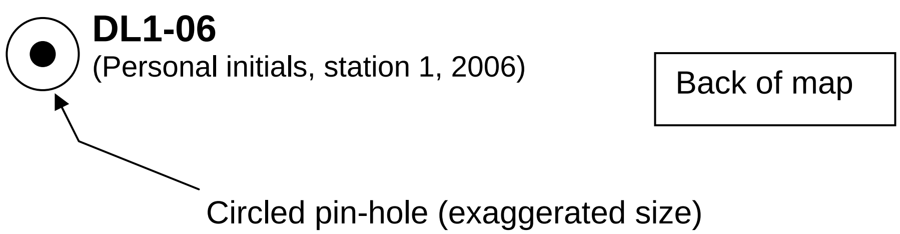

5. Typical notebook entries for a given station might include:
   - Rock descriptions
   - Identification of formations (or other mappable units) at the contact
   - Nature of the contact (disconformity; gradational; fault; igneous; etc.)
   - Strike-and-dip, trend-and-plunge, etc.
   - Estimates of formation thickness
   - Observations on topographic expression of rock units
   - Structural cross-section sketch
   - Stereonet sketch (to help visualize structural data)
   - Sketch of complex outcrop relationships
     (Be sure to distinguish facts/observations from interpretations)

   Good field notes are richly illustrated with clean, clear sketches; one good picture is worth a thousand words!

6. Next, draw the contact on your map as far as you can confidently see it, either on the ground or the air photo (use a thin/sharp pencil with a soft touch, in case you need to erase it). Do not forget the Rule of V's, but

don't exaggerate the contact migration in valleys. The contact location on your map should be accurate not generalized or theoretical. Your map IS data.

7. Then move on quickly to the next contact. Remember, try to cover as much ground as possible each day and <u>NEVER</u> plan to return to the same outcrop later – chances are, you never will.

   Also, don't stash your daypack expecting to return to it later. Once you get to a new spot, you may see something that dictates a different route than you planned on. Carry all your gear with you, all the time (this is a basic USGS rule of mapping).

8. To save time and energy, plan your traverse so it crosses the structural grain at a high angle (perpendicular to strike). Work back and forth over an area in a series of traverses, spaced according to the topography and complexity of the geology.

9. Take advantage of hilltops to check your mapping, refine your contacts, refine your traverse route, and predict contacts on the next leg of your traverse. Sometimes in rugged, high mountains, the view from a peak may be your only way to map cliffs, cirque headwalls, and other inaccessible places. In such instances, a good pair of lightweight field binoculars may be your best friend (the so-called "Swiss rock hammer").

10. On your geologic map, depict the hinge lines of folds at the point of maximum curvature and be sure that your strike-and-dip data support the interpretation. **Use medium-weight blue lines for fold hinges**.

11. **Use heavyweight red lines for faults** and apply the appropriate design for different fault types (e.g., barbs in the hanging wall of thrust faults).

TYPES OF CONTACTS

There are many different types of contacts between mappable units (refer to geologic map and structure symbols). However, for this field course, three types of contacts will be used to express your level of confidence:

- Solid line = definite contact (you are sure you have located the contact within the line width on your map); sometimes you can show the dip direction and amount with an arrow, as below (intrusive igneous contacts can sometimes dip inwards):

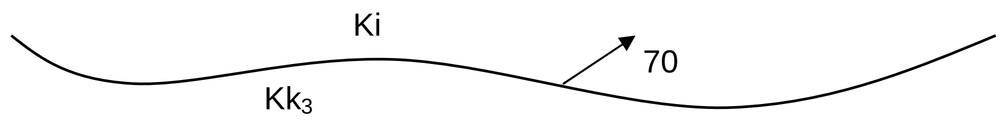

Figure 1. Contact position known well (50 ft on a 1:24,000 map)

- Dashed contact = the contact is reasonably well located, but possibly not within a line width on the map

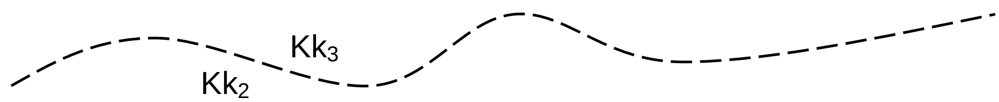

Figure 2. Contact known with less precision

- Dotted contact = concealed contact (i.e., beneath Quaternary alluvium)

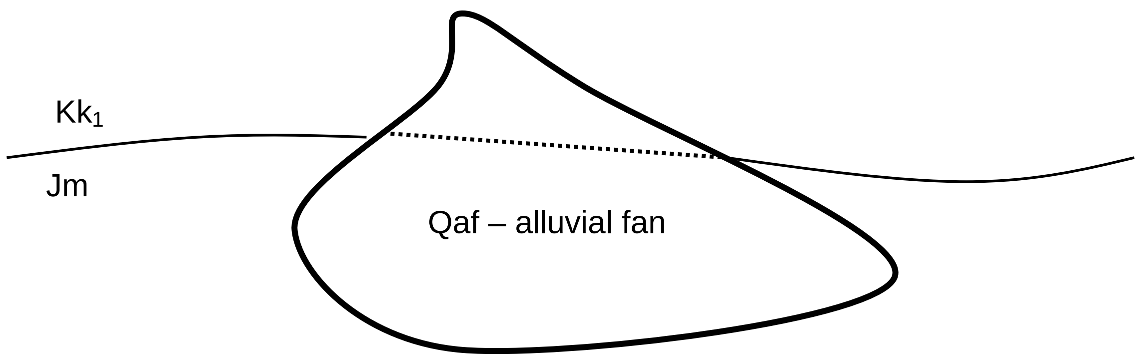

Figure 3. Contact concealed below a surficial unit.

If the rocks are well exposed (as they generally are in field camp), you should be able to draw solid contacts with confidence in most cases. Dotted contacts are certainly permissible where you need to extrapolate a contact beneath Quaternary cover. Dashed contacts should be used rarely in this class because, again, you are mapping some incredibly well exposed areas!

Air photos:
When available, air photos can be a great help in locating contacts. Even with black-and-white air photos, contacts can sometimes be clearly seen as tonal boundaries. Just be sure (through ground truthing) that a change in tone corresponds to a mappable contact (formational boundary) and not simply a change in vegetation; if the tone change does correspond to a contact, then you may be able to extrapolate the contact well beyond the area of your traverse and then transfer these data back to your topographic base map. Color air photos work even better for this application! Of course, working with stereo-pairs can assist in visualizing the 3-d relationship of contacts to topography. Be aware that distortion increases on an air photo from the center to its margins, thus affecting the shape of outcrops near the margins of the photo.

When traversing about a field area, pay attention to the plant cover that grows on different rock units. This will assist in your interpretation of air photos.

COMMON SYMBOLS USED ON GEOLOGIC MAPS

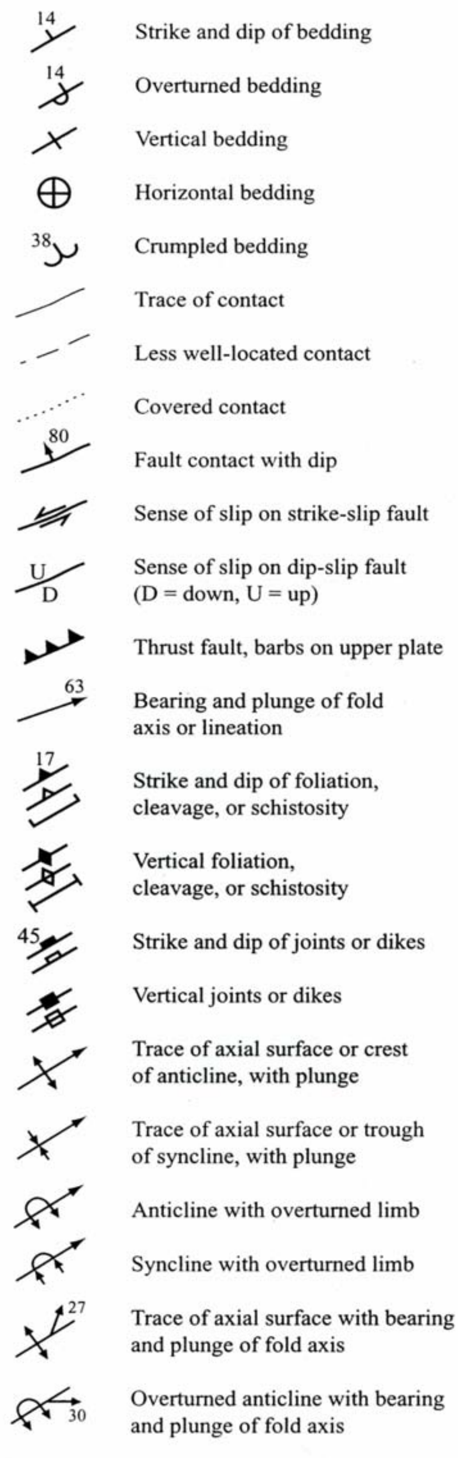

Figure 4. Common symbols on a geologic map (from Rowland et al., 2007, appendix F)

SURFICIAL DEPOSITS

Do not get carried away with mapping Quaternary alluvium in every little creek and arroyo; reserve the mapping of Qal for big creeks and rivers with broad, deep floodplains. If bedrock mapping is your goal, then map surficial deposits only where they hopelessly obscure bedrock; alternatively, if your goal is to map surficial deposits, then do not let the bedrock detain you. Do not map surficial deposits as “undifferentiated cover” and do not invent some meaningless designation, such as Quaternary hill wash.

Here is a short-list of some commonly encountered Quaternary deposits that you might need to map:

- Qal – alluvium
- Qaf or Qf – alluvial fan, typically at the base of a range
- Qls – landslide
- Qt – talus (particularly a talus apron at the base of a cliff)
- Qm - moraine

THE ISSUE OF SCALE

The amount of detail you can show on your map depends on its scale – basically on what you have room to draw. You can generally show more detail by resorting to a larger scale, depending of course on the size of the structures in your field area. When selecting a map scale for your field project (something you don’t have to worry about in field camp), consider the following:

- What is the goal or purpose of my mapping?
- What scale of structures do I want to “capture” through mapping?
- How much time do I have (is this a reconnaissance project, or can I go slow and map in great detail)?

The typical scale for USGS mapping projects is 1:24,000. At this scale, the USGS rule-of-thumb pace of mapping is one mile^2 per day. For projects involving detailed structural analysis, a better scale may be 1:12,000 and a pace of ~0.5 mile^2 per day.

THE IMPORTANCE OF THINKING

People who wander aimlessly from one outcrop to the next, with no traverse plan, are probably wasting their time. You should always have in mind one or more ***working hypotheses*** that predicts what rocks you will find at the next outcrop or ridge, based on an overall hypothesis about the structure. Geologic field mapping is the ultimate application of continuous hypothesis testing and juggling multiple hypotheses in your mind – the essence of scientific methodology! ***Every outcrop you visit should test one or more hypotheses.***

For this reason, good field mappers are generally very good scientists. The Classic paper *The Method of Multiple Working Hypotheses* by T.C. Chamberlain (1890) explains the benefits of this method in eloquent 19th century scientific prose. The paper is included in this tome for your edification. If you find that you do not have a working hypothesis, it is important to stop and think until you have one. Alternatively, if you find that you are able to consistently predict the next outcrop with ease, don't become too confident and allow your model to dictate the mapping, for Mother Nature has a way of throwing curve balls that can humble even the most experienced field mappers!

STRUCTURAL MEASUREMENTS

Every student in field camp is required to have successfully completed structural geology (GEOL 315 or equivalent from another university). Here are some points to keep in mind:

- Make sure the magnetic declination on your compass is set correctly (based on up-to-date information)
- There are a variety of ways to measure dip and strike with a compass:
    1. Observe an outcrop exposed in three dimensions (most accurate (Compton, 1962, p. 29)):
        - Step back from outcrop 10 feet or so.
        - Move until the bedding surface just disappears.
        - Sight a level line and read the azimuth (Fig. 2A)
        - Maintain position and measure the dip looking along the azimuth line (Fig. 2B).

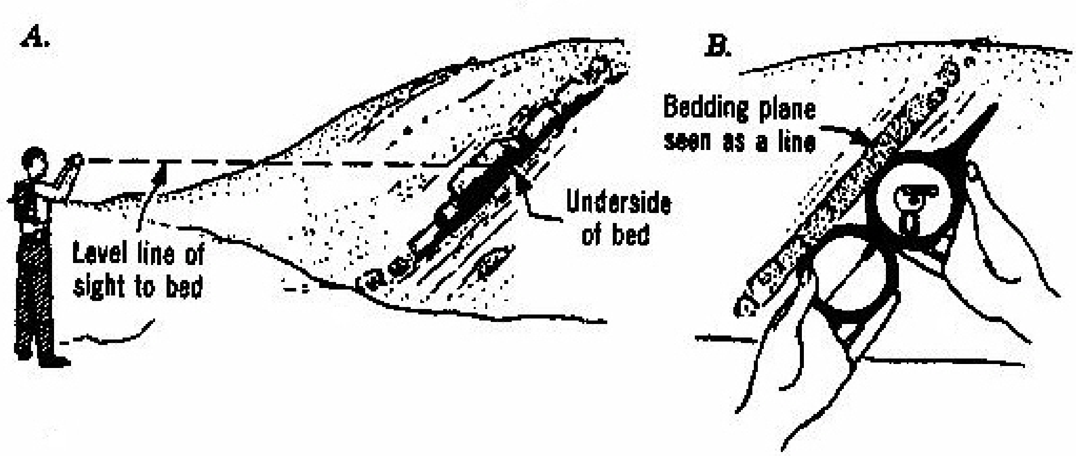

Figure 5. Dip and strike from outcrop 10 feet away (from Compton, 1962, p. 29)

2. On an outcrop (beware of surface irregularities)

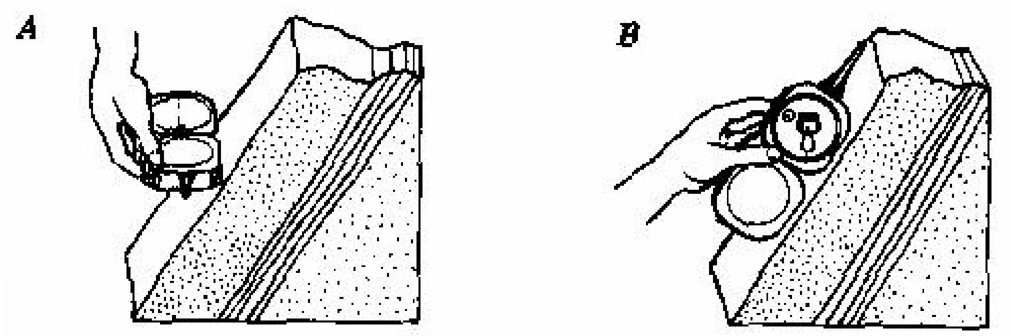

Figure 6. Measurement of dip and strike on outcrop (from Compton, 1962, p. 30).

3. On an outcrop with low dip angle splash water on surface and measure dip parallel to water flow and strike perpendicular to that (Compton, 1962, p. 31)
4. Visually sight a strike-and-dip across an outcrop or across a ravine; these are generally more accurate than measuring directly on an outcrop surface (especially an irregular bedding surface) unless there is a fault in the ravine that offsets the contact.

- For a given outcrop, you and your partner should both take a structural measurement. This provides a quick double-check of your measurement and allows you to take a numerical average, thus accounting for Mother Nature's variability. Your measurements should be within 5^o of one another; if not, then find out why.
- With accurate mapping of contacts across topography, you can also determine strike-and-dip through the application of the **three-point method** (three points in space define a plane); this is especially useful for measuring the dip of thrust faults.
- Record a strike-and-dip as: S = 305, 45 SW (always indicate dip direction!)
- Alternatively, record dip and dip direction as: 45, 215
- Record plunge and trend as: 35, 045 (i.e., 35^o in the direction 045^o)
- Never record a bunch of numbers without knowing exactly what they mean; take thorough field notes with lots of structure sketches and stereonet sketches
- Remember, if the trace of a contact (or dike) crosses irregular topography in a straight line, it is vertical or nearly so. If the map trace of a contact follows topographic contours, it must be horizontal. If the map trace of a contact wanders across irregular topography, then it dips!

- One can measure plunge and trend of the hinge line of a fold in one of two ways:
    - Stand on the nose of a fold and take a direct measurement of plunge angle and plunge direction at the point of maximum curvature, or
    - Simply plot strike-and-dip measurements on a stereonet from the limbs of a fold and determine the β-point or π-point (S-pole diagram) – this is the preferred method
- Structure sections should be drawn according to the MSU cross-section formatting rules, with no vertical exaggeration.
- Don't forget Occam's Razor: use the simplest explanation that fits your observed and measured field data.

MAP AND CROSS-SECTION KEY (EXPLANATION)

You will typically be asked to create one key for both the geologic map and cross-section(s). The key should provide the basic information needed to read the map, leaving nothing to guess about. It should be complete, yet concise and very clear. The key should include the following elements:

- The key should be on a separate piece of paper
- Every mapped rock unit should be identified by a colored box that matches the color on the map and cross-section(s), pattern (if used), symbol, and age
- Units should be vertically stacked from youngest at the top to oldest at the bottom
- Show igneous rocks in a separate section of the key (not lumped with sedimentary rocks)
- In some cases, you may be asked to represent stratigraphy as a columnar section instead of colored boxes – but you will receive specific instructions on this
- Each mapped unit should have a brief description adjacent to it, such as color (weathered versus fresh), texture, composition, thickness, outcrop expression, etc. – this information should be gathered by you in the field and recorded in your field notebook
- All structure and contact symbols must have an explanation (faults, folds, strike-and-dip of bedding and foliation, lineations, fold hinges, mine adits and trenches, etc.)
- The key should be specific to the project – it should not include units that do not appear on the map or cross-section

APPEARANCE

Geologic maps, cross-sections, keys, and field notes should please the eye and inform the mind. Always present your work as attractively and professionally as possible.

- Smooth, even, finely drawn ink lines inspire confidence; wavering and uncertain lines inspire doubt. Thick, sloppy lines virtually guarantee a very poor grade on the mapping project.
- Dashed and dotted lines should make smooth, continuous curves, not wayward chicken tracks.
- Lettering should be neat, precise, and easily readable.
- Letter your formation symbols on the map so they read the same way; don't have some upside-down, some sideways, and some right-side-up.
- If you do not have room within the contacts of a unit, place the symbol outside with a thin line connecting it to the unit.
- Be sure the cross section contact location matches the position on the map.

WRITTEN REPORT

We normally require a written report of a page or more on the important geologic aspects of the field area. The written report should be based solely on your own interpretations, not those of your instructors or fellow students. Furthermore, it is unethical to copy and/or slightly modify another student's field report.

- Field reports should address the questions posed in the project handout.
- Reports should not rehash rock descriptions and stratigraphy, unless you are so instructed.
- Reports should not rehash "Laramide history" or some other aspect of regional geology – keep the report focused on the geology of your map area and the leading questions.
- Spelling counts! Use dictionaries (geological and English language)
- The written report should be carefully phrased for the same reason your map and cross-section should be carefully drawn. No one wishes to struggle through a mess of superfluous verbiage and tortured syntax. Nothing makes you look worse than a written report that conveys the impression that you do not comprehend your own map!

FIELD NOTES

Field notes should be neat, clear, well organized, and richly illustrated. They should be written in such a manner that another geologist could easily comprehend what you wrote down. You should be able to pick up your notebook in 20 years and not guess about what your columns of numbers meant (like strike-and-dip). Many agencies (USGS) and companies catalog all field notebooks as archival records of your work. Your notebooks are part of your legacy, part of your professional reputation. Someone may read your notebook and form an impression of you long after you are gone, or worse, long before you are gone! Therefore, as always in your geologic work, strive for ***high-quality professionalism!***

- Use a bound notebook; two will be required for field camp.
- Use permanent ink or a hard pencil lead that will not smear; it is useful to have two separate pencils, a soft thin pencil for mapping and a harder-lead pencil for notes.
- You should start each day's notes with the date, location, identity of the map and/or air photos you are using, and other pertinent information about the field project (project number, land ownership, township-range-section, GPS coordinates, etc.)
- Basically, organize your notes by station number and GPS coordinates (if you are recording GPS).
- Enter your observations in an orderly manner. Try to be <u>consistent</u> in the order that you write down field data and observations.
- For structural data, it may be useful to place the appropriate structural symbol along the left margin, and then enter the numbers next to it (as a way to keep track of what the numbers represent).
- Consider making a "running" structural section along your line of traverse.
- **Make numerous sketches!** Many students resist sketching in their notebooks on the grounds that they are not artists and therefore cannot draw; if that logic were to prevail, then most could easily resist taking written notes on grounds that they are not published authors. Even a poorly executed sketch depicts ideas with clarity difficult to attain verbally.
- Many noted geologists recommend organizing notes with the left page reserved for writing and the right page for sketching, cross-sections, or columnar sections.
- Keep facts and interpretations physically separate and clearly identifiable.
- If you invent your own abbreviations (as we all tend to do), it is imperative to explain them with a "key" in the back of the notebook. An example might be "RBS" – rocks badly shattered – no one would have the foggiest idea what RBS meant without an explanation.

<u>GRADING CRITERIA</u>

Goals to strive for-

Map: accuracy, neatness, all map units present on the map, proper symbols and use of colors, logical field relationships, sufficient number of stations, and sufficient number of structural measurements.

Key: all units and symbols on map and cross-section are also on the key, mapping units in proper sequence (oldest on the bottom), accurate lithologic descriptions, and neatness.

Cross-section(s): consistent with your map, logical structural relationships (admissible), consistent bed thickness, properly formatted, and neatness.

Written report: addresses questions, succinct, correct sentence structure, correct spelling, and overall flow.

Stereonets: neat and clearly labeled, good explanation for each sheet, color or symbol coded if multiple fabrics are plotted on one sheet.

Field notes: organization, orderly presentation of data and interpretations, lots of clear sketches, running cross-sections, columnar sections where applicable, neatness, and overall readability.

PITFALLS

Common criticisms of geologic maps:
1. Inaccurately located contacts
2. Incorrect map symbol
3. Illogical contacts or other map relations (including missing mappable units – mostly commonly Jm)
4. Insufficient number of stations (strike-and-dips); in most field areas, you should easily be able to make at least 20 stations per day
5. Missing or inaccurately located fold hinge line, or the hinge is not drawn through the entire fold at all stratigraphic levels
6. Coloring so dark and streaky that it obscures the map
7. Inked lines too thick and/or not neatly drawn

Common criticisms of keys:
1. Map units or structure symbols missing
2. Poor lithologic descriptions
3. Improper sequence in the stratigraphic column
4. Sloppy lettering

Common criticisms of cross-sections:
1. Inconsistent with the geologic map
2. Inconsistent bed thickness (especially for competent units)
3. Illogical relationships – weak structural interpretation
4. Symbols missing
5. Formatting errors

Common criticisms of written reports:
1. Poor writing or spelling
2. Report does not address the salient questions posed at the onset of the project

Common criticisms of field notes:
1. Weak organization and/or lack of neatness
2. Using a pencil that is too soft, resulting in smudges and smears
3. Missing or inadequate sketches of structures and other relevant geologic features
4. Not enough structural data and/or poor organization of measurement data in the notebook
5. Inadequate lithologic descriptions
6. Overall inability to clearly follow what was written down

<u>ETHICS IN FIELD WORK (King, 1977)</u>

You will be required to work with a mapping partner, for the sake of field safety. That does not give you license to copy and plagiarize data. It is <u>fine</u> to discuss where a contact might be, or to compare strike-and-dip measurements to achieve a mean value, or to discuss rock descriptions, or to discuss and debate field relations, but it is <u>not fine</u> to blatantly copy from another student.

- Draw your own contacts on your own map – don't copy someone else's map
- Write your own field notes and do not "dry lab" them from another student in the evening
- Draw your own cross-sections and make your own interpretations
- Treat the land with respect and tread lightly, don't litter, don't carve your initials in rock, and don't break down fences (step through or crawl under when possible)
- *Be honest and set high standards for yourself, in geology field camp and in daily life! Take the ethical high road – it's a better view!*

REFERENCES CITED

Compton, R.R., 1962, *Manual of Field Geology*: New York, John Wiley and Sons, 378 p.

King, P.B., 1977, The *Evolution of North America* (revised edition): Princeton University Press, Princeton, N.J., 197 p.

Rowland, S.M., Duebendorfer,E.M., and Schiefelbein, I.M., 2007, *Structural Analysis and Synthesis. A Laboratory Course in Structural Geology* (3rd edition): Oxford, Blackwell Publishing, 300 p.

Chamberlain, T.C., 1890, The method of multiple working hypotheses: *Science*, v. 15, p. 92-97. Reprinted in *Science*, v. 148, p. 754-759 (1965).

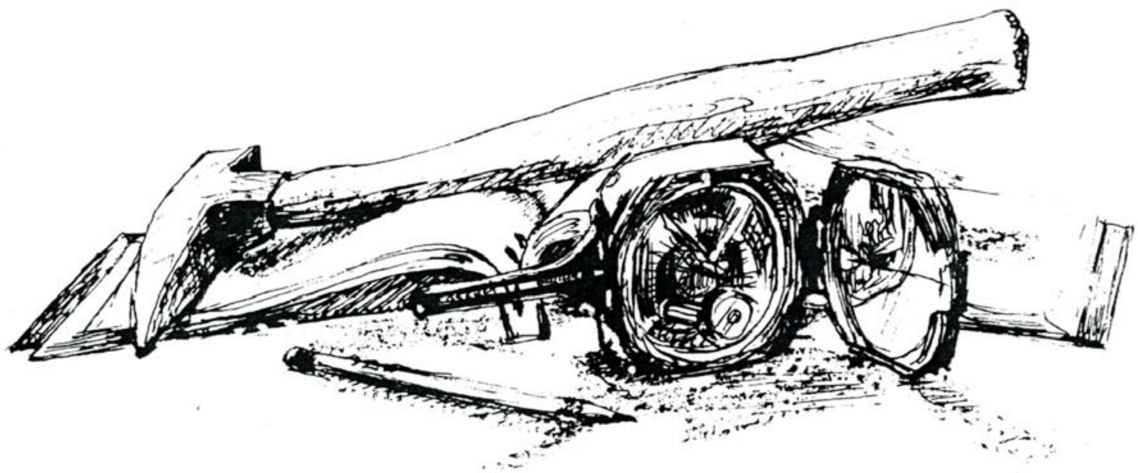

Brunton Compass Instruction Manual

POCKET TRANSIT
INSTRUCTION MANUAL

Printed in U.S.A.
form 51-600 rev 0011

1 -- Important Information

Congratulations on your purchase of the finest pocket transit instrument in the world. The Brunton Pocket Transit is not just a compass. It combines a surveyor's compass, prismatic compass, clinometer, hand level and a plumb into a single instrument. Use the Brunton Pocket Transit to measure azimuth (compass bearing), vertical angles, inclination of objects, percent grade, slopes, height of objects and for leveling.

Even though all Brunton Pocket Transits are made to be rugged, durable and withstand the rigor associated with outdoor use, care must be taken to assure long-life of your instrument. Avoid impacts, dropping, extreme temperatures, store in its case and the Brunton Pocket Transit will perform.

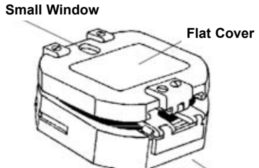

Figure 1

1.1 Opening The Pocket Transit

Rotate the pocket transit until the flat cover faces up, and the small window is positioned away from you. Unlatch the cover from the base. (Fig 1)

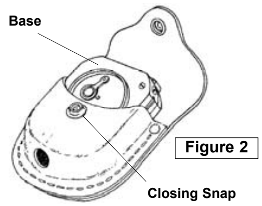

Figure 2

1.2 Protecting The Mirror

While in storage, Brunton recommends placing the pocket transit in the case, with the base against the closing snap. (Fig 2)

1.3 Direct Reading

Why are EAST & WEST switched?

Because the pocket transit is a ***direct reading*** compass. Read azimuth **directly** where the needle points on the graduated circle.

With the large sight toward the object, read azimuth directly where the north end of the needle points (**white** tip - 2001, 2061, 5005LM and 5006LM models, or "**N**" tip - 5007, 5008 and 8700 Com-Pro models). (Fig 3)

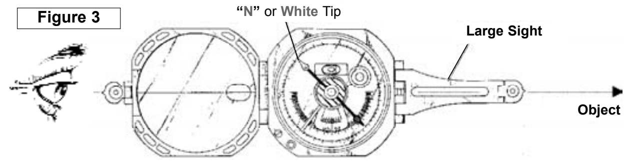

Figure 3

With the small sight toward the object, read azimuth directly where the south end of the needle points (**black** tip - 2001, 2061, 5005LM and 5006LM, or "**S**" tip - 5007, 5008 and 8700 Com-Pro models). (Fig 4)

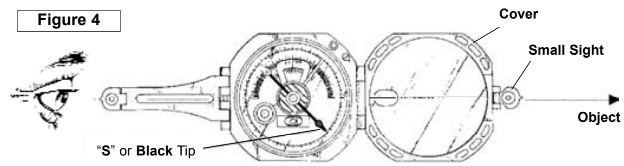

Figure 4

Detailed explanation of sighting an azimuth is in section 4.

2 -- Orientation

Orientation provides a description of important pocket transit parts. A detailed description of its operation is provided throughout the manual.

2.1 Needle (Fig 5)

The needle is induction damped, which allows the needle to seek magnetic north and come to a complete rest in a minimum amount of time, without accuracy degradation.

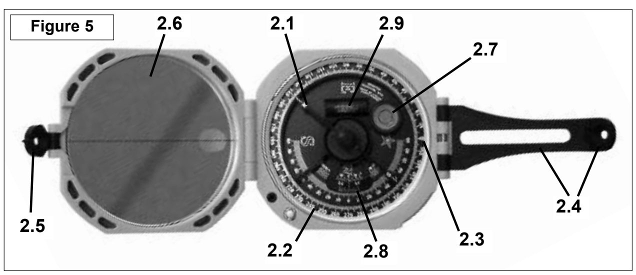

Figure 5

2.2 Graduated Circle (Fig 5)

In combination with the needle, the 1° graduated circle allows accurate 1/2° azimuth readings on both the Degree (0° through 360°) and Quadrant (0° through 90°) graduated circles.

2.3 Zero Pin (Fig 5)

The zero pin is the pointer used for magnetic declination adjustment. If no adjustment is necessary, the pin should point at 0°.

2.4 Large Sight w/ Peep Sight (Fig 5)

The large sight and the attached peep sight are used for precise azimuth measurement.

2.5 Small Sight (Fig 5)

Attached to the cover, the small sight is used for precise bearing and inclination sighting.

2.6 Mirror (Fig 5)

Located on the inside of the cover, the mirror and mirror center line are used for accurate azimuth measurements, when using the transit as a prismatic compass.

2.7 Round Level (Fig 5)

Use the round level to level the pocket transit for azimuth measurement.

2.8 Vernier (Fig 5)

The adjustable vernier is used in inclination measurements.

2.9 Long Level (Fig 5)

The long level for inclination measurement. Adjust the long level using the vernier adjustment - 2.11.

2.10 Circle Adjusting Screw (Fig 6)

With a screw driver, rotate the graduated circle by turning the circle adjusting screw.

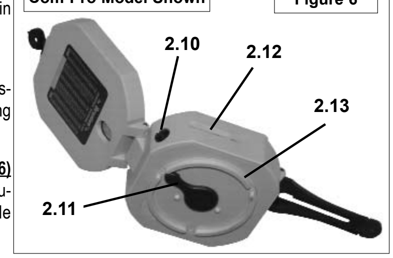

Figure 6

2.11 Vernier Adjustment (Fig 6)

Use the vernier adjustment to adjust the vernier and long level for inclination measurements.

2.12 Ball & Socket Tripod Mount (Fig 6)

The slots on both sides of the body are for mounting to an optional Brunton tripod.

2.13 Alidade Mount -- *Com-Pro Models Only* (Fig 6)

The circular extension with slots, located on the bottom of the body, is for the attachment of an optional Brunton alidade (protractor). Only the Com-Pro models have this feature.

3 -- Magnetic Declination

The Earth is completely surrounded by a magnetic field, and an unobstructed magnetized object will orient itself with the earth's magnetic north and south poles. Magnetic declination (variation) is the difference between true geographic north (north pole) and magnetic north (in northern Canada), with respect to your position. It is important to note magnetic declination at your position, because magnetic declination varies and fluctuate slowly at different rates, around the world. (Fig 7, p.5)

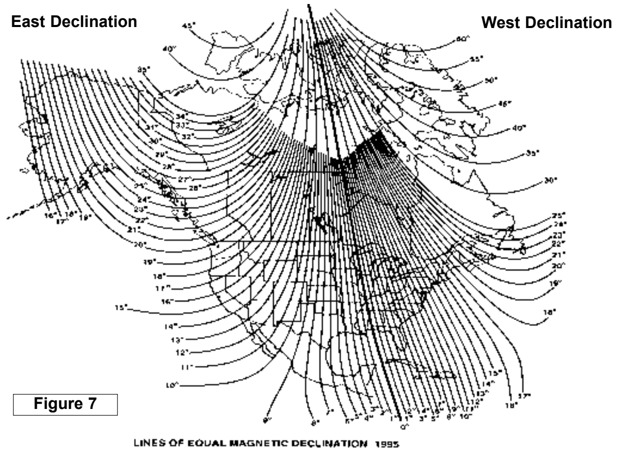

Figure 7

The isogonic chart shows North America, only. Use an isogonic chart, or current United States Geological Survey (USGS), Bureau of Land Management (BLM), or another map to determine magnetic declination at your position. Declination can be east, west or even 0°, from your current position. At 0° declination, true north and magnetic north are aligned.

Example: If magnetic declination at your position is 15° east, then magnetic north is 15° east of true geographic north. Figure 8 displays true geographic north and magnetic north, as indicated in the legends of USGS and BLM maps.

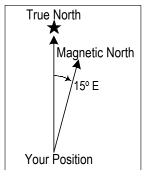

Figure 8

Most maps use true north as a reference. When adjustment for magnetic declination is complete, azimuth readings will be with respect to true north, same as the map.

To adjust for magnetic declination, rotate the graduated circle by turning the circle adjusting screw. Begin with the zero pin at 0°. For **East** declination, rotate graduated circle ***clockwise*** from the zero pin. (Fig 9A) For **West** declination, rotate graduated circle ***counter-clockwise***. (Fig 9B) If magnetic declination is 0°, no adjustment is necessary. (Fig 9C)

Figure 9A

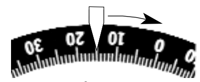

15° **East** Declination

Figure 9B

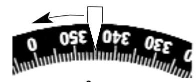

15° **West** Declination

Figure 9C

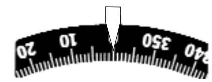

0° Declination

4 -- Azimuth Measurement

Azimuth is a term used for direction. Azimuth is normally measured clockwise, in degrees with true north being 0°. Bearing is a term often used when measuring with a quadrant type instrument. From this point forward, description of pocket transit use will involve the 0° through 360° graduated circle, and assume the pocket transit is adjusted for magnetic declination. Example of Azimuth: If a mountain is directly east of your position, the azimuth from your position to the mountain is 90°. If the mountain is directly south of your position, it would be at 180°.

Caution: The magnetic needle is highly sensitive. When sighting an azimuth, keep the pocket transit away from magnetic materials, such as watches, belt buckles, rings, knives, cigarette lighters, … etc.

4.1 Azimuth Using a Tripod or Unipod

When the greatest accuracy is required, mount the pocket transit on a Brunton non-magnetic

tripod using Brunton's Ball and Socket head. See section 11 for ordering information.

1. Adjust pocket transit for magnetic declinatio
   - See section 4, Magnetic Declination, for help.
2. Mount transit to the ball and socket hea
3. Open both the cover and large sight, until they exten parallel to the body. (Fig 10)
4. Flip small sight and peep sight up. (Fig 1
5. Rotate transit until large sight points at objec
6. Level the transit by centering bubble in round leve
7. Sight azimuth by aligning peep sights with object. (Fig 11)

Figure 10

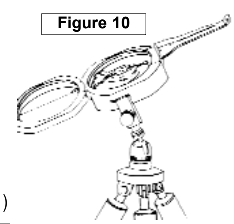

Figure 11

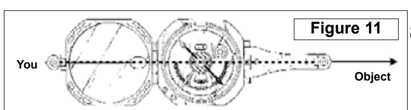

8. Read azimuth where the "N" end of the needle points at graduated circle -- 60°. (Fig 12)

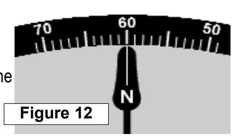

Figure 12

4.2 Azimuth Measurement Waist-Level

This method is often used when object is above or below the observer.

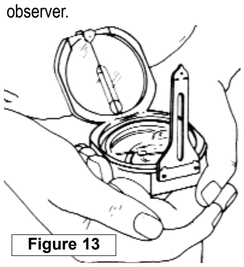

Figure 13

4.2.a Using "N" End of Needle

This method is often used when the object lies as much as 45° above, or 15° below the observer.

1. Hold transit waist high and in your left han
2. Open cover toward your body to approximately 45°.
3. Open large sight, until perpendicular to the bo . (Fig 13)

4. Press left forearm against your waist and steady with right han
5. Level compass using round bubble leve
6. Look into the mirr , and bisect the large sight and the object with mirror center line. (Fig 14)
   - Check that bubble is centered in round bubble level.
7. Read azimuth where the "N" end of needle points at the graduated circle.

Figure 14

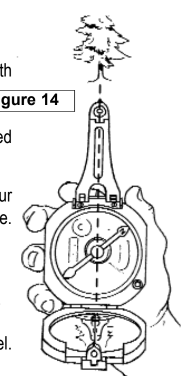

If object is more than 45° above you, open mirror further toward your body, and adjust large sight so that it leans over the bottom case. Then repeat the procedures described in 4.2.a.

4.2.b Using "S" End of Needle

Use this method when object is more than 15° below the observer.

1. Hold transit waist high and in your left han
2. Open cover away from your body to approximately 45° from level. (Fig 15)
3. Open large sight, until it leans over the body at approximately 45°. (Fig 1
4. Press left forearm against your waist and steady with right han
5. Level compass using round bubble leve
6. Look just over the large sight, and at the objec through window opening on mirror. (Fig 15)
   - Adjust mirror and large sight so the image of the large peep sight are bisected by the mirror center line.
   - Check that bubble is centered in round bubble level.
7. Read azimuth where the "S" end of needle points a the graduated circle. (Fig 16)

Figure 15

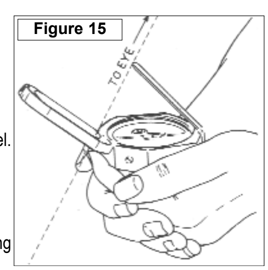

4.3 Using as a Prismatic Compass

Occasionally, objects may interfere with sighting using methods previously mentioned, or user may encounter circumstances which require the transit be held at eye-level to sight an object. If this is the case, follow the procedures below.

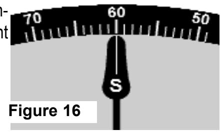

Figure 16

1. Open cover away from your body to approximately 45°, and open small sight. (Fig 17)
2. Lift large sight until perpendicular to the body, or leans slightly away from the base. (Fig 17)
3. Hold instrument at eye-level, with large sight toward you.
4. Align large sight and small sight on top of the cover with object.
   - OR - Sight object through the lower portion of large sight and the window in the mirror.
5. Level round bubble level in the reflection of the mirror.
6. Read azimuth in the reflection of the mirror, where the "S" end of needle points at the graduated circle.

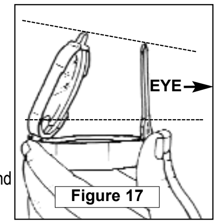

Figure 17

5 -- Vertical & Percent Grade Measurement

The Brunton Pocket Transit is capable of measuring vertical angles with accuracy better than 1°, with readings to 10 minutes. It can also display percent grade, without any calculation.

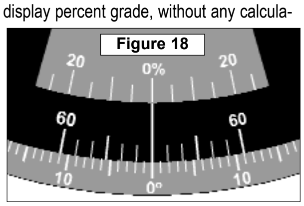

Figure 18

The bottom scale is incremented from 0° to 90° and is used for vertical inclination. The scale on the vernier is also used for vertical (inclination) measurement, but it is incremented from 0 to 60 minutes. (Fig 18) Closer to the center, the second scale increments from 0% to 100%. This scale is the percent grade scale.

5.1 Inclination and Percent Grade Using Tripod

Use a tripod, or unipod for greatest inclination accuracy possible.

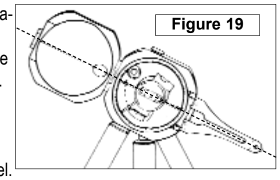
Figure 19

1. With pocket transit attached to the tripod using the ball and socket mount, tilt the head 90°. (Fig 19).
   - Transit should be on its side.
2. Lock into position using the clamp screw.
3. Align sights with object behind transit. (Fig 19)
4. Adjust vernier until bubble is centered in long level.
5. Read inclination at vernier's center line from the degree scale -- 26°. (Fig 20)

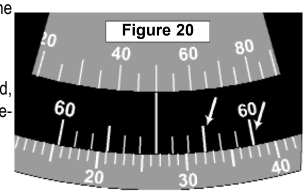

Figure 20

5.1.a -- inclination to the nearest 30 minutes
When 30 minute readable accuracy is required, use the vernier scale (0--60 min. with 10 min. increments).
1. Read inclination at vernier's center line -- 26° + ??.
2. Find minutes by determining whether the 30 or 60 min. line is closest to a degree marking.
   - A Loupe or magnifier may be required.

Since the 30 minute line is closest, the total angle is 26° + 30' (***26° 30' or 26.50°***)

5.1.b -- percent grade
When percent grade is required use the percent scale directly above the vernier.
1. Read nearest percent grade at the vernier's center line -- 50%. (Fig 20)

For greater accuracy, *calculate* the percent grade using the following equation.
Percent Grade = [tan(θ) x 100]

Measure the angle of inclination, θ = 26.5°. Then calculate the tangent of 26.5° using a calculator. Finally, move the decimal two places to the right (multiply by 100).

Example: Tan(26.5°) = .499 = 49.9% Grade

5.2 Inclination Using Prismatic Compass
The pocket transit can also measure angles of inclination without a tripod.

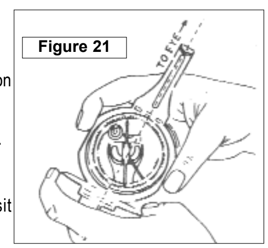

Figure 21

1. Open small sight and large sight as far as possible.
2. Flip peep sight up on large sight, .
3. Position Cover to approximately 45°.
4. With large sight pointing toward you, position transit at eye-level with cover open to the left. (Fig 21)
5. Sight object behind transit, aligning small sight, window and peep sight with object.
6. In mirror, adjust vernier until bubble in long level is centered.
5. Read inclination or percent grade at vernier's center line.

5.2.a Height Measurement Using Vertical Angles
1. Sight inclination, as described in section 5.2.
2. Apply height calculation as shown in Figure 22A or 22B.

Note: Do not calculate tangent of an angle by adding tangents of two smaller angles.

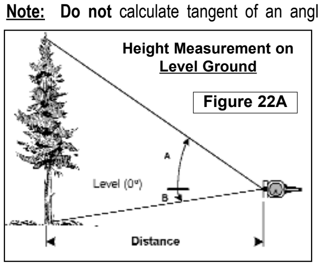

Figure 22A

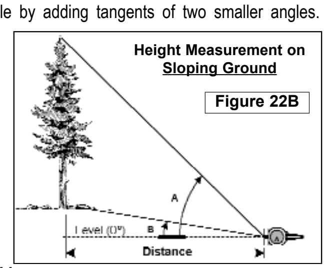

Figure 22B

Level Ground

Height = (TanA + TanB) x Distance

Example: A = 36°, B = 10° & Distance = 50 ft.

Height = (Tan(36°) + Tan (10°)) x 50'
Height = (.727 + .176) x 50
Height = (.903) x 50
Height = 45.15 ft. **= 45'**

Sloping Ground

Height = (TanA - TanB) x Distance

Example: A = 38°, B = 10° & Distance = 75 ft.

Height = (Tan(38°) - Tan (10°))} x 75'
Height = (.781 - .176) x 75
Height = (.605) x 75
Height = 45.38 ft. **= 45'**

Example: Tan(60°) ≠ Tan(30°) + Tan(30°) Find Tan(60°) from a table, use a calculator, or step back until angle of inclination is less than 45°.

5.2.b Height Measurements Using % Grade

Level Ground — Figure 23A
Height = (A + B) x Distance
Example: A = 72.7%, B = 17.6% & Distance = 50 ft.
Height = (72.7% + 17.6%)} x 50'
Height = (.903) x 50'
Height = 45.15 ft. **= 45'**

Sloping Ground — Figure 23B
Height = (A - B) x Distance
Example: A = 78.1%, B = 17.6% & Distance = 75 ft.
Height = (78.1% - 17.6%)} x 75'
Height = (.605) x 75'
Height = 45.38 ft. **= 45'**

6 -- Compass Use with a Topographic Map

1. Sight % Grade using level or sloping ground, same as in Figures 22A & B, p. 11.
2. Apply height calculation, as show in figures 23A & 24B.

A United States Geological Survey (USGS) topographic map is a 2-dimensional drawing of 3-dimensional terrain. Hills, valleys, ridges, cliffs and other terrain are represented through a series of contour lines. Each line represents constant elevation in feet or meters above sea level. Find the contour interval in the legend of the topo-map. With practice, you'll begin to recognize contours, labeling and identify passable routes.

6.1 Map Azimuth
1. On the topo-map, place a "point" at a starting position and an "X" at a destination.

2. Draw a line connecting both mark
3. At the starting position, draw a true north line. (F 24, p.13)
   - Use true north indicator in the legend, or the edge of printed topo-map for reference.
4. Using the Alidade (Com-Pro models only), or a p tractor, find the angle from the starting position to the destination, "X".

Remember, the true north line is 0°.

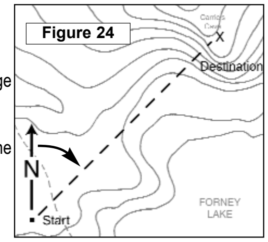

Figure 24

From the start position in the field, sight azimuth determined from the map, and you will be facing the destination. See section, 4 - Azimuth Measurement, for help.

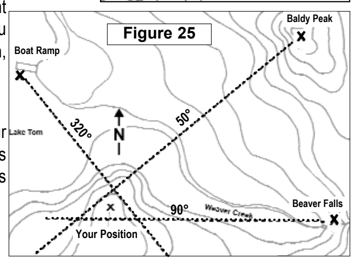

Figure 25

6.2 Triangulation

Triangulation is a method used to find your approximate position, using a compass and a map. Make sure the pocket transit is adjusted for magnetic declination.

1. Identify three landmarks in the field, th you can identify on a topo-map.
2. Sight an azimuth to each land mark an document.
3. Draw an azimuth line on the map fo each azimuth.

7 -- Additional Measurement

4. our position is within the small triangle, or position formed by the intersection of the three lines. (Fig 25)

7.1 Level

The transit can be used as a level, to run level lines, or to determine points of elevation which is the same as the users eyes.

1. Adjust ernier to 0° inclination, using the lever on the back of the body.
2. Place transit on its side, on an object, o use the tripod. (Fig 26)
3. Tilt instrument until the bubble is centered in the long level.

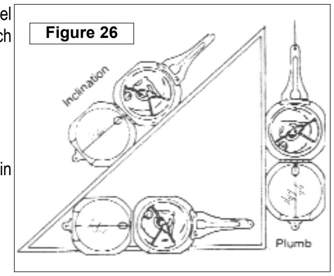

Figure 26

7.2 Plumb Bob

1. Suspend the transit in an open positio from the large peep sight. (Fig 26)
2. Use the small sight as the point .

7.3 Inclination

8 -- Prospecting

1. Place instrument on its side on and object. (Fig 2
2. Move lever on the back of the body until the bubble in the Long Level is centere
3. Read inclination in either degrees or % grad

If you were to discover gold, silver, or another valuable mineral deposit, you would want to "stake a claim". It would be necessary to construct a map of your claim, and tie (locate) your claim relative to some known position. Your Brunton Pocket Transit is ideally suited for this job, since it is essentially the same instrument used by geologists, mining engineers for prospecting and mapping around the world, since 1896.

8.1 Laws Governing Prospecting

In 1872 the General Mining Laws were enacted, and since then more laws have been passed governing the western United States. ***Currently, state laws vary widely and the federal laws concerning mining claims are quite vague. A discussion of the law is beyond the***

scope of this manual and it is strongly advised that you contact your state and federal agencies for information concerning "staking a claim".

Following, is general information on mining claims for basic understanding.
RULES AND LAWS MAY HAVE CHANGED.

1. **Lands Open to Mining Claims** - Lands available for mining claims can be determined by examining records from the Federal Land Office and the U.S. Bureau of Land Management (BLM), for your state. Generally, mining claims are limited to western states, where public land still exists. This includes public lands administered by the U.S. Forest Service, and U.S. BLM. It excludes national parks, monuments, state owned land and privately owned lands.
2. **Qualification** -- An individual must be a United States citizen, or one who has declared their intention to become a citizen. A corporation must be organized under the laws of the United States, or one of the fifty states. There are no restrictions as to age or residency.
3. **Federal Requirements** - The location must be distinctly marked on the ground so that its boundaries can be readily traced. All records of mining claims shall contain the name, or names of of the locators, the date of the location and such a description of the claim or claims located by reference to some natural object or permanent monument as will identify the claim.
4. **State Requirements** - Each mining district may make regulations not in conflict with the laws of the United States, or with the laws of the state or territory in which the district is situated governing the location, manner of recording and amount of work necessary to hold position of a mining claim. THis means the details of location are left to the states.
5. **Type of Claims** - There are four types of claims: lode claims, placer claims, mill sites, and tunnel sites. *Only lode claims are discussed here.*
6. **Lode Claims** - A lode is defined as a zone or belt of mineralized rock lying within boundaries clearly separating it from the neighboring rock. The dimensions of a lode claim are a maximum of 1,500 feet along the lode or vein, and no more than 300 feet to either side of the vein; end lines must be parallel.

Following, is an example of state regulations -- Nevada lode claim location requirements.

1. **E**rect a *discovery monument* at the point of discovery, and post thereon a *location notice* containing: (a) the name of the claim, (b) the name and mailing address of the locator, (c) the date of location, (d) the number of linear feet along the vein each way from the discovery monument, with the width claimed on either side of the vein, and (e) the general course of the vein. (NRS 517.010)
2. **A**ll monuments must consist of (a) a tree cut of 3 or more feet above the ground and blazed, (b) a rock pile 3 or more feet in height, or (c) a 4-inch diameter post at least 4 1/2 feet in length set 1 foot in the ground. (NRS 517.030)
3. **W**ithin 20 days of posting the location notice, mark the boundaries of the claim by placing monuments at the four corners and center of each side line. (NRS 517.030)
4. **W**ithin 90 days of posting the location notice, prepare two copies of a claim map (scale of 500 feet to the inch) showing the position of the claim monuments, the relationship of the claim monuments and the relationship of the claim group to a survey corner, or claim location marker. The marker must be a rock pile 4 feet in diameter and 4 feet high, or a steel post 3 inches in diameter and 5 feet high. The description must also include the sec tion, township and range. The map need not be perfect, but "in accordance with the locator's abilities." (NRS.030) The maps must then be filed with the county recorder. (NRS 517.040 (2))
5. **W**ithin 90 days of posting the location notice, record duplicate location certificates with the county recorder containing the following information *(NRS 517.050):
   a. The name of the lode or vei
   b. The name of the locator or locators, together with the post fice address of such locator or locators
   c. The date of the locatio
   d. The number of linear feet claimed in length along the course of the vein each way fr the point of discovery with width of each side of the center of the vein, and the general course of the lode or vein as near as may be.
   e. A statement that the location work consisted of making the maps as provided in (NR 517.040).

f. The location and description of each corner, with the markings thereon.

6. **O**nly one location may be claimed on each location notice or location certificate (NRS 517.020, 517.050).
7. **P**enalty for late recording: "any record of the location of a lode mining claim which shall not contain all the requirements named in this section recorded on or after July 1, 1971, shall be void, and every location of a mining claim recorded on or after July 1, 1971, shall be absolutely void unless a certificate of location thereof substantially complying with the above requirements is recorded with the county recorder of the county in which the claim is located within 90 days after the date of location." (NRS 517.050 (2))

Other states commonly require some form of discovery work other than preparation of a map. This may consist of digging a shaft or drilling a specified footage of discovery holes. *Check the mining statutes of every state to determine its specific requirements.*

8.2 Surveyed Land

In locating your mining claims and constructing your claim location map, it will be helpful to understand how lands are divided up by the rectangular system of surveys. This system is the basis for the identification, administration and disposal of public lands.

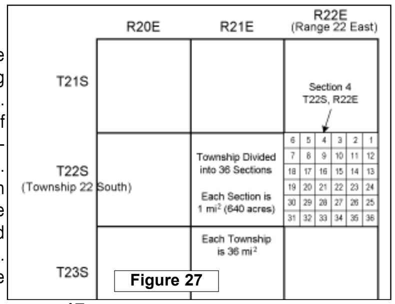

Figure 27

Figure 27 illustrates how lands are divided by survey. Lines running north-south are called range lines. R22E stands for Range 22 East of the principal meridian. Lines running east-west are township lines. T22S stands for Township 22 South of the base line. On a topo-map, the range lines are shown at the top and bottom of the printed map. Township lines are shown on the

east-west margin of the map.

By specifying the township and range, a township area of land is located. The large squares in figure 27 are townships. For example, T22S, R22E specifies the township area with 36 sections, each numbered and 1 mi^2 (640 acres) apiece. This makes a township is 36 mi^2. A 1mi^2 section of land is located by calling out the section number, township and range -- Section 4, T22S, R22E.

A section is further divided into quarter sections by straight lines connecting quarter section corners or opposite boundaries. There are eight monuments on each section. One monument on each corner and one midway between corners on the section boundary lines (not shown).

If your claim is in a surveyed area of public land, it will be located within a section shown on a topo-map. To locate your claim, it is then necessary to tie, or locate your claim relative to a section corner monument. The corner monument may be a pipe with a brass cap fastened to the top. It may be a brass tablet. 3 1/4 by 3 1/2 inches, attached to a rock outcropping and set in concrete. The brass is marked with letters and figures that give the section, township and range. It is marked so that it must be read while standing on the south side of the monument. The south side of the monument is marked with the date of the monument. (Fig 28)

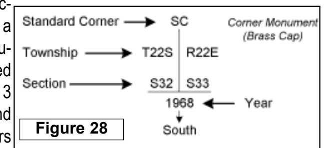

Figure 28

8.3 Sample Claim Location Map

Figure 29 on page 20, shows the location monument with claim extending 300 feet to each side of the vein center line and 1,500 feet long. The claim is tied or located to a section corner post by showing the bearing to the corner post, the number of feet to the post and the section, township and range.

The bearing is obtained with your Brunton Pocket Transit by selecting one of your claim corners as your tie point, and sighting from the tie point to the section corner post. The azimuth

to the South East corner of Section 32, T22S, R22E was found to be 110°. (Fig 29, p. 20). Note, the distance to the section corner must also be provided.

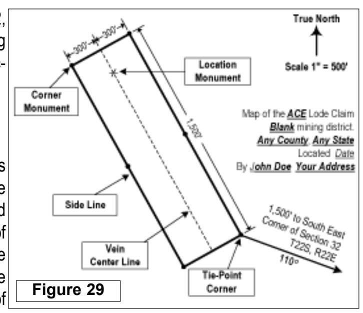

Figure 29

8.4 Location On Unsurveyed Land

Not all of the U.S. has been surveyed. As of 1970, about 500,000,000 acres were still unsurveyed. Most of the unsurveyed land is located in mountainous sections of the country. Since then, however, more has been surveyed. Check with the Federal Land office, or the U.S. Bureau of Land Management of your state.

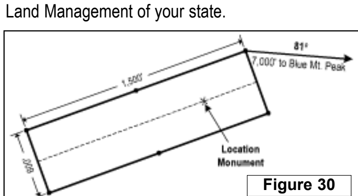

Figure 30

If your claim is located in one of the unsurveyed areas (no corner post to locate, or tie your claim), you must locate your claim in reference to some natural land mark. A natural land mark being a mountain top, intersection of a river and a stream, etc.

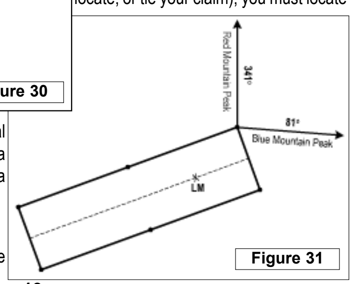

Figure 31

8.4.a Using Bearing & Distance

Figure 30 shows a claim tied to Blue

Mountain Peak by an azimuth of 81°, and a distance to Blue Mountain Peak of 7,000 feet from a corner monument.

8.4.b Using Two Bearings

The claim in figure 31 is tied to two azimuth readings from a corner monument. Using this method, distance is not required, since the intersection of both azimuth lines determine the location.

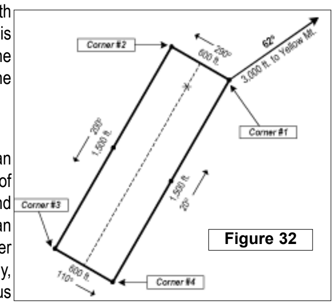

Figure 32

8.4.c Using Five Bearings

A more complete description of your claim can be determined by displaying the direction of the sides of your claim. The angles are found by standing on corner #1 and taking an azimuth to corner #2. Then standing on corner #2 and taking an azimuth to corner #3. Finally, from #3 to #4 and from #4 back to #1, thus completing the description.

9 -- Reference Material

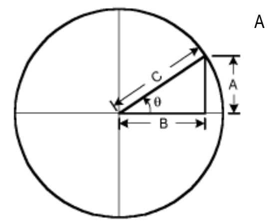

SIN(θ) = A/C **CSC(θ) = C/A**
COS(θ) = B/C **SEC(θ) = C/B**
TAN(θ) = A/B **COT(θ) = B/A**

A = side opposite angle θ
B = side adjacent to angle θ
C is the hypotenuse

$$C^2 = A^2 + B^2$$

Inches	Feet	mm	cm	Conversions	Conversions
1/8	0.0104	3.1750	.31750	1 inch = 2.54 centimeters	1 centimeter = 10 millimeters
1/4	0.0208	6.3500	.63500	1 foot = 12 inches	1 centimeter = 0.01 meters
3/8	0.0313	9.5250	.95250	1 foot = 0.305 meters	1 centimeter = 0.394 inches
1/2	0.0417	12.700	1.2700	1 yard = 3 feet	1 meter = 100 centimeters
5/8	0.0521	15.875	1.5875	1 yard = 0.914 meters	1 meter = 3.281 feet
3/4	0.0625	19.050	1.9050	1 chain = 66 feet	1 meter = 1.094 yards
7/8	0.0729	22.225	2.2225	1 mile = 5,280 feet	1 kilometer = 1,000 meters
1	0.0833	25.400	2.5400	1 mile = 80 chains	1 kilometer = 0.6214 miles
2	0.1667	50.800	5.0800	1 mile = 1.609 kilometers	1 hectare = 10,000 meters^2
3	0.2500	76.200	7.6200	1 acre = 43,500 feet^2	1 hectare = 2.471 acres
4	0.3333	101.60	10.160	1 acre = 0.4047 hectares	
5	0.4167	127.00	12.700		
6	0.5000	152.40	15.240		
12	1.0000	304.80	30.480		

10 -- Specifications

description of the claim shown in Figure 32, would read:
Beginning at Corner #1, the NE corner of the claim.
Thence 600 feet, 290° to Corner #2.
Thence 1,500 feet, 200° to Corner #3.
Thence 600 feet, 110° to Corner #4.
Thence 1,500 feet, 10° to Corner #1.

Magnetism: Models - 2001 & 2061 (*Alnico II Bar Magnet*)
Models - 5005LM & 5006LM (*Alnico V Bar Magnet*)
Models - 5007, 5008 & 8700 Com-Pro (*NdFeB Magnet*)

Accuracy: Bearing -- +/- 1/2° accurate
Inclination -- +/- 1° accurate (30 minute readable)

11 -- Service

Size (Closed): Width -- [2001, 2061, 5005LM & 5006LM models] - 2.79 in. (7.09 cm)
Width -- [5007, 5008, 8700 models] - 2.76 in. (7.01 cm)
Length -- [2001, 2061, 5005LM & 5006LM models] - 3.09 in. (7.84 cm)
Length -- [5007, 5008, 8700 models] - 3.14 in. (7.97 cm)
Height -- [2001, 2061, 5005LM & 5006LM models] - 1.31 in. (3.34 cm)
Height -- [5007, 5008, 8700 models] - 1.33 in. (3.38 cm)
Weight -- [2001, 2061 models] - 6.8 oz (19.3 g)
Weight -- [5005LM & 5006LM models] - 7.1 oz (20.1 g)
Weight -- [5007, 5008, 8700 models] - 5.7 oz (16.2 g)

Engraving - A Brunton Pocket Transit with a cast aluminum body can be personalized with engraving (up to 18 characters, including spaces). Com-Pro models have a decal which can have up to 6 lines of text (approximately 20 characters per each line, including spaces). Call Brunton at (307) 856-6559 for details.

Balancing - Brunton Pocket Transits can be balanced for use in a specific part of the world. Special balancing is required for use in the southern hemisphere. Call Brunton for details.

Repair - Brunton's repair department is capable of handling repairs, or conversions of any genuine BRUNTON Pocket Transit. Periodic maintenance and calibration is highly recommended and will prolong the life of your pocket transit. Call Brunton for details.

Accessories

3051
Jacob Staff
Thimble
Attaches transit to steel tipped wooden rod or Jacob's staff. Ball and socket head is also required.

3040
Ball & Socket
Attaches transit to tripod. Swivels 90o in any direction for reading verticle angle measurements and rotates 360o for horizontal measurements.

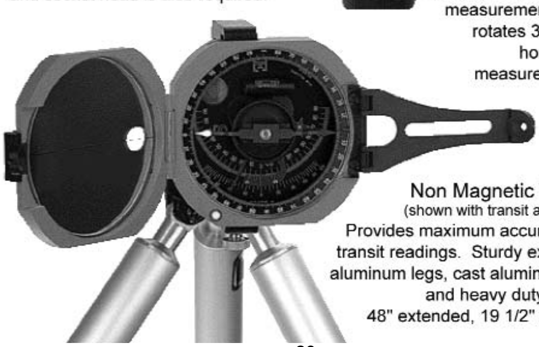

3051
Non Magnetic Tripod
(shown with transit attached)
Provides maximum accuracy for transit readings. Sturdy extruded aluminum legs, cast aluminum top and heavy duty joints.
48" extended, 19 1/2" closed.

Brunton Professional Instruments

Pocket Transits

MODEL	NEEDLE/GRADUATIONS
2001	Conventional, QUADS - 4x90^{o}
2061	Conventional, 0-360^{o}
5005LM	International, QUADS - 4x90^{o}
5006LM	International, 0-360^{o}
5007	COM-PRO, International, QUADS - 4x90^{o}
5008	COM-PRO, International, 0-360^{o}

5006LM

5008

SM 360LA

SUM 360LA

Sighting Compasses
Gives bearing, height, distance or inclination to objects. Sturdy anodized aluminum body. Available with nylon or leather case.

The Method of Multiple Working Hypotheses

With this method the dangers of parental affection for a favorite theory can be circumvented.

T. C. Chamberlin

As methods of study constitute the leading theme of our session, I have chosen as a subject in measurable consonance the method of multiple working hypotheses in its application to investigation, instruction, and citizenship.

There are two fundamental classes of study. The one consists in attempting to follow by close imitation the processes of previous thinkers, or to acquire by memorizing the results of their investigations. It is merely secondary, imitative, or acquisitive study. The other class is primary or creative study. In it the effort is to think independently, or at least individually, in the endeavor to discover new truth, or to make new combinations of truth, or at least to develop an individualized aggregation of truth. The endeavor is to think for one's self, whether the thinking lies wholly in the fields of previous thought or not. It is not necessary to this habit of study that the subject-material should be new; but the process of thought and its results must be individual and independent, not the mere following of previous lines of thought ending in predetermined results. The demonstration of a problem in Euclid precisely as laid down is an illustration of the former; the demonstration of the same proposition by a method of one's own or in a manner distinctively individual is an illustration of the latter; both lying entirely within the realm of the known and the old.

Creative study, however, finds its largest application in those subjects in which, while much is known, more remains to be known. Such are the fields which we, as naturalists, cultivate; and we are gathered for the purpose of developing improved methods lying largely in the creative phase of study, though not wholly so.

Intellectual methods have taken three phases in the history of progress thus far. What may be the evolutions of the future it may not be prudent to forecast. Naturally the methods we now urge seem the highest attainable. These three methods may be designated, first, the method of the ruling theory; second, the method of the working hypothesis; and, third, the method of multiple working hypotheses.

In the earlier days of intellectual development the sphere of knowledge was limited, and was more nearly within the compass of a single individual; and those who assumed to be wise men, or aspired to be thought so, felt the need of knowing, or at least seeming to know, all that was known as a justification of their claims. So, also, there grew up an expectancy on the part of the multitude that the wise and the learned would explain whatever new thing presented itself. Thus pride and ambition on the one hand, and expectancy on the other, developed the putative wise man whose knowledge boxed the compass, and whose acumen found an explanation for every new puzzle which presented itself. This disposition has propagated itself, and has come down to our time as an intellectual predilection, though the compassing of the entire horizon of knowledge has long since been an abandoned affectation. As in the earlier days, so still, it is the habit of some to hastily conjure up an explanation for every new phenomenon that presents itself. Interpretation rushes to the forefront as the chief obligation pressing upon the putative wise man. Laudable as the effort at explanation is in itself, it is to be condemned when it runs before a serious inquiry into the phenomenon itself. A dominant disposition to find out what is, should precede and crowd aside the question, commendable at a later stage, "How came this so?" First full facts, then interpretations.

Premature Theories

The habit of precipitate explanation leads rapidly on to the development of tentative theories. The explanation offered for a given phenomenon is naturally, under the impulse of self-consistency, offered for like phenomena as they present themselves, and there is soon developed a general theory explanatory of a large class of phenomena similar to the original one. This general theory may not be supported by any further considerations than those which were involved in the first hasty inspection. For a time it is likely to be held in a tentative way with a measure of candor. With this tentative spirit and measurable candor, the mind satisfies its moral sense, and deceives itself with the thought that it is proceeding cautiously and impartially toward the goal of ultimate truth. It fails to recognize that no amount of provisional holding of a theory, so long as the view is limited and the investigation partial, justifies an ultimate conviction. It is not the slowness with which conclusions are arrived at that should give satisfaction to the moral sense, but the thoroughness, the completeness, the all-sidedness, the impartiality, of the investigation.

It is in this tentative stage that the affections enter with their blinding influence. Love was long since represented as blind, and what is true in the personal realm is measurably true in the intellectual realm. Important as

---

Thomas C. Chamberlin (1843–1928), a geologist, was president of the University of Wisconsin at the time this lecture was written. Later he was professor and director of the Walker Museum of the University of Chicago. In 1893 he founded the *Journal of Geology*, which he edited until his death. In 1908 he was president of the AAAS. The article is reprinted from *Science* (old series), **15**, 92 (1890).

Reprints of this article are available.

Prices (*cash with order*):

1	50 cents (*or* 25 cents and stamped, self-addressed envelope)
2 to 9	45 cents each
10 to 24	30 cents each
25 or more	20 cents each

Address orders to AAAS, Chamberlin Reprints, 1515 Massachusetts Ave., NW, Washington, D.C. 20005.

the intellectual affections are as stimuli and as rewards, they are nevertheless dangerous factors, which menace the integrity of the intellectual processes. The moment one has offered an original explanation for a phenomenon which seems satisfactory, that moment affection for his intellectual child springs into existence; and as the explanation grows into a definite theory, his parental affections cluster about his intellectual offspring, and it grows more and more dear to him, so that, while he holds it seemingly tentative, it is still lovingly tentative, and not impartially tentative. So soon as this parental affection takes possession of the mind, there is a rapid passage to the adoption of the theory. There is an unconscious selection and magnifying of the phenomena that fall into harmony with the theory and support it, and an unconscious neglect of those that fail of coincidence. The mind lingers with pleasure upon the facts that fall happily into the embrace of the theory, and feels a natural coldness toward those that seem refractory. Instinctively there is a special searching-out of phenomena that support it, for the mind is led by its desires. There springs up, also, an unconscious pressing of the theory to make it fit the facts, and a pressing of the facts to make them fit the theory. When these biasing tendencies set in, the mind rapidly degenerates into the partiality of paternalism. The search for facts, the observation of phenomena and their interpretation, are all dominated by affection for the favored theory until it appears to its author or its advocate to have been overwhelmingly established. The theory then rapidly rises to the ruling position, and investigation, observation, and interpretation are controlled and directed by it. From an unduly favored child, it readily becomes master, and leads its author whithersoever it will. The subsequent history of that mind in respect to that theme is but the progressive dominance of a ruling idea.

Briefly summed up, the evolution is this: a premature explanation passes into a tentative theory, then into an adopted theory, and then into a ruling theory.

When the last stage has been reached, unless the theory happens, perchance, to be the true one, all hope of the best results is gone. To be sure, truth may be brought forth by an investigator dominated by a false ruling idea. His very errors may indeed stimulate investigation on the part of others. But the condition is an unfortunate one. Dust and chaff are mingled with the grain in what should be a winnowing process.

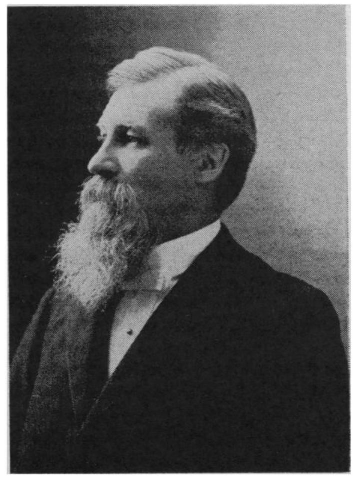

Thomas Chrowder Chamberlin was noted for his contributions to glaciology and for his part in formulating the Chamberlin-Moulton (planetesimal) hypothesis of the origin of the earth.

Ruling Theories Linger

As previously implied, the method of the ruling theory occupied a chief place during the infancy of investigation. It is an expression of the natural infantile tendencies of the mind, though in this case applied to its higher activities, for in the earlier stages of development the feelings are relatively greater than in later stages.

Unfortunately it did not wholly pass away with the infancy of investigation, but has lingered along in individual instances to the present day, and finds illustration in universally learned men and pseudo-scientists of our time.

The defects of the method are obvious, and its errors great. If I were to name the central psychological fault, I should say that it was the admission of intellectual affection to the place that should be dominated by impartial intellectual rectitude.

So long as intellectual interest dealt chiefly with the intangible, so long it was possible for this habit of thought to survive, and to maintain its dominance, because the phenomena themselves, being largely subjective, were plastic in the hands of the ruling idea; but so soon as investigation turned itself earnestly to an inquiry into natural phenomena, whose manifestations are tangible, whose properties are rigid, whose laws are rigorous, the defects of the method became manifest, and an effort at reformation ensued. The first great endeavor was repressive. The advocates of reform insisted that theorizing should be restrained, and efforts directed to the simple determination of facts. The effort was to make scientific study factitious instead of causal. Because theorizing in narrow lines had led to manifest evils, theorizing was to be condemned. The reformation urged was not the proper control and utilization of theoretical effort, but its suppression. We do not need to go backward more than twenty years to find ourselves in the midst of this attempted reformation. Its weakness lay in its narrowness and its restrictiveness. There is no nobler aspiration of the human intellect than desire to compass the cause of things. The disposition to find explanations and to develop theories is laudable in itself. It is only its ill use that is reprehensible. The vitality of study quickly disappears when the object sought is a mere collocation of dead unmeaning facts.

The inefficiency of this simply repressive reformation becoming apparent, improvement was sought in the method of the working hypothesis. This is affirmed to be *the* scientific method of the day, but to this I take exception. The working hypothesis differs from the ruling theory in that it is used as a means of determining facts, and has for its chief function the suggestion of lines of inquiry; the inquiry being made, not for the sake of the hypothesis, but for the sake of facts. Under the method of the ruling theory, the stimulus was directed to the finding of facts for the support of the theory. Under the working hypothesis, the facts are sought for the purpose of ultimate induction and demonstration, the hypothesis being but a means for the more ready development of facts and of their relations, and the arrangement and preservation of material for the final induction.

It will be observed that the distinction is not a sharp one, and that a working hypothesis may with the utmost ease degenerate into a ruling theory. Affection may as easily cling about an hypothesis as about a theory, and the demonstration of the one may become a ruling passion as much as of the other.

A Family of Hypotheses

Conscientiously followed, the method of the working hypothesis is a marked improvement upon the method of the ruling theory; but it has its defects—defects which are perhaps best expressed by the ease with which the hypothesis becomes a controlling idea. To guard against this, the method of multiple working hypotheses is urged. It differs from the former method in the multiple character of its genetic conceptions and of its tentative interpretations. It is directed against the radical defect of the two other methods; namely, the partiality of intellectual parentage. The effort is to bring up into view every rational explanation of new phenomena, and to develop every tenable hypothesis respecting their cause and history. The investigator thus becomes the parent of a family of hypotheses: and, by his parental relation to all, he is forbidden to fasten his affections unduly upon any one. In the nature of the case, the danger that springs from affection is counteracted, and therein is a radical difference between this method and the two preceding. The investigator at the outset puts himself in cordial sympathy and in parental relations (of adoption, if not of authorship) with every hypothesis that is at all applicable to the case under investigation. Having thus neutralized the partialities of his emotional nature, he proceeds with a certain natural and enforced erectness of mental attitude to the investigation, knowing well that some of his intellectual children will die before maturity, yet feeling that several of them may survive the results of final investigation, since it is often the outcome of inquiry that several causes are found to be involved instead of a single one. In following a single hypothesis, the mind is presumably led to a single explanatory conception. But an adequate explanation often involves the co-ordination of several agencies, which enter into the combined result in varying proportions. The true explanation is therefore necessarily complex. Such complex explanations of phenomena are specially encouraged by the method of multiple hypotheses, and constitute one of its chief merits. We are so prone to attribute a phenomenon to a single cause, that, when we find an agency present, we are liable to rest satisfied therewith, and fail to recognize that it is but one factor, and perchance a minor factor, in the accomplishment of the total result. Take for illustration the mooted question of the origin of the Great Lake basins. We have this, that, and the other hypothesis urged by different students as the cause of these great excavations; and all of these are urged with force and with fact, urged justly to a certain degree. It is practically demonstrable that these basins were river-valleys antecedent to the glacial incursion, and that they owe their origin in part to the pre-existence of those valleys and to the blocking-up of their outlets. And so this view of their origin is urged with a certain truthfulness. So, again, it is demonstrable that they were occupied by great lobes of ice, which excavated them to a marked degree, and therefore the theory of glacial excavation finds support in fact. I think it is furthermore demonstrable that the earth's crust beneath these basins was flexed downward, and that they owe a part of their origin to crust deformation. But to my judgment neither the one nor the other, nor the third, constitutes an adequate explanation of the phenomena. All these must be taken together, and possibly they must be supplemented by other agencies. The problem, therefore, is the determination not only of the participation, but of the measure and the extent, of each of these agencies in the production of the complex result. This is not likely to be accomplished by one whose working hypothesis is pre-glacial erosion, or glacial erosion, or crust deformation, but by one whose staff of working hypotheses embraces all of these and any other agency which can be rationally conceived to have taken part in the phenomena.

A special merit of the method is, that by its very nature it promotes thoroughness. The value of a working hypothesis lies largely in its suggestiveness of lines of inquiry that might otherwise be overlooked. Facts that are trivial in themselves are brought into significance by their bearings upon the hypothesis, and by their causal indications. As an illustration, it is only necessary to cite the phenomenal influence which the Darwinian hypothesis has exerted upon the investigations of the past two decades. But a single working hypothesis may lead investigation along a given line to the neglect of others equally important; and thus, while inquiry is promoted in certain quarters, the investigation lacks in completeness. But if all rational hypotheses relating to a subject are worked co-equally, thoroughness is the presumptive result, in the very nature of the case.

In the use of the multiple method, the re-action of one hypothesis upon another tends to amplify the recognized scope of each, and their mutual conflicts whet the discriminative edge of each. The analytic process, the development and demonstration of criteria, and the sharpening of discrimination, receive powerful impulse from the co-ordinate working of several hypotheses.

Fertility in processes is also the natural outcome of the method. Each hypothesis suggests its own criteria, its own means of proof, its own methods of developing the truth; and if a group of hypotheses encompass the subject on all sides, the total outcome of means and of methods is full and rich.

The use of the method leads to certain peculiar habits of mind which deserve passing notice, since as a factor of education its disciplinary value is one of importance. When faithfully pursued for a period of years, it develops a habit of thought analogous to the method itself, which may be designated a habit of parallel or complex thought. Instead of a simple succession of thoughts in linear order, the procedure is complex, and the mind appears to become possessed of the power of simultaneous vision from different standpoints. Phenomena appear to become capable of being viewed analytically and synthetically at once. It is not altogether unlike the study of a landscape, from which there comes into the mind myriads of lines of intelligence, which are received and co-ordinated simultaneously, producing a complex impression which is recorded and studied directly in its complexity. My description of this process

T. C. Chamberlin published two papers under the title of "The method of multiple working hypotheses." One of these papers, first published in the *Journal of Geology* in 1897, was quoted by John R. Platt in his recent article "Strong inference" (*Science,* 16 Oct. 1964). Platt wrote: "This charming paper deserves to be reprinted." Several readers, having had difficulty obtaining copies of Chamberlin's paper, expressed agreement with Platt. One wrote that the article had been reprinted in the *Journal of Geology* in 1931 and in the *Scientific Monthly* in November 1944. Another sent us a photocopy. Several months later still another wrote that the Institute for Humane Studies (Stanford, Calif.) had reprinted the article in pamphlet form this year. On consulting the 1897 version, we found a footnote in which Chamberlin had written: "A paper on this subject was read before the Society of Western Naturalists in 1892, and was published in a scientific periodical." Library research revealed that "a scientific periodical" was *Science* itself, for 7 February 1890, and that Chamberlin had actually read the paper before the Society of Western Naturalists on 25 October 1889. The chief difference between the 1890 text and the 1897 text is that, as Chamberlin wrote in 1897: "The article has been freely altered and abbreviated so as to limit it to aspects related to geological study." The 1890 text, which seems to be the first and most general version of "The method of multiple working hypotheses," is reprinted here. Typographical errors have been corrected, and subheadings have been added.

is confessedly inadequate, and the affirmation of it as a fact would doubtless challenge dispute at the hands of psychologists of the old school; but I address myself to naturalists who I think can respond to its verity from their own experience.

Drawbacks of the Method

The method has, however, its disadvantages. No good thing is without its drawbacks; and this very habit of mind, while an invaluable acquisition for purposes of investigation, introduces difficulties in expression. It is obvious, upon consideration, that this method of thought is impossible of verbal expression. We cannot put into words more than a single line of thought at the same time; and even in that the order of expression must be conformed to the idiosyncrasies of the language, and the rate must be relatively slow. When the habit of complex thought is not highly developed, there is usually a leading line to which others are subordinate, and the difficulty of expression does not rise to serious proportions; but when the method of simultaneous vision along different lines is developed so that the thoughts running in different channels are nearly equivalent, there is an obvious embarrassment in selection and a disinclination to make the attempt. Furthermore, the impossibility of expressing the mental operation in words leads to their disuse in the silent process of thought, and hence words and thoughts lose that close association which they are accustomed to maintain with those whose silent as well as spoken thoughts run in linear verbal courses. There is therefore a certain predisposition on the part of the practitioner of this method to taciturnity.

We encounter an analogous difficulty in the use of the method with young students. It is far easier, and I think in general more interesting, for them to argue a theory or accept a simple interpretation than to recognize and evaluate the several factors which the true elucidation may require. To illustrate: it is more to their taste to be taught that the Great Lake basins were scooped out by glaciers than to be urged to conceive of three or more great agencies working successively or simultaneously, and to estimate how much was accomplished by each of these agencies. The complex and the quantitative do not fascinate the young student as they do the veteran investigator.

Multiple Hypotheses and Practical Affairs

It has not been our custom to think of the method of working hypotheses as applicable to instruction or to the practical affairs of life. We have usually regarded it as but a method of science. But I believe its application to practical affairs has a value coordinate with the importance of the affairs themselves. I refer especially to those inquiries and inspections that precede the coming-out of an enterprise rather than to its actual execution. The methods that are superior in scientific investigation should likewise be superior in those investigations that are the necessary antecedents to an intelligent conduct of affairs. But I can dwell only briefly on this phase of the subject.

In education, as in investigation, it has been much the practice to work a theory. The search for instructional methods has often proceeded on the presumption that there is a definite patent process through which all students might be put and come out with results of maximum excellence; and hence pedagogical inquiry in the past has very largely concerned itself with the inquiry, "What is the best method?" rather than with the inquiry, "What are the special values of different methods, and what are their several advantageous applicabilities in the varied work of instruction?" The past doctrine has been largely the doctrine of pedagogical uniformitarianism. But the faculties and functions of the mind are almost, if not quite, as varied as the properties and functions of matter: and it is perhaps not less absurd to assume that any specific method of instructional procedure is more effective than all others, under any and all circumstances, than to assume that one principle of interpretation is equally applicable to all the phenomena of nature. As there is an endless variety of mental processes and combinations and an indefinite number of orders of procedure, the advantage of different methods under different conditions is almost axiomatic. This being granted, there is presented to the teacher the problem of selection and of adaptation to meet the needs of any specific issue that may present itself. It is important, therefore, that the teacher shall have in mind a full array of possible conditions and states of mind which may be presented, in order that, when any one of these shall become an actual case, he may recognize it, and be ready for the emergency.

Just as the investigator armed with many working hypotheses is more likely to see the true nature and significance of phenomena when they present themselves, so the instructor equipped with a full panoply of hypotheses ready for application more readily recognizes the actuality of the situation, more accurately measures its significance, and more appropriately applies the methods which the case calls for.

The application of the method of multiple hypotheses to the varied affairs of life is almost as protean as the phases of that life itself, but certain general aspects may be taken as typical of the whole. What I have just said respecting the application of the method to instruction may apply, with a simple change of terms, to almost any other endeavor which we are called upon to undertake. We enter upon an enterprise in most cases without full knowledge of all the factors that will enter into it, or all of the possible phases which it may develop. It is therefore of the utmost importance to be prepared to rightly comprehend the nature, bearings, and influence of such unforeseen elements when they shall definitely present themselves as actualities. If our vision is narrowed by a preconceived theory as to what will happen, we are almost certain to misinterpret the facts and to misjudge the issue. If, on the other hand, we have in mind hypothetical forecasts of the various contingencies that may arise, we shall be the more likely to recognize the true facts when they do present themselves. Instead of being biased by the anticipation of a given phase, the mind is rendered open and alert by the anticipation of any one of many phases, and is free not only, but is predisposed, to recognize correctly the one which does appear. The method has a further good effect. The mind, having anticipated the possible phases which may arise, has prepared itself for action under any one that may come up, and it is therefore ready-armed, and is predisposed to act in the line appropriate to the event. It has not set itself rigidly in a fixed purpose, which it is predisposed to follow without regard to contingencies. It has not nailed down the helm and predetermined to run a specific course, whether rocks lie in the path or not; but, with the helm in hand, it is ready to veer the ship according as danger or advantage discovers itself.

It is true, there are often advantages in pursuing a fixed predetermined course without regard to obstacles or adverse conditions. Simple dogged resolution is sometimes the salvation of an enterprise; but, while glorious successes have been thus snatched from the very brink of disaster, overwhelming calamity has in other cases followed upon this course, when a reasonable regard for the unanticipated elements would have led to success. So there is to be set over against the great achievements that follow on dogged adherence great disasters which are equally its result.

Danger of Vacillation

The tendency of the mind, accustomed to work through multiple hypotheses, is to sway to one line of policy or another, according as the balance of evidence shall incline. This is the soul and essence of the method. It is in general the true method. Nevertheless there is a danger that this yielding to evidence may degenerate into unwarranted vacillation. It is not always possible for the mind to balance evidence with exact equipoise, and to determine, in the midst of the execution of an enterprise, what is the measure of probability on the one side or the other: and as difficulties present themselves, there is a danger of being biased by them and of swerving from the course that was really the true one. Certain limitations are therefore to be placed upon the application of the method, for it must be remembered that a poorer line of policy consistently adhered to may bring better results than a vacillation between better policies.

There is another and closely allied danger in the application of the method. In its highest development it presumes a mind supremely sensitive to every grain of evidence. Like a pair of delicately poised scales, every added particle on the one side or the other produces its effect in oscillation. But such a pair of scales may be altogether too sensitive to be of practical value in the rough affairs of life. The balances of the exact chemist are too delicate for the weighing-out of coarse commodities. Despatch may be more important than accuracy. So it is possible for the mind to be too much concerned with the nice balancings of evidence, and to oscillate too much and too long in the endeavor to reach exact results. It may be better, in the gross affairs of life, to be less precise and more prompt. Quick decisions, though they may contain a grain of error, are oftentimes better than precise decisions at the expense of time.

The method has a special beneficent application to our social and civic relations. Into these relations there enter, as great factors, our judgment of others, our discernment of the nature of their acts, and our interpretation of their motives and purposes. The method of multiple hypotheses, in its application here, stands in decided contrast to the method of the ruling theory or of the simple working hypothesis. The primitive habit is to interpret the acts of others on the basis of a theory. Childhood's unconscious theory is that the good are good, and the bad are bad. From the good the child expects nothing but good; from the bad, nothing but bad. To expect a good act from the bad, or a bad act from the good, is radically at variance with childhood's mental methods. Unfortunately in our social and civic affairs too many of our fellow-citizens have never outgrown the ruling theory of their childhood.

Many have advanced a step farther, and employ a method analagous to that of the working hypothesis. A certain presumption is made to attach to the acts of their fellow-beings, and that which they see is seen in the light of that presumption, and that which they construe is construed in the light of that presumption. They do not go to the lengths of childhood's method by assuming positively that the good are wholly good, and the bad wholly bad; but there is a strong presumption in their minds that he concerning whom they have an ill opinion will act from corresponding motives. It requires positive evidence to overthrow the influence of the working hypothesis.

The method of multiple hypotheses assumes broadly that the acts of a fellow-being may be diverse in their nature, their moves, their purposes, and hence in their whole moral character; that they may be good though the dominant character be bad; that they may be bad though the dominant character be good; that they may be partly good and partly bad, as is the fact in the greater number of the complex activities of a human being. Under the method of multiple hypotheses, it is the first effort of the mind to see truly what the act is, unbeclouded by the presumption that this or that has been done because it accords with our ruling theory or our working hypothesis. Assuming that acts of similar general aspect may readily take any one of several different phases, the mind is freer to see accurately what has actually been done. So, again, in our interpretations of motives and purposes, the method assumes that these may have been any one of many, and the first duty is to ascertain which of possible motives and purposes actually prompted this individual action. Going with this effort there is a predisposition to balance all evidence fairly, and to accept that interpretation to which the weight of evidence inclines, not that which simply fits our working hypothesis or our dominant theory. The outcome, therefore, is better and truer observation and juster and more righteous interpretation.

Imperfections of Knowledge

There is a third result of great importance. The imperfections of our knowledge are more likely to be detected, for there will be less confidence in its completeness in proportion as there is a broad comprehension of the possibilities of varied action, under similar circumstances and with similar appearances. So, also, the imperfections of evidence as to the motives and purposes inspiring the action will become more discernible in proportion to the fulness of our conception of what the evidence should be to distinguish between action from the one or the other of possible motives. The necessary result will be a less disposition to reach conclusions upon imperfect grounds. So, also, there will be a less inclination to misapply evidence; for, several constructions being definitely in mind, the indices of the one motive are less liable to be mistaken for the indices of another.

The total outcome is greater care in ascertaining the facts, and greater discrimination and caution in drawing conclusions. I am confident, therefore, that the general application of this method to the affairs of social and civic life would go far to remove those misunderstandings, misjudgments, and misrepresentations which constitute so pervasive an evil in our social and our political atmospheres, the source of immeasurable suffering to the best and most sensitive souls. The misobservations, the misstatements, the misinterpretations, of life may cause less gross suffering than some other evils; but they, being more universal and more subtle, pain. The remedy lies, indeed, partly in charity, but more largely in correct intellectual habits, in a predominant, ever-present disposition to see things as they are, and to judge them in the full light of an unbiased weighing of evidence applied to all possible constructions, accompanied by a withholding of judgment when the evidence is insufficient to justify conclusions.

I believe that one of the greatest moral reforms that lies immediately before us consists in the general introduction into social and civic life of that habit of mental procedure which is known in investigation as the method of multiple working hypotheses.

Education as a Way of Life

Traditional arrangements for education must be supplemented by a system designed for lifelong learning.

John W. Gardner

Nothing is more obsolete than the notion that education is something that takes place in a solid block of years between, roughly, ages 6 and 22. From now on, the individual is going to have to seek formal instruction at many points throughout his career.

Under such a system, much of the present anxiety over young people who quit school prematurely will disappear. The anxiety stems from the fact that today leaving school signifies the end of education. Under the new system there will be no end to education.

Unfortunately, our institutional arrangements for lifelong education are ridiculously inadequate. Most educational institutions are still designed for young people who have nothing else to do. They are ill suited to men and women who must fit their learning into a busy life.

For years a small number of devoted educators have sought to meet the needs of this latter group, but they have not received much cooperation from the rest of the academic world. That state of affairs appears to be changing.

In the making now are some highly flexible arrangements to make education available to anyone able and willing to learn, under circumstances suited to his needs. To indicate in concrete terms what such a system might look like, I am going to describe certain activities of an imaginary university—let us call it Midland State University. (It is not necessary that all these activities be sponsored by a university—a point which I discuss later.)

The author is president of Carnegie Corporation of New York, 589 Fifth Avenue, New York 10017.

Annu. Rev. Earth Planet. Sci. 2004. 32:13–45
doi: 10.1146/annurev.earth.32.101802.120257

First published online as a Review in Advance on November 10, 2003

EVOLUTION OF THE NORTH AMERICAN CORDILLERA

William R. Dickinson
Department of Geosciences, University of Arizona, Tucson, Arizona 85721; email: wrdickin@geo.arizona.edu

Key Words continental margin, crustal genesis, geologic history, orogen, tectonics

■ **Abstract** The Cordilleran orogen of western North America is a segment of the Circum-Pacific orogenic belt where subduction of oceanic lithosphere has been underway along a great circle of the globe since breakup of the supercontinent Pangea began in Triassic time. Early stages of Cordilleran evolution involved Neoproterozoic rifting of the supercontinent Rodinia to trigger miogeoclinal sedimentation along a passive continental margin until Late Devonian time, and overthrusting of oceanic allochthons across the miogeoclinal belt from Late Devonian to Early Triassic time. Subsequent evolution of the Cordilleran arc-trench system was punctuated by tectonic accretion of intraoceanic island arcs that further expanded the Cordilleran continental margin during mid-Mesozoic time, and later produced a Cretaceous batholith belt along the Cordilleran trend. Cenozoic interaction with intra-Pacific seafloor spreading systems fostered transform faulting along the Cordilleran continental margin and promoted incipient rupture of continental crust within the adjacent continental block.

INTRODUCTION

Geologic analysis of the Cordilleran orogen, forming the western mountain system of North America, raises the following questions: 1. When was the Cordilleran system born, and from what antecedents; 2. which rock masses are integral to the Cordilleran continental margin, and how were they formed; 3. which rock masses were incorporated into the Cordilleran realm by tectonic accretion, and what were their origins; and 4. what geologic processes are promoting distension and disruption of the Cordilleran system today?

Figure 1 is a chronostratigraphic diagram of Cordilleran rock assemblages showing their relationships to major phases of Cordilleran evolution. The Cordilleran edge of the Precambrian basement, which forms the Laurentian craton, was first delineated by rifting to form a passive continental margin, along which a thick Neoproterozoic to Devonian miogeoclinal prism of sedimentary strata was deposited. From Late Devonian to Early Triassic time, oceanic allochthons were successively thrust across the miogeoclinal strata as internally deformed tectonic

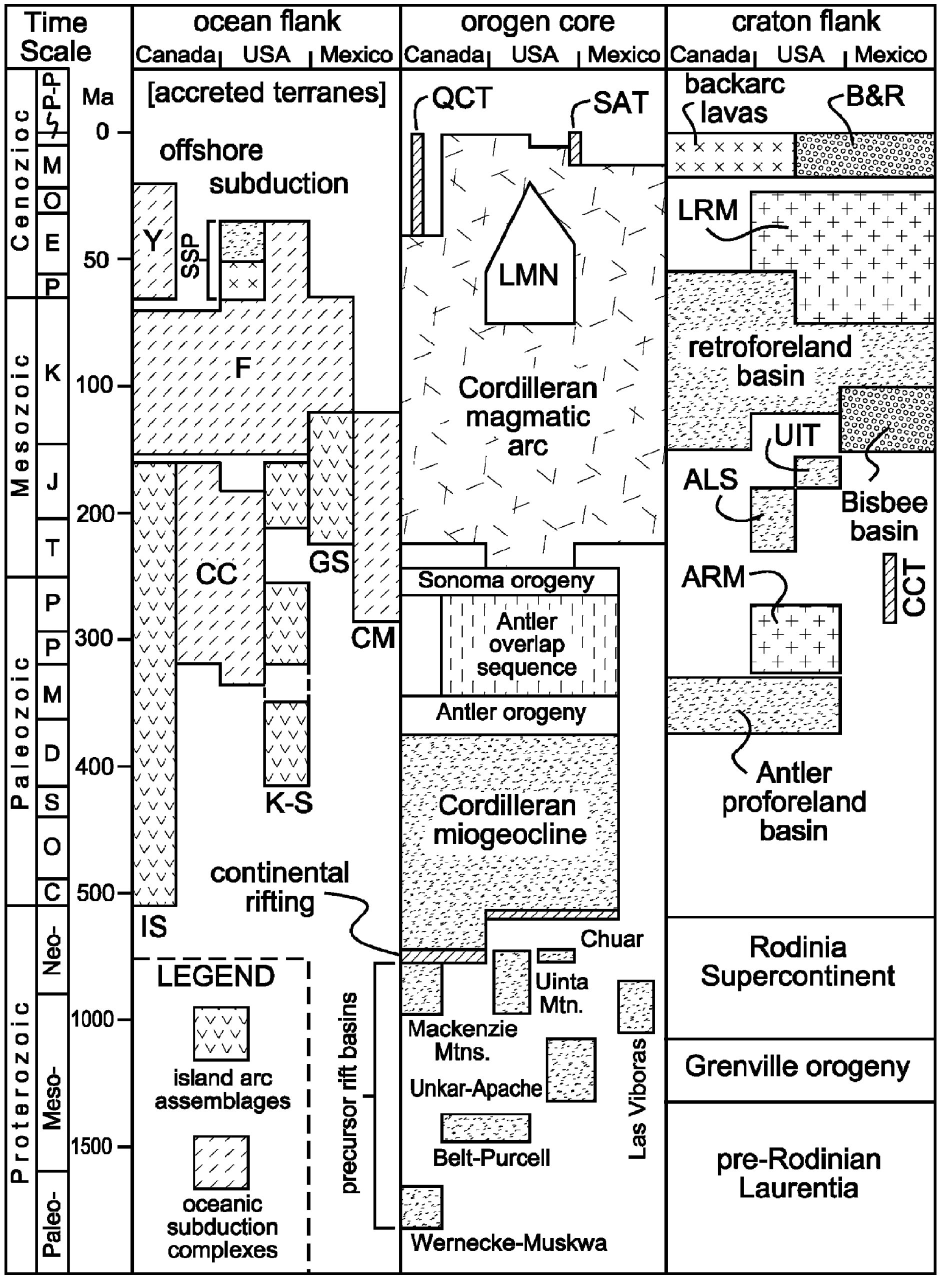

Figure 1 Schematic chronostratigraphic diagram of major Cordilleran rock assemblages (note changes in timescale at 100 Ma and 500 Ma). Canada includes the adjacent panhandle of southeastern Alaska, and Mexico includes the USA-Mexico border region south of the Colorado Plateau. Accreted island-arc assemblages: GS, Guerrero superterrane; IS, Insular superterrane; K-S, accreted arcs of Klamath Mountains and Sierra Nevada foothills. Subduction complexes: CC, Cache Creek; CM, central Mexico; F, Franciscan; Y, Yakutat. Transform faults (*diagonally ruled bars*): CCT, California-Coahuila; QCT, Queen Charlotte; SAT, San Andreas. Other features: ALS, Auld Lang Syne backarc basin; ARM, Ancestral Rocky Mountains province; B&R, Basin and Range taphrogen; LRM, Laramide Rocky Mountains province (LMN, Laramide magmatic null); SSP, accreted Siletzia and overlying forearc basin; UIT, Utah-Idaho trough.

assemblages accreted to the continent. An arc-trench system initiated along the modified continental margin in Triassic time was the tectonic regime that produced Mesozoic-Cenozoic subduction complexes and batholiths most characteristic of the Cordilleran orogen. During the subduction of oceanic lithosphere beneath the Cordilleran margin, Jurassic-Cretaceous accretion of intraoceanic island arcs contributed to the outward growth of the continental block. Beginning in mid-Cenozoic time, impingement of intra-Pacific seafloor spreading systems on the subduction zone at the continental margin gave birth to transform fault systems lying near the edge of the continental block and to associated inland deformation that distended continental crust previously overthickened by Cordilleran orogenesis.

On paleotectonic maps showing the distributions of Cordilleran rock assemblages adapted in part from Dickinson (2000, 2001, 2002) and Dickinson & Lawton (2001a,b; 2003), rock masses are plotted on present geography, with state and province boundaries for orientation, without palinspastic restoration to correct for distortion of rock masses by deformation. Offsets of rock masses across major Cenozoic strike-slip faults are shown, however, and curvatures of tectonic trends by oroclinal bending are indicated by annotations where appropriate.

To aid analysis of accretionary tectonics, the North American Cordillera has been subdivided into nearly 100 formally named tectonostratigraphic terranes (Coney et al. 1980) separated by faulted boundaries of varying tectonic significance and structural style (Silberling et al. 1992). For graphic display at feasible scale, various terranes are combined into generic groupings.

CORDILLERAN OROGEN

The Cordilleran mountain chain of western North America is an integral segment of the Circum-Pacific orogenic belt, which extends along a great circle path for 25,000+ km from the Antarctic Peninsula to beyond Taiwan (Figure 2). The length of the Cordilleran orogen from the Gulf of Alaska to the mouth of the Gulf of California is ~5000 km, or ~20% of the total length of the orogenic belt.

Characteristic geologic features of the Circum-Pacific orogenic belt derive from persistent subduction of oceanic lithosphere at trenches along the flanks of continental margins and offshore island arcs linked spatially to form a nearly continuous chain along the Pacific rim (Figure 2). The rock assemblages of subduction zones where oceanic plates are progressively consumed and of the parallel magmatic arcs built by related igneous activity are the prime signatures of Circum-Pacific orogenesis in the rock record. The oldest rock assemblages of the Cordilleran continental margin that reflect this style of tectonism mark initiation of the Cordilleran orogenic system in mid-Early Triassic time. Older rock assemblages exposed within the mountain chain record preceding tectonic regimes of different character.

Global Orogenic Patterns

In the Philippine-Indonesian region, the Circum-Pacific orogenic belt intersects the Alpine-Himalayan orogenic belt, which is aligned along a different great circle

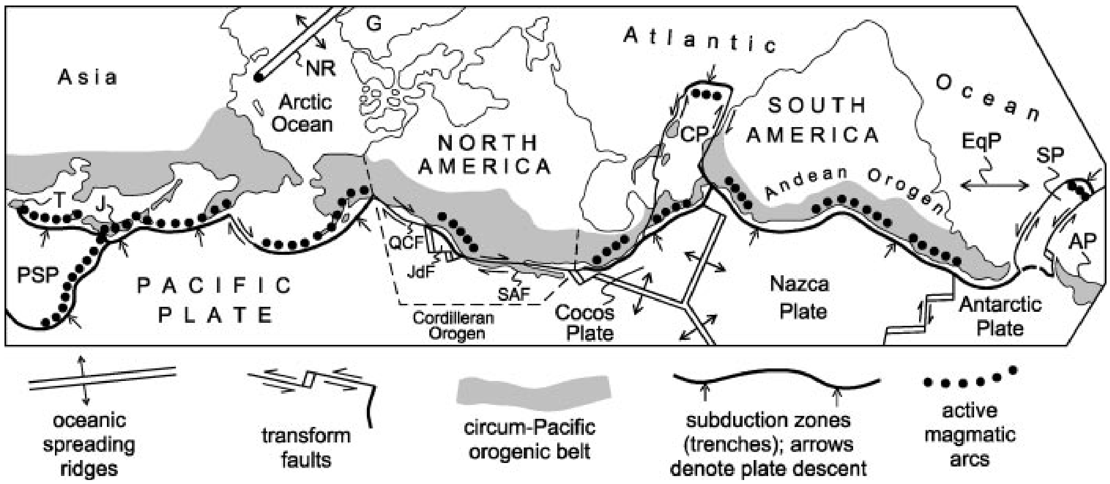

Figure 2 Position of the Cordilleran orogen of western North America along the Circum-Pacific orogenic belt (after Dickinson et al. 1986). Mercator projection with pole at 25° N Lat, 15° E Long (EqP is equatorial plane of projection). AP, Antarctic Peninsula; C, Cascades volcanic chain; CP, Caribbean plate; G, Greenland; J, Japan; JdF, Juan de Fuca plate; NR, Nansen Ridge (northern extremity of Atlantic spreading system); PSP, Philippine Sea plate; QCf, Queen Charlotte fault; SAf, San Andreas fault; SP, Scotia plate; T, Taiwan.

of the globe (Figure 3). Both orogenic belts relate to the breakup of the Permian-Triassic supercontinent of Pangea beginning early in Mesozoic time, but in different ways, as the Atlantic and Indian oceans opened to disrupt Pangea by seafloor spreading. Alpine-Himalayan evolution has involved the successive juxtaposition of disparate continental blocks (e.g., Africa, India, Australia against Eurasia) at suture belts marking the former positions of trenches where intervening ocean basins were closed by plate consumption (Figure 3), but no crustal blocks of comparable size have lodged against the Pacific margin of the Americas.

The ancestral Circum-Pacific orogenic system along the margin of Pangea was born along a great circle path (Le Pichon 1983), rimming an ocean (Panthalassa) that was effectively a paleo-Pacific realm with a Tethyan gulf that projected into the angle between Laurasian and Gondwanan segments of Pangea (Figure 4). The great circle configuration was maintained as expansion of the Atlantic and Indian Oceans led to a modern Pacific only 60% the size of the paleo-Pacific (Le Pichon et al. 1985) by insertion of Australia and its surrounding seas into the Pacific arena to step the Pacific rim eastward for ~5500 km along the Indonesian archipelago (Figure 3). During Circum-Pacific evolution, intra-Pacific seafloor spreading renewed oceanic lithosphere so rapidly that no vestiges of pre-Jurassic paleo-Pacific seafloor remain (Dickinson 1977).

Supercontinent History

The composite supercontinent of Pangea (Figure 4) formed during late Paleozoic time when Gondwana lodged against Laurasia along the Appalachian-Hercynian

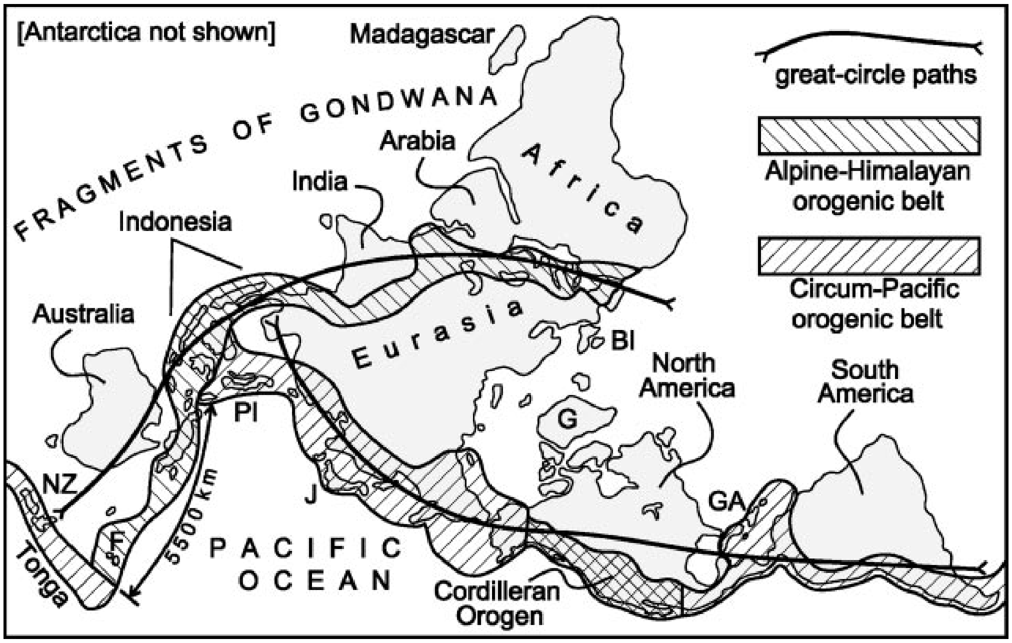

Figure 3 Distribution of continents in relation to the Alpine-Himalayan and Circum-Pacific orogenic belts (Cordilleran orogen: *cross-hatched*) in "circular" projection (after Challand & Rageau 1985). BI, British Isles; F, Fiji; G, Greenland; GA, Greater Antilles; J, Japan; NZ, New Zealand; PI, Philippine Islands.

orogen, a Paleozoic precursor of the modern Alpine-Himalayan system in that both achieved assembly of supercontinents (Pangea and Eurasia) through juxtaposition of previously separate continental blocks. Gondwana was a paleocontinent assembled in Neoproterozoic time (800–550 Ma) by juxtaposition of continental fragments across multiple internal suture belts (Meert & Van der Voo 1997). Laurasia included the ancient continental nuclei of Laurentia (North America) and Baltica (Europe), which had been conjoined in early Paleozoic time and linked in mid-Paleozoic time with Siberia. The Paleozoic precursor of the modern Circum-Pacific system was the Gondwanide orogenic belt, which lay along the Panthalassan (paleo-Pacific) margin of Gondwana, from South America past Antarctica to Australia (Figure 4), where consumption of oceanic lithosphere proceeded without interruption during the progressive assembly of Pangea (Ramos & Aleman 2000, Foster & Gray 2000).

The assembly of Pangea and its subsequent breakup during the assembly of Eurasia over the course of Phanerozoic time finds a Precambrian parallel in the geologic history of an earlier supercontinent, Rodinia, from which continental fragments were at first widely dispersed and then rearranged to form Gondwana and eventually Pangea. Rodinia was aggregated during Grenville orogenesis in Mesoproterozoic time (1325–1050 Ma), and the Cordilleran continental margin first took shape from Neoproterozoic breakup of Rodinia. As yet, however, there is no final consensus on the arrangement of continental cratons within the Rodinian

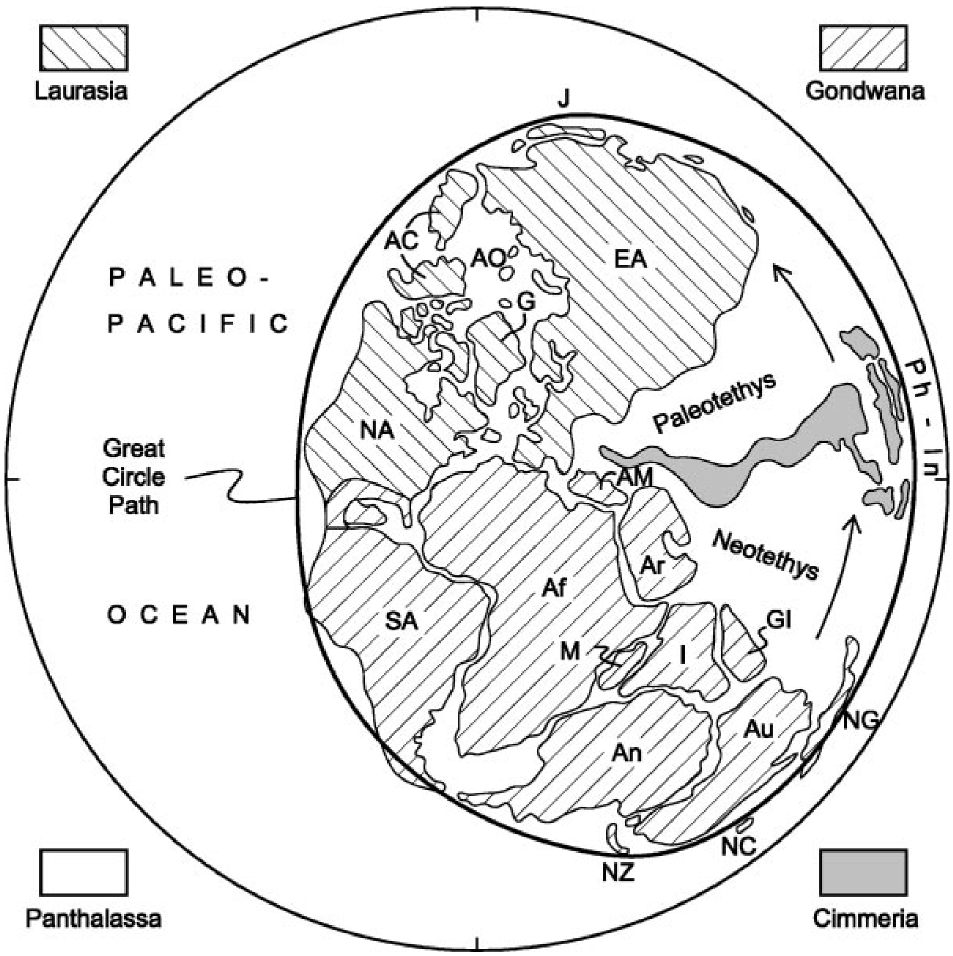

Figure 4 Permian-Triassic configuration of Pangea (Gondwana after Lawver & Scotese 1987) surrounded by Panthalassa (global sea including paleo-Pacific ocean and Tethys gulf) in Lambert equal-area projection (whole Earth). The Arctic Ocean closed by restoring transform slip of Alaska-Chukotka (Patrick & McClelland 1995). Arrows schematically denote the motion of Cimmerian landmasses in transit across the Tethys gulf, originating by rifting off the margin of Gondwana, toward Mesozoic accretion along the southern flank of Eurasia by closure of Paleothys as Neotethys opened. AC, Alaska-Chukotka; Af, Africa; AM, Asia Minor; An, Antarctica; AO, Arctic Ocean (closed); Ar, Arabia; Au, Australia; EA, Eurasia; G, Greenland; GI, Greater India; I, India; J; Japan; M, Madagascar; NA, North America; NC, New Caledonia; NG, New Guinea; NZ, New Zealand; Ph-In, Philippine-Indonesian archipelago; SA, South America.

supercontinent. Continental blocks suggested as conjugate to the Cordilleran rifted margin of Laurentia include Siberia (Sears & Price 2000), Antarctica-Australia (Dalziell 1992), Australia together with an unknown block farther north (Karlstrom et al. 1999), and China (Li et al. 2002). Of the various options, Siberia currently seems the most viable (Sears & Price 2003).

PRECAMBRIAN–PALEOZOIC MIOGEOCLINE

Along the Cordilleran margin of Laurentia, an elongate belt of thick sediment was deposited in Neoproterozoic and lower Paleozoic time as a miogeoclinal prism draped over a passive continental margin formed by rifting during the breakup of Rodinia (Figure 1). The narrow miogeoclinal belt truncates disrupted older Precambrian age provinces of interior Laurentia (Figure 5). The miogeoclinal prism thickened westward from a zero edge along a hinge line at the edge of the Laurentian craton. Miogeoclinal sedimentation continued, unbroken by tectonic disruption, until Late Devonian time, but the timing of its inception was apparently diachronous.

Cordilleran Rifting

North of the trans-Idaho discontinuity (Yates 1968), where the elongate trend of the miogeocline is offset by >250 km (Figure 5), basaltic rocks associated with glaciomarine diamictite in basal horizons of the miogeoclinal succession have been dated isotopically at 770–735 Ma (Armstrong et al. 1982, Devlin et al. 1988, Rainbird et al. 1996, Colpron et al. 2002). This time frame provides an age bracket for rifting that initiated deposition of the Windermere Supergroup along a newly formed passive continental margin open to the west in Canada (Ross 1991, MacNaughton et al. 2000). South of the trans-Idaho discontinuity, coeval rifting apparently formed only intracontinental basins in which redbed units such as the Chuar Group (775–735 Ma) of the Grand Canyon were deposited (Timmons et al. 2001), with continental separation delayed in the Death Valley region to the west until after 600 Ma (Prave 1999).

The subparallelism of the trans-Idaho discontinuity and a paleotransform delimiting the southwest margin of Laurentia (Figure 5) suggests that both originated as transform offsets of the nascent Cordilleran margin. Miogeoclinal strata present locally along the trans-Idaho discontinuity form a narrow band exposed only within roof pendants of the Idaho batholith (Lund et al. 2003) and contain intercalated bimodal volcanic rocks (685 Ma), which perhaps reflect prolonged deformation along a marginal offset at the edge of the continental block during the evolution of the rifted Cordilleran margin.

Published subsidence analyses for the Cordilleran miogeocline in both Canada and the USA imply that postrift thermotectonic subsidence of the passive continental margin did not begin until 560–555 Ma in Early Cambrian time (Bond et al. 1983, Armin & Mayer 1983, Bond & Kominz 1984, Levy & Christie-Blick 1991). Replotting the subsidence curves for revised estimates of the beginning of Cambrian time (545 Ma versus 570 Ma) puts onset of thermotectonic subsidence at 525–515 Ma, still within Early Cambrian time on the revised timescale. Projecting subsidence curves backward in time to allow for 1.1–1.2 km of synrift tectonic subsidence (~2 km of sediment accumulation) in the Great Basin area of the USA (Levy & Christie-Blick 1991) suggests that rifting that led directly to

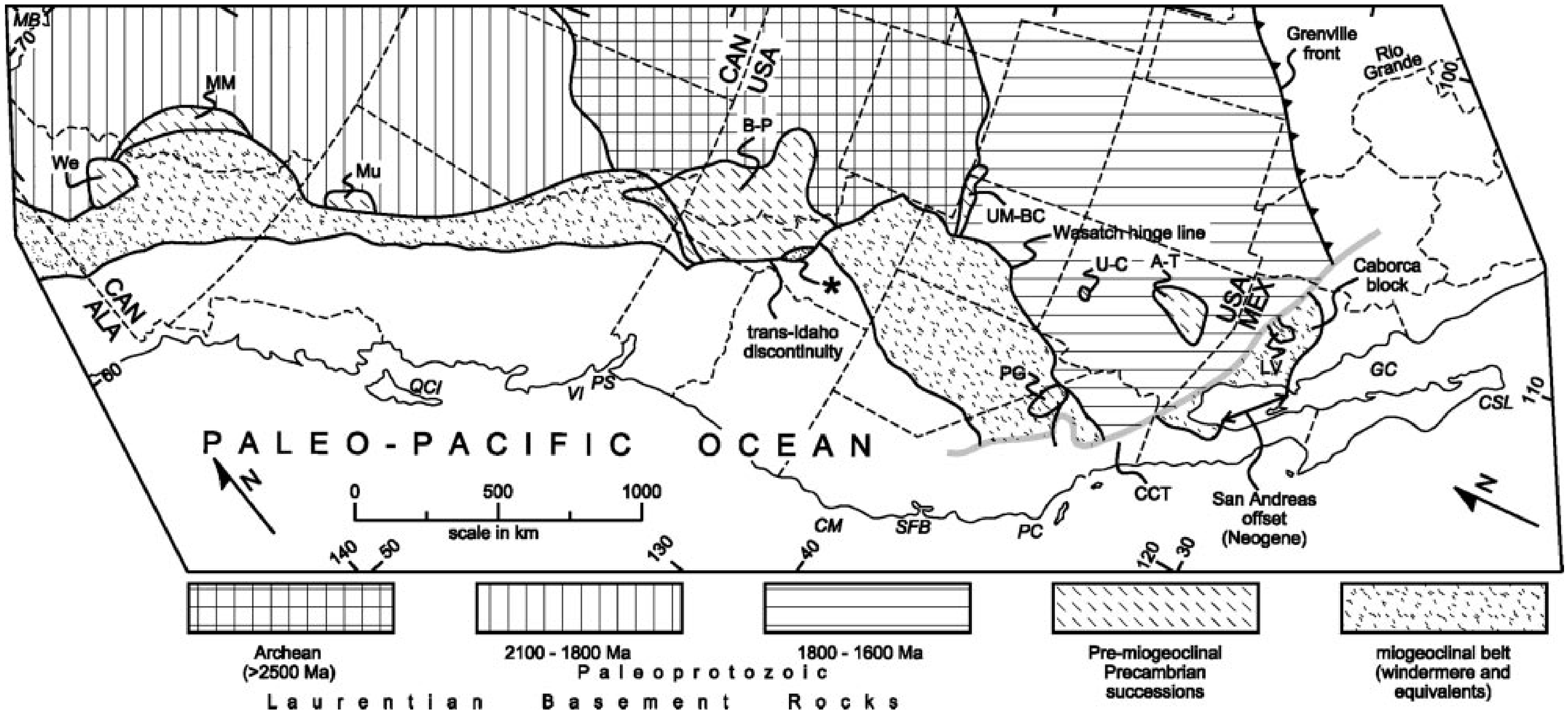

Figure 5 Neoproterozoic-Early Paleozoic Cordilleran miogeocline and premiogeoclinal sedimentary basins along the trend of the North American Cordillera (rock assemblages now present west of the miogeoclinal belt were added to the continental block after mid-Late Devonian time). Asterisk (*) denotes miogeoclinal strata along trans-Idaho discontinuity (Lund et al. 2003). Grenville front is margin of Mesoproterozoic Grenville orogen along which Rodinia was assembled. CCT is Permian-Triassic California-Coahuila transform (Dickinson 2000), which offset the Cordilleran miogeoclinal assemblage of the Caborca block by overprinting an older paleotransform system that delimited the early Paleozoic southwest margin of Laurentia (Dickinson & Lawton 2001a). See text for ages of premiogeoclinal successions. (A-T, Apache-Troy; B-P, Belt-Purcell; LV, Las Víboras; MM, Mackenzie Mountains; Mu, Muskwa; PG, Pahrump Group; U-C, Unkar-Chuar; UM-BC, Uinta Mountain—Big Cottonwood; We, Wernecke). Coastal locales (*italics*): CM, Cape Mendocino; CSL, Cabo San Lucas; GC, Gulf of California; MB, Mackenzie Bay of Arctic Ocean; PC, Point Conception; PS, Puget Sound; QCI, Queen Charlotte Islands; SFB, San Francisco Bay; VI, Vancouver Island.

continental separation south of the trans-Idaho discontinuity occurred during the interval 600–575 Ma (Armin & Mayer 1983). Isotopic dating of synrift volcanic rocks in southern British Columbia at 570 ± 5 Ma (Colpron et al. 2002) documents that active rifting persisted into latest Neoproterozoic time, north as well as south of the trans-Idaho discontinuity.

The indicated time span of 45–65 million years between initial rifting and onset of passive thermotectonic subsidence is comparable to the time span of 55 million years between initial development of Triassic rift basins and the first emplacement of Jurassic oceanic crust along the modern Atlantic continental margin (Manspeizer & Cousminer 1988). Cordilleran unconformities near the Precambrian-Cambrian time boundary (Devlin & Bond 1988, Lickorish & Simony 1995) may stem from reactivation of rift faults or from the influence of eustasy on a rift hinge undergoing flexure from sediment loading of oceanic crust offshore (Fedo & Cooper 2001).

The evidence for two rift events (Colpron et al. 2002), spaced 160–170 million years apart in pre-Windermere and latest Neoproterozoic time, suggests the possibility that two different continental blocks, one west of Canada and one west of USA-Mexico, were once conjugate with Laurentia, but no current Rodinian models are readily compatible with that interpretation. In any case, the onset of thermotectonic subsidence at the same time in both Canada and southward implies that the Windermere passive margin was reactivated at the time of the second rifting event, as suggested by stratal relationships near the USA-Canada border (Devlin 1989).

Precursor Rifts

A number of premiogeoclinal Precambrian sedimentary successions occur along the trend of the Cordillera but lack the longitudinal continuity of the overlying miogeocline (Figure 5). Each was deposited within an intracratonic basin formed by incipient rift extension within Rodinia or before its assembly (Figure 1). From the trans-Idaho discontinuity northward, isotopic dating of basin substratum, intercalated volcanics, and local intrusions establishes age brackets as follows for deep local rift troughs: Wernecke Supergroup, 1820–1710 Ma (Ross et al. 2001); Muskwa Assemblage, 1760–1660 Ma (Ross et al. 2001); Belt-Purcell Supergroup, 1470–1370 Ma (Evans et al. 2000, Luepke & Lyons 2001); Mackenzie Mountains Supergroup, 975–775 Ma (Rainbird et al. 1996); Uinta Mountain Group (and Big Cottonwood Formation), 975?–725? Ma. Farther south, thinner premiogeoclinal successions, deposited either in rift basins or on the craton, include the following: Unkar Group, Apache Group (including Troy Quartzite), and lower Pahrump Group, 1220–1070 Ma (Timmons et al. 2001), with the lowermost Apache Group as old as 1335 Ma (Stewart et al. 2001); Las Víboras Group, 1050?–850? Ma (Stewart et al. 2002); and the Chuar Group, 775–735 Ma (Timmons et al. 2001).

The precursor rift troughs may have acted as subregional guides helping to control the trend of eventual continental separation that initiated miogeoclinal sedimentation. In the Death Valley region, for example, diamictites of the Kingston Peak Formation in the upper Pahrump Group probably include correlatives of both syn-Windermere (∼750 Ma) rift fill and younger (∼600 Ma) synrift deposits at the base of the miogeoclinal succession (Prave 1999). Recent interpretations from deep seismic reflection profiles propose that pre-Windermere Canadian assemblages (Wernecke, Muskwa, Mackenzie Mountains) in the region north of the Belt-Purcell basin are all parts of a composite sediment prism built westward along an evolving passive continental margin that flanked the youngest basement components of the Laurentian craton and persisted over a time span that exceeded a billion years (Snyder et al. 2002). If so, no continental separation by Neoproterozoic rifting was required to form the Windermere continental margin, but the disparate age ranges and outcrop discontinuity of the pre-Windermere successions are difficult to reconcile with the postulate of a pre-Windermere passive continental margin continuous for the length of the Canadian Cordillera.

LATE PALEOZOIC–EARLY TRIASSIC ACCRETION

Between Late Devonian and Early Triassic time, internally deformed allochthons (Figure 6) of oceanic strata were thrust eastward as accretionary prisms across the seaward flank of the miogeoclinal belt when the margin of the Laurentian continental block was drawn into the subduction zones of intraoceanic island arcs that faced the Cordilleran margin and subducted offshore oceanic crust of marginal seas downward to the west (Dickinson 2000). Lithic constituents of the allochthons include pillow basalts, peridotite, and serpentinite of oceanic crust and subjacent mantle, as well as more voluminous argillite, ribbon chert, and turbidites of overlying seafloor sediment profiles. The turbidites of the allochthons include continental slope and rise deposits originally transported off the Laurentian margin and then thrust back toward the craton over the miogeoclinal shelf edge. Exposures where later tectonism and erosion has exhumed the thrust contact show that the allochthons traveled 100+ km across the structurally underlying miogeoclinal assemblage.

Antler-Sonoma Allochthons

Stratigraphic and structural analysis of the overthrust allochthons has documented their emplacement during two discrete episodes of incipient continental subduction termed the Antler and Sonoma orogenies in the USA. The two events were spaced ∼110 million years apart during comparatively brief intervals of time (∼25 million years each) spanning the Devonian-Mississippian and Permian-Triassic time boundaries (Figure 1). The two separate allochthons have been delineated with greatest confidence in the Great Basin of Nevada (USA), where allochthonous but unmetamorphosed oceanic facies of multiple Paleozoic horizons were thrust over autochthonous miogeoclinal facies of the same ages along the Roberts Mountains

(Antler) and Golconda (Sonoma) thrusts (Figure 6). Farther north, the lack of clearcut evidence for the presence of either allochthon along the trend of the trans-Idaho discontinuity (Figures 5 and 6) may stem from engulfment by batholiths, widespread erosion, and burial beneath volcanic cover, but may also reflect anomalous tectonic behavior along that atypical segment of the Cordilleran margin.

Within Canada, post-Triassic internal deformation and tectonic transport of Paleozoic Antler-Sonoma allochthons during Mesozoic arc-continent collision and subsequent retroarc thrusting complicate interpretations of their original character and positions (Hansen 1990, Ghosh 1995). Allochthons of both Antler (Smith & Gehrels 1991; 1992a,b) and Sonoma (Roback et al. 1994, Roback & Walker 1995) age have been identified in the Kootenay structural arc (Figure 6) spanning the USA-Canada border. Farther north, the Sylvester allochthon emplaced above the Cassiar platform (Figure 6) is composed exclusively of post-Devonian rocks (Nelson 1993) and apparently represents only the younger allochthon of Sonoma age. Nearby, however, the widespread and internally complex Yukon-Tanana terrane (Hansen 1988) probably includes both allochthons as well as underthrust miogeoclinal facies (Hansen & Dusel-Bacon 1998). Blueschists of both Devonian (∼345 Ma) and Permian (270–260 Ma) ages are present in allochthonous Yukon-Tanana assemblages lying structurally above miogeoclinal strata along the west flank of the Cassiar platform and in the isolated Anvil allochthon (Figure 6) to the east (Erdmer et al. 1998). Juxtaposition of the Anvil allochthon against the Cassiar platform implies ∼485 km of post-thrust dextral displacement along the Tintina fault (Figure 6).

Antler-Sonoma Foreland

Tectonic loads of the overthrust Antler-Sonoma allochthons downflexed the Laurentian margin to form an elongate system of markedly asymmetric proforeland sedimentary basins extending across the miogeoclinal belt into the fringe of the interior craton (Lawton 1994, Savoy & Mountjoy 1995). The extent of the Antler foreland basin is defined by an apron of clastic sediment shed toward carbonate platforms of the interior craton, but the Sonoma foreland basin is defined only by the limit of Triassic marine strata (Figure 6). Widespread syndepositional normal faulting of Antler age along the foreland belt in Canada (Gordey et al. 1987) can be interpreted as a response to local extension induced by flexure of the foreland basin floor (Smith et al. 1993).

Proximal sandstone petrofacies along the western fringe of the Antler foreland belt are dominantly quartzolithic, a composition reflective of sediment recycling from the uplifted accretionary prisms of allochthons exposed farther west as sediment sources (Smith et al. 1993). Near the Canada-Alaska border, the ages of detrital zircons in Cambrian and Devonian sandstones suggest derivation of foreland sediment near the northern end of the Cordilleran orogen (Figure 6) from the Paleozoic Innuitian-Ellesmerian orogen of the Canadian Arctic to the northeast (Gehrels et al. 1999).

During the time interval between Antler and Sonoma thrusting along the Cordilleran margin, part of the continental block extending as far west as the Antler foreland basin and thrust front in the USA was disrupted by intracontinental reverse faulting to form yoked basins and uplifts of the Ancestral Rocky Mountains province (Figure 6). The intracontinental deformation, centered on Pennsylvanian time (Figure 1), was related to sequential intercontinental suturing along the Ouachita orogenic belt (Figure 6), where the southern flank of the Laurentian craton was drawn progressively, from east to west, into a subduction zone along the leading edge of Gondwana during the assembly of Pangea (Dickinson & Lawton 2003).

Accreted Island Arcs

Segments of accreted Devonian and Permian island arcs, composed of volcanic and volcaniclastic strata and paired geotectonically with Antler and Sonoma accretionary prisms to the east, are present in the Klamath-Sierran region (Figure 6) of the Cordilleran orogen to the south of volcanic cover in the Pacific Northwest (USA). The Paleozoic Klamath-Sierran arc system evolved as a system of frontal arcs and remnant arcs during slab rollback related to closure of marginal seas between the offshore arc complex and the Cordilleran continental margin (Dickinson 2000).

Farther north in Canada, remnants of comparable Devonian to Permian arc assemblages (Rubin et al. 1990, Brown et al. 1991), underlying the Mesozoic arc assemblages of Quesnellia and Stikinia (Figure 6), are interpreted here as northern analogues of the accreted Klamath-Sierran island arcs. Both east and west of the Cassiar platform (Figure 6), overthrust allochthonous assemblages include both Devonian (365–340 Ma) and Permian (∼260 Ma) granitic plutons of arc affinity (Mortensen 1992). Permian island-arc volcanics are closely associated with deformed seafloor volcanics within the internally complex Sylvester allochthon emplaced structurally above the Cassiar platform (Nelson 1993) and in correlative assemblages farther south (Ferri 1997). These occurrences of island-arc remnants within allochthonous Paleozoic assemblages suggest that severe structural telescoping in Canada during superposed mid-Mesozoic arc-continent suturing and later Mesozoic-Cenozoic retroarc thrusting closely juxtaposed island-arc and subduction-zone tectonic elements of Antler-Sonoma age that remain largely separate farther south.

MESOZOIC-CENOZOIC ARC-TRENCH SYSTEM

A Permian-Triassic (284–232 Ma) magmatic arc, built along the edge of Gondwanan crust in eastern Mexico (Dickinson & Lawton 2001a), was sustained by subduction of oceanic crust beneath present-day central Mexico (Figure 6). The northern margin of the subducting Mezcalera plate along the southwestern edge of

Laurentia was defined by the sinistral California-Coahuila transform, which offset the Caborca block of miogeoclinal strata, together with underlying basement and a structurally superposed allochthon of overthrust Paleozoic strata (Figure 6), from southern California into northwestern Mexico (Dickinson 2000, Dickinson & Lawton 2001a). Farther northwest, the transform fault obliquely truncated, along a northwest-southeast trend, island-arc complexes trending northeast-southwest that were accreted to the continental block in the Klamath-Sierran region by Antler-Sonoma orogenesis. Initiation of subduction beneath the truncated continental margin in mid-Early Triassic time (Dickinson 2000) closely preceded the breakup of Pangea, and was the earliest record of Cordilleran orogenesis as an integral facet of the circum-Pacific orogenic belt.

Subsequent evolution of the active Cordilleran continental margin was marked by incremental accretion of subduction complexes at a trench along the continental slope, and by arc magmatism involving both plutonism and volcanism along the edge of the continental block. Multiple imbricate thrust panels of accretionary mélange belts incorporate disrupted stratal successions of seafloor turbidites, argillite, and chert, together with pillow lavas of underlying oceanic crust and structural slices of peridotite and serpentinite derived from oceanic mantle, and with limestone enclaves representing carbonate platforms built on oceanic seamounts. Combined plutonic and volcanic contributions to arc magmatism were emplaced into and erupted through the composite Cordilleran crustal profile along a shifting belt of igneous activity that lay 100–250 km inland from the evolving subduction zone along the continental margin (Armstrong 1988, Armstrong & Ward 1991). The principal record of arc magmatism is a discontinuous alignment of deeply eroded Cretaceous granitic batholiths extending the full length of the Cordilleran orogen. Isotopic studies indicate that the granitic magmas were composed in part of juvenile mantle components and in part of recycled crustal materials (DePaolo 1981, Samson et al. 1991).

Mid-Triassic to Mid-Jurassic Cordilleran Arc

Volcanic assemblages and associated plutons of Upper Triassic to Middle Jurassic age developed within a continuous magmatic arc established along the margin of North America as modified by Antler-Sonoma tectonism. The central segment of the Triassic-Jurassic arc transected miogeoclinal and Laurentian cratonic crust along the truncated continental margin of the southwest USA (Busby-Spera 1988, Schweickert & Lahren 1993), but the arc trend extended southward across the Ouachita suture into Gondwanan crust of eastern Mexico (Dickinson & Lawton 2001a) and northward along the continental margin, as expanded by tectonic accretion, to merge with the Quesnellia or Nicola arc (Mortimer 1987) of the Canadian Cordillera (Figure 7).

The local preservation of forearc basins along the western flank of the nascent Cordilleran arc in both the Canadian Cordillera (Travers 1978) and the USA Pacific Northwest (Dickinson 1979) show that the arc-trench system faced west, subducting seafloor downward beneath North America, even where relations of the arc assemblage to Laurentian basement or miogeoclinal strata are unexposed. Past speculation that the Quesnellia arc was a freestanding intraoceanic structure only accreted to North America by later collapse of an intervening marginal sea or open ocean has been discounted by recent isotopic studies (Unterschutz et al. 2002, Erdmer et al. 2002). The backarc region was flooded in Canada by marine waters, but was occupied in the USA by desert ergs (Figure 7), with the accommodation space for both sedimentary assemblages probably provided by subsidence of the flank of the continental block under the geodynamic influence of a subducted slab in the mantle beneath (Lawton 1994).

West of the Triassic-Jurassic Cordilleran arc assemblage lies a paired subduction complex of mélange and variably deformed thrust panels of oceanic strata forming the Cache Creek terrane and its correlatives in the Canadian Cordillera, the central mélange belt (Baker terrane) of the Pacific Northwest, coeval assemblages in the central Klamath Mountains and the Sierra Nevada foothills of California, and remnants of the Arperos oceanic realm formed on the Mezcalera plate in central Mexico. This nearly continuous alignment of disrupted oceanic materials, conveniently termed the Cache Creek belt (Mortimer 1986), forms a suture zone trapped between the Triassic-Jurassic continental margin and various accreted arc assemblages lying farther west (Figure 7).

The suture belt is probably a compound subduction complex formed of combined tectonic elements added to the flank of North America at a trench lying just offshore from the Triassic-Jurassic Cordilleran arc but also accreted to the flank of intraoceanic arc structures as they approached the Cordilleran margin, with both components representing offscrapings from intervening paleo-Pacific seafloor. Cache Creek blueschists formed by subduction-zone metamorphism have yielded isotopic ages of 230–210 Ma (Late Triassic) in both Canada and the USA (Erdmer et al. 1998), where stratal components of the suture belt range in age from Carboniferous (locally Devonian) to Early or Middle Jurassic (Cordey et al. 1987, Blome and Nestell 1991, Cordey & Schiarizza 1993, Dickinson 2000, Struik et al. 2001, Orchard et al. 2001). In Mexico, where accretion of an intraoceanic arc to the continental margin occurred much later than farther north, only Permian to Early Cretaceous rocks are present within the suture belt of central Mexico (Dickinson & Lawton 2001a).

Mid-Jurassic to Mid-Cretaceous Arc Accretion

In Jurassic-Cretaceous time, tectonic accretion at the Cordilleran subduction zone was punctuated by the arrival of intraoceanic island arcs subducting seafloor downward to the west, rather than to the east, to produce arc-continent collisions (Godfrey & Dilek 2000, Ingersoll 2000, Dickinson 2001). For evaluating accretionary tectonism, a distinction must be drawn (Wright 1982) between incremental accretion within evolving subduction complexes (so-called disrupted terranes), even where far-traveled oceanic components are incorporated, and bulk accretion of tectonic elements transported intact, as integral exotic terranes, to the continental margin. Arc accretion expanded the continental edge by closing the Cache Creek suture and induced the subduction zone and the magmatic arc along the Cordilleran margin to step outward away from the continental interior. Subsequent Cordilleran arc magmatism was widely superimposed on the accreted arc and mélange terranes (van der Heyden 1992, Friedman & Armstrong 1995). The ages of the oldest superimposed plutons of the Cordilleran magmatic arc reflect north-south diachroneity of arc accretion from Middle Jurassic (∼170 Ma) as far south as central California (Schweickert et al. 1999) to Early Cretaceous (∼120 Ma) in Mexico (Dickinson & Lawton 2001a).

CANADIAN TECTONIC ELEMENTS In Canada, two principal accreted tectonic elements, the Stikinia arc and the Insular superterrane, lie west of the Cache Creek suture belt (Figure 7). The Insular superterrane along the present continental fringe includes the Alexander terrane, a Paleozoic arc assemblage of largely pre-Devonian rocks overlain by less deformed Devonian to Permian strata including abundant limestone (Butler et al. 1997), and the Wrangellia terrane, a largely post-Carboniferous succession of Permian arc volcanics and overlying Triassic basalt capped by Upper Triassic limestone (Jones et al. 1977). The two components of the Insular superterrane were amalgamated by Carboniferous time, long before their joint incorporation into the Cordilleran continental margin, for they were both locally intruded by the same pluton (Gardner et al. 1988).

The Stikinia arc farther east is composed dominantly of Upper Triassic to Middle Jurassic volcanic and volcaniclastic rocks, intruded by cogenetic plutons (Marsden & Thorkelson 1992, Mihalynuk et al. 1994, Anderson 1993, Currie & Parrish 1997, MacIntyre et al. 2001). The arc assemblage is flanked on the northeast by a forearc basin (Dickie & Hein 1995, Johannson et al. 1997), lying adjacent to the Cache Creek suture in a position showing that the Stikinia arc faced the Cordilleran margin and subducted seafloor downward to the west. The ages of the youngest arc-forearc strata and the oldest strata in the postaccretion Jurassic-Cretaceous Bowser basin (MacLeod & Hills 1990), resting unconformably on Stikinia (Figure 7), indicate accretion of the northern part of Stikinia by early Middle Jurassic closure of the Cache Creek suture in either Aalenian (Ricketts et al. 1992) or early Bajocian (Thomson et al. 1986, Anderson 1993) time. The youngest strata known from the adjacent segment of the Cache Creek suture belt are Early Jurassic in age (Struik et al. 2001), but farther south in Canada deformed strata of the Cache Creek belt include strata as young as late Middle Jurassic (Callovian) in the Bridge River terrane (Cordey & Schiarizza 1993). The difference in stratal ages along tectonic strike suggest progressive southward closure of the Cache Creek suture from a tectonic hinge point on the north.

STIKINIA-QUESNELLIA OROCLINE Along tectonic strike to the north, the Stikinia arc merges, around the northern limit of the Cache Creek belt, with the northern end of the petrologically and lithologically similar Quesnellia arc along the edge of Triassic-Jurassic North America (Figure 7). This spatial relationship suggests that the Stikinia arc formed originally as a northern extension of the Quesnellia arc, but that oroclinal bending of the Quesnellia-Stikinia arc trend during continued subduction backfolded Stikinia against the Cordilleran margin to juxtapose Stikinia against Quesnellia across the Cache Creek suture, which was thereby enclosed within the tectonic orocline (Nelson & Mihalynuk 1993, Mihalynuk et al. 1994). Paleomagnetic data (May & Butler 1986, Vandall & Palmer 1990) showing no detectable latitudinal movement of Stikinia with respect to North America are compatible with the enclosure interpretation, and isotopic data indicating juvenile crustal origins are similar for Stikinia and Quesnellia arc assemblages (Samson et al. 1989, Smith et al. 1995). Pre-Mesozoic underpinnings of both Stikinia and Quesnellia include Devonian to Permian arc assemblages (Brown et al. 1991, Currie & Parrish 1997), inferred here to have been accreted to Laurentia during Antler-Sonoma events (Figure 6). Both Mesozoic arc assemblages also overlap depositionally upon deformed Paleozoic assemblages (Mortensen 1992, Roback & Walker 1995, Dostal et al. 2001, Acton et al. 2002), interpreted here as overthrust Antler-Sonoma allochthons.

Most of the contact zone between the Stikinia arc and the Insular superterrane is occupied by a sliver of strongly deformed pre-Mesozoic strata, forming a western arm of the Yukon-Tanana terrane (Gehrels et al. 1991, 1992) including the Taku terrane (Gehrels 2002), which underlie the Mesozoic arc assemblage of Stikinia and are regarded here as a product of Antler-Sonoma orogenesis oroclinally deformed along with Stikinia (Figures 6 and 7). The contact zone was overlapped by thick Upper Jurassic (Oxfordian) to Lower Cretaceous (Albian) strata of the intraarc Gravina basin (McClelland et al. 1992), but underlying metavolcanic rocks that also overlap the contact zone document initial accretion of the Insular superterrane to the western flank of Stikinia by Middle Jurassic (~175 Ma) time (Gehrels 2001). Mid-Cretaceous thrusting later carried rocks east of the contact zone over the Gravina basin and the Insular superterrane (Gehrels et al. 1990, Rubin & Saleeby 1992).

INSULAR ARC ACCRETION As the Stikinia arc demonstrably faced east, subduction along its western flank could not have drawn the Insular superterrane toward the continental margin. Accordingly, Early to Middle Jurassic arc magmatism (190–165 Ma) within the Insular superterrane, as displayed in the Queen Charlotte Islands (Lewis et al. 1991) and on Vancouver Island (DeBari et al. 1999), is viewed here as evidence for activation of subduction along the eastern flank of the Insular superterrane, to draw the Insular superterrane closer to the back side of the Stikinia arc by subducting intervening seafloor downward to the west. The polarity of the Jurassic arc along the Insular superterrane is seemingly confirmed along tectonic strike to the northwest, beyond the head of the Gulf of Alaska, where Lower to Middle Jurassic plutons intruding the Wrangellia component of the Insular superterrane on the Alaska Peninsula display transverse compositional gradients indicative of a magmatic arc facing the continent (Reed et al. 1983).

Paleomagnetic data suggest that the Alexander terrane lay in the Arctic region near Baltica in mid-Paleozoic time, but that the associated Wrangellia terrane lay near the paleolatitude of the Pacific Northwest by Late Triassic time (Butler et al. 1997). Apparently, the Insular superterrane drifted as an intraoceanic arc structure within the paleo-Pacific Ocean, along paths that cannot be specified with present information, through late Paleozoic and early Mesozoic time before its accretion to the Cordilleran margin along the back side of Stikinia. If the sliver of the Yukon-Tanana terrane along the west flank of Stikinia includes miogeoclinal facies, as seems likely (Gehrels 2000), the oroclinal rotation of Stikinia was apparently initiated by calving of Stikinia off the edge of the Laurentian margin during backarc rifting. The complex plate motions required to achieve accretion of both the Stikinia arc and the Insular superterrane to the Cordilleran margin in the same general time frame (intra-Jurassic) are indeterminate with present information.

PACIFIC NORTHWEST RECONSTRUCTION The longitudinal correlation of premid-Cretaceous tectonic elements southward across the Pacific Northwest from Canada into the USA has long been a challenge (Monger et al. 1982) because of widespread Neogene volcanic cover (Figure 8*A*), the complex kinematics of an intersecting knot of strike-slip faults of latest Cretaceous to Eocene age spanning the USA-Canada border (Figures 7, 9), and structural complexity within the metamorphic cores of mountain ranges near the USA-Canada border where Cretaceous structural telescoping obscured earlier tectonic relationships between older rock masses.

An apparently satisfactory tectonic reconstruction is achieved here (Figure 8*B*) by reversing 105–110 km of Eocene (44–34 Ma) dextral slip on the Fraser River–Straight Creek fault zone and 110–115 km of previous dextral slip on the offset Yalakom–Ross Lake fault system of latest Cretaceous (<75 Ma) to Eocene age (Kleinspehn 1985, Umhoefer & Kleinspehn 1995, Umhoefer & Miller 1996, Umhoefer & Schiarizza 1996) and by backrotating the Oregon-Washington Coast Range and the Blue Mountains by 50° each (Figure 8) to recover clockwise tectonic rotations imposed during Eocene time (Heller et al. 1987, Dickinson 2002).

In Figure 8, the southern extension of the Stikinia arc assemblage includes the Cadwallader terrane of southern British Columbia (Rusmore 1987, Rusmore et al. 1988, Umhoefer 1990, Rusmore & Woodsworth 1991) and the Triassic-Jurassic Cascade River–Holden belt (Hopson & Mattinson 1994) in the Cascade Mountains east of the Straight Creek fault. Inland extensions of the Insular superterrane include the Chilliwack, Bowen Lake, and Harrison Lake terranes of southern British Columbia (Friedman et al. 1990, Mahoney et al. 1995), the Swakane Gneiss (Nason terrane) east of the Straight Creek fault in the Cascade Mountains (Mattinson 1972), and the Wallowa–Seven Devils segment of Wrangellia in the Blue Mountains. The Cache Creek suture belt flanking the Triassic-Jurassic continental margin is reconstructed as an alignment of similar lithologic units, including the Cache Creek and Bridge River terranes of southern British Columbia, the Hozameen terrane spanning the USA-Canada border, the Baker terrane of the Blue Mountains, and

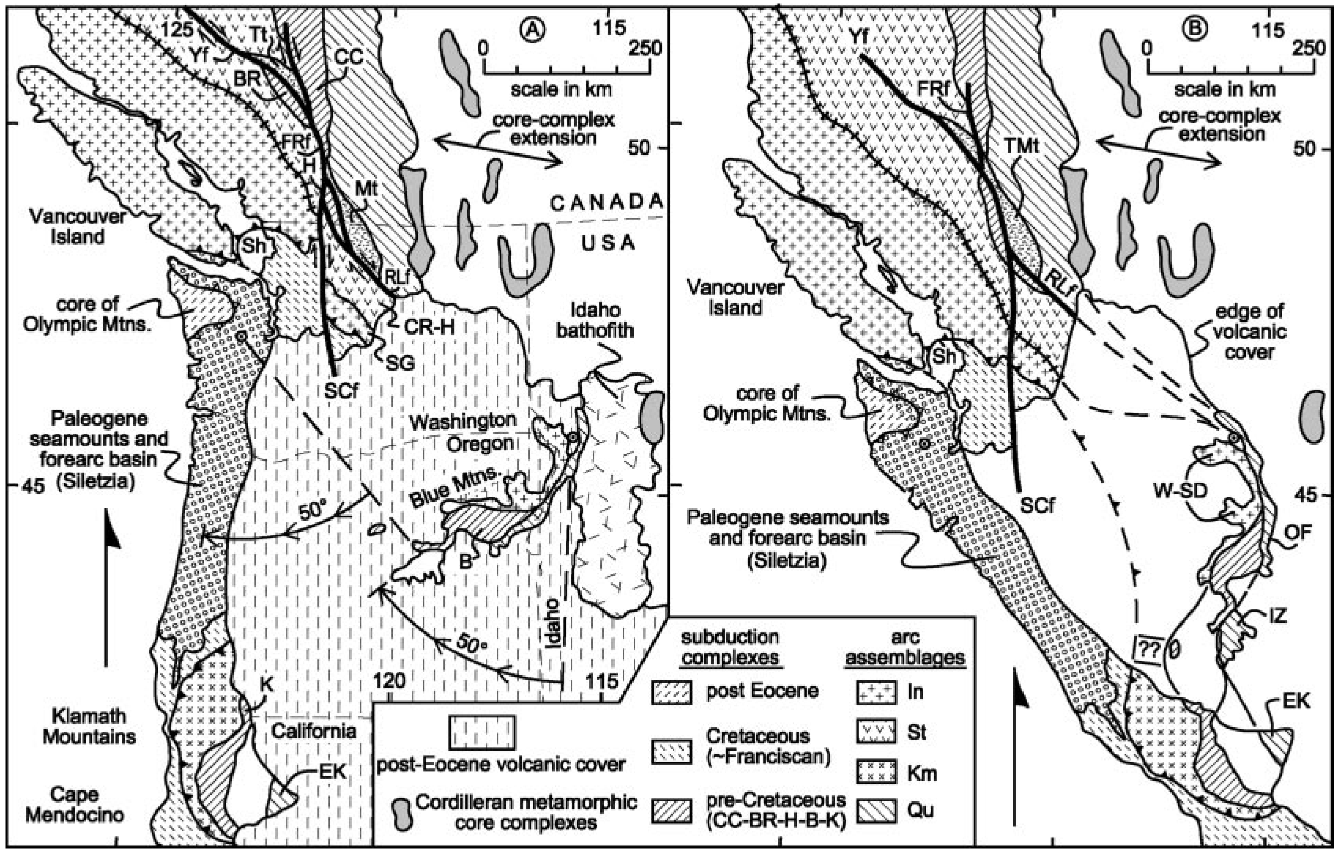

Figure 8 Pre-Oligocene geotectonic features in the Pacific Northwest (USA) and adjacent Canada at present (*A*) and as reconstructed (*B*) before clockwise rotations of the Oregon-Washington Coast Range and Blue Mountains provinces, and before dextral slip on branching faults near the USA-Canada border. Arc assemblages: In, Insular (SG, Swakane Gneiss; W-SD, Wallowa–Seven Devils); Km, accreted western Klamath Mountains arcs; Qu, Quesnellia and related terranes (IZ, Izee forearc basin; EK, eastern Klamath Mountains Mesozoic arc, OF, Olds Ferry terrane or Huntington arc); St, Stikinia (CR-H, Cascade River–Holden belt). Pre-Late Jurassic subduction-complex terranes: B, Baker; BR, Bridge River; CC, Cache Creek; H, Hozameen, K, central Klamath Mountains mélange belt. Other geologic features: Sh, Shuksan thrust system (schematic); TMt, Tyaughton–Methow trough (offset segments: Mt, Methow trough; Tt, Tyaughton trough).

the central mélange belt of the Klamath Mountains (Figure 8*B*). Closer proximity of restored tectonic elements near the USA-Canada border to counterparts in the Blue Mountains could be achieved by additional recovery of the significant Eocene intracontinental extension recorded by Cordilleran core complexes (Figure 8) in southeastern British Columbia (Dickinson 2002).

The Tyaughton-Methow trough (Figure 8) was initiated in Early Jurassic time as a forearc basin flanking the Quesnellia arc (Anderson 1976), but evolved during Late Jurassic and Early Cretaceous time to overlap the accreted Stikinia arc (Garver 1992, Umhoefer et al. 2002). West and south of the Shuksan thrust system (Figure 8), an internally deformed underthrust assemblage, including Upper Jurassic to Lower Cretaceous blueschists and clastic strata (Brown 1987, Brandon et al. 1988, Monger 1991), is presumed to be a northern counterpart of the late Mesozoic Franciscan subduction complex and associated forearc basins of coastal California to the south (Brown & Blake 1987).

USA-MEXICO ARC ACCRETION The Insular superterrane extends as far south as the Blue Mountains (Figure 8) of the Pacific Northwest, where intense mid-Cretaceous crustal telescoping near the Snake River has thrust strata of Wrangellia beneath the Mesozoic continental margin (Lund & Snee 1988). Stratigraphic analysis of Blue Mountains terranes indicates, however, that initial accretion of the Wrangellia component of the Insular superterrane was completed in Middle Jurassic (Bajocian) time (Follo 1992, White et al. 1992, Avé Lallemant 1995), coordinate with accretion farther north in Canada. The oroclinally deformed Stikinia arc apparently does not extend farther south than the Cascades Mountains along the USA-Canada border (Figure 8), and there is no indication that active magmatism was still underway at the southern end of the Insular superterrane when the Wallowa–Seven Devils segment (Figure 8) of Wrangellia was drawn passively into a subduction zone along the continental margin (Dickinson 1979).

Accreted intraoceanic arc assemblages of Jurassic age in the Klamath Mountains and Sierra Nevada foothills of California rest on ophiolitic basement formed near the Triassic-Jurassic time boundary (Dilek 1989, Edelman 1990, Hacker & Ernst 1993, Wright & Wyld 1994, Hacker et al. 1995), as does the Guerrero superterrane (Figure 7) of western Mexico (Dickinson & Lawton 2001a). The accreted Mesozoic arc complexes in the USA and Mexico can perhaps be regarded as southern extensions and descendants of the Jurassic arc along the Insular superterrane where subduction continued southward across paleo-Pacific oceanic crust lying beyond the southern limits of the older Alexander and Wrangellia terranes. In California, severely deformed mélange belts separate accreted arc assemblages on the west from the pre-Jurassic continental margin (Wright 1982, Edelman & Sharp 1989, Edelman et al. 1989b, Dilek et al. 1990, Hacker et al. 1993), but a superimposed magmatic arc built along the Cordilleran continental margin across the accreted tectonic elements by late Middle Jurassic (Callovian) time (Wright & Fahan 1988, Edelman 1990, Edelman et al. 1989a, Harper et al. 1994, Girty et al. 1995) implies arc accretion during early Middle Jurassic (Bajocian) time (170–165 Ma).

In the southwestern USA and Mexico, final closure of the oceanic realm between accreted Mesozoic arcs and the Cordilleran continental margin in Early Cretaceous time promoted slab rollback of the Mezcalera plate to induce crustal extension within the overriding continental block (Dickinson & Lawton 2001a). The resulting border rift belt, including the Bisbee basin and Chihuahua trough, supplanted arc magmatism along the USA-Mexico border region (Figure 7), with Late Jurassic rifting accompanied by bimodal magmatism and followed by Early Cretaceous thermotectonic subsidence (Dickinson & Lawton 2001b). Farther north, the extensional Utah-Idaho trough (Figure 7) of Middle to Late Jurassic age and development of a wide zone of Late Jurassic to Early Cretaceous backarc magmatism (Figure 7) closely followed arc accretion along the California continental margin to the west (Dickinson 2001). Earlier Middle Jurassic thrusting along the Luning-Fencemaker thrust (Wyld 2002), which carried the fill of the Auld Lang Syne backarc basin eastward (Figure 7), coincided closely in timing with arc accretion farther west.

Mid-Cretaceous to Mid-Tertiary Cordilleran Arc

Following Jurassic-Cretaceous arc accretion at the evolving subduction zone along the continental margin, the Cordilleran magmatic arc stepped oceanward to a trend that was largely superimposed upon accreted terranes (Figure 9). Massive Late Cretaceous plutonism, continuing until mid-Eocene time in Canada, formed the major Cordilleran batholith belt along the arc axis. To the west, a parallel belt of Jurassic-Cretaceous forearc basins is prominent along the coastal fringes of the USA and Mexico, and lies immediately inland from exposures of the Jurassic-Cretaceous subduction complex forming the Franciscan superterrane (Figure 9). Farther north in Canada, however, Cenozoic modification of the continental margin by strike slip along the Cenozoic Queen Charlotte transform and its splays has largely disrupted or submerged tectonic elements of the late Mesozoic forearc region.

Past speculation (Cowan et al. 1997), based on paleomagnetic data, that the western part of the Canadian Cordillera, including a large segment of the Cretaceous batholith belt, was transported northward in Cretaceous-Paleocene time from an origin along the continental margin of California or Mexico encounters the insuperable difficulty that no segment of the Cretaceous arc-trench system is missing from California or Mexico (Figure 9). The anomalously shallow paleomagnetic vectors that gave rise to the hypothesis of large lateral displacements can be interpreted instead as the result of widespread pluton tilt coupled with compaction in sedimentary strata (Butler et al. 2001).

Crustal shortening across the Cordilleran orogen gave rise by Late Jurassic time in Canada (Cant & Stockmal 1989) and mid-Early Cretaceous time in the USA (Dickinson 2001) to initiation of a backarc thrust belt that was continuous from the interior flank of the Canadian Cordillera into the Sevier thrust belt (Figure 9). The tectonic load of the thrust sheets downflexed an extensive retroforeland basin with a distal fringe that extended well into the continental interior. Deformation within the Canadian Cordillera produced intraorogen thrusting associated with development of the Skeena foldbelt (Evenchick 1991) accompanied by downflexure of the Sustut basin, and analogous intraorogen deformation formed the Eureka thrust belt in the USA (Figure 9).

Scattered plutons of Late Cretaceous age present in the interior hinterland of the backarc thrust belt, but most prominent in the Omineca region of the Canadian Cordillera (Figure 9), were not an integral facet of the arc magmatism active farther west, but instead were derived largely from sources within underthrust continental crust. Backarc thrusting and the associated retroforeland basin did not extend as far south as the region occupied until mid-Cretaceous time by the Bisbee basin and related rift troughs along the USA-Mexico border. Although somewhat diachronous in timing, backarc rifting (Figure 7) and backarc thrusting (Figure 9) occupied different realms marked by distinct contrasts in geodynamics along the Cordilleran orogen.

In Canada, arc magmatism along the eastern flank of the Coast batholith continued until mid-Eocene time (~45 Ma), as did deformation along the backarc thrust belt. Farther south, however, in both the USA and Mexico, subhorizontal subduction of the Farallon plate during latest Cretaceous through Eocene time altered the progress of both magmatism and tectonism (Dickinson & Snyder 1978). Inland migration and diminution of igneous activity led to a magmatic null through much of the USA Cordillera (Figure 1), and basement-involved crustal shortening produced yoked uplifts and basins of the Laramide Rocky Mountains well inland from the continental margin (Figure 9).

Deformation began ~70 Ma throughout the Laramide Rocky Mountains while thrusting was still underway along the Sevier thrust belt to the west, but its termination was diachronous (Dickinson et al. 1988). The development of Laramide basins and uplifts was complete in the northern part of the Laramide province by mid-Eocene time (~50 Ma), coincident with the terminal phase of deformation along the Sevier thrust belt to the west (DeCelles 1994). Farther south, however, Laramide deformation continued until the end of Eocene time. In Mexico, south of the magmatic null, Laramide basin evolution (Figure 9) during Late Cretaceous and Paleocene time (Dickinson & Lawton 2001b) was accompanied by arc magmatism that migrated inland from the Cretaceous batholith belt near the coast. The time-space pattern of Laramide magmatism and deformation suggests that the shallow angle of plate descent that gave rise to both resulted from subduction of a buoyant oceanic plateau beneath the continental margin (Dickinson et al. 1988).

In the Pacific Northwest, the elongate oceanic seamount chain of Siletzia (Figure 9), which formed during Paleocene-Eocene time (Figure 1) at some unknown distance offshore, was accreted in bulk to the Cordilleran margin early in Eocene time, and was subsequently buried beneath the Eocene forearc basin (Figure 8) of the Oregon-Washington Coast Range (Heller et al. 1987). A subduction complex (Brandon & Vance 1992), composed of premid-Miocene Cenozoic strata underthrust beneath the accreted mass of Siletzia, forms the core of the Olympic Mountains near the USA-Canada border (Figure 9). Incrementally accreted Paleocene-Eocene components of the Franciscan subduction complex are exposed along the coastal fringe of California farther south, but elsewhere most Cenozoic subduction along the Cordilleran margin occurred along an offshore zone still unexposed underwater.

CENOZOIC TAPHROGENY

The Cordilleran arc orogen as a typical segment of the Circum-Pacific orogenic belt reached peak development in Late Cretaceous time. During Tertiary time, arrival at the Cordilleran margin of successive segments of spreading systems bounding the Pacific plate progressively converted segments of the continental margin into transform fault systems along the Pacific plate boundary. As the transform continental margin evolved, subsidiary strike slip and associated crustal extension disrupted the adjacent continental block and gave rise to the rift trough of the Gulf of California, an incipient ocean basin that is expanding obliquely within the transform regime (Figure 10).

North of the Tofino triple junction (Figure 10), subduction associated with waning phases of batholith generation along the coastal fringe of the Canadian Cordillera was supplanted in mid-Eocene time (Hyndman & Hamilton 1993) by dextral slip along the Queen Charlotte transform fault. The change in coastal geodynamics, from convergence to strike slip, was triggered by amalgamation of the offshore Kula and Pacific plates at ∼42.5 Ma (Lonsdale 1988). Subsequent Oligocene-Miocene magmatism within the Queen Charlotte Islands was associated with evolution of a slab window (Hamilton & Dostal 2001), and the Neogene Queen Charlotte basin farther east (Figure 10) developed as a pull-apart basin within the transform system (Lewis et al. 1991). The Chatham Strait–Denali fault system, initiated in mid-Eocene time as a branch of the Queen Charlotte transform (Cole et al. 1999), has displaced segments of the Insular superterrane laterally along the continental margin (Figure 10). A discrepancy between 370 km of slip along the Denali fault and 150 km of slip along the linked Chatham Strait fault suggests that 220 km of slip parallel to the continental margin, southward from the elbow where those two fault segments meet, was accommodated by the Coast shear zone along the eastern flank of the Insular superterrane (Gehrels 2000).

Farther south, subduction along the Cordilleran margin continues at the foot of the continental slope along an offshore trend parallel to and coextensive with the active Cascades volcanic arc of the Pacific Northwest (Figure 10). Arc volcanism, which extended southward through the USA in Miocene time (Figure 10), was progressively extinguished south of the Cascades arc by evolution of the San Andreas transform system along the continental margin as the Mendocino triple junction (Figure 10) migrated northward to shorten the Cascades subduction zone. Beginning near the Oligocene-Miocene time boundary, slab-window volcanism evolved in coastal California along a belt parallel to the evolving San Andreas transform (Dickinson 1997). Neogene arc volcanism was extinguished in similar fashion within Baja California when the Rivera triple junction (Figure 10) migrated southward in mid-Miocene time to a position near the mouth of the modern Gulf of California.

Following Laramide events, establishment of mid-Cenozoic arc magmatism along a trend near the USA-Mexico continental margin had been accomplished by the migration of successive volcanic fronts toward the coast (Figure 10) as the slab of oceanic lithosphere subducting beneath the Cordilleran orogen steepened or foundered (Dickinson 2002). Subsequent initiation of the San Andreas transform along the continental margin in Early Miocene time triggered crustal extension within the Basin and Range taphrogen (Figure 10), where multiple fault blocks distended the Cordilleran orogen once the continental block was partly coupled to the Pacific plate. A largely intact remnant of the mid-Cenozoic arc assemblage lies along the Sierra Madre Occidental (Figure 10), where flat-lying volcanic strata form an enclave of largely undistended crust enclosed within the Basin and Range taphrogen. Baja California was calved from mainland Mexico when the San Andreas transform plate boundary south of the USA jumped inland in Late Miocene time to open the Gulf of California by oblique extension.

In the Pacific Northwest (USA), extensive volcanic fields of flood basalt that have erupted behind the Cascades volcanic arc since Early Miocene time mask older rock assemblages over wide areas (Figure 10). The volcanism may have been related to mantle advection induced by deformation of the continental lithosphere after shear was imposed on the continental block by interaction of the Pacific and American plates along the San Andreas transform system at the continental margin (Dickinson 1997). Less voluminous but comparably extensive Middle Miocene and younger volcanic fields of basaltic character in the Canadian Cordillera (Edwards & Russell 2000) may reflect analogous shear coupling of the Pacific and American plates along the nearby Queen Charlotte transform.

SUMMARY PERSPECTIVES

The questions posed in the introduction can be answered as follows:

1. The Cordilleran system, as an integral segment of the circum-Pacific orogenic belt, was established when subduction was initiated between Early and Late Triassic time along a continental margin that had been delineated by Neoproterozoic rifting during the breakup of Rodinia, and later modified in late Paleozoic and earliest Mesozoic time by the emplacement of oceanic allochthons upon the edge of the continental block during the final assembly of Pangea.
2. Rock masses native to the Cordilleran margin include the miogeoclinal prism deposited between Neoproterozoic and Late Devonian time along a passive continental margin, volcanic and plutonic rocks of the Cordilleran magmatic

arc built along an active continental margin from mid-Triassic time to the present, and the sedimentary and volcanic assemblages of basins and lava fields superimposed upon the miogeoclinal succession and the arc assemblage.

3. Accreted tectonic elements include subduction complexes thrust bodily over the miogeoclinal prism in Devonian-Mississsippian and Permian-Triassic time; intraoceanic island arcs sutured to the continental block at those times and also later, between Middle Jurassic and Early Cretaceous time; and subduction complexes accreted incrementally to the continental block at the Cordilleran subduction zone between Late Triassic and mid-Cenozoic time.
4. Postmid-Cenozoic internal distension and incipient dislocation of Cordilleran crust has occurred in response to transform tectonism imposed on the continental margin when intra-Pacific seafloor spreading systems impinged on the Cordilleran trench.

The *Annual Review of Earth and Planetary Science* is online at http://earth.annualreviews.org

LITERATURE CITED

Acton SL, Simony PS, Heaman LM. 2002. Nature of the basement to Quesnel terrane near Christina Lake, southeastern British Columbia. *Can. J. Earth Sci.* 39:65–78

Anderson P. 1976. Oceanic crust and arc-trench gap tectonics in southwestern British Columbia. *Geology* 4:443–46

Anderson RG. 1993. A Mesozoic stratigraphic and plutonic framework for northwestern Stikinia (Iskut River area), northwestern British Columbia, Canada. In *Mesozoic Paleogeography of the Western United States—II*, ed. GC Dunne, KA McDougall, Book 74, pp. 477–94. Los Angeles: Pacif. Sect. SEPM (Soc. Sediment. Geol.)

Armin RA, Mayer L. 1983. Subsidence analysis of the Cordilleran miogeocline: implications for timing of late Proterozoic rifting and amount of extension. *Geology* 11:702–5

Armstrong RL. 1988. Mesozoic and early Cenozoic magmatic evolution of the Canadian Cordillera. In *Processes in Continental Lithospheric Deformation*, ed. SP Clark Jr, BC Burchfiel, J Suppe, Spec. Pap. 218, pp. 55– 91. Boulder, CO: Geol. Soc. Am.

Armstrong RL, Ward PL. 1991. Late Triassic to earliest Eocene magmatism in the North America Cordillera: implications for the Western Interior Basin. In *The Evolution of the Western Interior Basin*, ed. WGE Caldwell, EG Kauffman, Spec. Pap. 39, pp. 49–72. Ottawa, Can: Geol. Assoc. Can.

Armstrong RL, Eisbacher GH, Evans PD. 1982. Age and stratigraphic-tectonic significance of Proterozoic diabase sheets, Mackenzie Mountains, northwestern Canada. *Can. J. Earth Sci.* 19:316–23

Avé Lallemant HG. 1995. Pre-Cretaceous tectonic evolution of the Blue Mountains province, northeastern Oregon. *U.S. Geol. Surv. Prof. Pap.* 1438:271–304

Blome CD, Nestell MK. 1991. Evolution of a Permo-Triassic sedimentary mélange, Grindstone terrane, east-central Oregon. *Geol. Soc. Am. Bull.* 103:1280–96

Bond GC, Kominz M. 1984. Construction of tectonic subsidence curves for the early Paleozoic miogeocline, southern Canadian Rocky Mountains: implications for subsidence mechanisms, age of breakup, and crustal thinning. *Geol. Soc. Am. Bull.* 95: 155–73

Bond GC, Kominz MA, Devlin WR. 1983. Thermal subsidence and eustasy in the lower Palaeozoic miogeocline of western North America. *Nature* 306:775–79

Brandon MT, Vance JA. 1992. Tectonic evolution of the Cenozoic Olympic subduction complex, Washington state, as deduced from fission track ages for detrital zircons. *Am. J. Sci.* 292:565–636

Brandon MT, Cowan DS, Vance JA. 1988. *The Late Cretaceous San Juan Thrust System, San Juan Islands, Washington,* Spec. Pap. 221. Boulder, CO: Geol. Soc. Am. 81 pp.

Brown EH. 1987. Structural geology and accretionary history of the northwest Cascades system, Washington and British Columbia. *Geol. Soc. Am. Bull.* 99:201–14

Brown EH, Blake MC, Jr. 1987. Correlation of Early Cretaceous blueschists in Washington, Oregon, and northern California. *Tectonics* 6:795–806

Brown DA, Logan JM, Gunning MH, Orchard MJ, Bamber WE. 1991. Stratigraphic evolution of the Paleozoic Stikine assemblage in the Stikine and Iskut River area, northwestern British Columbia. *Can. J. Earth Sci.* 28:958–72

Busby-Spera CJ. 1988. Speculative tectonic model for the early Mesozoic arc of the southwest Cordilleran United States. *Geology* 16:1121–25

Butler RF, Gehrels GE, Bazard DR. 1997. Paleomagnetism of Paleozoic strata of the Alexander terrane, southeastern Alaska. *Geol. Soc. Am. Bull.* 109:1372–88

Butler RF, Gehrels GE, Kodama KP. 2001. A moderate translation alternative to the Baja British Columbia hypothesis. *GSA Today* 11(6):4–10

Cant DE, Stockmal GS. 1989. The Alberta foreland basin: relationship between stratigraphy and Cordilleran terrane-accretion events. *Can. J. Earth Sci.* 26:1964–75

Challand G, Rageau J-P. 1985. *A Strategic Atlas.* New York: Harper & Row. 224 pp.

Cole RB, Ridgway KD, Layer PW, Drake J. 1999. Kinematics of basin development during the transition from terrane accretion to strike-slip tectonics, Late Cretaceous–early Tertiary Cantwell Formation, south central Alaska. *Tectonics* 18:1224–44

Colpron M, Logan JM, Mortensen JK. 2002. U-Pb zircon age constraint for late Neoproterozoic rifting and initiation of the lower Paleozoic passive margin of western Laurentia. *Can. J. Earth Sci.* 39:133–43

Coney PJ, Jones DL, Monger JWH. 1980. Cordilleran suspect terranes. *Nature* 288: 329–33

Cordey F, Schiarizza P. 1993. Long-lived Panthalassic remnant: the Bridge River accretionary complex, Canadian Cordillera. *Geology* 21:263–66

Cordey F, Mortimer N, DeWever P, Monger JWH. 1987. Significance of Jurassic radiolarians from the Cache Creek terrane, British Columbia. *Geology* 15:1151–54

Cowan DS, Brandon MT, Garver JI. 1997. Geologic tests of hypotheses for large coastwise displacements—a critique illustrated by the Baja British Columbia controversy. *Am. J. Sci.* 297:117–73

Currie LD, Parrish RK. 1997. Paleozoic and Mesozoic rocks of Stikinia exposed in northwestern British Columbia: implications for correlations in the northern Cordillera. *Geol. Soc. Am. Bull.* 109:1402–20

Dalziell IWD. 1992. Antarctica: a tale of two supercontinents? *Annu. Rev. Earth Planet. Sci.* 20:501–26

DeBari SM, Anderson RG, Mortensen JK. 1999. Correlation among lower to upper crustal components in an island arc, Vancouver Island, Canada. *Can. J. Earth Sci.* 36:1371–413

DeCelles PG. 1994. Late Cretaceous-Paleocene synorogenic sedimentation and kinematic history of the Sevier thrust belt, northeast Utah and southwest Wyoming. *Geol. Soc. Am. Bull.* 106:32–56

DePaolo DJ. 1981. A neodymium and strontium isotopic study of the Mesozoic calc-alkaline granitic batholiths of the Sierra Nevada and Peninsular Ranges, California. *J. Geophys. Res.* 86:10470–88

Devlin WJ. 1989. Stratigraphy and sedimentology of the Hamill Group in the northern Selkirk Mountains, British Columbia: evidence for latest Proterozoic–Early Cambrian extensional tectonism. *Can. J. Earth Sci.* 26:515–33

Devlin WJ, Bond GC 1988. The initiation of the early Proterozoic Cordilleran miogeocline: evidence from the uppermost Proterozoic–Lower Cambrain Hamill Group of southeastern British Columbia. *Can. J. Earth Sci.* 25:1–19

Devlin WJ, Brueckner HK, Bond GC. 1988. New isotopic data and a preliminary age for volcanics near the base of the Windermere Supergroup, northeastern Washington, U.S.A. *Can. J. Earth Sci.* 25:1906–11

Dickie JR, Hein FJ. 1995. Conglomeratic fan deltas and submarine fans of the Jurassic Laberge Group, Whitehorse trough, Yukon Territory, Canada: fore-arc sedimentation and unroofing of a volcanic island arc complex. *Sediment. Geol.* 98:263–92

Dickinson WR. 1977. Subduction tectonics in Japan. *Am. Geophys. Union Trans.* 58:948–52

Dickinson WR. 1979. Mesozoic forearc basin in central Oregon. *Geology* 7:166–70

Dickinson WR. 1997. Tectonic implications of Cenozoic volcanism in coastal California. *Geol. Soc. Am. Bull.* 109:936–54

Dickinson WR. 2000. Geodynamic interpretation of Paleozoic tectonic trends oriented oblique to the Mesozoic Klamath-Sierran continental margin in California. In *Paleozoic and Triassic Paleogeography and Tectonics of Western Nevada and Northern California*, ed. MJ Soreghan, GE Gehrels, Spec. Pap. 347, pp. 209–45. Boulder, CO: Geol. Soc. Am.

Dickinson WR. 2001. Tectonic setting of the Great Basin through geologic time: implications for metallogeny. In *Regional Tectonics and Structural Control of Ore: The Major Gold Trends of Northern Nevada,* ed. DR Shaddrick, E Zbinden, DC Mathewson, C Prenn, Spec. Publ. 33, pp. 27–53. Reno, NV: Geol. Soc. Nev.

Dickinson WR. 2002. The Basin and Range province as a composite extensional domain. *Int. Geol. Rev.* 44:1–38

Dickinson WR, Lawton TF. 2001a. Carboniferous to Cretaceous assembly and fragmentation of Mexico. *Geol. Soc. Am. Bull.* 113:1142–60

Dickinson WR, Lawton TF. 2001b. Tectonic setting and sandstone petrofacies of the Bisbee basin (USA-Mexico). *J. S. Am. Earth Sci.* 14:475–501

Dickinson WR, Lawton TF. 2003. Sequential intercontinental suturing as the ultimate control for Pennsylvanian Ancestral Rocky Mountains deformation. *Geology* 31:609–12

Dickinson WR, Snyder WS. 1978. Plate tectonics of the Laramide orogeny. In *Laramide Folding Associated With Basement Block Faulting in the Western United States*, ed. V Mathews III, Mem. 151, pp. 355–66. Boulder: Geol. Soc. Am.

Dickinson WR, Swift PN, Coney PJ. 1986. Tectonic strip maps of Alpine-Himalayan and Circum-Pacific orogenic belts (great circle projections). *Geol. Soc. Am. Map Chart Ser.* MC-58

Dickinson WR, Klute MA, Hayes MJ, Janecke SU, Lundin ER, et al. 1988. Paleogeographic and paleotectonic setting of Laramide sedimentary basins in the central Rocky Mountain region. *Geol. Soc. Am. Bull.* 100:1023–39

Dilek Y. 1989. Tectonic significance of post-accretion rifting of an early Mesozoic oceanic basement in the northern Sierra Nevada metamorphic belt, California. *J. Geol.* 97:503–18

Dilek Y, Thy P, Moores EM, Grundvig S. 1990. Late Paleozoic–early Mesozoic oceanic basement of a Jurassic arc terrane in the northwestern Sierra Nevada, California. See Harwood & Miller 1990, pp. 351–69

Dilek Y, Moores EM, Elthon D, Nicolas A, eds. 2000. *Ophiolites and Oceanic Crust: New Insights from Field Studies and the Ocean Drilling Program*, Spec. Pap. 349. Boulder, CO: Geol. Soc. Am.

Dostal J, Church BN, Hoy T. 2001. Geological and geochemical evidence for variable magmatism and tectonics in the southern Canadian Cordillera: Paleozoic to Jurassic suites, Greenwood, southern British Columbia. *Can. J. Earth Sci.* 38:75–90

Dunne GC, McDougall KA, eds. 1993. *Mesozoic Paleogeography of the Western United States—II*. Los Angeles: Pacif. Sect., SEPM (Soc. Sediment. Geol.). Book 71

Edelman SH. 1990. *Paleozoic and Early Mesozoic Paleogeographic Relations; Sierra Nevada, Klamath Mountains, and Related Terranes*, See Harwood & Miller 1990, pp. 371–78

Edelman SH, Sharp WD. 1989. Terranes, early faults, and pre-Late Jurassic amalgamation of the western Sierra Nevada metamorphic belt, California. *Geol. Soc. Am. Bull.* 101:1420–33

Edelman SH, Day HW, Bickford ME. 1989a. Implications of U-Pb ages for the tectonic settings of the Smartville and Slate Creek complexes, northern Sierra Nevada, California. *Geology* 17:1032–35

Edelman SH, Day HW, Moores EM, Zigan SM, Murphy TP, Hacker BR. 1989b. *Structure Across a Mesozoic Ocean-Continent Suture Zone in the Northern Sierra Nevada, California*, Spec. Pap. 224. Boulder, CO: Geol. Soc. Am. 56 pp.

Edwards BR, Russell JK. 2000. Distribution, nature, and origin of Neogene-Quaternary magmatism in the northern Cordilleran volcanic province, Canada. *Geol. Soc. Am. Bull.* 112:1280–95

Erdmer P, Ghent ED, Archibald DA, Stout MZ. 1998. Paleozoic and Mesozoic high-pressure metamorphism at the margin of ancestral North America in central Yukon. *Geol. Soc. Am. Bull.* 110:615–29

Erdmer P, Moore JM, Heaman L, Thompson RI, Daughtry KL, Creaser RA. 2002. Extending the ancient margin outboard in the Canadian Cordillera: record of Proterozoic crust and Paleocene regional metamorphism in the Nicola horst, southern British Columbia. *Can. J. Earth Sci.* 39:1605–23

Evans KV, Aleinikoff JN, Obradovich JD, Fanning JM. 2000. SHRIMP U-Pb geochronology of volcanic rocks, Belt Supergroup, western Montana: evidence for rapid deposition of sedimentary strata. *Can. J. Earth Sci.* 37:1287–300

Evenchick CA. 1991. Geometry, evolution, and tectonic framework of the Skeena fold belt, north central British Columbia. *Tectonics* 10:527–46

Fedo CM, Cooper JD. 2001. Sedimentology and sequence stratigraphy of Neoproterozoic and Cambrian units across the craton-margin hinge zone, southeastern California, and implications for the early evolution of the Cordilleran margin. *Sediment. Geol.* 141-142:501–22

Ferri F. 1997. Nina Creek Group and Lay Range assemblage, north-central British Columbia: remnants of late Paleozoic oceanic and arc terranes. *Can. J. Earth Sci.* 34:854–74

Follo MF. 1992. Conglomerates as clues to the sedimentary and tectonic evolution of a suspect terrane: Wallowa Mountains, Oregon. *Geol. Soc. Am. Bull.* 104:1561–76

Foster DA, Gray DR. 2000. Evolution and structure of the Lachlan fold belt (orogen) of eastern Australia. *Annu. Rev. Earth Planet. Sci.* 28:47–80

Friedman RM, Armstrong RL. 1995. Jurassic and Cretaceous geochronology of the southern Coast Belt, British Columbia, 49° to 51° N. See Miller & Busby 1995, pp. 95–139

Friedman RM, Monger JWH, Tipper HW. 1990. Age of the Bowen Island Group, southwestern Coast Mountains, British Columbia. *Can. J. Earth Sci.* 27:1456–61

Gardner MC, Bergman SC, Cushing GW, MacKevett EM Jr, Plafker G, et al. 1988. Pennsylvanian stitching of Wrangellia and the Alexander terrane, Wrangell Mountains, Alaska. *Geology* 16:967–71

Garver JI. 1992. Provenance of Albian-Cenomanian rocks of the Methow and Tyaughton basins, southern British Columbia: a mid-Cretaceous link between North America and the Insular terrane. *Can. J. Earth Sci.* 29:1274–95

Gehrels GE. 2000. Reconnaissance geology and U-Pb geochronology of the western flank of the Coast Mountains between Juneau and Skagway, southeastern Alaska. In *Tectonics of the Coast Mountains, Southeastern Alaska and British Columbia*, ed. HH Stowell, WC McClelland, Spec. Pap. 343, pp. 213–33. Boulder, CO: Geol. Soc. Am.

Gehrels GE. 2001. Geology of the Chatham Sound region, southeast Alaska and coastal British Columbia. *Can. J. Earth Sci.* 38: 1579–99

Gehrels GE. 2002. Detrital zircon geochronology of the Taku terrane, southeast Alaska. *Can. J. Earth Sci.* 39:921–31

Gehrels GE, McClelland WC, Samson SD, Patchett PJ, Jackson JL. 1990. Ancient continental margin assemblage in the northern Coast Mountains, southeast Alaska and northwest Canada. *Geology* 18:208–11

Gehrels GE, McClelland WC, Samson SD, Patchett PJ. 1991. U-Pb geochronology of detrital zircons from a continental margin assemblage in the northern Coast Mountains, southeastern Alaska. *Can. J. Earth Sci.* 28:1285–300

Gehrels GE, McClelland WC, Samson SD, Patchett PJ. 1992. Geology of the western flank of the Coast Mountains between Cape Fanshaw and Taku Inlet, southeastern Alaska. *Tectonics* 11:567–85

Gehrels GE, Johnsson MJ, Howell DG. 1999. Detrital zircon geochronology of the Adams Argillite and Nation River Formation, east-central Alaska, U.S.A. *J. Sediment. Res.* 69:135–44

Girty GH, Hanson RE, Girty MS, Schweickert RA, Harwood DS, et al. 1995. Timing of emplacement of the Haypress Creek and Emigrant Gap plutons: implications for the timing and controls of Jurassic orogenesis, northern Sierra Nevada, California. See Miller & Busby 1995, pp. 191–201

Ghosh DK. 1995. Nd-Sr isotopic constraints on the interactions of the Intermontane Superterrane with the western edge of North America in the southern Canadian Cordillera. *Can. J. Earth Sci.* 32:1740–58

Godfrey NJ, Dilek Y. 2000. Mesozoic assimilation of oceanic crust and island arc into the North American continental margin in California and Nevada: insights from geophysical data. See Dilek et al. 2000, pp. 365–82

Gordey SP, Abbott JG, Tempelman-Kluit DJ, Gabrielse H. 1987. "Antler" clastics in the Canadian Cordillera. *Geology* 15:103–7

Hacker BR, Ernst WG. 1993. Jurassic orogeny in the Klamath Mountains: a geochronological analysis. See Dunne & McDougall 1993, pp. 37–59

Hacker BR, Ernst WG, McWilliams MO. 1993. Genesis and evolution of a Permian-Jurassic magmatic arc/accretionary wedge, and reevaluation of terranes in the central Klamath Mountains. *Tectonics* 12:387–409

Hacker BR, Donato MM, Barnes CG, McWilliams MO, Ernst WG. 1995. Timescales of orogeny: Jurassic construction of the Klamath Mountains. *Tectonics* 14:677–703

Hamilton TS, Dostal J. 2001. Melting of heterogeneous mantle in a slab window environment: examples from the middle Tertiary Masset basalts, Queen Charlotte Islands, British Columbia. *Can. J. Earth Sci.* 38:825–38

Hansen VL. 1988. A model for terrane accretion, Yukon-Tanana and Slide Mountain terranes, northwest North America. *Tectonics* 6:1167–77

Hansen VL. 1990. Yukon-Tanana terrane: a partial acquittal. *Geology* 18:365–69

Hansen VL, Dusel-Bacon C. 1998. Structural and kinematic evolution of the Yukon-Tanana upland tectonites, east-central Alaska: a record of late Paleozoic to Mesozoic crustal assembly. *Geol. Soc. Am. Bull.* 110:211–30

Harper GD, Saleeby JB, Heizler M. 1994. Formation and emplacement of the Josephine ophiolite and the Nevadan orogeny in the Klamath Mountains, California-Oregon: U/Pb sircon and $^{40}Ar/^{39}Ar$ geochronology. *J. Geophys. Res.* 99:4293–321

Harwood DS, Miller MM, eds. 1990. *Paleozoic and Early Mesozoic Paleogeographic*

Relations; Sierra Nevada, Klamath Mountains, and Related Terranes, Spec. Pap. 225. Boulder, CO: Geol. Soc. Am.

Heller PL, Tabor RW, Suczek CA. 1987. Paleogeographic evolution of the United States Pacific Northwest during Paleogene time. *Can. J. Earth Sci.* 24:1652–67

Hopson CA, Mattinson JM. 1994. Chelan migmatite complex, Washington: field evidence for mafic magmatism, crustal anatexis, mixing, and protodiapiric emplacement. In *Guides to Field Trips, 1994 Geological Society of America Annual Meeting, Seattle, Washington*, ed. DA Swanson, RA Haugerud, pp. 22–23. Seattle: Univ. Wash.

Hyndman RD, Hamilton TS. 1993. Queen Charlotte area Cenozoic tectonics and volcanism and their association with relative plate motions along the northeastern Pacific margin. *J. Geophys. Res.* 98:14257–77

Ingersoll RV. 2000. Models for emplacement of Jurassic ophiolites of northern California. See Dilek et al. 2000, pp. 395–402

Johannson GG, Smith PL, Gordey SP. 1997. Early Jurassic evolution of the northern Stikinian arc: evidence from the Laberge Group, northwestern British Columbia. *Can. J. Earth Sci.* 34:1030–57

Jones DJ, Silberling NJ, Hillhouse J. 1977. Wrangellia—a displaced terrane in northwestern North America. *Can. J. Earth Sci.* 14:2565–77

Karlstrom KE, Harlan SS, Williams HL, McClelland J, Geissman JW, Ahäll KI. 1999. Refining Rodinia: geologic evidence for the Australia–western U.S. connection in the Proterozoic. *GSA Today* 9(10):1–7

Kleinspehn KL 1985. Cretaceous sedimentation and tectonics, Tyaughton–Methow basin, southwestern British Columbia. *Can. J. Earth Sci.* 22:154–74

Lawton TF. 1994. Tectonic setting of Mesozoic sedimentary basins, Rocky Mountain region, United States. In *Mesozoic Systems of the Rocky Mountain Region, USA*, ed. MV Caputo, JA Peterson, KJ Franczyk, pp. 1–25. Denver, CO: Rocky Mountain Sec., SEPM (Soc. Sediment. Geol.).

Lawver LA, Scotese CR. 1987. A revised reconstruction of Gondwanaland. In *Gondwanaland Six: Structure, Tectonics, and Geophysics*, Monogr. 40, pp. 17–23. Washington, DC: Am. Geophys. Union Geophys.

Le Pichon X. 1983. Pangée, géoïde et convection. *C.R. Acad. Sci. Paris (Ser. II).* 296:1313–20

Le Pichon X, Huchon P, Barrier, E. 1985. Pangea, the geoid and the evolution of the western margin of the Pacific Ocean. In *Formation of Active Ocean Margins*, ed. N Nasu, K Kobayashi, S Uyeda, I Kushiro, H Kagami, pp. 3–42. Tokyo: Terra Sci.

Levy M, Christie-Blick N. 1991. Tectonic subsidence of the early Paleozoic passive continental margin in eastern California and southern Nevada. *Geol. Soc. Am. Bull.* 103:1590–606

Lewis PD, Haggart JW, Anderson RG, Hickson CJ, Thompson RI, et al. 1991. Triassic to Neogene geologic evolution of the Queen Charlotte region. *Can. J. Earth Sci.* 28:854–69

Li Z-X, Li X-H, Zhou H, Kinny PD. 2002. Grenvillian continental collision in south China: new SHRIMP U-Pb zircon results and implications for the configuration of Rodinia. *Geology* 30:163–66

Lickorish HW, Simony PS. 1995. Evidence for late rifting of the Cordilleran margin outlined by stratigraphic division of the Lower Cambrian Gog Group, Rocky Mountain main ranges, British Columbia and Alberta. *Can. J. Earth Sci.* 32:860–74

Lonsdale P. 1988. Paleogene history of the Kula plate: offshore evidence and onshore implications. *Geol. Soc. Am. Bull.* 100:733–54

Luepke JJ, Lyons TW. 2001. Pre-Rodinian (Mesoproterozoic) supercontinental rifting along the western margin of Laurentia: geochemical evidence from the Belt-Purcell Supergroup. *Precambrian Res.* 111:79–90

Lund K, Snee LW. 1988. Metamorphism, structural development, and age of the continent–island arc juncture in west-central Idaho. In *Metamorphism and Crustal Evolution of the Western United States*, ed. WG Ernst, pp. 296–331. Englewood Cliffs, NJ: Prentice Hall

Lund K, Aleinikoff JN, Evans KV, Fanning CM. 2003. SHRIMP U-Pb geochronology of the Neoproterozoic Windermere Supergroup, central Idaho: implications for rifting of western Laurentia and synchroneity of Sturtian glacial deposits. *Geol. Soc. Am. Bull.* 113:349–72

MacIntyre DG, Villeneuve ME, Schiarizza P. 2001. Timing and tectonic setting of Stikine terrane magmatism, Babine–Takla Lakes area, central British Columbia. *Can. J. Earth Sci.* 38:579–601

MacLeod SE, Hills LV. 1990. Conformable Late Jurassic–Early Cretaceous strata, northern Bowser basin, British Columbia: a sedimentological and paleontological model. *Can. J. Earth Sci.* 27:988–98

MacNaughton RB, Narbonne GM, Dalrymple RW. 2000. Neoproterozoic slope deposits, Mackenzie Mountains, northwestern Canada: implications for passive-margin development and Ediacaran faunal ecology. *Can. J. Earth Sci.* 37:997–1020

Mahoney JB, Friedman RM, McKinley SD. 1995. Evolution of a Middle Jurassic volcanic arc: stratigraphic, isotopic, and geochemical characteristics of the Harrison Lake Formation, southwestern British Columbia. *Can. J. Earth Sci.* 32:1759–76

Manspeizer W, Cousminer HL. 1988. Late Triassic–Early Jurassic synrift basins of the U.S. Atlantic margin. In *The Atlantic Continental Margin*, ed. RE Sheridan, JA Grow, Vol. I-2, pp. 197–216. Boulder, CO: Geol. Soc. Am. Geol. N. Am.

Marsden H, Thorkelson DJ. 1992. Geology of the Hazelton volcanic belt in British Columbia: implications for the Early to Middle Jurassic evolution of Stikinia. *Tectonics* 11:1266–87

Mattinson JM. 1972. Ages of zircons from the northern Cascade Mountains, Washington. *Geol. Soc. Am. Bull.* 83:3769–84

May SR, Butler RF. 1986. North American Jurassic apparent polar wander: implications for plate motion, paleogeography, and Cordilleran tectonics. *J. Geophys. Res.* 91:11519–44

McClelland WC, Gehrels GE, Saleeby JB. 1992. Upper Jurassic–Lower Cretaceous basinal strata along the Cordilleran margin: implications for the accretionary history of the Alexander-Wrangellia-Peninsular terrane. *Tectonics* 11:823–35

Meert JG, Van der Voo R. 1997. The assembly of Gondwana 800–550 Ma. *J. Geodyn.* 23:223–35

Mihalynuk MG, Nelson JL, Diakow LJ. 1994. Cache Creek terrane entrapment: oroclinal paradox within the Canadian Cordillera. *Tectonics* 13:575–95

Miller DM, Busby C, eds. 1995. *Jurassic Magmatism and Tectonics of the North American Cordillera*, Spec. Pap. 299. Boulder, CO: Geol. Soc. Am.

Monger JWH. 1991. Correlation of the Settler Schist with the Darrington Phyllite and Shuksan Greenschist and its tectonic implications, Coast and Cascade Mountains, British Columbia and Washington. *Can. J. Earth Sci.* 28:447–58

Monger JWH, Price RA, Tempelman-Kluit DJ. 1982. Tectonic accretion and the origin of the two major metamorphic and plutonic welts in the Canadian Cordillera. *Geology* 10:70–75

Mortensen JK. 1992. Pre-mid-Mesozoic tectonic evolution of the Yukon-Tanana terrane, Yukon and Alaska. *Tectonics* 11:836–53

Mortimer N. 1986. Late Triassic, arc-related, potassic igneous rocks in the North American Cordillera. *Geology* 14:1035–38

Mortimer N. 1987. The Nicola Group: Late Triassic and Early Jurassic subduction-related volcanism in British Columbia. *Can. J. Earth Sci.* 24:2521–36

Nelson JL. 1993. The Sylvester allochthon: upper Paleozoic marginal-basin and island-arc terranes in northern British Columbia. *Can. J. Earth Sci.* 30:631–43

Nelson JA, Mihalynuk M. 1993. Cache Creek ocean: closure or enclosure? *Geology* 21:173–76

Orchard MJ, Cordey F, Rui L, Bamber EW, Mamet B, et al. 2001. Biostratigraphic and biogeographic constraints on the Carboniferous to Jurassic Cache Creek terrane in central British Columbia. *Can. J. Earth Sci.* 38:551–78

Patrick BE, McClelland WC. 1995. Late Proterozoic granitic magmatism on Seward Peninsula and a Barentian origin for Alaska-Chukotka. *Geology* 23:81–84

Prave AR. 1999. Two diamictites, two cap carbonates, two δ^{13} excursions, two rifts. *Geology* 27:339–42

Rainbird RH, Jefferson CW, Young GM. 1996. The early Neoproterozoic sedimentary succession B of northwestern Laurentia: correlations and paleogeographic significance. *Geol. Soc. Am. Bull.* 108:454–70

Ramos VA, Aleman A. 2000. Tectonic evolution of the Andes. In *Tectonic Evolution of South America*, ed. UG Cordani, EJ Milani, AT Filho, DA Campos, pp. 635–85. Rio de Janeiro: Int. Geol. Congr. (31st)

Reed BL, Miesch AT, Lanphere MA. 1983. Plutonic rocks of Jurassic age in the Alaska-Aleutian Range batholith: chemical variations and polarity. *Geol. Soc. Am. Bull.* 94:1232–40

Ricketts BD, Evenchick CA, Anderson RG, Murphy DC. 1992. Bowser basin, northern British Columbia: constraints on the timing of initial subsidence and Stikinia–North America terrane interactions. *Geology* 20:1119–22

Roback JC, Walker NW. 1995. Provenance, detrital zircon U-Pb geochronometry, and tectonic significance of Permian to Lower Triassic sandstone in southeastern Quesnellia, British Columbia and Washington. *Geol. Soc. Am. Bull.* 107:665–75

Roback RC, Sevigny JH, Walker NW. 1994. Tectonic setting of the Slide Mountain terrane, southern British Columbia. *Tectonics* 13:1242–58

Ross GM. 1991. Tectonic setting of the Windermere Supergroup revisited. *Geology* 19:1125–28

Ross GM, Parrish RR, Winston W. 1992. Provenance and U-Pb geochronology of the Mesoproterozoic Belt Supergroup (northwestern United States): implications for age of deposition and pre-Panthalassa reconstructions. *Earth Planet. Sci. Lett.* 113:57–76

Ross GM, Villenueve ME, Theriault RJ. 2001. Isotopic provenance of the lower Muskwa assemblage (Mesoproterozoic, Rocky Mountains, British Columbia): new clues to correlation and source areas. *Precambrian Res.* 111:57–77

Rubin CM, Saleeby JB. 1992. Tectonic history of the eastern edge of the Alexander terrane, southeast Alaska. *Tectonics* 11:586–602

Rubin CM, Miller MM, Smith GM. 1990. Tectonic development of Cordilleran mid-Paleozoic volcano-plutonic complexes: evidence for convergent-margin tectonism. See Harwood & Miller 1990, pp. 1–16

Rusmore ME. 1987. Geology of the Cadwallader Group and the Intermontane–Insular superterrane boundary, southwestern British Columbia. *Can. J. Earth Sci.* 24:2279–91

Rusmore ME, Woodsworth GJ. 1991. Distribution and tectonic significance of Upper Triassic terranes in the eastern Coast Mountains and adjacent Intermontane Belt, British Columbia. *Can. J. Eath Sci.* 28:532–41

Rusmore ME, Potter CJ, Umhoefer PJ. 1988. Middle Jurassic terrane accretion along the western edge of the Intermontane Superterrane, southwestern British Columbia. *Geology* 16:891–94

Samson SD, McClelland WC, Patchett PJ, Gehrels GE, Anderson RG. 1989. Evidence from neodymium isotopes for mantle contributions to Phanerozoic crustal genesis in the Canadian Cordillera. *Nature* 337:705–9

Samson SD, Patchett PJ, McClelland WC, Gehrels GE. 1991. Nd and Sr isotopic constraints on the petrogenesis of the west side of the northern Coast Mountains batholith, Alaskan and Canadian Cordillera. *Can. J. Earth Sci.* 28:939–46

Savoy LE, Mountjoy EW. 1995. Cratonic-margin and Antler-age foreland basin strata (Middle Devonian to Lower Carboniferous) of the southern Canadian Rocky Mountains and adjacent plains. In *Stratigraphic Evolution of Foreland Basins*, ed. DL Dorobek, GM Ross, Spec. Publ. 52, pp. 213–31. Tulsa, OK: SEPM (Soc. Sediment. Geol.)

Schweickert RA, Hanson RE, Girty GH. 1999. Accretionary tectonics of the western Sierra Nevada metamorphic belt. In *Geologic Field Trips in Northern California*, ed. DL Wagner, SA Graham, Spec. Publ. 119, pp. 33–79. Sacramento: Calif. Div. Mines Geol.

Schweickert RA, Lahren MM. 1993. Triassic-Jurassic magmatic arc in eastern California and western Nevada: arc evolution, cryptic tectonic breaks, and significance of the Mojave–Snow Lake fault. See Dunne & McDougall 1993, pp. 227–46

Sears JW, Price RA. 2000. New look at the Siberian connection: no SWEAT. *Geology* 28:423–26

Sears JW, Price RA. 2003. Tightening the Siberian connection to western Laurentia. *Geol. Soc. Am. Bull.* 115:943–53

Silberling NJ, Jones DL, Monger JW, Coney PJ. 1992. Lithotectonic terrane map of the North American Cordillera. *U.S. Geol. Surv. Misc. Inv. Ser. Map* I-2176

Smith AD, Brandon AD, Lambert RStJ . 1995. Nd–Sr systematics of Nicola Group volcanic rocks, Quesnel terrane. *Can. J. Earth Sci.* 32:437–46

Smith MT, Gehrels GE. 1991. Detrital zircon geochronology of upper Proterozoic to lower Paleozoic continental margin strata of the Kootenay arc: implications for the early Paleozoic tectonic development of the eastern Canadian Cordillera. *Can. J. Earth Sci.* 28:1271–84

Smith MT, Gehrels GE. 1992a. Structural geology of the Lardeau Group near Trout Lake, British Columbia: implications for the structural evolution of the Kootenay arc. *Can. J. Earth Sci.* 29:1305–19

Smith MT, Gehrels GE. 1992b. Stratigraphic comparison of the Lardeau and Covada Groups: implications for revision of stratigraphic relations in the Kootenay arc. *Can. J. Earth Sci.* 29:1320–29

Smith MT, Dickinson WR, Gehrels GE. 1993. Contractional nature of Devonian-Mississippian Antler tectonism along the North American continental margin. *Geology* 21:21–24

Snyder DB, Clowes RM, Cook FA, Erdmer P, Evenchick CA, et al. 2002. Proterozoic prism arrests suspect terranes: insights into the ancient Cordilleran margin from seismic reflection data. *GSA Today* 12 (10):4–10

Stewart JH, Amaya-Martínez R, Palmer AR. 2002. Neoproterozoic and Cambrian strata of Sonora, Mexico: Rodinian supercontinent to Laurentian continental margin. In *Contributions to Crustal Evolution of the Southwestern United States*, ed. A Barth, Spec. Pap. 365, pp. 5–48. Boulder, CO: Geol. Soc. Am.

Stewart JH, Gehrels GE, Barth AP, Link PK, Christie-Blick N, Wrucke CT. 2001. Detrital zircon provenance of Mesoproterozoic to Cambrian arenites in the western United States and northwestern Mexico. *Geol. Soc. Am. Bull.* 113:1343–56

Struik LC, Schiarizza P, Orchard MJ, Cordey E, Sano H, et al. 2001. Imbricate architecture of the upper Paleozoic to Jurassic oceanic Cache Creek terrane, central British Columbia. *Can. J. Earth Sci.* 38:496–514

Thomson RC, Smith PL, Tipper HW. 1986. Lower to Middle Jurassic (Pliensbachian to Bajocian) stratigraphy of the northern Spatsizi area, north-central British Columbia. *Can. J. Earth Sci.* 23:1965–73

Timmons JM, Karlstrom KE, Dehler CM, Geissman JW, Heizler MT. 2001. Proterozoic multistage (ca. 1.1 and 0.8 Ga) extension recorded in the Grand Canyon Supergroup and establishment of northwest- and north-trending tectonic grains in the southwestern United States. *Geol. Soc. Am. Bull.* 113:163–80

Travers WB. 1978. Overturned Nicola and Ashcroft strata and their relation to the Cache Creek Group, southwestern Intermontane Belt, British Columbia. *Can. J. Earth Sci.* 15:99–116

Umhoefer PJ. 1990. Stratigraphy and tectonic setting of the upper part of the Cadwallader terrane, southwestern British Columbia. *Can. J. Earth Sci.* 27:702–11

Umhoefer PJ, Kleinspehn KL. 1995. Mesoscale and regional kinematics of the northwestern Yalakom fault system: major Paleogene dextral faulting in British Columbia, Canada. *Tectonics* 14:78–94

Umhoefer PJ, Miller RB. 1996. Mid-Cretaceous thrusting in the southern Coast Belt, British Columbia, after strike-slip reconstruction. *Tectonics* 15:545–65

Umhoefer PJ, Schiarizza P. 1996. Latest Cretaceous to early Tertiary dextral strike-slip faulting on the southeastern Yalakom fault system, southeastern Coast Belt, British Columbia. *Geol. Soc. Am. Bull.* 108:768–85

Umhoefer PJ, Schiarizza P, Robinson M. 2002. Relay Montain Group, Tyaughton–Methow basin, southwest British Columbia: a major Middle Jurassic to Early Cretaceous terrane overlap assemblage. *Can. J. Earth Sci.* 39:1143–67

Unterschutz JLE, Creaser RA, Erdmer P, Thompson RI, Daughtry KL. 2002. North American origin of Quesnel terrane strata in the southern Canadian Cordillera: inferences from geochemical and Nd isotopic characteristics of Triassic metasedimentary rocks. *Geol. Soc. Am. Bull.* 114:462–75

Vandall TA, Palmer HC. 1990. Canadian Cordilleran displacement: paleomagnetic results from the Early Jurassic Hazelton Group, Terrane I, British Columbia, Canada. *Geophys. J. Int.* 103:609–19

Van der Heyden P. 1992. A Middle Jurassic to early Tertiary Andean-Sierran arc model for the Coast Belt of British Columbia. *Tectonics* 11:82–97

White JDL, White DL, Vallier TL, Stanley GD Jr, Ash SR. 1992. Middle Jurassic strata link Wallowa, Olds Ferry, and Izee terranes in the accreted Blue Mountains island arc, northeastern Oregon. *Geology* 20:729–32

Wright JE. 1982. Permo-Triassic accretionary subduction complex, southwestern Klamath Mountains, northern California. *J. Geophys. Res.* 87:3805–18

Wright JE, Fahan MR. 1988. An expanded view of Jurassic orogenesis in the western United States Cordillera: Middle Jurassic (pre-Nevadan) regional metamorphism and thrust faulting within an active arc environment, Klamath Mountains, California. *Geol. Soc. Am. Bull.* 100:859–76

Wright JE, Wyld SJ. 1994. The Rattlesnake Creek terrane, Klamath Mountains, California: an early Mesozoic volcanic arc and its basement of tectonically disrupted oceanic crust. *Geol. Soc. Am. Bull.* 106:1033–56

Wyld SJ. 2002. Structural evolution of a Mesozoic backarc fold-thrust belt in the U.S. Cordillera: new evidence from northern Nevada. *Geol. Soc. Am. Bull.* 114:1452–68

Yates RG. 1968. The trans-Idaho discontinuity. *23rd Int. Geol. Congr.* 1:117–23

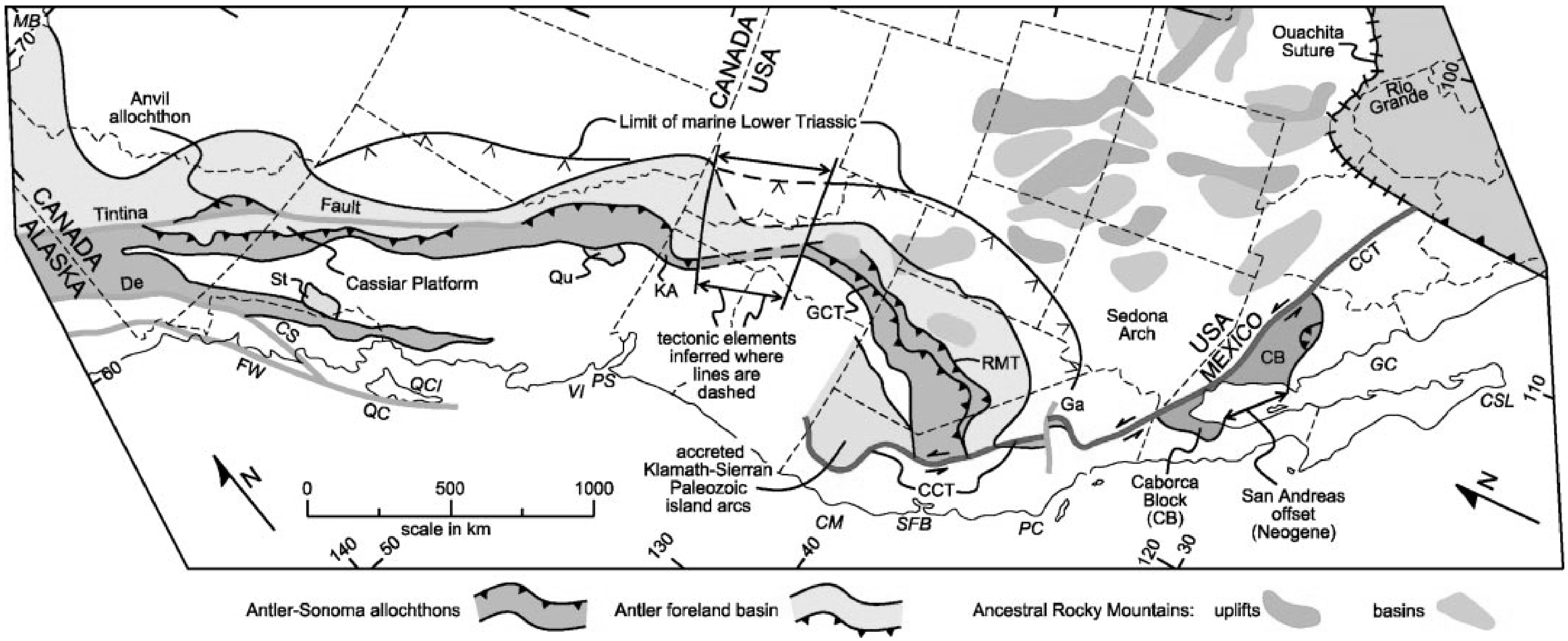

Figure 6 Geotectonic features of the Antler orogen (Late Devonian–Early Mississippian), the Ancestral Rocky Mountains province (Pennsylvanian–Early Permian), and the Sonoma orogen (Late Permian–Early Triassic) of the North American Cordillera (allochthons of Antler and Sonoma age are combined, but note the uncertain continuity of tectonic trends along the trans-Idaho discontinuity of Figure 5). See text for discussion of Kootenay structural arc (KA) and remnants of Paleozoic arc assemblages in Quesnellia (Qu) and Stikinia (St). Key active faults: RMT, Devonian-Mississippian Roberts Mountains thrust; GCT, Permian-Triassic Golconda thrust; CCT, Permian-Triassic California-Coahuila transform. Gondwanan Mexico restored (after Dickinson & Lawton 2001a) to position before mid-Mesozoic opening of the Gulf of Mexico. Tintina and De-CS-FW-QC fault systems are Cenozoic structures. See Figure 5 for geographic legend.

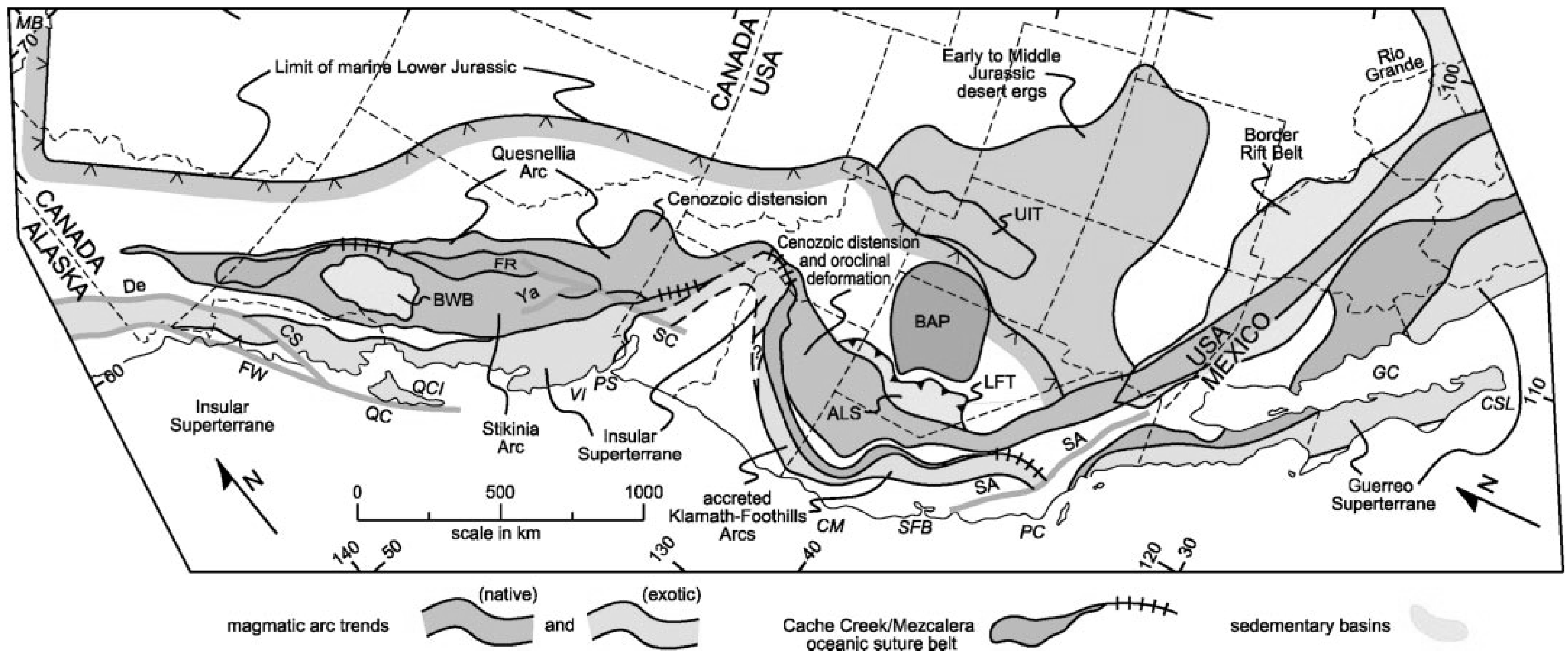

Figure 7 Mid-Early Triassic (~247.5 Ma) to mid-Early Cretaceous (~120 Ma) geotectonic features of the Cordilleran arc-trench system, including intraoceanic arc structures accreted to the Cordilleran continental margin between Middle Jurassic and Early Cretaceous time. Selected geologic features: ALS, Late Triassic to Early Jurassic Auld Lang Syne backarc basin; LFT, Middle Jurassic Luning-Fencemaker backarc thrust system; BAP, zone of diffuse Middle to Late Jurassic backarc plutonism (Nevada-Utah); UIT, Middle to Late Jurassic Utah-Idaho backarc trough; BWB, Late Jurassic to Early Cretaceous Bowser successor basin (superimposed on accreted Stikinia arc). Border rift belt (Late Jurassic to Early Cretaceous) includes Bisbee basin and Chihuahua trough. Cenozoic faults (*gray*): De-CS, Denali-Chatham Strait; FR, Fraser River; FW, Fairweather; QC, Queen Charlotte; RL, Ross Lake; SA, San Andreas; SC, Straight Creek; Ya, Yalakom. See Figure 5 for geographic legend.

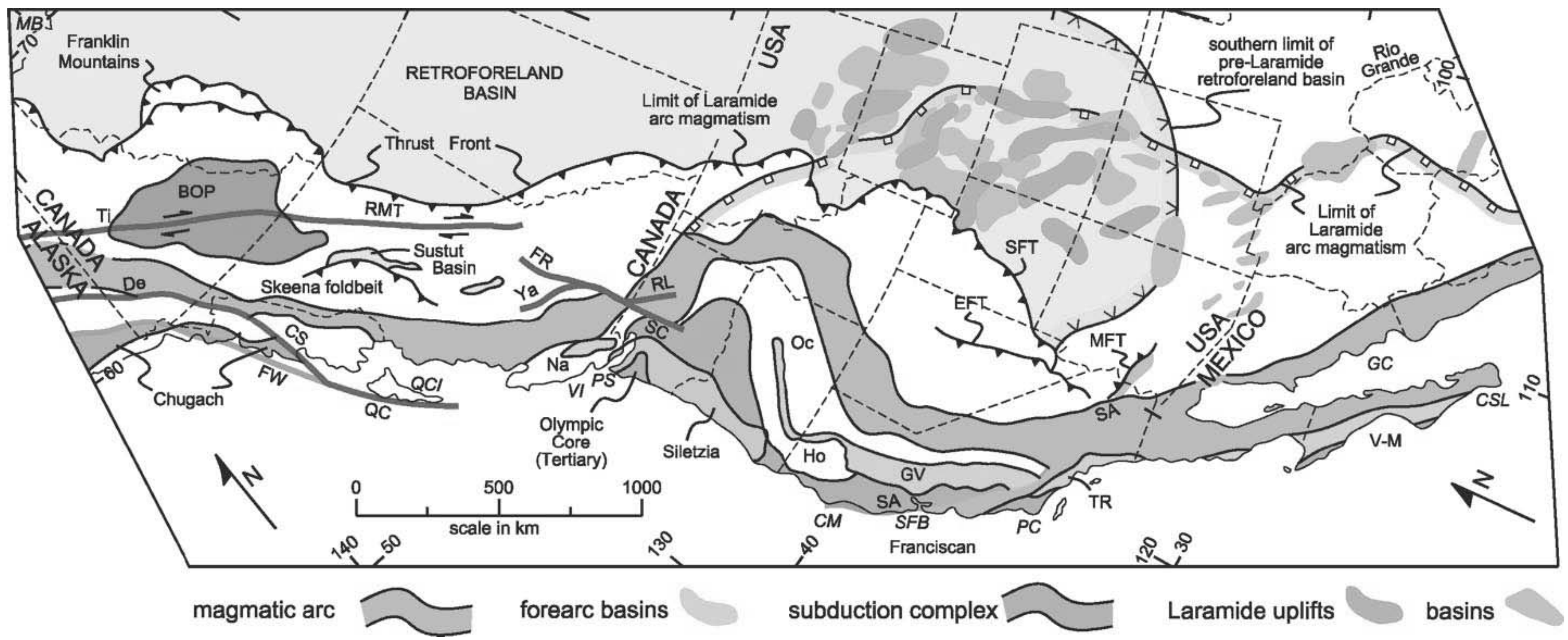

Figure 9 Mid-Early Cretaceous (~120 Ma) to mid-Cenozoic (Eocene/Oligocene boundary) geotectonic features of the Cordilleran arc-trench system, including the Laramide province of intracontinental deformation. The main batholith belt is delineated as the magmatic arc, but subsidiary arc magmatism spread inland for varying distances (BOP, Omineca zone of backarc mid-Cretaceous plutonism). Active Paleogene strike-slip faults (*red lines*): De-CS, Denali-Chatham Strait; FR, Fraser River; QC, Queen Charlotte; RL, Ross Lake; SC, Straight Creek; Ti-RMT, Tintina–Rocky Mountain Trench; Ya, Yalakom. Younger Neogene strike-slip faults (*gray lines*): FW, Fairweather; SA, San Andreas. Key active fold-thrust belts: EFT, Eureka; MFT, Maria; SFT, Sevier. Key forearc basin segments: GV, Great Valley (California); Ho, Hornbrook; Oc, Ochoco; Na, Nanaimo; TR, Transverse Ranges; V-M, Vizcaino-Magdalena. See Figure 5 for geographic legend.

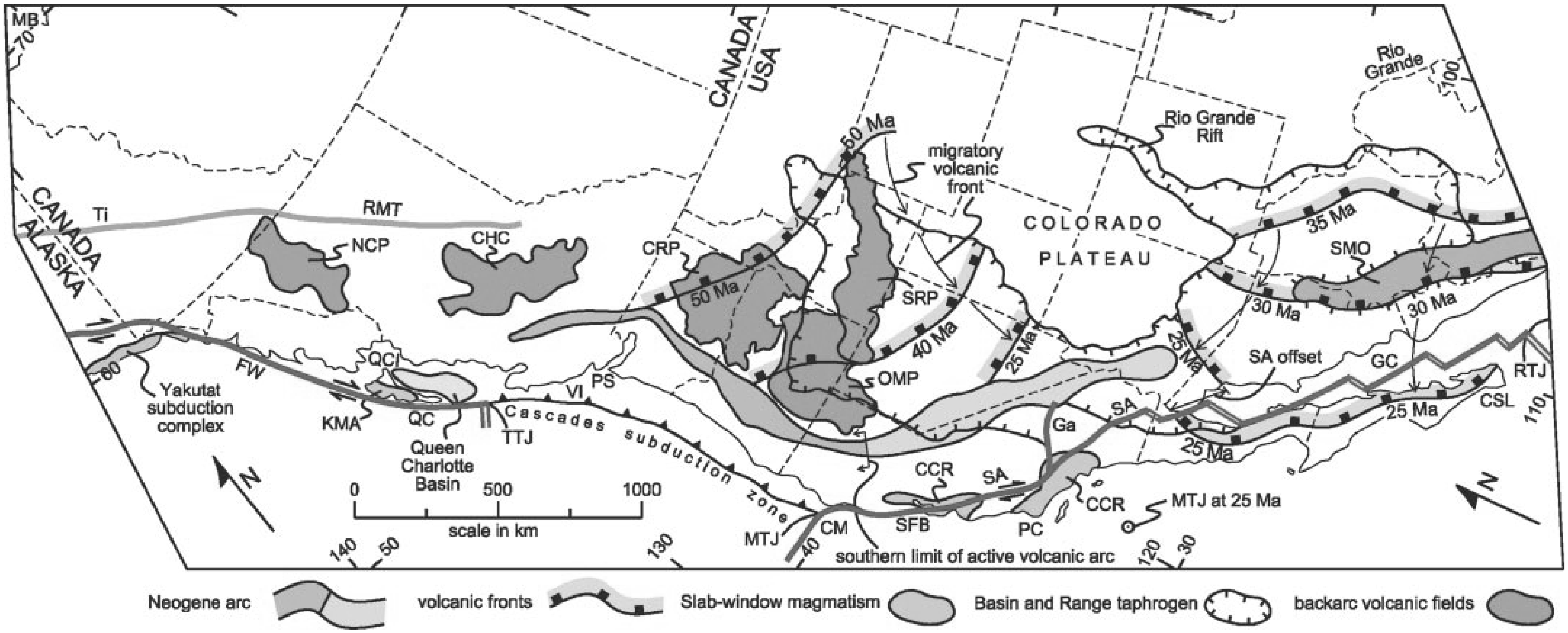

Figure 10 Post-Eocene geotectonic features of the North American Cordillera, including the Basin and Range taphrogen (SMO, Paleogene magmatic arc remnant in the Sierra Madre Occidental). Active Neogene strike-slip faults (*red lines*): FW, Fairweather; Ga, Garlock; QC, Queen Charlotte; SA, San Andreas. Offshore triple plate junctions: MTJ, Mendocino (FFT); RTJ, Rivera (RTF); TTJ, Tofino (RTF). Slab-window magmatism (near the coastal transform systems): CCR, California Coast Ranges (28–0 Ma); KMA, Queen Charlotte Islands (46–17 Ma). Backarc lava fields (erupted inland from main Cordilleran arc trend): CHC, Chilcotin (14–6 Ma); CRP, Columbia River Plateau (17–8 Ma); NCP, Northern Cordilleran Province (8–0 Ma); OMP, Oregon-Modoc Plateau (17–7 Ma); SRP, Snake River Plain (16–0 Ma). See Figure 5 for geographic legend.

Reference Material

Evolution of the northern Cordilleran foreland basin during the middle Cretaceous

Yongtai Yang[†]
Andrew D. Miall
Department of Geology, University of Toronto, 22 Russell Street, Toronto, Ontario M5S 3B1, Canada

ABSTRACT

A detailed study of the middle–late Cenomanian Belle Fourche Formation in southern Alberta helps to elucidate the evolution of the Cordilleran foreland basin during the middle Cretaceous. By combining isopach data from the study area with previously published research on middle Cretaceous stratigraphy in adjacent areas of northern Alberta and Montana, it is possible to define the position of the proximal foredeep, forebulge, and backbulge depozones from late Albian to Cenomanian time.

The foredeep probably lay to the west of the present fold-thrust belt in western Montana from the late Albian to middle Cenomanian, with the forebulge extending northwestward through the northwest corner of Wyoming and curving northeastward through the present-day location of Calgary. Thick Dunvegan deposits (middle Cenomanian) of northwestern Alberta are interpreted as foredeep deposits. Palinspastic reconstruction of the southern Rocky Mountains of Alberta is consistent with a location of the foredeep within the area of the present fold-thrust belt.

At the end of the middle Cenomanian the forebulge retreated westward within Alberta, defining a nearly straight northwest-southeast trend through the present position of the Foothills and Front Ranges of Alberta and northwestern Montana. The change in trend of the foreland basin at the end of the middle Cenomanian may reflect the change of convergence vectors along the western margin of North America during the middle Cretaceous.

Keywords: Cordilleran tectonics, foreland basin, middle Cretaceous, Alberta, Montana.

[†]E-mail: yongtai.yang@utoronto.ca

INTRODUCTION

Quantitative flexural models have demonstrated that the subsidence in the Cretaceous Cordilleran foreland basin was mainly driven by the lithospheric loading of Cordilleran thrust sheets (Beaumont, 1981; Jordan, 1981). Flexural subsidence and sedimentary infilling in the basin can be correlated with thrusting events. For example, the thick deltaic and coastline deposits of the late Albian–Santonian Colorado Group in northwestern Alberta (Leckie and Smith, 1992; Bhattacharya, 1994; Leckie et al., 1994) and in western Montana (Schwartz, 1982; Schwartz and DeCelles, 1988; Dyman et al., 1997) reflect intense flexural subsidence of the foreland basin during the middle Cretaceous (Figs. 1A and 2). However, in southern Alberta and northwestern Montana the Colorado Group consists primarily of marine shale with an almost uniform thickness of 500–700 m and does not show the typical isopach pattern of a foreland basin with a thick foredeep deposit (Fig. 1A). At times of widespread shale deposition through northern Montana and southern Alberta, the area may not have undergone much flexural subsidence, with sedimentary accommodation reflecting eustatic sea-level change and regional downflexing of the North American craton (e.g., McMechan and Thompson, 1993; Pang and Nummedal, 1995).

A foreland basin system comprises four distinct zones: the wedge-top, foredeep, forebulge, and backbulge depozones (DeCelles and Giles, 1996). The position, orientation, and tectonic evolution of these components are dependent on the orientation and rate of convergence of the supracrustal load. A synthesis of stratigraphic and structural data for the U.S. portion of the Cordilleran foreland basin enabled DeCelles (2004) to reconstruct the position of the foredeep and forebulge several times during the Late Jurassic to Eocene evolution of that basin. Isopach patterns outline the changing positions of the foredeep and forebulge of the foreland basin in response to the changes in orientation of crustal stress. Preservation of a stratigraphic record over the forebulge may require that accommodation was available as a result of high eustatic sea levels or subsidence from dynamic topography, or both. This paper attempts to make a comparable reconstruction of the Montana-Alberta portion of the basin, based on a synthesis of stratigraphic data.

The reconstructed displacement history between western North America and adjacent oceanic plates shows that, along the western margin of North America, convergence was in a more-or-less east-west direction at a velocity of ~100 km/m.y. during the Late Jurassic–Early Cretaceous and in a northeast-southwest direction at a rate of ~200 km/m.y. during the Late Cretaceous–Eocene (Engebretson et al., 1985). This change is reflected in the structural evolution of the Front Range fold-thrust belt. The formation of several northwest-dipping reverse faults in the southern Canadian Cordillera has been attributed to the Late Jurassic–Early Cretaceous phase of convergence (Price and Sears, 2000) (Fig. 1A). The Late Cretaceous–Paleocene convergence resulted in intense northeast-verging folding and thrusting in the Rocky Mountain fold and thrust belt and horizontal shortening of >250 km across the belt near lat 53°N (Price 1994; Price and Sears, 2000) (Fig. 1A).

The middle to late Cenomanian Belle Fourche Formation of southern Alberta has been chosen as the main focus of this paper in order to explore the evolution and subsidence mechanisms of the northern Cordilleran foreland basin during the middle Cretaceous (Fig. 2). We investigated an area of ~60,000 km^2 in southern Alberta, using data from 61 cores and 1515 wells, including 35 wells in northwestern Montana (Fig. 1B) in order to establish a detailed allostratigraphy for this unit. Based on the more subtle stratigraphic features of the forebulge and backbulge zones, where strata are well preserved, this study focuses on deducing the position of the foredeep zone and the evolutionary history of the northern Cordilleran foreland basin during

GSA Bulletin; March/April 2009; v. 121; no. 3/4; p. 483–501; doi: 10.1130/B26374.1; 11 figures.

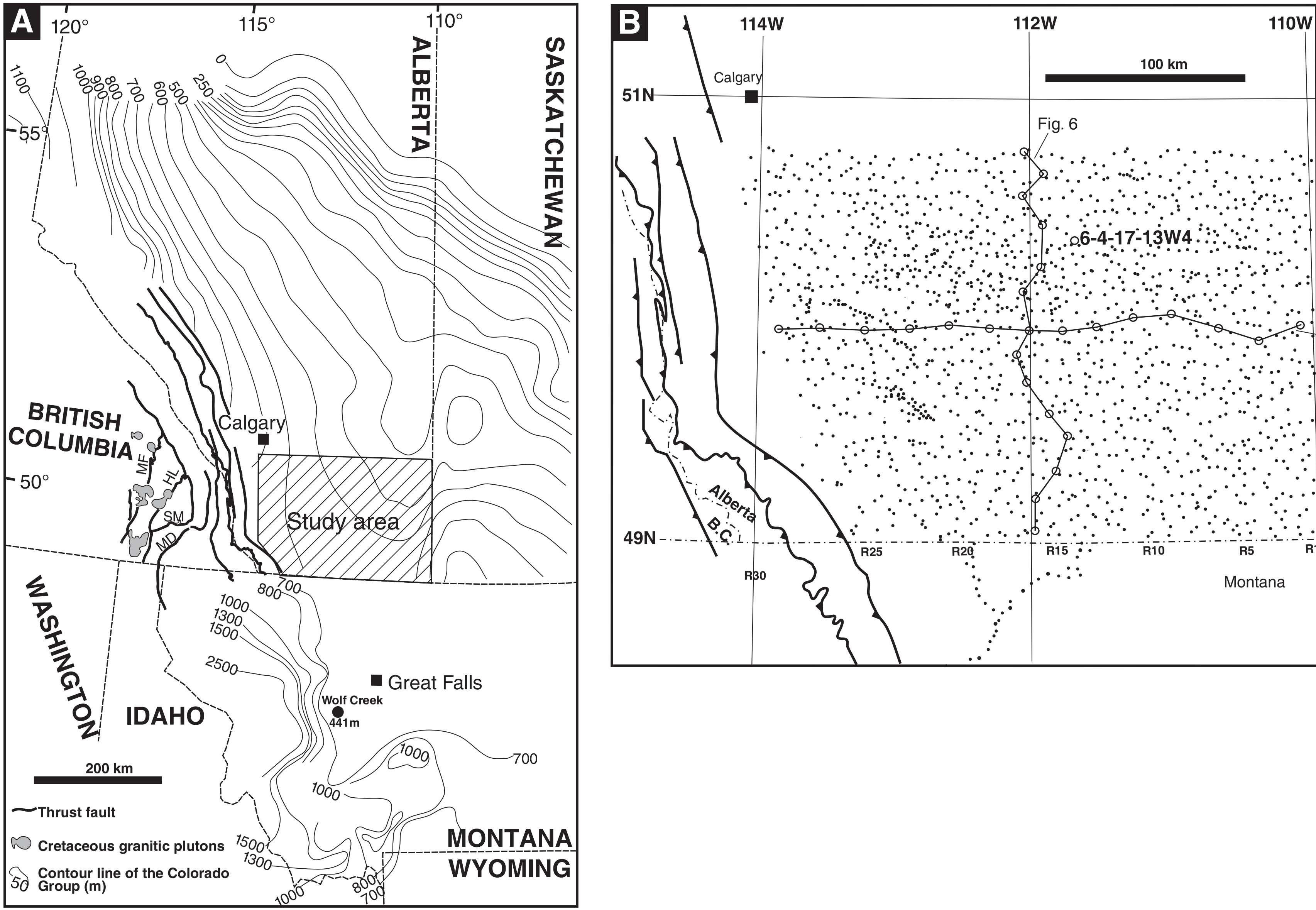

Figure 1. Location of study area. (A) Isopach map of the late Albian to Santonian Colorado Group in Alberta and western Saskatchewan (Leckie and Smith, 1992), restored isopach map of the Colorado Group in western Montana (Schwartz and DeCelles, 1988), and thickness of the Colorado Group at Wolf Creek (tp. 15N, rge. 4W) in western Montana (Schmidt, 1978). Thicknesses in meters. Cretaceous granitic plutons and major thrust faults of the Cordilleran orogenic belt are shown (Price and Sears, 2000). MF—Mount Forester fault; HL—Hall Lake fault; SM—St. Mary fault; MD—Moyie–Dibble Creek fault. (B) Locations of 1480 wells in southern Alberta and 35 wells in northwestern Montana from which logs were used to define the allostratigraphy of the Belle Fourche Formation. Also, locations of wells from which logs were used to construct cross sections (Figs. 5 and 6) are shown.

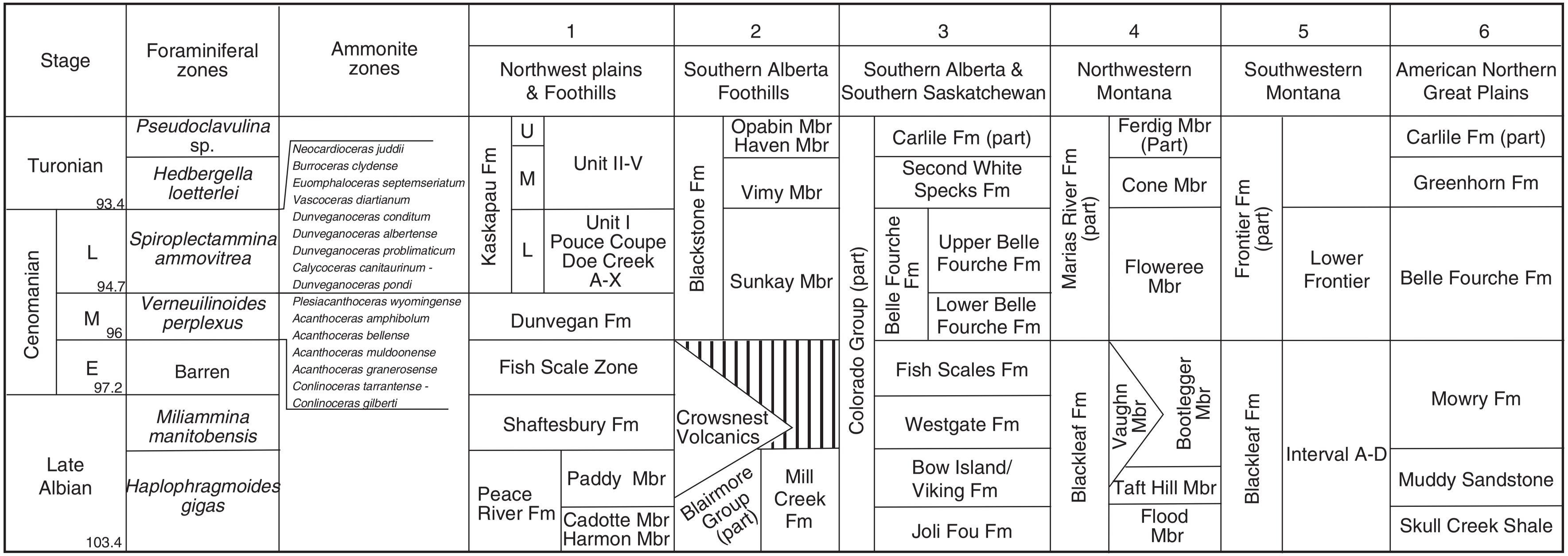

Figure 2. Stratigraphic nomenclature and microfaunal zones of the late Albian to Turonian strata in the northern Cordilleran foreland basin. Stage boundaries and ages are from Kauffman et al. (1993). Foraminiferal zones are after Caldwell et al. (1978) and Tyagi et al. (2007). Ammonite zones are after Obradovich (1993). Column 1 nomenclature is after Leckie et al. (1994), Plint (2000), and Varban and Plint (2005); column 2 after Glaister (1959) and Stott (1963); column 3 after Bloch et al. (1993), SchroderAdams et al. (1996), and Tyagi et al. (2007); column 4 after Cobban et al. (1976) and Lang and McGugan (1988); column 5 after Schwartz (1982) and Dyman and Tysdal (1998); and column 6 after McGookey (1972).

the middle Cretaceous. It is suggested that the foredeep zone of the foreland basin would have been located within the area of the Front Ranges of the Rocky Mountains during the middle Cretaceous, but it is now mostly missing owing to postdepositional erosion and cannibalization. This paper provides an example for studies in other foreland basins in which facies patterns and the geometries of strata may be used to deduce the subsidence patterns and basin evolution through time.

STRATIGRAPHY

A stratigraphic framework for the undifferentiated shale of the Colorado Group in the subsurface of southern Alberta and southern Saskatchewan includes, in ascending order, the Westgate, Fish Scales, Belle Fourche, and Second White Specks Formations (Bloch et al., 1993; Schroder-Adams et al., 1996) (Fig. 2). The Belle Fourche Formation consists of shale and siltstone coarsening upward to fine-grained sandstone near the top, and in general conformably overlies the Fish Scales Formation (Bloch et al., 1993). The Belle Fourche Formation is subdivided into lower and upper parts (Ridgley et al., 2001; Pedersen, 2004; Tyagi et al., 2007). The Lower Belle Fourche Formation contains the *Verneuilinoides perplexus* foraminiferal zone and the *Conlinoceras tarrantense–Conlinoceras gilberti* ammonite zones, and is of middle Cenomanian age (Ridgley et al., 2001; Tyagi et al., 2007) (Fig. 2). The Upper Belle Fourche Formation contains the *Spiroplectammina ammovitrea* foraminiferal zone, which equates approximately with the late Cenomanian *Dunveganoceras pondi–Dunveganoceras conditum* ammonite zones, and is of late Cenomanian age (Ridgley et al., 2001; Tyagi et al., 2007) (Fig. 2). On the basis of our detailed well-log correlation, an isopach map of the Belle Fourche Formation in southern Alberta has been constructed (Fig. 3). In general, it shows a markedly northwest-trending prismatic geometry, thinning from 50 to 70 m in a central thick zone southwestward to <30 m and northeastward to <40 m.

ALLOSTRATIGRAPHY

An allostratigraphic unit is defined and identified as a mappable body of rocks bounded by discontinuities (NACSN, 1983). These bounding discontinuities can include unconformities, disconformities, omission surfaces, discontinuity surfaces, and flooding surfaces (Bhattacharya and Walker, 1991). Allostratigraphic methods have been used for many subdivisions of the Cretaceous rocks of western Canada, and major flooding surfaces correlatable over hundreds of kilometers are usually selected as representing chronostratigraphically significant bounding discontinuities (e.g., Bhattacharya and Walker, 1991; Plint, 2000).

This study also uses widespread flooding surfaces as the boundaries of allomembers and subdivides the Belle Fourche Formation into five allomembers, A–E (Figs. 4, 5A, and 6A). Our Allomember A and Allomembers B–E correspond with the Lower and Upper Belle Fourche Formation as named by Tyagi et al. (2007), respectively (Fig. 2). These allomembers coarsen upward from dark shale to bioturbated or laminated shaly siltstone. In southeastern Alberta and southwestern Saskatchewan, hummocky cross-stratified or parallel-laminated fine sandstones are at the top of Allomember A and Allomember E, which are important reservoirs for biogenic gas.

Allomember A is mainly composed of shale with thin, shaly siltstone and fine sandstone at the top (Figs. 4, 5A, and 6A). It forms a thinning wedge, decreasing from 20 m at the Alberta-Saskatchewan border westward to 0–8 m in southwestern Alberta (Fig. 7A). Its isopach lines trend north in southeastern Alberta but north-northwest in southwestern Alberta. Well-log correlation in southwestern Saskatchewan shows that the Lower Belle Fourche Formation (Allomember A), with a thickness of 20–45 m, extends beyond central southern Saskatchewan (Pedersen, 2004) (Fig. 8).

Allomembers B and C mainly consist of shale, coarsening upward into shaly siltstone (Figs. 4, 5A, 6A). They have similar isopach patterns, with a northwest-trending thick zone near the southern Alberta Foothills, thinning northeastward to several meters at the Alberta-Saskatchewan border (Figs. 7B and 7C). The thickest zones show a southwestward-tapering tendency toward the southwestern corner of the study area.

Allomember D mainly consists of shale, coarsening upward into shaly siltstone (Figs. 4, 5A, and 6A). It shows a markedly northwest-trending prismatic geometry, thinning from 16 to 20 m in the central part of the study area southwestward to zero and northeastward to <2 m (Fig. 7D).

Allomember E is mainly composed of shale and shaly siltstone with fine sandstone at the top (Figs. 4, 5A, and 6A). Its thick zone trends northwest in the northeastern part of the study area, with a tapering tendency northeastward, and thins southwestward to a northwest-trending thin zone with a thickness of 0–4 m in southwestern Alberta (Fig. 7E). Note that Allomember E gradually thickens southwestward to 8 m in the southwestern corner of the study area.

In comparison with isopach maps of the other four allomembers of the Belle Fourche Formation, that of Allomember A has a notably different pattern (Fig. 7). The isopach lines of Allomember A trend mainly north in southeastern Alberta and show a north-northwest–trending thin zone ~150–200 km wide in southwestern Alberta. However, it can be seen that the thin and thick zones shift progressively northeastward from Allomember B to E (Figs. 5–7). Younger strata of the Upper Belle Fourche Formation onlap underlying Allomember A northeastward, and the whole Upper Belle Fourche Formation thins northeastward. The gradually thinning Upper Belle Fourche Formation dies out in central southern Saskatchewan (Pedersen, 2004) (Fig. 8). Therefore, we disagree with the suggestion by Ridgley et al. (2001) that the thinning of the Upper Belle Fourche Formation is because of a widespread unconformity between the Belle Fourche Formation and the Second White Specks Formation in southern Alberta, southern Saskatchewan, and northern Montana.

COLORADO GROUP IN ALBERTA AND MONTANA

In order to develop a regional picture of the evolution of the Belle Fourche Formation, we discuss here the correlation of this unit with older and younger strata in Montana and elsewhere in Alberta. In northeastern British Columbia and northwestern Alberta the late Albian–Santonian Colorado Group has a thickness of >1150 m, and its isopach lines intersect the Rocky Mountain thrust belt at a high angle (Leckie and Smith, 1992) (Figs. 1A and 2). In western Montana the Colorado Group has a maximum thickness of 2500 m, and it thins eastward markedly to 411 m in the Wolf Creek area (Schmidt, 1978; Schwartz and DeCelles, 1988) (Fig. 1A).

Upper Albian

The late Albian Joli Fou and Viking Formations thin from 160 m in northeastern British Columbia to 20–40 m in central Alberta and then thicken to 60–160 m in southern Alberta and southern Saskatchewan (Reinson et al., 1994) (Figs. 2 and 9A). The latest Albian Shaftesbury Formation has a thickness of 500 m in northeastern British Columbia, and its equivalent Westgate Formation is 0–20 m thick in central Alberta and 140 m in southwestern Saskatchewan (Leckie et al., 1994) (Figs. 2 and 9B). Well-log cross sections for southern Alberta show thinning and pinch-out of the Westgate Formation westward to the Alberta Foothills (Fig. 5A). Using outcrop and subsurface sections, Glaister (1959) correlated the Early Cretaceous strata in central and southern Alberta and northwestern Montana, and Lang and McGugan (1988)

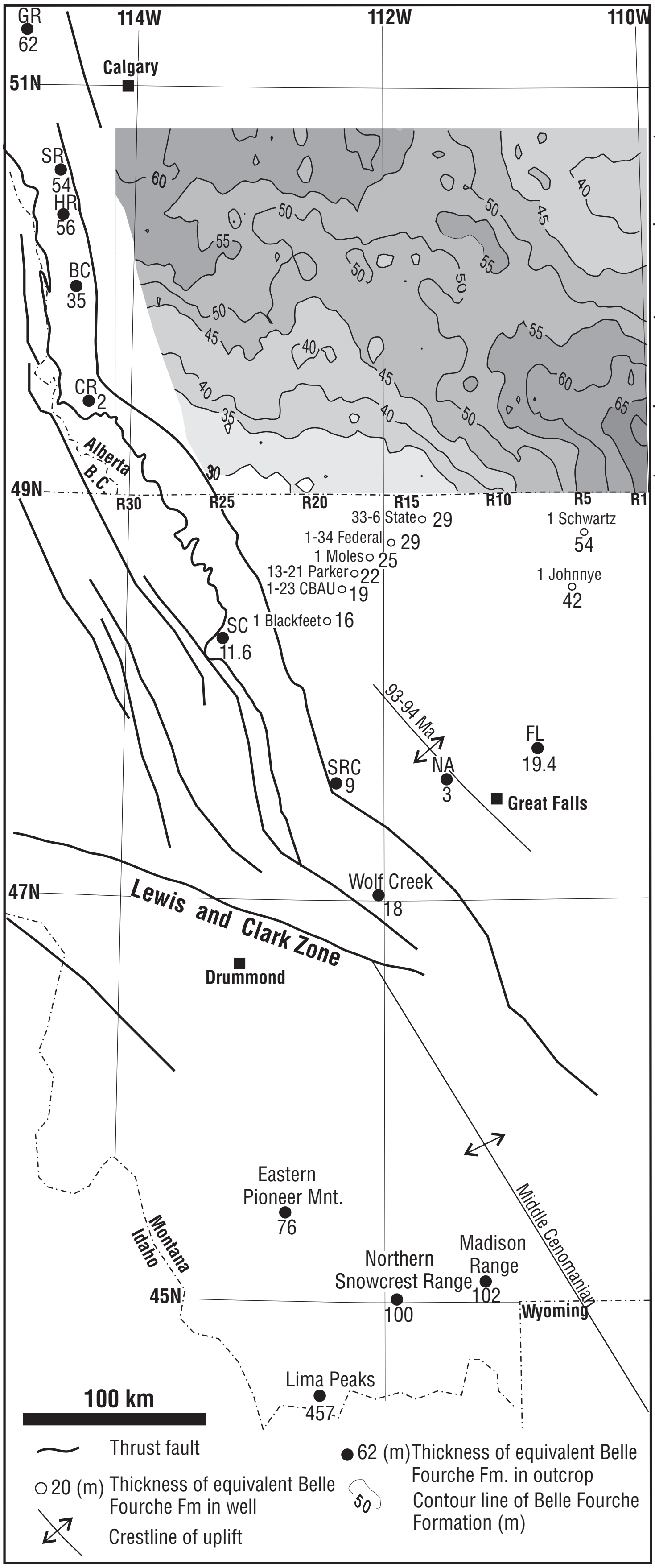

Figure 3. Distribution of the time equivalent Belle Fourche Formation in southern Alberta and western Montana. Thicknesses (in meters) of the Belle Fourche Formation in outcrops in southern Alberta Foothills are from Stott (1963) and Leckie et al. (2000): GR—Ghost River (sec. 4, tp. 27, rge. 7, W5); SR—Sheep River (tp. 19, rge. 5, W5); HR—Highwood River (sec. 28, tp. 18, rge. 3, W5); BC—Bruin Creek (50°00.919′, 114°24.926′); CR—Castle River (sec. 11, tp. 6, rge. 4, W5). Thicknesses of the Floweree Member of the Marias River Formation in outcrops in northwestern Montana are from Cobban et al. (1976): SC—Summit Creek (tp. 30N, rge. 13W); SRC—Sun River Canyon (tp. 22N, rge. 8W); VA—Vaughn (sec. 6, tp. 21N, rge. 1E); FL—Floweree (sec. 16, tp. 23N, rge. 6E). The well 1 Schwartz and the well 1 Johnnye in northern Montana are from Ridgley et al. (2001), and the Wolf Creek outcrop (tp. 15N, rge. 4W) in western central Montana is from Schmidt (1978). Middle and late Cenomanian crestlines of uplift are from Merewether and Cobban (1986). Thicknesses of the Lower Frontier Formation in outcrops in southwestern Montana: Eastern Pioneer Mountains (sec. 28, tp. 4S, rge. 9W) is from Dyman and Tysdal (1998), Madison Range (sec. 7, tp. 9S, rge. 4E) from Tysdal (1991), Northern Snowcrest Range (sec. 18, tp. 9S, rge. 3W) from Dyman et al. (1988), and Lima Peaks (sec. 18, tp. 15S, rge. 8W) from Dyman et al. (1989).

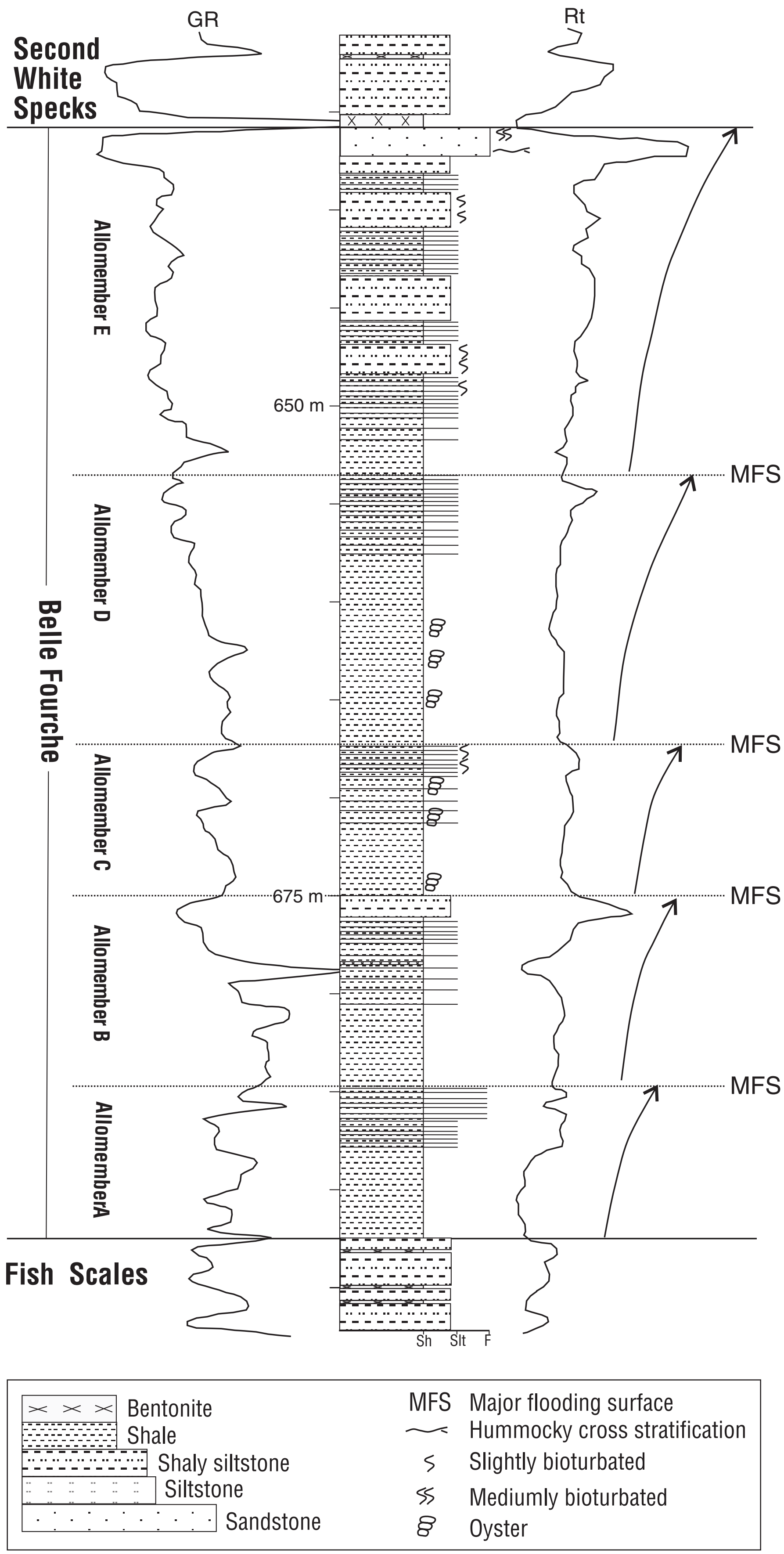

Figure 4. Allostratigraphy of the Belle Fourche Formation in well 6–4-17–13W4 (see Fig. 1B for location). Subdivision of the formation into five allomembers was based on the recognition of major flooding surfaces (MFS) from well logs and core logs. Arrows show shallowing upward of relative sea level. GR—gamma ray; Rt—true resistivity.

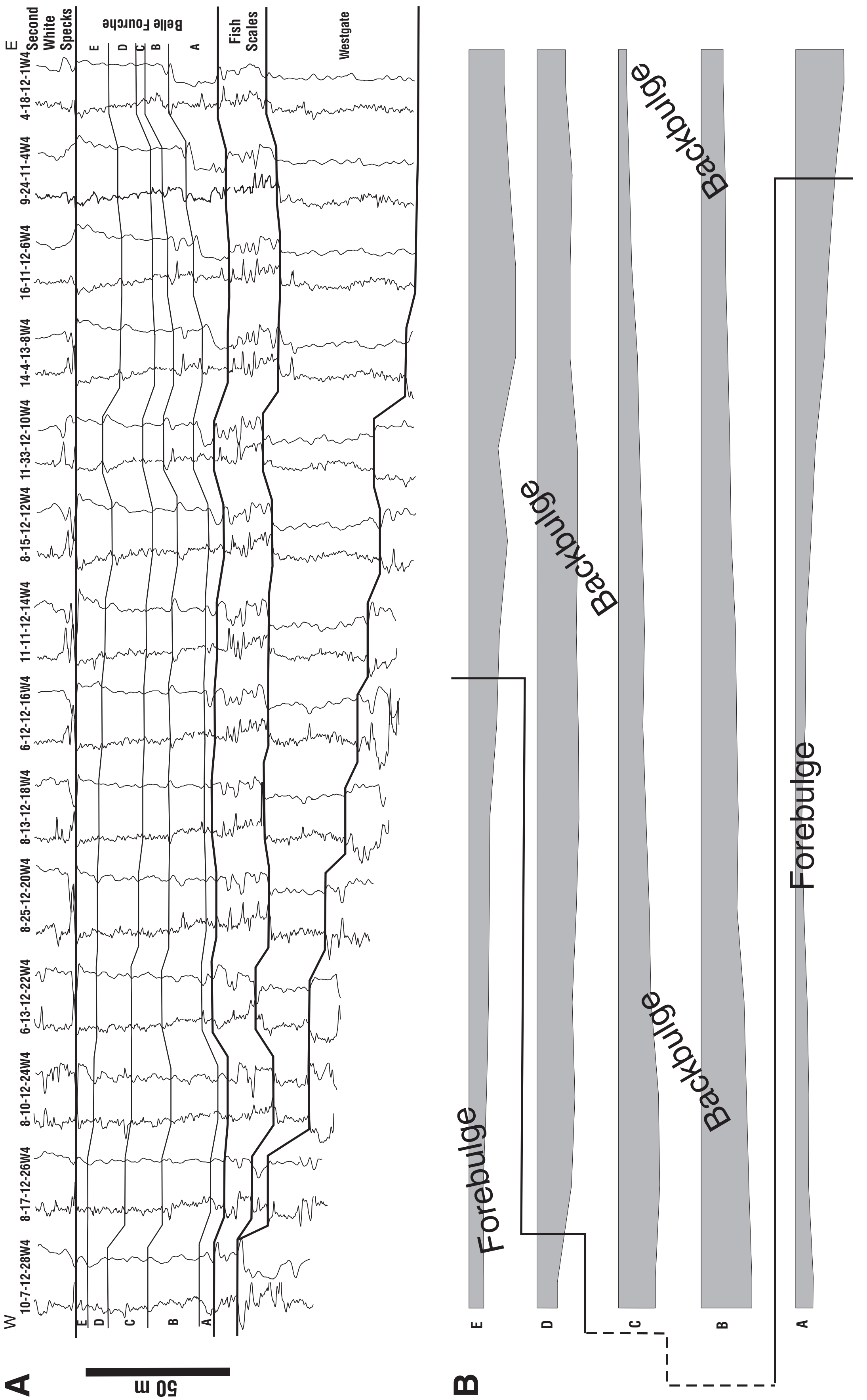

Figure 5. (A) West-east cross section of the Belle Fourche Formation in southern Alberta, using gamma ray log (left curve) and resistivity log (right curve) for each well (see Fig. 1B for line of sections). (B) Interpretation of basin evolution of five allomembers according to the foreland-basin-system concept (DeCelles and Giles, 1996).

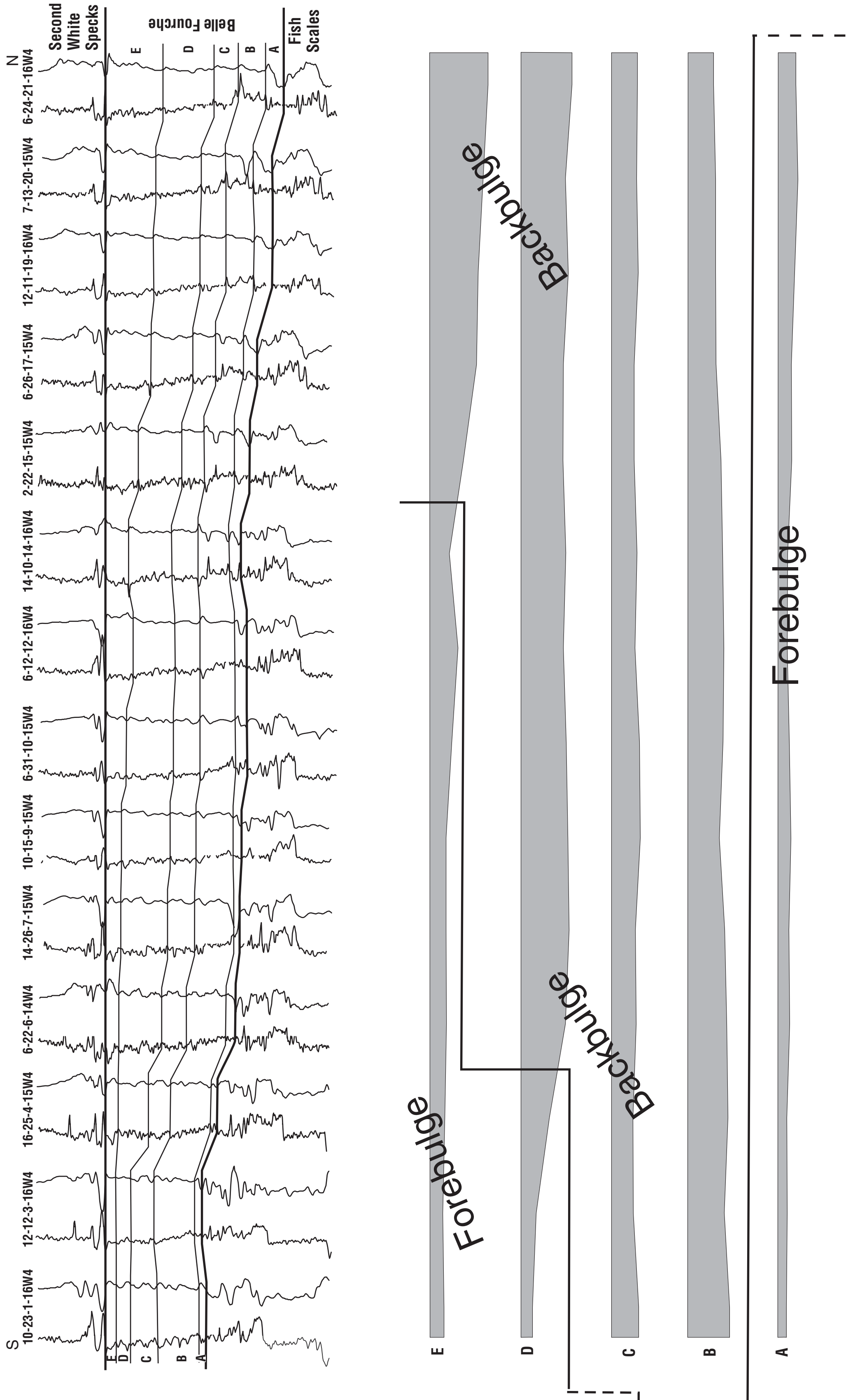

Figure 6. (A) South-north cross section of the Belle Fourche Formation in southern Alberta, using gamma ray log (left curve) and resistivity log (right curve) for each well (see Fig. 1B for line of section). (B) Interpretation of basin evolution of five allomembers according to the foreland-basin-system concept (DeCelles and Giles, 1996).

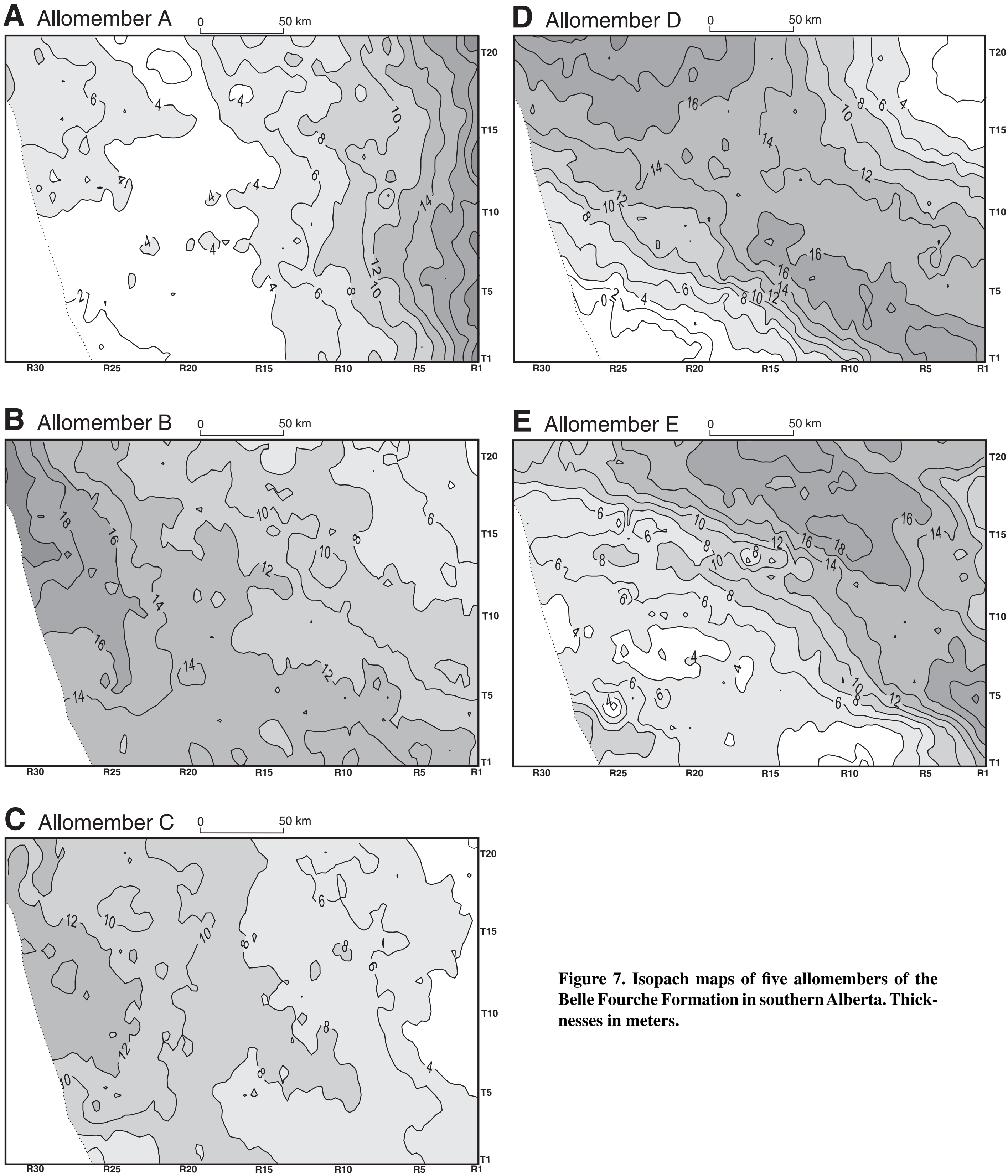

Figure 7. Isopach maps of five allomembers of the Belle Fourche Formation in southern Alberta. Thicknesses in meters.

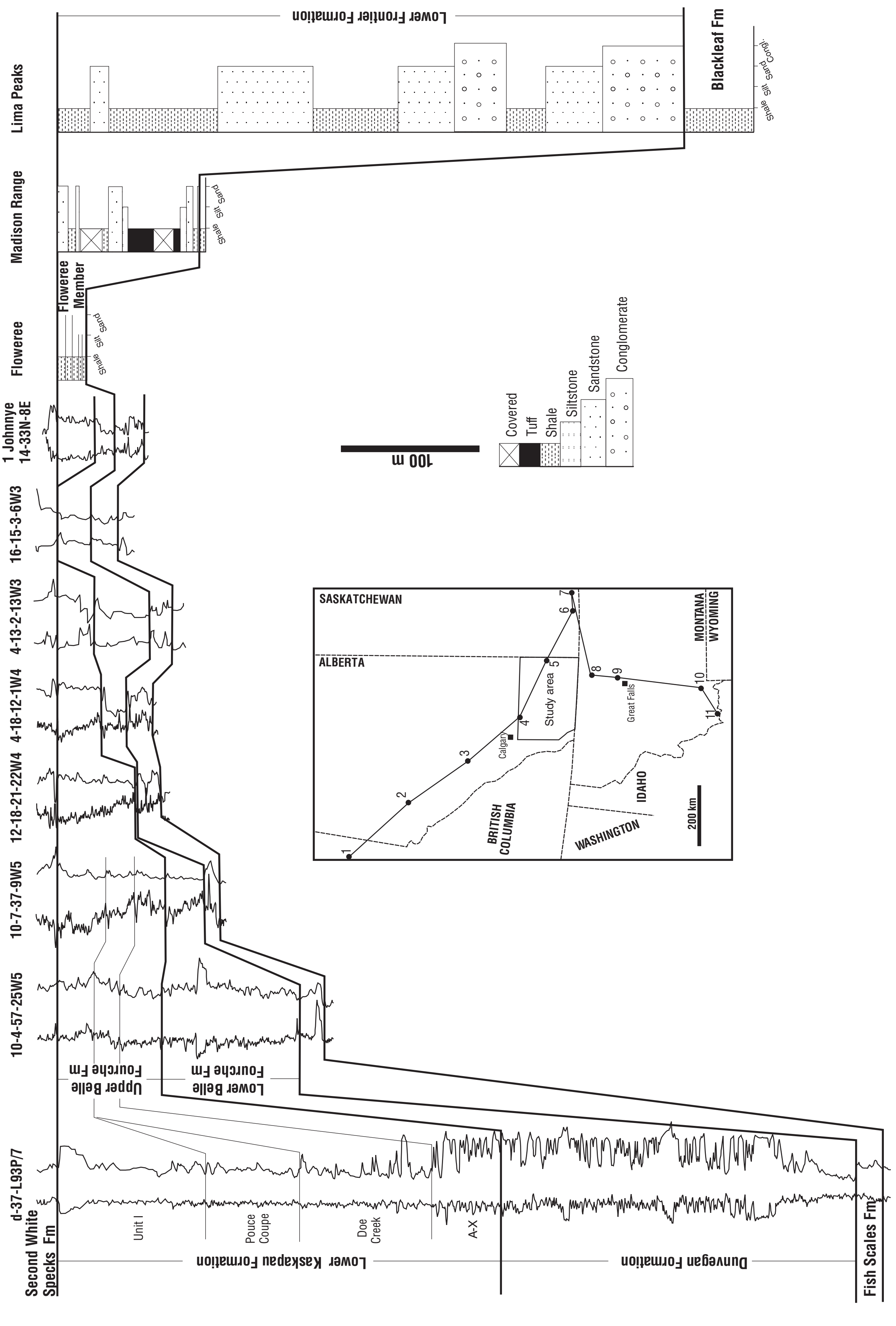

Figure 8. Cross section of Cenomanian strata in the northern Cordilleran foreland basin: 1 is from Plint (2000), Varban and Plint (2005), and Kreitner and Plint (2006); 2 and 3 are from Tyagi et al. (2007); 6 and 7 are from Pedersen (2004); 8 is from Ridgley et al. (2001); 9 is from Cobban et al. (1976); 10 is from Tysdal (1991); and 11 is from Dyman et al. (1988).

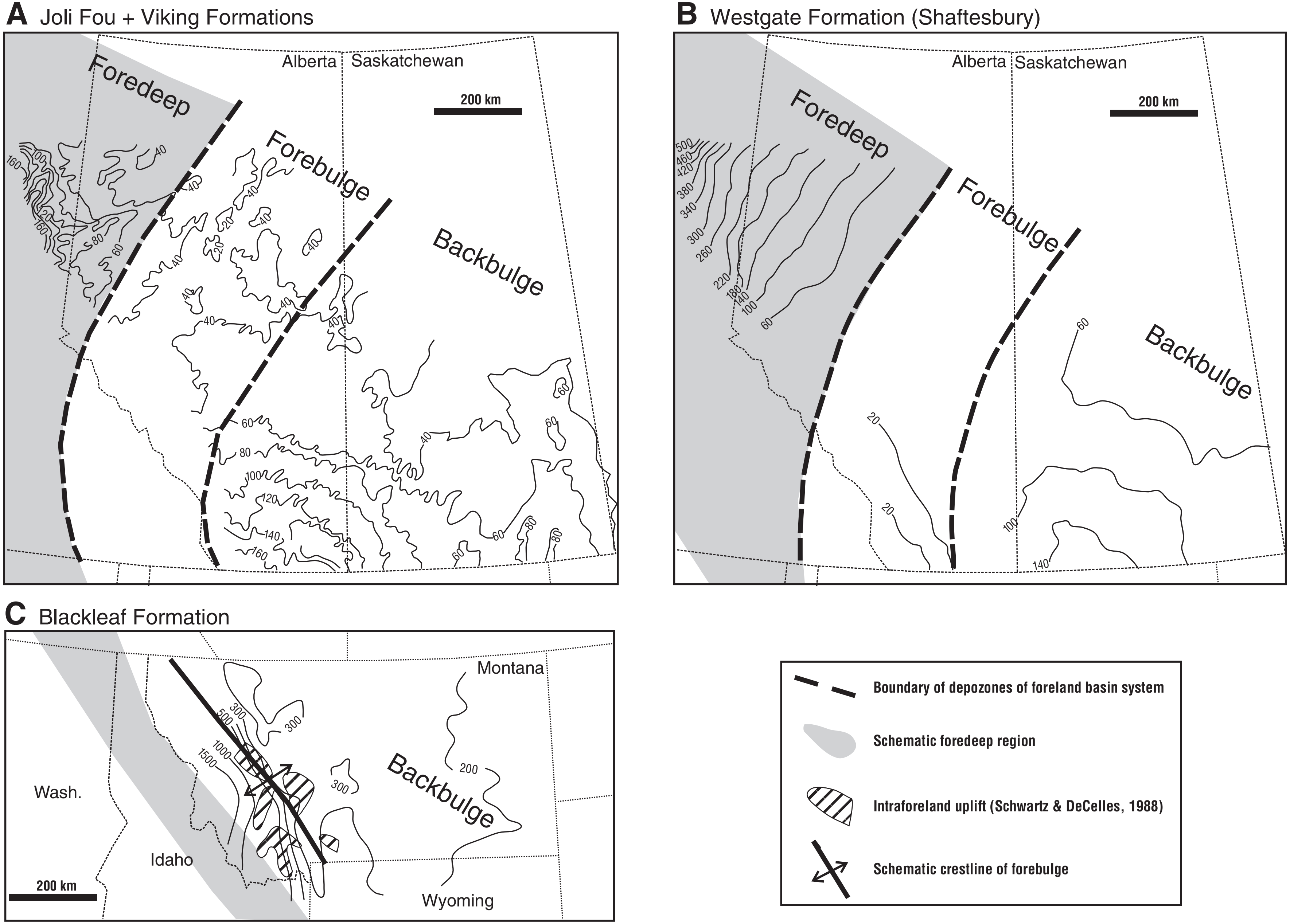

Figure 9. (A) Late Albian foreland basin system in southern Canada. Isopach map of Joli Fou and Viking Formations is from Reinson et al. (1994). (B) Latest Albian foreland basin system in southern Canada. Isopach map of Westgate Formation in southern Alberta and southern Saskatchewan, and isopach map of Shaftesbury Formation in northwestern Alberta and northeastern British Columbia, are from Leckie et al. (1994). (C) Late Albian foreland basin system in the northern United States. Isopach map of the upper Albian in Montana is from DeCelles (2004), and intraforeland uplifts in southwestern Montana are from Schwartz and DeCelles (1988). Thicknesses in meters.

correlated the late Albian–early Turonian strata in southern Alberta and northwestern Montana (Fig. 2). These studies show a remarkable feature of the isopach lines of the late Albian strata, curving from a northeast trend in southern Alberta to a northwest trend in northwestern Montana. Lang and McGugan (1988) suggested that the present north-northwest–trending Sweetgrass Arch in northwestern Montana may have been tectonically active during the middle Cretaceous because of the rapid thinning of the Vaughn Member of the Blackleaf Formation from >210 m in northwestern Montana northeastward to zero in central northern Montana (Fig. 2). A series of north-northwest–trending intraforeland uplifts developed in southwestern Montana during the Early Cretaceous–early Late Cretaceous and were interpreted as possible manifestations of migratory forebulge uplift (Schwartz, 1982; Schwartz and DeCelles, 1988) (Figs. 9C and 10).

Lower Cenomanian

The early Cenomanian Fish Scales Formation is a regional stratigraphic marker in the Western Interior of Canada and is mainly composed of silty mudstone with abundant fish remains and bentonite beds (Figs. 2 and 8). This formation was correlated with the upper part of the Bootlegger Formation and Mowry Formation in northern Montana, where it mostly consists of interbedded and interlaminated sandstone, siltstone, and sandy shale with abundant fish scales (Glaister, 1959; Cobban et al., 1976; Lang and McGugan, 1988) (Fig. 2).

Middle–Upper Cenomanian

Detailed well-log correlation shows that the Dunvegan Formation and the lower part of the Kaskapau Formation in northeastern British Columbia and northwestern Alberta are correlative with the Belle Fourche Formation in central and southern Alberta (Tyagi et al., 2007) (Figs. 2 and 8). The Dunvegan Formation contains the *Verneuilinoides perplexus* foraminiferal zone and can be correlated with the Lower Belle Fourche Formation (Allomember A). It is a large deltaic complex comprising 10 coarsening-upward allomembers, showing a southeastward thinning tendency (Bhattacharya and Walker, 1991; Bhattacharya, 1994; Plint, 2000; Tyagi et al., 2007) (Fig. 10). The lower Kaskapau Formation shallow marine mudstones consist of A-X, Doe Creek, Pouce Coupe, and Unit I units and can be correlated with the Upper Belle Fourche Formation (Allomembers B–E) (Tyagi et al., 2007) (Figs. 2 and 8). The *Dunveganoceras* ammonite zone, indicative of a late Cenomanian age, was found in the Pouce Coupe and Unit I units in northwestern Alberta (Warren and Stelck, 1940; Varban and Plint, 2005). The A-X unit exhibits a wedge shape, thinning from ~50 m in northeastern British Columbia to ~10 m in central northern Alberta (Plint, 2000). An isopach map of the Doe Creek unit also shows a wedge shape, thinning from 115 m in northeastern British Columbia to <5 m in central northern Alberta (Kreitner and Plint, 2006). The Pouce Coupe unit, with a thickness of 0–100 m, occurs mainly in northeastern British Columbia and dies out at the British Columbia–Alberta border (Kreitner and Plint, 2006) (Figs. 8 and 11). Unit I shows a wedge shape, thinning from ~110 m in northeastern British Columbia to ~10 m in northwestern Alberta (Varban and Plint, 2005). The Upper Belle Fourche Formation in central Alberta thins eastward from ~70–80 m near the foothills to 4–6 m near the Alberta-Saskatchewan border (Tyagi et al., 2007) (Figs. 8 and 11).

In the central and southern Alberta Foothills there is an unconformity between the Sunkay Member of the Blackstone Formation and the Blairmore Group (Stott, 1963, 1984) (Fig. 2). The Sunkay Member, composed of marine shale interbedded with siltstone and very fine sandstone, shows a northward-thickening tendency, with a minimum thickness of 2–5 m at the Castle River, thickening to 62 m at the Ghost River (Stott, 1963, 1984; Leckie et al., 2000) (Fig. 3). The lower part of the Sunkay Member, containing the *Verneuilinoides perplexus* foraminiferal zone (Caldwell et al., 1978; Tyagi et al., 2007), and the upper part, containing the *Dunveganoceras* ammonite zone (Stott, 1963), are of middle and late Cenomanian age, respectively (Fig. 2). Tyagi et al. (2007) correlated the Sunkay Member and the subsurface Belle Fourche Formation in central and southern Alberta. Leckie et al. (2000) attributed the late Albian–middle Cenomanian unconformity and thickness change of the Sunkay Member in the Alberta Foothills to a paleohigh created mainly by deposition of the volcaniclastic sediments of the Crowsnest Formation during the late Albian (Fig. 2). However, the Crowsnest Formation has a highly restricted distribution area near three volcanic source areas or pipes in the southern Alberta Foothills (Pearce, 1970; Leckie and Burden, 2001).

In northwestern Montana the late Cenomanian *Dunveganoceras albertense* and *Calycoceras canitaurinum* ammonite zones are present in the Floweree Member of the Marias River Formation (Cobban et al., 1976) (Fig. 2). This unit is mainly composed of marine shale interbedded with shaly siltstone and generally shows a southwestward-thinning tendency (Fig. 3). In the subsurface it has a thickness of 42–54 m in central northern Montana (Ridgley et al., 2001), and 16–29 m in northwestern Montana. It is 3–19.4 m thick in the exposed sections near Great Falls, 11.6 m thick at Summit Creek, and 9 m thick in Sun River Canyon (Cobban et al., 1976). Merewether and Cobban (1986) suggested that a north-northwest–trending uplift developed near Great Falls during the 93–94 Ma period (Fig. 3).

Upper Cenomanian–Santonian strata, >2000 m thick, are exposed near Drummond, Montana, and consist of interbedded sandy limestone and sandstone deposited in shallow brackish-water (Wallace et al., 1990) (Fig. 3). In the Wolf Creek area, Montana, the middle–late Cenomanian Floweree Member of the Marias River Shale, with a thickness of 18 m, consists of marine shale, sandstone, bentonite, and conglomerate and rests disconformably on the Blackleaf Formation (Schmidt, 1978) (Fig. 3). Wallace et al. (1990) suggested a barrier at the present location of the Lewis and Clark line during the Late Cretaceous, which separated the sedimentation in different foreland basins north

Figure 10. Reconstructed middle Cenomanian foreland basin system in western North America. Palinspastically restored thrust faults are from Price and Sears (2000). Isopach map of Allomember A of the Belle Fourche Formation is drawn for southern Alberta. Isopach map of the Dunvegan Formation in northwestern Alberta is from Bhattacharya (1994). Thicknesses (in meters) of the Lower Belle Fourche Formation in central Alberta are measured from well logs *in* Tyagi et al. (2007), and in southwestern Saskatchewan from well logs *in* Pedersen (2004). Thicknesses of the Lower Belle Fourche Formation in the well 1 Schwartz and well 1 Johnnye in northern Montana are from Ridgley et al. (2001). Crestlines of uplift and intraforeland uplifts in southwestern Montana are after Merewether and Cobban (1986) and Schwartz and DeCelles (1988), respectively. Although the equivalent Belle Fourche Formation in outcrops of western Montana cannot be subdivided into middle and upper Cenomanian parts, we mark the outcrops with thickness of the whole formation for correlation convenience.

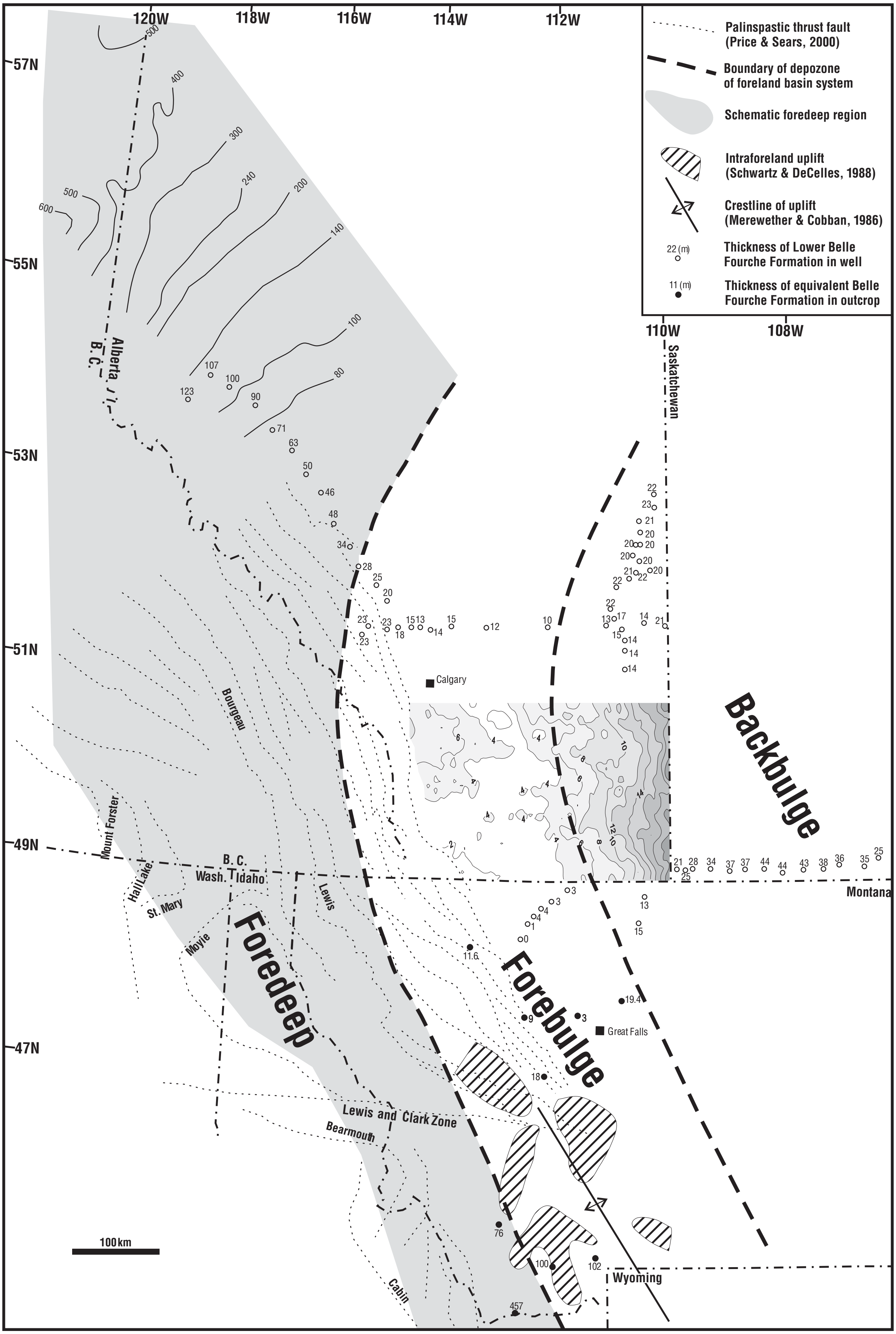
Palinspastic thrust fault (Price & Sears, 2000)
Boundary of depozone of foreland basin system
Schematic foredeep region
Intraforeland uplift (Schwartz & DeCelles, 1988)
Crestline of uplift (Merewether & Cobban, 1986)
22 (m) Thickness of Lower Belle Fourche Formation in well
11 (m) Thickness of equivalent Belle Fourche Formation in outcrop
120W
118W
116W
114W
112W
110W
108W
57N
55N
53N
51N
49N
47N
Alberta
B.C.
Saskatchewan
Calgary
Bourgeau
Mount Forster
Hall Lake
St. Mary
Moyie
B. C.
Wash.
Idaho
Lewis
Montana
Foredeep
Forebulge
Backbulge
Great Falls
Lewis and Clark Zone
Bearmouth
Cabin
Wyoming
100 km

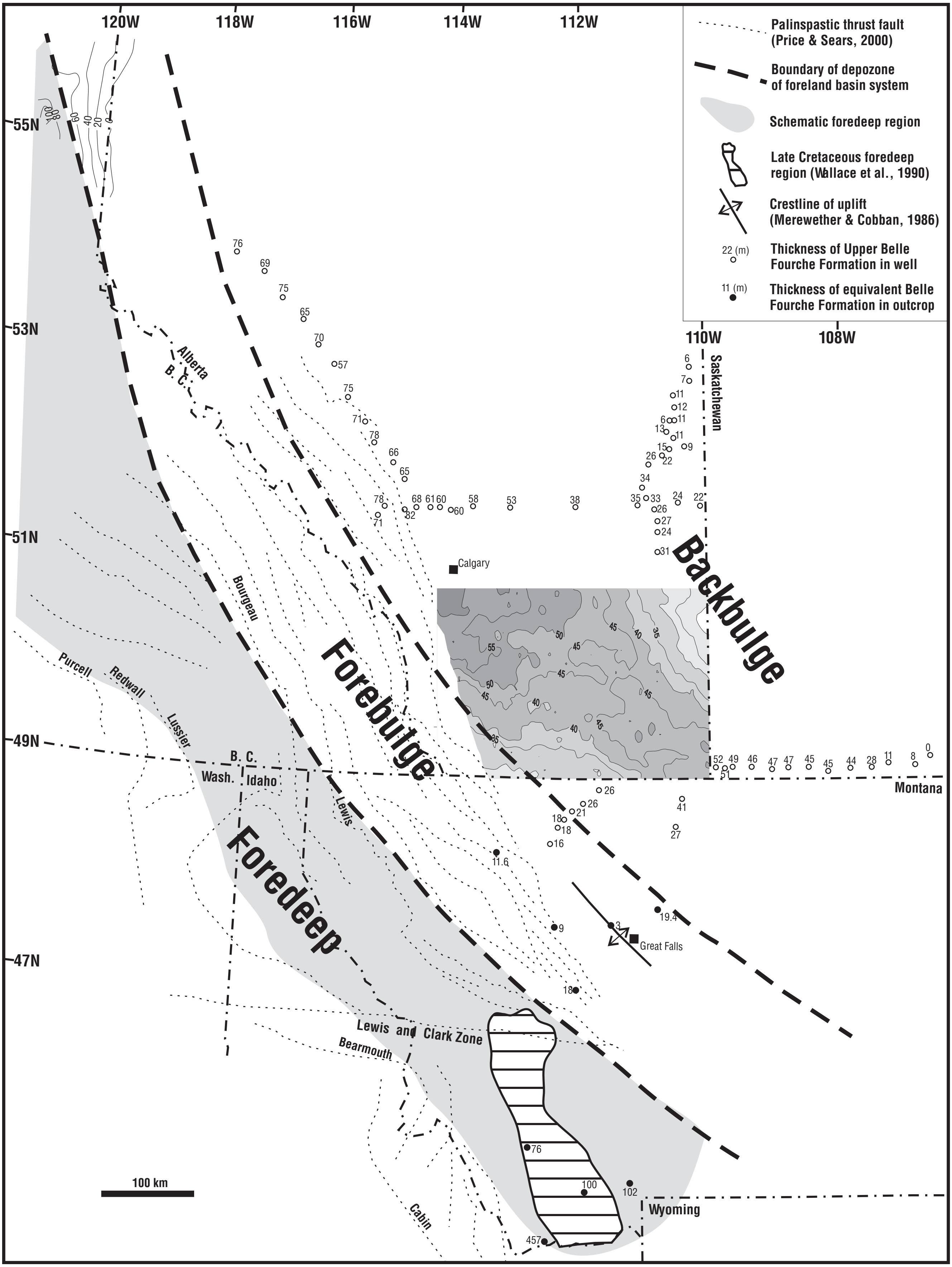
Palinspastic thrust fault (Price & Sears, 2000)
Boundary of depozone of foreland basin system
Schematic foredeep region
Late Cretaceous foredeep region (Wallace et al., 1990)
Crestline of uplift (Merewether & Cobban, 1986)
22 (m) Thickness of Upper Belle Fourche Formation in well
11 (m) Thickness of equivalent Belle Fourche Formation in outcrop
120W
118W
116W
114W
112W
110W
108W
55N
53N
51N
49N
47N
Alberta
B. C.
Saskatchewan
Montana
Wash.
Idaho
Wyoming
Calgary
Great Falls
Bourgeau
Purcell
Redwall
Lussier
Lewis
Lewis and Clark Zone
Bearmouth
Cabin
Foredeep
Forebulge
Backbulge
100 km

Figure 11. Reconstructed late Cenomanian foreland basin system in western North America. Palinspastically restored thrust faults are from Price and Sears (2000). The isopach map of Allomembers B–E of the Belle Fourche Formation is drawn for southern Alberta. The isopach map of the Pouce Coupe unit in northeastern British Columbia is from Kreitner and Plint (2006). Thicknesses of the Upper Belle Fourche Formation in central Alberta are measured from well logs *in* Tyagi et al. (2007), and in southwestern Saskatchewan from well logs *in* Pedersen (2004). Thicknesses of the Upper Belle Fourche Formation in well 1 Schwartz and well 1 Johnnye in northern Montana are from Ridgley et al. (2001). Crestline of uplift in northwestern Montana is after Merewether and Cobban (1986). The Late Cretaceous foredeep region in southwestern Montana is after Wallace et al. (1990). Although the equivalent Belle Fourche Formation in outcrops of western Montana cannot be subdivided into middle and upper Cenomanian parts, we mark the outcrops with thickness of the whole formation for convenience of correlation. Thicknesses in meters.

and south of the line (Figs. 3 and 11). The foreland basin to the south of the Lewis and Clark line lay in southwestern Montana.

The thick middle Cenomanian–early Santonian Frontier Formation is exposed in southwestern Montana, with a maximum thickness of 2135 m in the Lima Peaks (Dyman et al., 1997) (Figs. 2, 3, and 8). U-Pb data for porcellanitic samples from the top of the underlying Blackleaf Formation indicate that the Frontier Formation was deposited after 95 Ma (Dyman et al., 1997). Palynologic data show that the lower coarse-clastic unit of the formation is of Cenomanian age (Dyman et al., 1989, 1997). Therefore, the Lower Frontier Formation was deposited during the middle–late Cenomanian, coeval with the Belle Fourche Formation in other areas in the northern Great Plains, United States (McGookey, 1972), and in southern Alberta and southern Saskatchewan. This unit shows a northeastward-thinning tendency, from 457 m in the Lima Peaks to 102, 100, and 76 m, respectively, in the Madison Range, northern Snowcrest Range, and eastern Pioneer Mountains (Dyman et al., 1988, 1989; Tysdal, 1991; Dyman and Tysdal, 1998) (Figs. 3 and 8). Merewether and Cobban (1986) proposed that the middle Cenomanian *Acanthoceras* ammonite zone is represented by a north-northwest–trending unconformity in southwestern Montana and northwestern Wyoming (Fig. 3). The Lower Frontier Formation in the Lima Peaks area was deposited in a fluvial environment and is mainly composed of nonmarine siltstone, mudstone, sandstone, and conglomerate with a strong volcaniclastic component (Dyman et al., 1988, 1989, 1997) (Fig. 8). It mainly consists of interbedded mudstone, silty mudstone, sandstone, and tuff in the eastern Pioneer Mountains and Madison Range and was deposited in a broad deltaic environment (Tysdal, 1991; Dyman and Tysdal, 1998) (Fig. 8). Data from fluvial and delta plain sandstones and conglomerates in the Lower Frontier Formation suggest a north-to-south paleocurrent direction (Dyman et al., 1988). Because no data support a further subdivision of the Lower Frontier Formation into middle and upper Cenomanian parts, the consistent lithologic and sedimentary characteristics of the unit and its northeastward thinning reflect continuous subsidence and infilling in southwestern Montana under a similar tectonic condition during the middle–late Cenomanian.

RECONSTRUCTION OF THE MIDDLE CRETACEOUS FORELAND BASIN

Based on our detailed stratigraphic study for the Belle Fourche Formation in southern Alberta, combined with tectonic studies in the Cordilleran fold and thrust belt in southern Canada and the northern United States, especially by Price and Sears (2000), and stratigraphic studies for the equivalent Belle Fourche Formation and older and younger strata in Alberta and Montana mentioned above, we have restored the evolution of the northern Cordilleran foreland basin for late Albian–Cenomanian time (Figs. 9–11).

The Albian–Santonian Colorado Group consists of strata deposited during orogenic loading (synorogenic or thrusting) periods alternating with strata deposited during orogenic unloading (postorogenic or tectonic quiescence) periods (Yang and Miall, 2008) in accordance with a two-phase stratigraphic model for foreland basins (Heller et al., 1988; Jordan and Flemings, 1991; Beaumont et al., 1993; Catuneanu et al., 1998). The strata produced during the orogenic loading period show a typical foreland basin system as defined by DeCelles and Giles (1996), with wedge-top, foredeep, forebulge, and backbulge depozones. During an orogenic unloading period a peripheral sag is developed in front of the uplifted orogenic belt and the proximal part of the foredeep zone of the preceding orogenic loading period, with a depocenter over the forebulge zone of the preceding orogenic loading period.

Owing to intense postdepositional thrusting and cannibalization in the Rocky Mountains, the precise locations of the western margin of the foreland basin cannot be determined.

Late Albian

Because we have not carried out a detailed stratigraphic study for the upper Albian strata, orogenic loading and unloading deposits for these intervals cannot be recognized. Mainly on the basis of published stratigraphic data, according to the definition of the foreland basin system (DeCelles and Giles, 1996), we present a simple analysis of basin evolution during the late Albian here (Fig. 9). This reconstruction indicates that the proximal margin of the foredeep may have been much farther to the west than present outcrop patterns would suggest. The positioning of the foredeep and forebulge is consistent with the significant northwest-southeast shortening in southern Canada during the Early Cretaceous (Price and Sears, 2000; major faults are shown in Fig. 1A).

The stratigraphic pattern of the equivalent Joli Fou and Viking Formations indicates that a north-northeast–trending foreland basin system was developed in western Canada during the late Albian, with a foredeep in northeastern British Columbia and northwestern Alberta, a forebulge in central Alberta, and a backbulge in southern Alberta and Saskatchewan (Fig. 9A). The strata of the Cadotte and Harmon Members in northwestern Alberta consist mainly of marine shale onlapping the forebulge zone southeastward, and the equivalent Joli Fou Formation in southern Alberta consists of marine shale onlapping the forebulge zone northwestward (Leckie et al., 1994; Reinson et al., 1994) (Fig. 2), probably reflecting deposition during an orogenic loading period. The Paddy Member in northwestern Alberta and the equivalent Viking Formation in southern Alberta are mainly composed of regressive fluvial, coastal plain, and coastline deposits (Leckie et al., 1994; Reinson et al., 1994) (Fig. 2), probably reflecting uplift of the proximal foreland basin and cratonward shifting of the depocenter during an orogenic unloading period. The Westgate Formation shale, deposited in the backbulge zone in southern Alberta and southern Saskatchewan, thinning to zero westward onto the forebulge (Fig. 5A), together with the Shaftesbury Formation in northwestern Alberta, deposited in the foredeep zone, reflect a pattern typical of a foreland basin system developed during orogenic loading (Fig. 9B). Because proximal parts of the foredeep depozones have been uplifted and cannibalized, mainly distal marine shale is found in the Albian formations in northeastern British Columbia and northwestern Alberta (Leckie et al., 1994; Reinson et al., 1994).

The curving of the upper Albian strata from a northeast trend in southern Alberta to a northwest trend in northwestern Montana (Glaister, 1959; Lang and McGugan, 1988) reflects the change of the trend of the late Albian foreland basin around the international border (Fig. 9). It trends north-northwest in the northern United States, with a foredeep depozone in eastern Idaho and westernmost Montana, a forebulge depozone in western Montana, and a backbulge depozone in eastern Montana (Fig. 9C). In the foredeep region in southwestern Montana the Blackleaf Formation is 490–1170 m thick and consists mainly of fluvial deposits (Schwartz, 1982). In northern Montana the abrupt thinning of the Vaughn Member of the Blackleaf Formation northeastward (Lang and McGugan, 1988) reflects the onlap of the foredeep deposits on the forebulge depozone. The forebulge inherited the Early Cretaceous forebulge developed in southwestern Montana (DeCelles, 2004), and the north-northwest–trending intraforeland uplifts reflect the continuous migration of the foreland basin during the late Albian (Schwartz, 1982; Schwartz and DeCelles, 1988). In the backbulge depozone in eastern Montana, shoreface sandstone and marine shale were deposited with a thickness of ~200–300 m (McGookey, 1972; Schwartz, 1982; DeCelles, 2004) (Fig. 9C).

Early Cenomanian

According to the two-phase stratigraphic model for foreland basins (Heller et al. 1988; Jordan and Flemings 1991; Beaumont et al., 1993; Catuneanu et al., 1998), we interpret that the early Cenomanian Fish Scales Formation was deposited during an orogenic unloading period (Yang and Miall, 2008). The Westgate Formation below and the Lower Belle Fourche Formation (Allomember A) above the Fish Scales Formation in southern Alberta, together with their equivalent strata in northwestern Alberta, exhibit typical isopach patterns of foreland basin systems (Figs. 5, 6, 9B, and 10). However, the Fish Scales Formation has a relatively constant thickness of 10–20 m (Fig. 8). The relationship among the Westgate, Fish Scales, and Lower Belle Fourche Formations suggests that strata were deposited alternately during orogenic loading periods and unloading periods.

Middle Cenomanian

The reconstructed middle Cenomanian foreland basin system is drawn on the background of the palinspastic map of the Rocky Mountains in southern Canada and the northern United States (Price and Sears, 2000) (Fig. 10). It trends north-northeast in southern Canada and changes to a north-northwest trend in the northern United States.

The deltaic Dunvegan Formation was deposited in the foredeep depozone in northeastern British Columbia and northwestern Alberta, and progressively onlapped the forebulge depozone southeastward (Fig. 10). Based on the estimated shortening of ~100 km in the Rocky Mountain fold and thrust belt and Foothills near 56°N (McMechan and Thompson, 1989), and the distribution of middle Cenomanian strata in the subsurface and outcrop sections (Plint, 2000), a foredeep zone with a width of ~500–600 km is estimated for northwestern Alberta. The isopach lines of the Dunvegan Formation are oriented at a high angle to the Rocky Mountain fold and thrust belt (Fig. 10). We therefore suggest that the middle Cenomanian foredeep zone can be extended to southeastern British Columbia. The northeastward-thinning, northeastward facies change from fluvial to deltaic, and the northward paleocurrent direction of the middle–late Cenomanian Lower Frontier Formation in southwestern Montana (Figs. 8 and 10), coupled with the distribution of the thick Colorado Group in western Montana (Fig. 1A), suggest that a foredeep zone was developed in western Montana and eastern Idaho during the middle Cenomanian. Owing to the northeast-southwest shortening of the Rocky Mountains during Late Cretaceous–Paleocene time (Price and Sears, 2000; Sears, 2001; Ross et al., 2005), the foredeep deposits in southeastern British Columbia, eastern Idaho, and northwestern Montana were uplifted and cannibalized.

A forebulge ~250 km wide was developed in central and southwestern Alberta (Fig. 10). Well-log correlation shows that the Lower Belle Fourche Formation is 10–18 m thick above the forebulge in central Alberta (Tyagi et al., 2007) and 0–8 m in southwestern Alberta and northwestern Montana. Submarine erosion above the forebulge formed a local erosional surface between the Belle Fourche Formation and the underlying Fish Scales Formation in southwestern Alberta (Yang and Miall, 2008). We also postulate that the middle Cenomanian north-northwest–trending unconformity in southwestern Montana and northwestern Wyoming described by Merewether and Cobban (1986) represents a forebulge, just as White et al. (2002) suggested for the Cenomanian–Turonian unconformities in Colorado documented by Merewether and Cobban (1986). This interpretation is in accordance with the formation of intraforeland uplifts in southwestern Montana during the Early–early Late Cretaceous (Schwartz, 1982; Schwartz and DeCelles, 1988) (Fig. 10). The locations of forebulges show that the foreland basin system propagated progressively east-southeastward in Alberta from the late Albian to the middle Cenomanian (Figs. 9 and 10).

The Lower Belle Fourche Formation (Allomember A) in southeastern Alberta and its equivalent strata in eastern central Alberta (Tyagi et al., 2007), Saskatchewan (Ridgley et al., 2001; Pedersen, 2004), and northeastern Montana (Ridgley et al., 2001) were deposited in the extensive backbulge depozone (Figs. 8 and 10). According to the cross section in southern Saskatchewan constructed by Pedersen (2004) and our isopach map of Allomember A, a width of ~300 km is estimated from the axis of the backbulge to the crestline of the forebulge (Fig. 10).

Late Cenomanian

A palinspastic reconstruction of the Rocky Mountains in southern Alberta and northern Montana indicates significant shortening in a northeast-southwest direction during the Late Cretaceous–Paleocene (Price and Sears, 2000) (Fig. 11). The reconstruction of the late Cenomanian foreland basin system is consistent with the palinspastic reconstruction and the following stratigraphic data.

All the features of the Lower Frontier Formation in southwestern Montana—northeastward thinning, northeastward facies change from fluvial to deltaic, and northward paleocurrent direction—reflect proximal foredeep deposition, onlapping the forebulge depozone northeastward, in accordance with the proposed rapidly subsiding foreland basin to the south of the Lewis and Clark line during the Late Cretaceous (Wallace et al., 1990) (Figs. 8 and 11). The restored Colorado Group in western Montana (Fig. 1) also indicates that a foredeep developed in western Montana during the late Cenomanian. The foredeep depozone extended northwestward to southeastern British Columbia. However, continuous northeast-verging thrusting and shortening of the Rocky Mountains resulted in cannibalization of the late Cenomanian foredeep depozone in southeastern British Columbia and the northern United States (Price and Sears, 2000; Sears, 2001; Ross et al., 2005). The marine shale interbedded with shoreline and delta front sandstone of the Lower Kaskapau Formation in northeastern British Columbia, with a thickness of ~350 m, represents deposition in the foredeep depozone (Plint, 2000; Varban and Plint, 2005; Kreitner and Plint, 2006) (Fig. 8). Based on the estimated shortening of ~100 km in the Rocky Mountain fold and thrust belt and Foothills near 56°N (McMechan and Thompson, 1989), and the distribution of the upper Cenomanian in the subsurface and outcrop sections (Plint, 2000; Kreitner and Plint, 2006), a foredeep zone with a width of ~200–250 km is estimated for northwestern Alberta.

Based mainly on the thicknesses of the middle–late Cenomanian strata in western Montana, the north-northwest–trending late Cenomanian uplift in northwestern Montana (Merewether and Cobban, 1986), and the isopach map of the Upper Belle Fourche Formation (Allomembers B–E), a north-northwest–trending forebulge ~150 km wide is restored for western Montana and southeastern British Columbia (Fig. 11). Although we use the total thickness of the Upper Belle Fourche Formation to define this forebulge, it is clearly indicated that the formation of the forebulge resulted from propagation of the foreland basin system cratonward, as suggested by DeCelles and Giles (1996) (Figs. 5–7). The equivalent Belle Fourche Formation in northwestern Montana and the southern Alberta Foothills cannot be subdivided into middle and upper Cenomanian parts, but based on its thickness in these areas the Upper Cenomanian strata are 0–10 m above the crestline of the forebulge (Figs. 3 and 11). The forebulge in southeastern British Columbia and northwestern Montana has been uplifted and cannibalized (Price and Sears, 2000; Sears, 2001; Ross et al., 2005). Kreitner and Plint (2006) mentioned that there is a hinge zone at the border between northeastern British Columbia and northwestern Alberta, and the Pouce Coupe unit is mainly distributed west of it (Figs. 8 and 11). The cross sections in Kreitner and Plint (2006) also show that the sandstone in the Doe Creek unit is mainly distributed west of the hinge zone. Several allomembers of overlying Unit I of the Lower Kaskapau Formation are absent west of the hinge zone but appear abruptly east of it (Varban and Plint, 2005). Kreitner and Plint (2006) attributed the hinge zone to control by the Precambrian basement. However, Ross and Eaton (1999) suggested that there is little direct relationship between the Precambrian basement and presence and orientation of faults in the sedimentary section in the Alberta basin. In addition, in an earlier study by Plint et al. (1993) it was suggested that at the British Columbia–Alberta border a forebulge zone controlled deposition of the Doe Creek and Pouce Coupe sandstones. Therefore, we interpret the hinge zone as a migratory forebulge (Fig. 11).

The Late Cenomanian backbulge depozone trends north-northwest, with deposition of the Upper Belle Fourche Formation in central Alberta (Tyagi et al., 2007) and Allomembers B–E of the Belle Fourche Formation in southern Alberta (Fig. 11). In southern Alberta, Allomembers B–E show a key isopach pattern of backbulge accumulation, with regional closure around a central thick zone (DeCelles and Giles, 1996) (Figs. 7B–E and 11). A width of ~200 km is estimated from the axis of the backbulge to the crestline of the forebulge. The depocenters of the backbulge depozones propagated progressively cratonward from Allomembers B–E, thinning and onlapping the eastern margin of the Western Interior Seaway (Figs. 5–8). The backbulge strata thin to zero in central southern Saskatchewan (Figs. 8 and 11). Based on the northwest-trending tendency of the backbulge depozone in southern Alberta, the Upper Belle Fourche Formation, with thicknesses of 60–82 m near the central Alberta Foothills (Tyagi et al., 2007), represents deposition in the axis of the backbulge, and part of the backbulge deposition near the forebulge side has been uplifted and cannibalized (Fig. 11). In northwestern Alberta the Lower Kaskapau Formation east of the forebulge shows a similar pattern and thickness as the Upper Belle Fourche Formation in central Alberta (Tyagi et al., 2007) and southern Alberta, thinning east-northeastward from ~80–100 m in northwestern Alberta to ~10 m in central northern Alberta (Plint, 2000; Varban and Plint, 2005; Kreitner and Plint, 2006) (Fig. 8).

DISCUSSION

It has been argued here that the Cordilleran foreland basin was developed with a north-northeast trend in southern Canada and a north-northwest trend in the northern United States during the late Albian–middle Cenomanian (Figs. 9 and 10). During the late Cenomanian a north-northwest–trending foreland basin was developed, which extended through southern Canada and the northern United States (Fig. 11). The foredeep depozone and part of the forebulge depozone in the present Rocky Mountains in southern Canada and the northern United States were uplifted and cannibalized by postdepositional thrusting and shortening during the Late Cretaceous–Paleocene. The unconformity between the Sunkay Member and the Blairmore Group, and the northward thickening of the Sunkay Member in the southern and central Alberta Foothills (Stott, 1963, 1984; Leckie et al., 2000), are related to uplift of the forebulge zones during the late Albian–late Cenomanian (Figs. 2 and 3).

Four major northwest-dipping thrust faults in the southern Canadian Cordillera—Moyie–Dibble Creek, St. Mary, Hall Lake, and Mount Forster faults—change southward into west-dipping or southwest-dipping thrust faults in the northern United States (Price and Sears, 2000) (Figs. 1A and 10). A series of west-northwest–dipping reverse faults have been documented in southeastern Yukon Territory in the Omineca Belt west of the Canadian Rockies (McMechan and Thompson, 1993; Price, 1994). Geochemical and geochronological studies of granitic plutons that intruded these thrust faults near the international border and in southeastern Yukon Territory show that the latest movement on the faults was at ca. 94 Ma (Baadsgaard et al., 1961; Archibald et al., 1984; Höy and van der Heyden, 1988; Price and Sears, 2000; Coulson et al., 2002). By the end of the middle Cenomanian (ca. 94 Ma), thrusting and folding west of the Moyie fault had ended (Price and Sears, 2000), approximately consistent with the end of a regional metamorphism and deformation event along the Salmon River suture zone in western Idaho before ca. 93 Ma (Lund and Snee, 1988). Therefore, we suggest that the episode of crustal loading and shortening represented by the activity of these faults resulted in formation of the foreland basin with a north-northeast trend in southern Canada and a north-northwest trend in the northern United States during the late Albian–middle Cenomanian. Our interpreted late Albian–middle Cenomanian foreland basin in the northern Cordilleran foreland basin, together with the Early Cretaceous north-northeast–trending foreland basin in the central Cordilleran foreland basin (Currie, 2002), reflects the east-west convergence vector at the North American plate margin during the Late Jurassic–Early Cretaceous (Engebretson et al., 1985). Because the palinspastic reconstruction by Price and Sears (2000) was mainly focused on the Late Cretaceous and Paleocene northeast-southwest shortening in the Rocky Mountains, the palinspastic locations of the Moyie–Dibble Creek, St. Mary, Hall Lake, and Mount Forster faults may not reflect their original locations before 94 Ma. We suggest that the western margin of the late Albian–middle Cenomanian foreland basin might have been east of the original locations of these faults before the end of the middle Cenomanian.

The northeast-verging thrusting and folding in the Rocky Mountains in southern Canada began after the end of the middle Cenomanian (ca. 94 Ma) and are related to the northeast-southwest convergence at the North American margin during the Late Cretaceous–Eocene (Engebretson et al., 1985). This is consistent with the formation of a north-northwest–trending foreland basin in western North America during the late Cenomanian (Fig. 11). We suggest that the western margin of the late Cenomanian foreland basin might have been northeast of the palinspastic locations of the westernmost northwest-trending thrust faults (Purcell, Redwall, and Lussier) in southern Canada (Fig. 11).

We attribute the westward retreat of the forebulges within Alberta at the end of the middle Cenomanian not only to the change of thrusting directions of the Cordilleran thrust belt as mentioned above, but also to the increase of orogenic load due to more intense thrusting of the Cordilleran thrust belt since the late Cenomanian (Figs. 10 and 11). The more intense thrusting was caused by higher convergence velocities of ~200 km/m.y. along the western margin of North America during the Late Cretaceous–Eocene in comparison with that of ~100 km/m.y. during the Late Jurassic–Early Cretaceous (Engebretson et al., 1985). The bigger load, as a result of more intense thrusting of the Cordilleran thrust belt, resulted in the formation of a foreland basin with a shorter wavelength in the late Cenomanian than the one that formed in the middle Cenomanian, in accordance with the predictions of numerical modeling (Flemings and Jordan, 1989; Sinclair et al., 1991). Therefore, the middle Cenomanian foreland basin system has wider foredeep, forebulge, and backbulge depozones. Study of the Karoo foreland basin of South Africa also shows that the change of orogenic loads resulted in the orogenward migration of the foreland basin system during the Triassic–Middle Jurassic (Catuneanu et al., 1998).

CONCLUSIONS

Using widely distributed flooding surfaces as the boundaries of allomembers, the middle–late Cenomanian Belle Fourche Formation is subdivided into five allomembers, A–E, in southern Alberta. The Belle Fourche Formation in southern Alberta is correlative with the Dunvegan Formation and the Lower Kaskapau Formation in northeastern British Columbia and northwestern Alberta, the Sunkay Member of the Blackstone Formation in the central and southern Alberta Foothills, the Floweree Member of the Marias River Formation in northwestern Montana, and the Lower Frontier Formation in southwestern Montana.

The reconstructed late Albian–middle Cenomanian foreland basin trends north-northeast in southern Canada and changes to a north-northwest trend in the northern United States. The formation of the basin was driven by thrusting of northwest-dipping thrust faults in the Canadian Cordillera and west-dipping or southwest-dipping thrust faults in the northern U.S. Cordillera. The reconstructed late Cenomanian foreland basin trends north-northwest in the northern Cordilleran foreland basin. The formation of the basin was driven by northeast-verging thrusting and folding in the Rocky Mountains since the late Cenomanian. The foredeep zones and part of the forebulge zones of the middle Cretaceous foreland basin in the present Rocky Mountains in southern Canada and the northern United States were uplifted and cannibalized by postdepositional thrusting and shortening during the Late Cretaceous–Paleocene. The change in trend of the foreland basins at the end of the middle Cenomanian may reflect the change of convergence vectors along the western margin of North America during the middle Cretaceous.

ACKNOWLEDGMENTS

We thank Guy Plint, Bogdan Varban, Aditya Tyagi, and other members of the Basin Analysis Group, University of Western Ontario, for their many good suggestions and much help in well-log selection and core measurement. We also thank Jennie Ridgley of the U.S. Geological Survey for her review of Yang's Ph.D. proposal. Feedback from Peter DeCelles and Paul Heller helped to improve an earlier version of the paper. Critical reviews by Brian Currie, Brendan Murphy, James Schmitt, and Tim White assisted greatly in improving the paper.

REFERENCES CITED

Archibald, D.A., Krogh, T.E., Armstrong, R.L., and Farrar, E., 1984, Chronology and tectonic implications of magmatism and metamorphism, southern Kootenay Arc and neighbouring regions, southeastern British Columbia, Part II: Mid-Cretaceous to Eocene: Canadian Journal of Earth Sciences, v. 21, p. 567–583.

Baadsgaard, H., Folinsbee, R.E., and Lipson, J.I., 1961, Potassium-argon dates of biotites from Cordilleran granites: Geological Society of America Bulletin, v. 72, p. 689–701, doi: 10.1130/0016-7606(1961)72[689:PDOBFC]2.0.CO;2.

Beaumont, C., 1981, Foreland basins: Royal Astronomical Society Geophysical Journal, v. 65, p. 291–329.

Beaumont, C., Quinlan, G., and Stockmal, G.S., 1993, The evolution of the western interior basin: Causes, consequences and unsolved problems, *in* Caldwell, W.G., and Kauffman, E.G., eds., Evolution of the Western Interior Basin: Geological Association of Canada Special Paper 39, p. 97–117.

Bhattacharya, J.P., 1994, Cretaceous Dunvegan Formation of the Western Canada Sedimentary Basin, *in* Mossop, G., and Shetsen, I., eds., Geological Atlas of the Western Canada Sedimentary Basin: Calgary, Canadian Society of Petroleum Geology and Alberta Research Council, p. 365–373.

Bhattacharya, J., and Walker, R.G., 1991, Allostratigraphic subdivision of the Upper Cretaceous Dunvegan, Shaftesbury, and Kaskapau formations in the northwestern Alberta subsurface: Bulletin of Canadian Petroleum Geology, v. 39, p. 145–164.

Bloch, J., Schroderadams, C., Leckie, D.A., McIntyre, D.J., Craig, J., and Staniland, M., 1993, Revised stratigraphy of the Lower Colorado Group (Albian to Turonian), Western Canada: Bulletin of Canadian Petroleum Geology, v. 41, p. 325–348.

Caldwell, W.G.E., North, B.R., Stelck, C.R., and Wall, J.R., 1978, A foraminiferal zonal scheme for the Cretaceous System in the interior plains of Canada, *in* Stelck, C.R., and Chatterton, B.D.E., eds., Western and Arctic Canadian Biostratigraphy: Geological Association of Canada Special Paper 18, p. 495–575.

Catuneanu, O., Hancox, P.J., and Rubidge, B.S., 1998, Reciprocal flexural behaviour and contrasting stratigraphies: A new basin development model for the Karoo retroarc foreland system, South Africa: Basin Research, v. 10, p. 417–439, doi: 10.1046/j.1365-2117.1998.00078.x.

Cobban, W.A., Erdmann, C.E., Lemke, R.W., and Maughan, E.K., 1976, Type sections and stratigraphy of the members of the Blackleaf and Marias River formations (Cretaceous) of the Sweetgrass Arch, Montana: U.S. Geological Survey Professional Paper 974, 66 p.

Coulson, I.M., Villeneuve, M.E., Dipple, G.M., Duncan, R.A., Russell, J.K., and Mortensen, J.K., 2002, Timescales of assembly and thermal history of a composite felsic pluton: Constraints from the Emerald Lake area, northern Canadian Cordillera, Yukon: Journal of Volcanology and Geothermal Research, v. 114, p. 331–356, doi: 10.1016/S0377-0273(01)00294-3.

Currie, B.S., 2002, Structural configuration of the Early Cretaceous Cordilleran Foreland-Basin System and Sevier Thrust Belt, Utah and Colorado: Journal of Geology, v. 110, p. 697–718, doi: 10.1086/342626.

DeCelles, P.G., 2004, Late Jurassic to Eocene evolution of the Cordilleran Thrust Belt and foreland basin system, western U.S.A.: American Journal of Science, v. 304, p. 105–168, doi: 10.2475/ajs.304.2.105.

DeCelles, P.G., and Giles, K.A., 1996, Foreland basin system: Basin Research, v. 8, p. 105–123, doi: 10.1046/j.1365-2117.1996.01491.x.

Dyman, T.S., and Tysdal, R.G., 1998, Stratigraphy and depositional environment of nonmarine facies of Frontier Formation, eastern Pioneer Mountains, southwestern Montana: Mountain Geologist, v. 35, p. 115–125.

Dyman, T.S., Perry, W.J., and Nichols, D.J., 1988, Stratigraphy, petrology, and provenance of the Albian Blackleaf Formation and the Cenomanian to Turonian lower part of the Frontier Formation in part of Beaverhead and Madison counties, Montana: Mountain Geologist, v. 25, p. 113–128.

Dyman, T.S., Perry, W.J., Nichols, D.J., Davis, L.E., and Haley, J.C., 1989, Stratigraphy, petrology, and provenance of the Cenomanian to Turonian Frontier Formation near Lima, southwest Montana, *in* French, D.E., and Grabb, R.F., eds., Montana Geological Society 1989 Field Conference Guidebook: Billings, Montana Geological Society, p. 103–114.

Dyman, T.S., Tysdal, R.G., Perry, W.J., Obradovich, J.D., Haley, J.C., and Nichols, D.J., 1997, Correlation of Upper Cretaceous strata from Lima Peaks area to Madison Range, southwestern Montana and southeastern Idaho, USA: Cretaceous Research, v. 18, p. 751–766, doi: 10.1006/cres.1997.0079.

Engebretson, D.C., Cox, A., and Gordon, R.G., 1985, Relative Motions between Oceanic and Continental Plates in the Pacific Basin: Geological Society of America Special Paper 206, 59 p.

Flemings, P.B., and Jordan, T.E., 1989, A synthetic stratigraphic model of foreland basins development: Journal of Geophysical Research, v. 94, p. 3851–3866, doi: 10.1029/JB094iB04p03851.

Glaister, R.P., 1959, Lower Cretaceous of southern Alberta and adjoining areas: American Association of Petroleum Geologists Bulletin, v. 43, p. 590–640.

Heller, P.L., Angevine, C.L., Winslow, N.S., and Paola, C., 1988, Two-phase model of foreland basin sequences: Geology, v. 16, p. 501–504, doi: 10.1130/0091-7613(1988)016<0501:TPSMOF>2.3.CO;2.

Höy, T., and van der Heyden, P., 1988, Geochemistry, geochronology, and tectonic implications of two quartz monzonite intrusions, Purcell Mountains, southeastern British Columbia: Canadian Journal of Earth Sciences, v. 25, p. 106–115.

Jordan, T.E., 1981, Thrust loads and foreland basin evolution, Cretaceous, western United States: American Association of Petroleum Geologists Bulletin, v. 65, p. 2506–2520.

Jordan, T.E., and Flemings, P.B., 1991, Large-scale stratigraphic architecture, eustatic variation, and unsteady tectonism: A theoretical evaluation: Journal of Geophysical Research, v. 96, p. 6681–6699, doi: 10.1029/90JB01399.

Kauffman, E.G., Sageman, B.B., Kirkland, J.I., Elder, W.P., Harries, P.J., and Villamil, T., 1993, Molluscan biostratigraphy of the Cretaceous Western Interior Basin, North America, *in* Caldwell, W.G.E., and Kauffman, E.G., eds., Evolution of the Western Interior Basin: Geological Association of Canada Special Paper 39, p. 397–434.

Kreitner, M.A., and Plint, A.G., 2006, Allostratigraphy and paleogeography of the upper Cenomanian, lower Kaskapau Formation in subsurface and outcrop, Alberta and British Columbia: Bulletin of Canadian Petroleum Geology, v. 54, p. 110–137, doi: 10.2113/gscpgbull.54.2.110.

Lang, H.R., and McGugan, A., 1988, Cretaceous (Albian-Turonian) foraminiferal biostratigraphy and paleogeography of northern Montana and southern Alberta: Canadian Journal of Earth Sciences, v. 25, p. 316–342.

Leckie, D.A., and Burden, E.T., 2001, Stratigraphy, sedimentology, and palynology of the Cretaceous (Albian) Beaver Mines, Mill Creek, and Crowsnest formations (Blairmore Group) of southwestern Alberta: Geological Survey of Canada Bulletin 563, 103 p.

Leckie, D.A., and Smith, D.G., 1992, Regional setting, evolution, and depositional cycles of the western Canada Foreland Basin, *in* Macqueen, R.W., and Leckie, D.A., eds., Foreland Basins and Fold Belts: American Association of Petroleum Geologists Memoir 55, p. 9–46.

Leckie, D.A., Bhattacharya, J.P., Bloch, J., Gilboy, C.F., and Norris, B., 1994, Cretaceous Colorado/Alberta Group strata of the Western Canada Sedimentary Basin, *in* Mossop, G., and Shetsen, I., eds., Geological Atlas of the Western Canada Sedimentary Basin: Calgary, Canadian Society of Petroleum Geology and Alberta Research Council, p. 335–352.

Leckie, D.A., Schroeder-Adams, C.J., and Bloch, J., 2000, The effect of paleotopography on the late Albian and Cenomanian sea-level record of the Canadian Cretaceous interior seaway: Geological Society of America Bulletin, v. 112, p. 1179–1198, doi: 10.1130/0016-7606(2000)112<1179:TEOPOT>2.3.CO;2.

Lund, K., and Snee, L.W., 1988, Metamorphism, structural development, and age of the continent–island arc juncture in west-central Idaho, *in* Ernst, W.G., ed., Metamorphism and Crustal Evolution of the Western United States: Englewood Cliffs, New Jersey, Prentice Hall, p. 296–331.

McGookey, D.P., compiler, 1972, Cretaceous System, *in* Mallory, W.W., ed., Geologic Atlas of the Rocky Mountain Region: Denver, Rocky Mountain Association of Geologists, p. 190–228.

McMechan, M.E., and Thompson, R.I., 1989, Structural style and history of the Rocky Mountain Fold and Thrust Belt, *in* Ricketts, B.D., ed., Western Canada Sedimentary Basin, a Case History: Calgary, Canadian Society of Petroleum Geologists, p. 47–76.

McMechan, M.E., and Thompson, R.I., 1993, The Canadian Cordilleran fold and thrust belt south of 66°N and its influence on the Western Interior Basin, *in* Caldwell, W.G.E., and Kauffman, E.G., eds., Evolution of the Western Interior Basin: Geological Association of Canada Special Paper 39, p. 73–90.

Merewether, E.A., and Cobban, W.A., 1986, Biostratigraphic units and tectonism in the mid-Cretaceous foreland of Wyoming, Colorado and adjoining areas, *in* Peterson, J.A., ed., Paleotectonics and Sedimentation: American Association of Petroleum Geologists Memoir 41, p. 443–468.

NACSN (North American Commission on Stratigraphic Nomenclature), 1983, North American Stratigraphic Code: American Association of Petroleum Geologists Bulletin, v. 67, p. 841–875.

Obradovich, D.J., 1993, A Cretaceous time scale, *in* Caldwell, W.G.E., and Kauffman, E.G., eds., Evolution of the Western Interior Basin: Geological Association of Canada Special Paper 39, p. 379–396.

Pang, M., and Nummedal, D., 1995, Flexural subsidence and basement tectonics of the Cretaceous Western Interior basin, United States: Geology, v. 23, p. 173–176, doi: 10.1130/0091-7613(1995)023<0173:FSABTO>2.3.CO;2.

Pearce, T.H., 1970, The analcite-bearing volcanic rocks of the Crowsnest Formation, Alberta: Canadian Journal of Earth Sciences, v. 7, p. 46–66.

Pedersen, P.K., 2004, Shallow Gas Research Project in Southwestern Saskatchewan: Revised Lithostratigraphy of the Colorado Group and Reservoir Architecture of the Belle Fourche and Second White Specks in the Senate Pool: Saskatchewan Geological Survey Summary of Investigations, 15 p.

Plint, A.G., 2000, Sequence stratigraphy and paleogeography of a Cenomanian deltaic complex: The Dunvegan and lower Kaskapau formations in sub-surface and outcrop, Alberta and British Columbia, Canada: Bulletin of Canadian Petroleum Geology, v. 48, p. 43–79, doi: 10.2113/48.1.43.

Plint, A.G., Hart, B.S., and Donaldson, W.S., 1993, Lithospheric flexure as a control on stratal geometry and facies distribution in Upper Cretaceous rocks of the Alberta foreland basin: Basin Research, v. 5, p. 69–77, doi: 10.1111/j.1365-2117.1993.tb00058.x.

Price, R.A., 1994, Cordilleran tectonics and the evolution of the Western Canada Sedimentary Basin, *in* Mossop, G., and Shetsen, I., eds., Geological Atlas of the Western Canada Sedimentary Basin: Calgary, Canadian Society of Petroleum Geology and Alberta Research Council, p. 13–24.

Price, R.A., and Sears, J.W., 2000, A preliminary palinspastic map of the Mesoproterozoic Belt-Purcell Supergroup, Canada and USA: Implications for the tectonic setting and structural evolution of the Purcell anticlinorium and Sullivan deposit, *in* Lydon, J.W., et al., eds., The Sullivan Deposit and Its Geological Environment: Geological Association of Canada, Mineral Deposits Division, p. 61–81.

Reinson, G.E., Warters, W.J., Cox, J., and Price, P.R., 1994, Cretaceous Viking Formation of the Western Canada Sedimentary Basin, *in* Mossop, G., and Shetsen, I., eds., Geological Atlas of the Western Canada Sedimentary Basin: Calgary, Canadian Society of Petroleum Geology and Alberta Research Council, p. 353–364.

Ridgley, J.L., McNeil, D.H., Gilboy, C.F., Condon, S.M., and Obradovich, J.D., 2001, Structural and stratigraphic controls on sites of shallow biogenic gas accumulations in the Upper Cretaceous Belle Fourche and Second White Specks–Greenhorn Formations of southern Alberta, Saskatchewan and northern Montana, *in* Anderson, D., et al., eds., Gas in the Rockies: Denver, Rocky Mountain Association of Geologists, p. 241–270.

Ross, G.M., and Eaton, D.W., 1999, Basement reactivation in the Alberta Basin: Observation and rationale: Bulletin of Canadian Petroleum Geology, v. 47, p. 391–411.

Ross, G.M., Patchett, P.J., Hamilton, M., Heaman, L., DeCelles, P.G., Rosenberg, E., and Giovanni, M.K., 2005, Evolution of the Cordilleran orogen (southwestern Alberta, Canada) inferred from detrital mineral geochronology, geochemistry, and Nd isotopes in the foreland basin: Geological Society of America Bulletin, v. 117, p. 747–763, doi: 10.1130/B25564.1.

Schmidt, R.G., 1978, Rocks and Mineral Resources of the Wolf Creek Area, Lewis and Clark and Cascade Counties, Montana: U.S. Geological Survey Bulletin 1441, 91 p.

Schroder-Adams, C.J., Leckie, D.A., Bloch, J., Craig, J., McIntyre, D.J., and Adams, P.J., 1996, Paleoenvironmental changes in the Cretaceous (Albian to Turonian) Colorado Group of western Canada: Microfossil, sedimentological and geochemical evidence: Cretaceous Research, v. 17, p. 311–365, doi: 10.1006/cres.1996.0022.

Schwartz, R.K., 1982, Broken Early Cretaceous foreland basin in southwestern Montana: Sedimentation related to tectonism, *in* Powers, R.B., ed., Geologic Studies of the Cordilleran Thrust Belt: Denver, Rocky Mountain Association of Geologists, p. 159–183.

Schwartz, R.K., and DeCelles, P.G., 1988, Cordilleran foreland basin evolution in response to interactive Cretaceous thrusting and foreland partitioning, southwestern Montana, *in* Schmidt, C.J., and Perry, W.J., eds., Interaction of the Rocky Mountain Foreland and the Cordilleran Thrust Belt: Geological Society of America Memoir 171, p. 489–513.

Sears, J.W., 2001, Emplacement and denudation history of the Lewis-Eldorado-Hoadley thrust slab in the northern Montana Cordillera, USA: Implications for steady-state orogenic processes: American Journal of Science, v. 301, p. 359–373, doi: 10.2475/ajs.301.4-5.359.

Sinclair, H.D., Coakley, B.J., Allen, P.A., and Watts, A.B., 1991, Simulation of foreland basin stratigraphy using a diffusion model of mountain belt uplift and erosion: An example from the central Alps, Switzerland: Tectonics, v. 10, p. 599–620, doi: 10.1029/90TC02507.

Stott, D.F., 1963, The Cretaceous Alberta Group and Equivalent Rocks, Rocky Mountain Foothills, Alberta: Geological Survey of Canada Memoir 317, 306 p.

Stott, D.F., 1984, Cretaceous sequences of the foothills of the Canadian Rocky Mountains, *in* Stott D.F., and Glass, D.J., eds., The Mesozoic of Middle North America: Calgary, Canadian Society of Petroleum Geologists Memoir 9, p. 85–107.

Tyagi, A., Plint, A.G., and McNeil, D.H., 2007, Correlation of physical surfaces, bentonites and biozones in the Cretaceous Colorado Group from the Alberta Foothills to south-west Saskatchewan, and a revision of the Belle Fourche/Second White Specks formational boundary: Canadian Journal of Earth Sciences, v. 44, p. 871–888, doi: 10.1139/E07-004.

Tysdal, R.G., 1991. Depositional Environments for Strata of Composite Section of Frontier Formation, Madison Range, Southwestern Montana: U.S. Geological Survey Bulletin 1949, 23 p.

Varban, B.L., and Plint, A.G., 2005, Allostratigraphy of the Kaskapau Formation (Cenomanian–Turonian) in subsurface and outcrop: NE British Columbia and NW Alberta, Western Canada Foreland Basin: Bulletin of Canadian Petroleum Geology, v. 53, p. 357–389, doi: 10.2113/53.4.357.

Wallace, C.A., Lidke, D.J., and Schmidt, R.G., 1990, Faults of the central part of the Lewis and Clark Line and fragmentation of the Late Cretaceous foreland basin in west-central Montana: Geological Society of America Bulletin, v. 102, p. 1021–1037, doi: 10.1130/0016-7606(1990)102<1021:FOTCPO>2.3.CO;2.

Warren, P.S., and Stelck, C.R., 1940, Cenomanian and Turonian faunas in Pouce Coupe district, Alberta and British Columbia: Transactions of the Royal Society of Canada, v. 34, p. 143–152.

White, T., Furlong, K., and Arthur, M., 2002, Forebulge migration in the Cretaceous Western Interior Basin of the central United States: Basin Research, v. 14, p. 43–54, doi: 10.1046/j.1365-2117.2002.00165.x.

Yang, Y., and Miall, A.D., 2008, Marine transgressions in the mid-Cretaceous of the Cordilleran foreland basin re-interpreted as orogenic unloading deposits: Bulletin of Canadian Petroleum Geology, v. 56, no. 3, p. 179–198.

Manuscript Received 19 November 2007
Revised Manuscript Received 12 June 2008
Manuscript Accepted 18 June 2008

Printed in the USA

Arctic and Alpine Research, Vol. 22, No. 1, 1990, pp. 1-13

LATE PLEISTOCENE GLACIERS AND THE CLIMATE OF WESTERN MONTANA, U.S.A.

William W. Locke
Department of Earth Sciences, Montana State University
Bozeman, Montana 59717, U.S.A.

ABSTRACT

Western Montana is ideally situated to have both its climate affected by the presence of Pleistocene ice sheets and those effects be apparent in its distribution of mountain glaciers. Paleoequilibrium line altitudes (paleoELAs) determined through a weighted average of cirque floor elevations, highest lateral moraines, and interpreted glacial extents define a complex pattern which reflects sources of moisture, directions of airflow, and sites of local convergence and divergence of airmasses.

The regional trend of paleoELAs is parallel to that of present glacier ELAs but lies about 450 m lower. The parallelism suggests that the regional controls on moisture availability during late Pleistocene time were similar to those at present. Numerical reconstructions of precipitation required to maintain glaciers assuming a uniform regional 10°C summer temperature depression indicate a Pleistocene decrease in precipitation, relative to present, of about 25 cm H_2O. Decreases were greater (more than 50 cm H_2O) over the high mountains of southwest Montana and snowfall may have increased (by more than 50 cm H_2O) in west-central Montana. Glacial Lakes Missoula and Great Falls may have served as significant local moisture sources during periods of maximum glaciation. Windflow patterns were similar to those at present, except that convergence of prevailing westerlies and katabatic winds from the Laurentide and Cordilleran ice sheets apparently generated local forceful uplift and increased precipitation.

INTRODUCTION

The study of the regional distribution of snowlines (altitudinal distribution of permanent snow and ice) is justified by Bradley (1985) as providing "an integrated measure of . . . climate in mountainous regions" (p. 230). Specifically, they provide "a means of obtaining important regional information on the state of glaciation, integrated regional climatic characteristics, and the sensitivity of present glaciers to climatic changes" (Humlum, 1985: 311). More importantly, because some former snow and ice bodies leave evidence of their presence, the reconstructions of paleosnowlines can provide proxy indicators of past climates. Leonard (1984) interprets snowline changes as indicative of changes in moisture source, wind direction, and effective continentality. Meierding (1982) summarizes past studies of modern and former snowlines, many of which have interpreted minimum temperature change associated with Pleistocene glaciation.

The term "snowline" is generic, as it can refer to many separate characteristics of present or past snow or ice bodies. On existing glaciers the most important elevation is that of the firn line, which separates the zone of net accumulation to date from that of net ablation (neglecting superimposed ice). The average position of the highest annual firn line over a number of years approximates the equilibrium line altitude (ELA) for that glacier, and the regional distribution of ELAs (RELA) is a common measure of integrated climate (Hawkins, 1985).

The major advantage of RELAs over other snowlines is that the approximate position of the steady-state (10^2 to 10^4 yr) ELA can be estimated for former glaciers from a number of criteria related to cirque and moraine morphology (Meierding, 1982). Of these criteria (below), the one which has had the widest use is that of the lowest elevations of northeast-facing cirque floors. Because the mass turnover is greatest at the ELA, the highest velocities in a cirque glacier, thus the greatest erosional potential, should occur near that level (Andrews, 1975). However, Bradley (1985) and Hawkins (1985) warn that cirque floors represent the integrated erosional history of a region across many glaciations; they may not therefore correctly indicate climate during any single event. They also warn that uncertainties as to the modern climates of mountainous regions and their relationship to present glaciation render the results of paleoclimatic interpretation equivocal.

Nevertheless, the ubiquitous distribution of cirques across vast areas of the North American cordillera makes at least simplistic evaluations of paleoclimate possible. Richmond (1965) generated north-south cirque floor elevation transects along the crest of the Rockies and interpreted a roughly equal Pleistocene depression of ELAs along the length of the range. Flint (1971) portrayed ELA trends across the entire American west and commented on the decrease in cirque floor elevation to the north and west, indicating the effects of decreasing average temperature (south to north) and the increase in precipitation (east to west). Porter et al. (1983) presented similar, but revised data and recognized that anomalies from the general trend represented moisture availability. They interpreted the Snake River Plain to be of particular importance as an avenue for moisture introduction into the Central Rockies. Porter et al. (1983) also recognized that the trend in ELAs across space was not smooth, but that they increased in a stepwise fashion where air masses penetrated inland across major orographic barriers.

The major trends of paleoELAs across the western United States are clear, as are the dominant controls on them. There are, however, critical subregions which have both the potential and the need for higher resolution than had been accomplished previously. Conspicuous among these regions are the San Juan Mountains of southwestern Colorado, where the combined effects of both Pacific Ocean/Gulf of California and Gulf of Mexico moisture may have been evident, and the Montana ranges, where the interactions between regional airflow and the Laurentide and Cordilleran ice sheets could have been significant. The San Juan Mountains have recently been studied by Leonard (1984); Montana is the area of this study (Figure 1).

The significance of the study area is threefold: the isolated mountain ranges of western and central Montana were nearly all occupied by mountain glaciers during ice maxima (Alden, 1953), the climate of the area is extremely varied and supports minor glaciation at present (Meier, 1961), and Laurentide and Cordilleran ice masses were juxtaposed with the locally glaciated mountains (Montagne, 1972). Locke (1989) evaluated the present climate and glaciation of the region, which serves as a modern standard against which to compare late Pleistocene glaciation and climate. Many workers (e.g., Kutzbach and Wright, 1985) have modeled the effects of continental ice sheets on regional climates; this study serves as a test of some of those reconstructions.

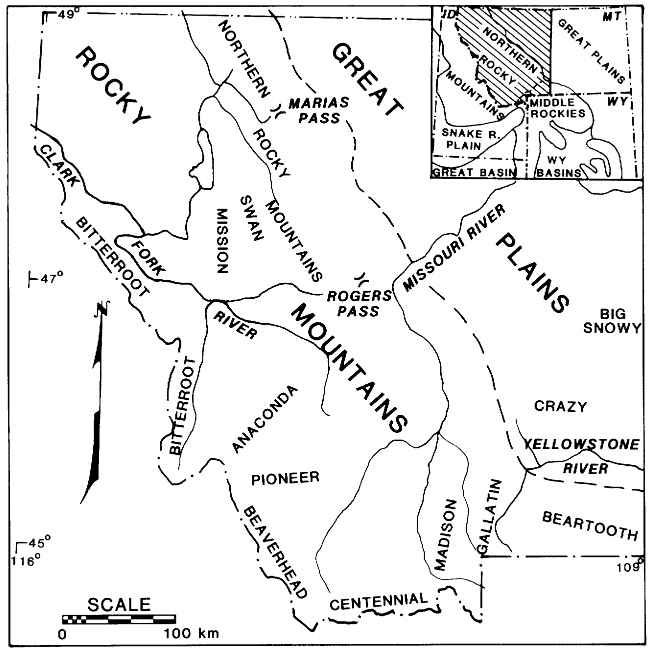

FIGURE 1. Physiography of western Montana, showing mountain ranges and other locations referred to in the text. All named ranges supported glaciers during the Pleistocene.

Montana has over 40 named mountain ranges (Taylor and Ashley, undated). Most (>35) of the ranges have summit elevations sufficient to have allowed late Pleistocene glaciation (Alden, 1953; Montagne, 1972; Taylor and Ashley, undated), yet the small area and high relief of most of the ranges lead to the formation only of cirque and valley glaciers (contrast with the San Juan Mountains: Atwood and Mather, 1932; Leonard, 1984). The even distribution of these ranges throughout the western half of the state allows the detailed reconstruction of RELAs, thus of paleoclimates of the glacial maximum.

The paleoclimate of Montana during past glaciations must have been significantly different from the present. Not only does paleoglaciation imply a decrease in temperature and/or an increase in precipitation, but the albedo and even the topography of the state, thus regional airflow patterns, must have differed as well. The northwestern portion of the state was occupied by the terminus of the Cordilleran ice sheet (Waitt and Thorson, 1983), while the northeastern segment was covered by Laurentide ice (Colton et al., 1961; Mickelson et al., 1983). In southwestern Montana, the Yellowstone ice cap and its northern outlet glacier was perhaps the longest non-ice sheet glacial flowline in the contiguous 48 states (Pierce, 1979). The presence of these major ice masses in addition to the numerous cirque and valley glaciers may have led to significant modification of local and regional windflow patterns, and consequently climate (Kutzbach and Wright, 1985).

PRESENT CONDITIONS

The extent and climatic implications of present cirque glaciers in Montana are summarized by Locke (1989). These glaciers decrease in ELA from southeast to northwest, with 92% explanation on easting and northing alone. This trend parallels a decrease in summer temperature and an increase in winter precipitation, both due to the introduction of cool, moist Pacific air in the lower northwest corner of the state. The residuals to the trend reflect control of cirque glacier ELA by local airflow, cirque orientation, and cirque backwall height.

The winter precipitation interpreted by Locke (1989) for Montana glaciers is less than has generally been reported for temperate zone glaciers, but is supported by two studies on (Alford and Clark, 1968) and near (Dightman, 1967) glaciers in the region (Figure 2). These data further support the suggestions by Loewe (1971) and Andrews (1975) that the relationship between winter precipitation and summer temperature at glacier ELAs is a complex one, and is related to continentality and/or latitude. The rationale for that relationship is discussed by Locke (in press) and probably reflects the mix of summer energy sources (and to a lesser extent, sinks) in maritime versus continental or temperate versus polar environments.

To test that relationship, multiple regression analysis was performed on the data from Alford and Clark (1968), Loewe (1971), and Sutherland (1984). The curvilinear relationship previously documented between winter precipitation and summer temperature (both at the ELA) and the requirement for precipitation to exceed zero dictated the use of the logarithm of winter precipitation, which is used as the dependent variable because precipitation is far less regionally consistent than temperature (Locke, 1989). The equation:

$$\log_{10}PPT = 1.88 + 0.13(\mathrm{sum}TEMP) - 0.19 \times 10^{-3}(CONT) \qquad (1)$$

defines the relationship, where PPT is accumulation = ablation at the ELA (cm), sum$TEMP$ is mean summer temperature (months vary—see Loewe, 1971) (°C), and $CONT$ is distance from the nearest seacoast along prevailing summer streamlines (km). This equation explains 74% of the variance in the data set (compared with 59% by summer temperature alone), with $p<0.01$ (n = 25). The addition of latitude provides little improvement in prediction (76%), thus a decrease in statistical significance. Uncertainty varies from as little as 10% near the center of the data set to as much as 100% at the extremes (Figure 2). This empirical relationship provides the mechanism for using known continentality and estimated Pleistocene temperature depression to predict Pleistocene winter precipitation at former glacier ELAs.

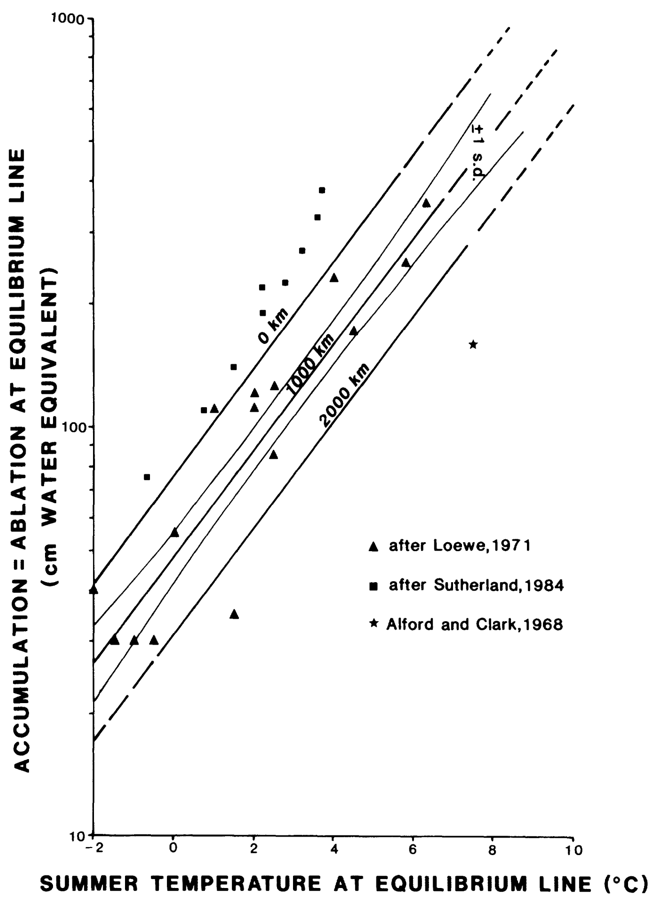

FIGURE 2. Empirical relationship among accumulation (= ablation) and summer temperature, both at the ELA, and continentality (after Alford and Clark, 1968; Loewe, 1971; Sutherland, 1984).

METHOD

The proxy data which are used to interpret Pleistocene paleoclimates of the region are the ELAs of the glaciers which formerly occupied the region. PaleoELAs are estimated from 500 different former small cirque and valley glaciers throughout western and central Montana (Figure 3). Small glaciers, regardless of aspect, were chosen as representative of maximum glacial conditions. Where ranges supported only minor glaciation, all cirques and their glaciers were evaluated. Only a representative sampling of glaciers was collected from larger or higher ranges which were extensively glaciated. Where ranges with broad crests were glaciated the presence of ice caps precluded the application of any of the techniques discussed below.

Indicators of former ELAs include the elevation of cirque floors and lateral moraines, and elevational and areal relationships based on the estimated extent of former glaciers (Richmond, 1965; Flint, 1971; Andrews, 1975; Meierding, 1982). Meierding (1982) found that the following four indicators gave similar results (within 27 m): the altitude of small, north- to east-facing cirque floors (*CIR*); the maximum altitude of lateral moraines (*MOR*); an estimate of 40% of the vertical distance between the glacier toe and the top of the cirque headwall (*THAR*); and an estimate of 65% of the former glacier area falling within the accumulation area (*AAR*). The root mean square error of these techniques varied from 80 m (*THAR*) to 81 m (*AAR*) to 109 m (*CIR*) to 148 m (*MOR*). The former two techniques were characterized as time-consuming and objective and the latter two as rapid and subjective. In all cases the estimates are subject to local variability and to error caused by the use of features of multiple ages (Bradley, 1985). Leonard (1984) used *AAR*s with less than 50-m error on existing glaciers and 75- to 100-m error on paleoglaciers. Hawkins (1985) used *MOR* and *THAR* as well as *AAR*, but found that *MOR* lies significantly lower (by ca. 50 m) than the other two, which agree within 28 m.

The density of points used in past studies has varied with study area size. Hawkins used a density of about 14 points/1000 km^2 in a 2500-km^2 area, whereas Leonard (1984) used a density of about 4 points/1000 km^2 in a 22,500-km^2 area. In this study a density of 3 points/1000 km^2 is achieved across 176,000 km^2.

In this study, data are interpreted from topographic maps at scales of 1:24,000 and 1:62,500 and contour intervals ranging from 20 to 80 ft (6 to 24 m). The four complementary methods (*CIR, MOR, THAR,* and *AAR*) are applied wherever possible. Analysis of preliminary data (Table 1) shows that although all of the measures of paleoELA are strongly related to one another ($r > 0.99$), highest lateral moraines generally lie about 230 m below

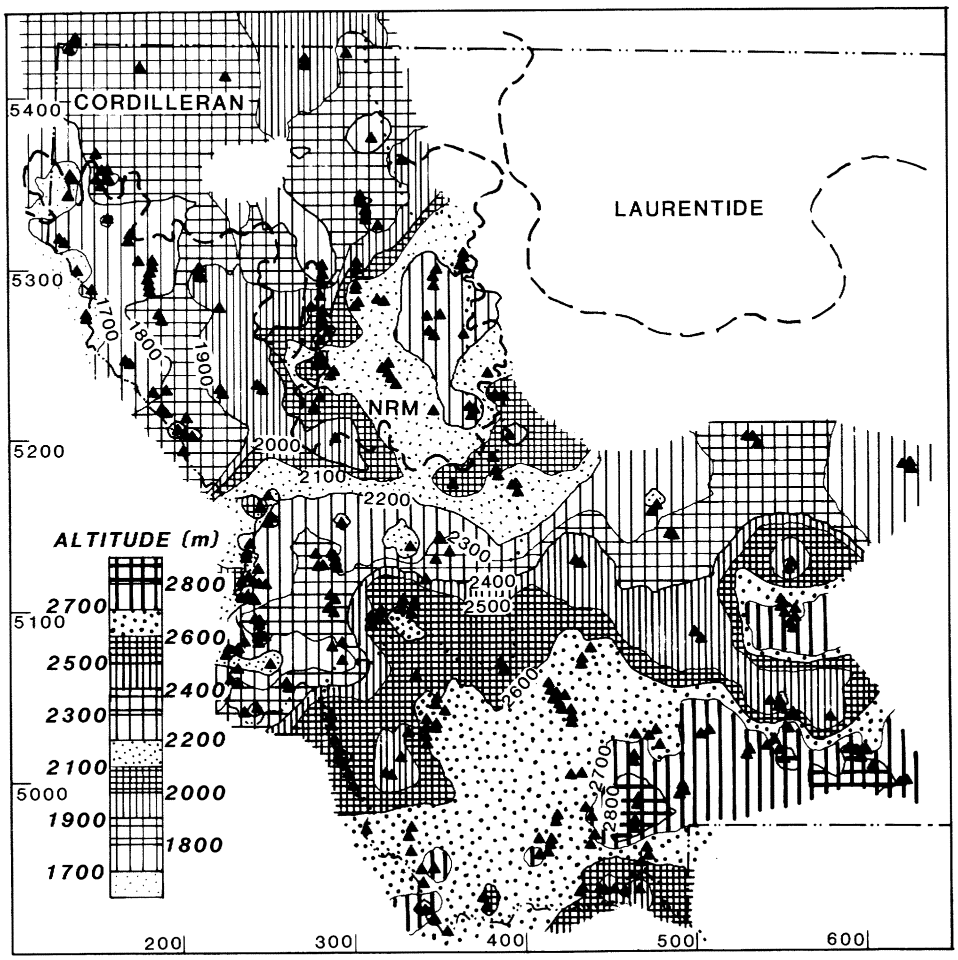

FIGURE 3. Composite Pleistocene paleoequilibrium line altitudes in western Montana. Contour interval is 100 m. Triangles indicate locations of paleoELA estimates. Margins of former ice caps and ice sheets (dashed – NRM indicates Northern Rocky Mountains ice cap) and the Continental Divide (dotted) are also shown. Ticks show Universal Transverse Mercator grid, forced to Zone 12T, in kilometers. Note: Colored versions of Figures 3–8 are available as a set of 35-mm slides from the author for $5.00.

the others. This phenomenon, which doubtless results from nonpreservation of moraines in steep valleys, requires that *MOR* be disregarded in this study. Because it is not possible to use all methods for all glaciers because of uncertainties as to ice-affected area (*AAR*) and poorly formed cirques (*CIR*), the techniques are weighted in order of their estimated precision and accuracy (*THAR* = 3, *AAR* = 2, *CIR* = 1). The weighted mean paleoELAs is then plotted at its approximate geographic location.

Because *THAR* and *AAR* required the identification of maximum ice extent based on morainal topography, and because the moraines of the last glaciation (Pinedale) are far more prominent on topographic maps than those of prior glaciations, the interpretation presented here logically represents the climate at the peak of the last glaciation. Where *CIR* is used alone it may include cirques occupied during prior glaciations, thus the results must be considered composite in age. In general, however, the interpretations should be comparable to other last-glacial climatic reconstructions (e.g., CLIMAP, 1981; Kutzbach and Wright, 1985).

TABLE 1
Statistical comparison of paleosnowline indicators[a]

	MOR	*CIR*	*THAR*	*AAR*
MOR	2121 ± 334	0.91	0.96	0.95
	321	285	317	251
CIR	28.6	2347 ± 355	0.95	0.96
	285	400	293	236
THAR	−40.4	**3.4**	2355 ± 342	0.99
	317	293	330	260
AAR	−37.4	**1.8**	**−3.0**	2353 ± 356
	251	236	260	264

[a]Upper right shows linear correlation coefficient and number of pairs, diagonal shows mean ±1 standard deviation and number of measurements, and lower left shows *T* statistic and number of pairs. Differences not significant at $p<0.001$ are shown in boldface.

RESULTS

The point data, located by easting and northing (forced to UTM Grid Zone 12), are contoured in all of the following figures using SURFER (Golden Graphics, Golden, Colorado). The closest ten points within a 50-km radius are averaged in a 20 × 20 km grid using a kriging algorithm. This analysis removes investigative bias at the cost of reduced precision where gradients are locally steep. Blank areas in the maps show regions without data points within 50 km.

Pleistocene paleoELAs in western Montana (Figure 3) were lowest (<1600 m) in the northern Bitterroot Mountains in the northwest corner of the state. From there the ELAs rose northward onto the Cordilleran Ice Sheet as well as eastward and southward. To the east a marked high in ELAs over the Northern Rocky Mountains (>2200 m) separated lows in the RELA surface. A minor trough in that surface extended north of the high and across the Northern Rocky Mountains (near present-day Marias Pass). The major trough in ELAs (generally below 2100 m) extended across the western part of the state south of the Northern Rocky Mountains. South of that trough, ELAs rose southeastward onto the highlands of southwest Montana, several of which supported local ice caps. Highest ELAs (>2900 m) were located in the highest mountain ranges (Beartooth, Madison, Gallatin, and Crazy mountains) in the southeast corner of the study area. From the western and southern boundaries of the state ELAs also increased toward the center of the state.

These results are comparable to those generated in past studies of the region, but show greater detail. Flint (1971: 475), using only *CIR*, defined a pattern which he equated to the orographic snowline which decreased northwestward from 10,000 ft (3050 m) over the Beartooth Plateau to 6000 ft (1830 m) over the northern Bitterroot Range. Similarly, Porter et al. (1983: 72) defined a trend which decreased northward across central Montana from 2700 m on the Beartooth Plateau to 2100 m near the Laurentide ice and northwestward to 1800 m in the northern Bitterroot Range. Neither of those studies used methods other than *CIR* and neither attempted a detailed study and explanation of paleoELA distribution. In the southeast corner of the study area former snowlines were estimated by Zwick (1980) on the Beartooth Plateau at >2700 m and by Pierce (1979) for the northern Yellowstone ice cap at 2850 m. Neither study is strictly comparable because of the difference in ice masses studied and techniques used, but the results of both are in agreement with the results of this study.

DISCUSSION—GEOGRAPHY

The pattern of paleoELAs can be defined in terms of the major geographic controls on glaciation—latitude, longitude, altitude, and aspect—and the major climatic controls—temperature and precipitation. A first-order trend surface fit to the data of Figure 3 decreases in elevation to the north at 1.8 m km^{-1} and to the west at 1.0 m km^{-1} (r^2 = 0.80, n = 483; Table 2). Cirque aspect (as deviation from 45°—the mean value) is insignificant when added to the regression, perhaps reflecting a dominance of optimally oriented glaciers in the data set.

The observed gradient is statistically indistinguishable from that defined by the ELAs of present glaciers (Locke, 1989), which in turn is consistent with a control largely by regional airflow bringing cool, moist Pacific air into the northwest corner of the state. The gradient of the trend surface is lower than those determined for both maritime (Østrem, 1966; Porter, 1977) and interior (Leonard, 1984) regions. Although Miller and others (1975) interpreted low gradients inland as suggestive of arctic desert conditions, with low moisture availability, in Montana the low gradients appear to represent *average* gradients. Major mountain fronts show RELA

TABLE 2
Trend-surface analysis of late-Pleistocene cirque and valley glacier equilibrium-line altitudes (m) ($n = 483$)

Model	Variable	Slope	S.E.	r	r^2	F	p
A	Northing (km)	-2.355	0.067	-0.85	0.72	1246	0.000
B	Easting (km)	0.992	0.068	0.55	0.80	1001	0.000
	Northing (km)	-1.806	0.067	-0.77			
C	Dev from 45°	0.696	0.193	0.16	0.81	688	0.000
	Easting (km)	1.005	0.067	0.56			
	Northing (km)	-1.785	0.067	-0.77			

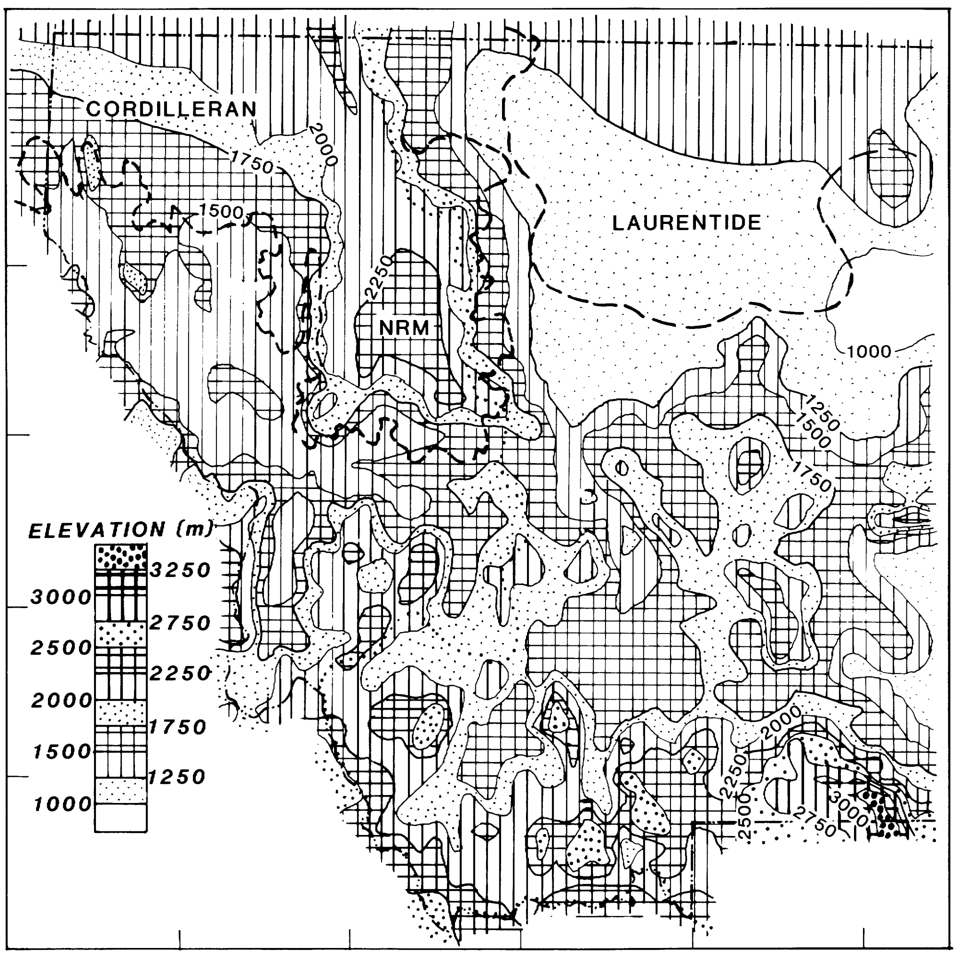

FIGURE 4. Late Pleistocene topography of western Montana. Contour interval 250 m; other symbols as in Figure 3. Areas lower than 1250 m west of the Continental Divide were inundated by Glacial Lake Missoula and east of the Divide and southwest of the Laurentide Ice Sheet were covered by Glacial Lake Great Falls. Note that closed contours reflect computer smoothing of the terrain, not the actual drainage.

gradients comparable to those determined in other studies; the low average values include intermountain areas where airmasses are often well below saturation because of locally descending air and the lack of significant local moisture recharge sources. The northward gradient exceeds those calculated by Østrem (1966) and Meierding (1982), perhaps because of local topographic factors. The presence of the continental ice masses may have generated a latitudinal temperature gradient well above normal.

The 20% of the variance which is not explained by latitude and continentality is logically dictated by regional topographic control over airflow and local topography such as headwall height. In contrast to the present topography, the late Pleistocene topography is dominated by "highlands" (including the continental ice sheets) both north and south (Figure 4), rather than dominantly in the south (cf. Locke, 1989, Figure 1). Only in the center of the study area were there passes with lowest elevations below 1750 m. This gap in the Continental Divide, nearly 1000 m lower than the mountains to the south and the ice sheets to the north, was a logical path for regional airflow.

Anomalously low RELAs (>100 m below the trend surface) occurred along the Bitterroot Range of western Montana (with protrusions to the northwest and southeast), the Centennial Range of southern Montana, and from the front of the Beartooth Range to the isolated Big Snowy Mountains of the eastern plains. Each of these anomalies most logically represents the effect of a moisture source.

The Bitterroot Range served as a barrier to Pacific moisture, allowing penetration only up the Clark Fork River valley and across two passes below 2000 m. To the south the Beaverhead Range and the high ranges of adjacent Idaho diverted moisture both north and south into the Snake River Plain. Orographic and convergent lifting of air penetrating eastwards along the Snake River Plain is evident in lowered ELAs along the Centennial Range and into adjacent Yellowstone Park, but farther northeastward penetration was minor. The greatest negative RELA anomaly was on the edge of the Great Plains, where Gulf of Mexico moisture was significant. Finally, Glacial Lake Missoula occupied the entire lowland area of western Montana (Pardee, 1942), with surface elevations up to 1280 m asl (Figure 4). Airflow from west to east would not only have been relatively high in moisture from its Pacific source but would have been seasonally recharged from Glacial Lake Missoula as well. The effects of topographic funnelling and moisture recharge are evident in the paleoELA data, with troughs in the RELA pattern across Lake Missoula toward Marias Pass (presently 1600 m, but ice covered to ca. 2100 m during the late Pleistocene: Locke, unpubl.) in the north and several passes below 2000 m in the south. RELA depression (<2000 m) east of these Continental Divide passes may be explained by recharge from Glacial Lake Great Falls (Colton et al., 1961). It may also reflect convergence of katabatic winds draining southward along the confluence of the Laurentide and Cordilleran ice sheets with prevailing westerlies, thus forceful lifting and enhanced precipitation.

Regional ELAs which lie well above (>100 m) the trend surface are restricted to the northwesternmost corner of the state and the cores of the major mountain massifs: Northern Rockies/Swan/Mission, Beartooth/Gallatin/Madison, and Anaconda/Pioneer/Beaverhead. The rise to the north (based entirely on cirque floor elevations above Cordilleran ice) may indicate the exclusion of moisture from the main mass of the Cordilleran Ice Sheet, perhaps by descending cold air. An alternative explanation is that the mountains to the north of the Clark Fork River have been affected by isostatic compensation since deglaciation. Waitt and Thorson (1983) document up to 200 m of isostatic compensation along the US–Canada boundary at Puget Sound, also affected by Cordilleran ice, thus all or part of the observed paleoELA rise may be explained by that mechanism. The irregular topography, poorly constrained ice thickness, and uncertain crustal and asthenospheric parameters preclude rigorous testing of this hypothesis at present.

The remaining areas of high RELA are located in the major mountain massifs of Montana, including the Mission/Swan/Northern Rocky Mountains downwind of Glacial Lake Missoula. These areas are probably the result of airflow diversion around the high ranges, with a "snow shadow" in the center of the ranges. Each of these ranges has local relief >2000 m, suggesting that the major moisture transport involved surface winds (<2 km above ground level) with divergence around the ranges rather than orographic rising over them. This is in agreement with the conclusions of Meierding (1982), Leonard (1984), and Humlum (1985), and with the normal distribution of atmospheric moisture (e.g., Barry and Chorley, 1976; Price, 1981).

DISCUSSION—CLIMATE CHANGE

The comparison of integrated indicators of present and past climate allows the interpretation of relative climatic change. The most striking evidence indicates that the pattern of modern snowpack (Locke, 1989, Table 3) and paleoELAs (Table 2) are parallel, with both changing to the north twice as rapidly as to the west. This is in agreement with Leonard (1984) and with Porter et al. (1983), who concluded that "the Pleistocene pattern of airmass movements apparently was similar to that at present" (p. 103). The dominant moisture source, then as now, was the Gulf of Alaska. In detail, however, this study suggests noticeable differences in airflow pattern between Pleistocene and present.

Prior studies of paleosnowlines have interpreted minimum Pleistocene snowline lowering of at least 300 m (Zwick, 1980; Leonard, 1984) relative to present. The estimates are minima because modern glaciers only exist in favorable localities (Leonard, 1984; Locke, 1989). The trend surface defined by ELAs in this study lies about 450 m below that of modern glaciers in the region (Locke, 1989), compared with estimated Pleistocene ELA depression of about 1000 m in much of the Rocky Mountains (Barry, 1983). Interpretation of these data has resulted in estimates of minimum temperature depression assuming no change in precipitation (Zwick, 1980; Porter et al., 1983). The regional consistency of temperature data and the variability of precipitation (Locke, 1989) suggests that the inverse model – assuming temperature to estimate precipitation – may be more appropriate.

Glaciation is the balance between accumulation and ablation. If we assume a known summer temperature and Pleistocene continentality equal to the present (thus defining ablation), the relationship of equation (1) allows the estimation of past snowpacks (accumulation) from ELAs. There are no paleotemperature data from within the study area; however, published summaries by Peterson et al. (1979), Barry (1983), and Péwé (1983) suggest Pleistocene summer temperatures were *at least* 10°C lower than present in the northern Rocky Mountain states. Accordingly, mean summer temperatures at glacial ELAs are estimated from the trend surface of Locke (1989) minus 10°C and that value (Figure 5) is used with equation (1) to estimate Pleistocene snowpack.

There are several weaknesses to the assumption of summer temperatures. Trend surface estimates of modern summer temperatures have an uncertainty of about 0.75°C (Locke, 1989), thus that uncertainty applies to consequent estimates of paleotemperatures. Modern summer temperatures are controlled by latitude and windflow patterns. The latitudinal paleotemperature gradient was probably affected by the presence of the ice sheets to the north, and former windflow patterns may have differed

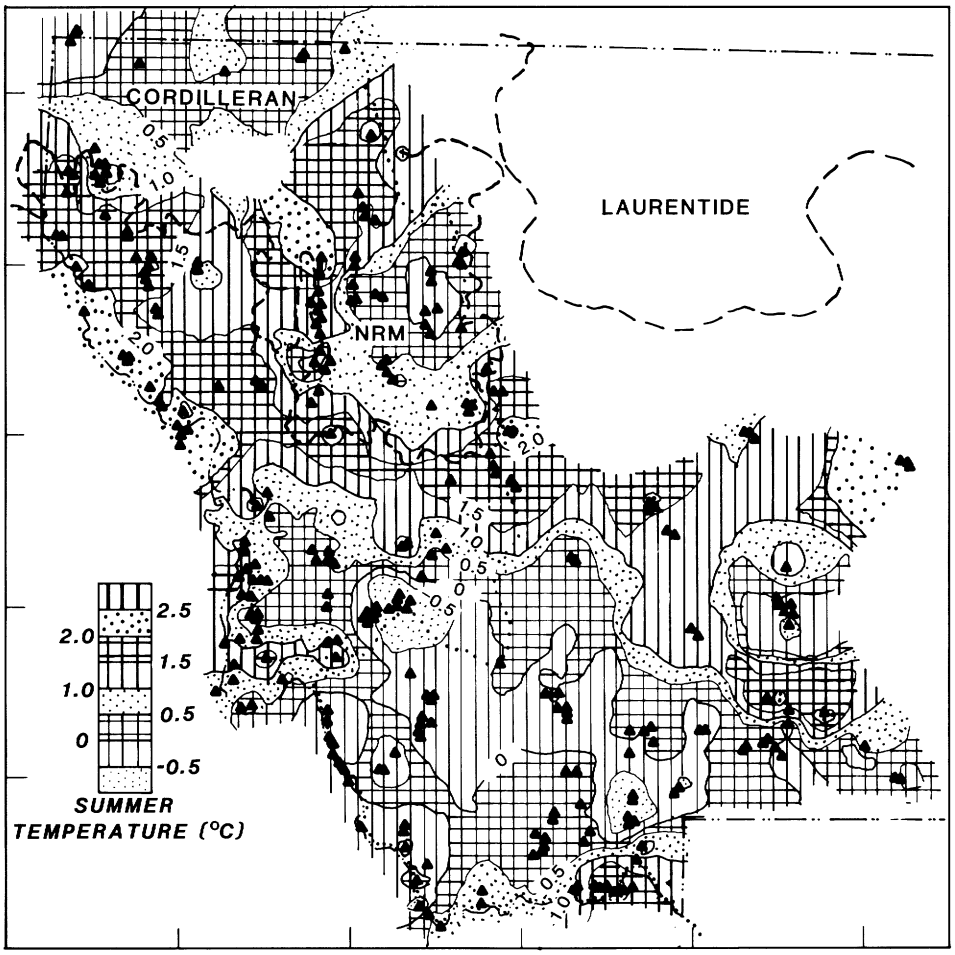

FIGURE 5. Assumed summer (June–August mean) temperatures (°C) at former glacier ELAs using modern temperature (after Locke, 1989) lowered by 10°C. Contour interval of 0.5°C shows trends, but differences of less than 1°C are not considered significant. Symbols as in Figure 3.

from present, although probably not substantially (above). The estimates are sensitive to vertical temperature gradients, which are assumed to have been similar to the present summer environmental lapse rate (-5.86°C km^{-1}; Locke, 1989). Because most modern lapse rates from glacierized areas do not differ significantly from that value (e.g., Andrews and Miller, 1972), no bias is evident in that assumption. Finally, the estimate of an average cooling by 10°C may be in error. It is likely, however, that the trends and major anomalies in summer temperatures at glacial ELAs are valid, and that the numerical values are conservative with respect to difference from present inasmuch as some published estimates (e.g., Mears, 1981, from adjacent Wyoming) suggest a cooling of greater than 10°C.

The assumed summer temperatures at ELAs range from -1.5 to +2.5°C (Figure 5). Because those temperatures are strongly elevation dependent, the pattern is very similar to that of paleoELAs (Figure 3). Assumed summer temperatures at ELAs were lowest where ELAs were highest: in the major massifs of southernmost western Montana and the northern Rocky Mountains and in the northwest corner of the state. Highest summer temperatures at ELAs are inferred along the western border, across the center of the study area, at the edge of the Great Plains, and at the end of the Snake River Plain. These temperatures lie within the range reported for modern glaciers (Figure 2) albeit near the low end of that range.

If the temperature estimates are valid, winter snowpack can be estimated using equation (1) (Figure 6). Because higher accumulation is required to offset higher ablation-season temperatures, the pattern is again similar to that of paleoELAs – the initial data set. Relatively low winter accumulation (<60 cm H_2O) was required to support glaciation in the high massifs of southern, central, and northwesternmost western Montana, whereas relatively high accumulation (>80 cm H_2O) was required along the western boundary of the state, across the center of the study area, along the edge of the Great Plains, and at the end of the Snake River Plain. This reconstruction assumes that the evaluation of modern analogs was valid

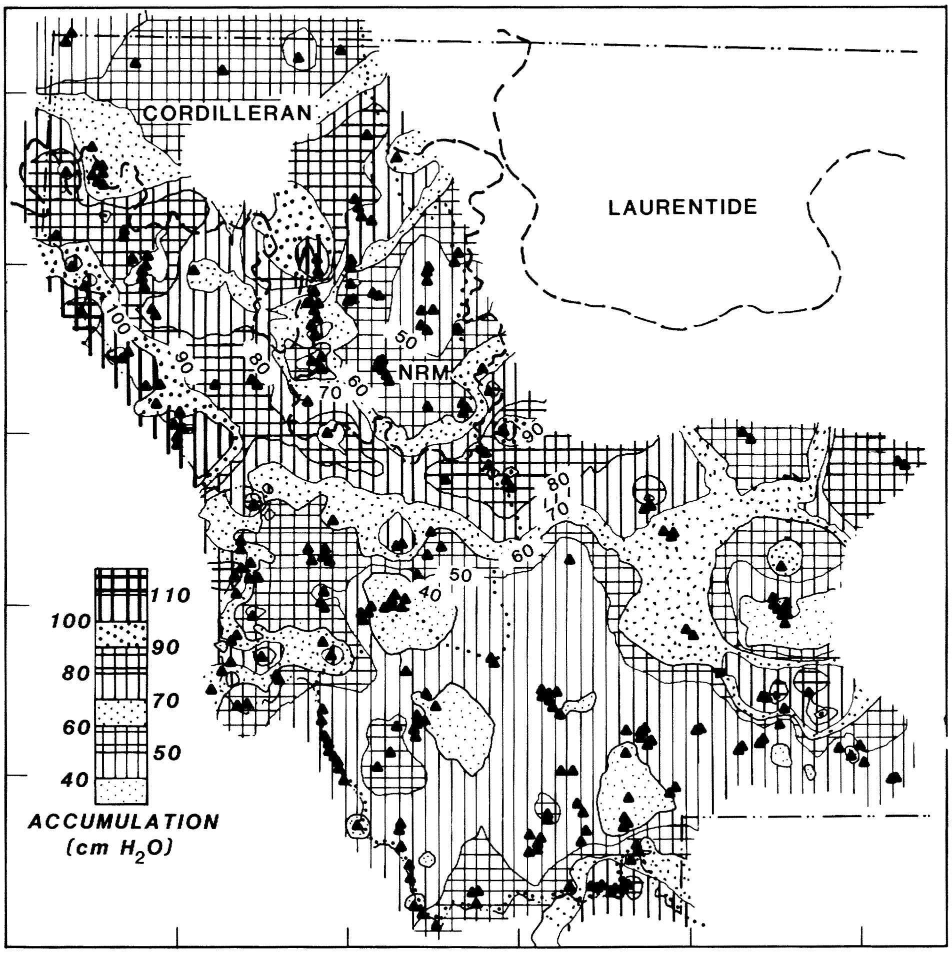

FIGURE 6. Calculated accumulation (cm H_2O) at former glacier ELAs using temperatures of Figure 5 and relationship of equation (1). Contour interval of 10 cm H_2O shows trends, but differences of less than 25% are not considered significant. Symbols as in Figure 3.

and, if so, is accurate within about 25% (10 to 20 cm H_2O). The significance of this reconstruction lies not so much in the individual values as in the trends across space and time.

Spatial trends are explicit in Figure 6; temporal trends require a modern data set for comparison. The best modern data are those of maximum snowpack (Soil Conservation Service, 1988), which are collected at elevations close to those of former glacier ELAs. Because modern snowpack begins to melt in spring and continues to melt into the fall, maximum snowpack is an underestimate of total snowfall. Comparisons with glacial accumulation will thus minimize glacial precipitation decreases and maximize apparent increases relative to present. Glacial accumulation also underestimates total precipitation, so the net error should be minor. Modern maximum snowpack data show consistent regional trends, but are affected by strong, coherent residuals (Locke, 1989). For comparison to reconstructed paleoprecipitation, modern maximum snowpack at glacial ELAs (Figure 7) is estimated using the trend surface of Locke (1989) at glacial elevations, with the modern spatial anomalies (residuals to that trend surface) added. This method assumes that the modern residuals result from regional (spatial) variability in moisture availability rather than variability with elevation. Although this assumption may be invalid, our present lack of understanding of vertical precipitation gradients (e.g., Zielinski and McCoy, 1987) makes it necessary. Uncertainty of estimation of modern snowpack is about 25%.

The pattern of modern maximum snowpack at Pleistocene glacial ELAs (Figure 7) differs substantially from the pattern of the ELAs themselves (Figure 3). Snowpack maxima (> 100 cm H_2O) occur over both the high Beartooth/Gallatin/Madison massif (because of high Pleistocene ELAs) and over the western border (because of modern moisture availability). Snowpack minima trend northeast-southwest across the center of the study area because of low Pleistocene ELAs (northeast) and low modern moisture availability (southwest).

The difference between modern maximum snowpack and glacial accumulation (Figure 8) can be calculated by

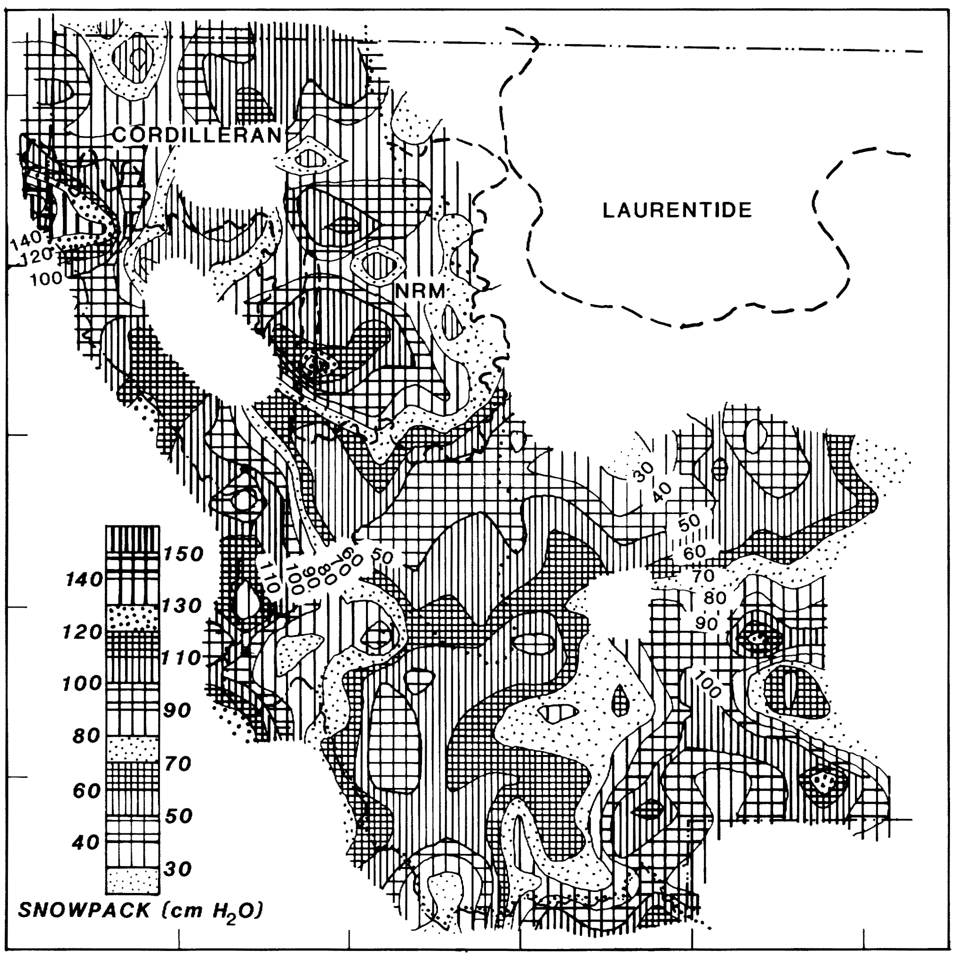

FIGURE 7. Modern maximum snowpack (cm H_2O) at former glacier ELAs (after Locke, 1989). Contour interval of 10 cm H_2O shows trends and is indicative of precision of available data. Symbols as in Figure 3.

subtracting the gridded estimates of those variables. Because of the differences between the data types, inferred precipitation decreases (glacial relative to present) are minimum estimates and inferred increases are maximum. If 25 cm H_2O differences are considered to be insignificant, Pleistocene winter accumulation exceeded modern only in the central portion of the study area, where calculated accumulation exceeded 150% of modern maximum snowpack. Under the assumed conditions of a 10°C cooling this increase very probably reflects both moisture recharge from Glacial Lakes Missoula and Great Falls and convergence of prevailing and katabatic winds.

Interpreted Pleistocene winter accumulation was significantly (>25 cm H_2O) less than modern maximum snowpack across much of the rest of the state. The maximum relative decreases are evident within the high massifs of southern and central Montana and along the margin of the Cordilleran Ice Sheet. This corresponds to a >25% reduction in winter snowfall. Considering that this difference is a minimum because of the differences in the data sets, it is clear that on average the mountainous region of Montana was about 25% or 25 cm H_2O drier in winter during the maximum of the last glaciation than it is at present. This estimate is a minimum because of the conservative effects of the estimates of regional cooling and the noncomparable data sets.

Quantitative estimates of snowfall at the last glacial maximum to which this reconstruction can be compared are rare. However, in an entirely independent study, Murray (in preparation; Murray and Locke, in press) has used glacier flow theory to reconstruct glacier mass balance, including average annual accumulation above the ELA. Results from individual glaciers in the Crazy Mountains and northern Beaverhead Mountains (Figure 1) are within 20% (the limits of accuracy of that study) of the values determined in this study (Figure 6). In both cases the calculated average annual accumulation above the ELAs (Murray, in preparation) exceeds the calculated accumulation = ablation at the ELA (this study). We conclude therefore, that an independent test has failed to discredit the results of this study despite the numerous assumptions required for this analysis. Other estimates

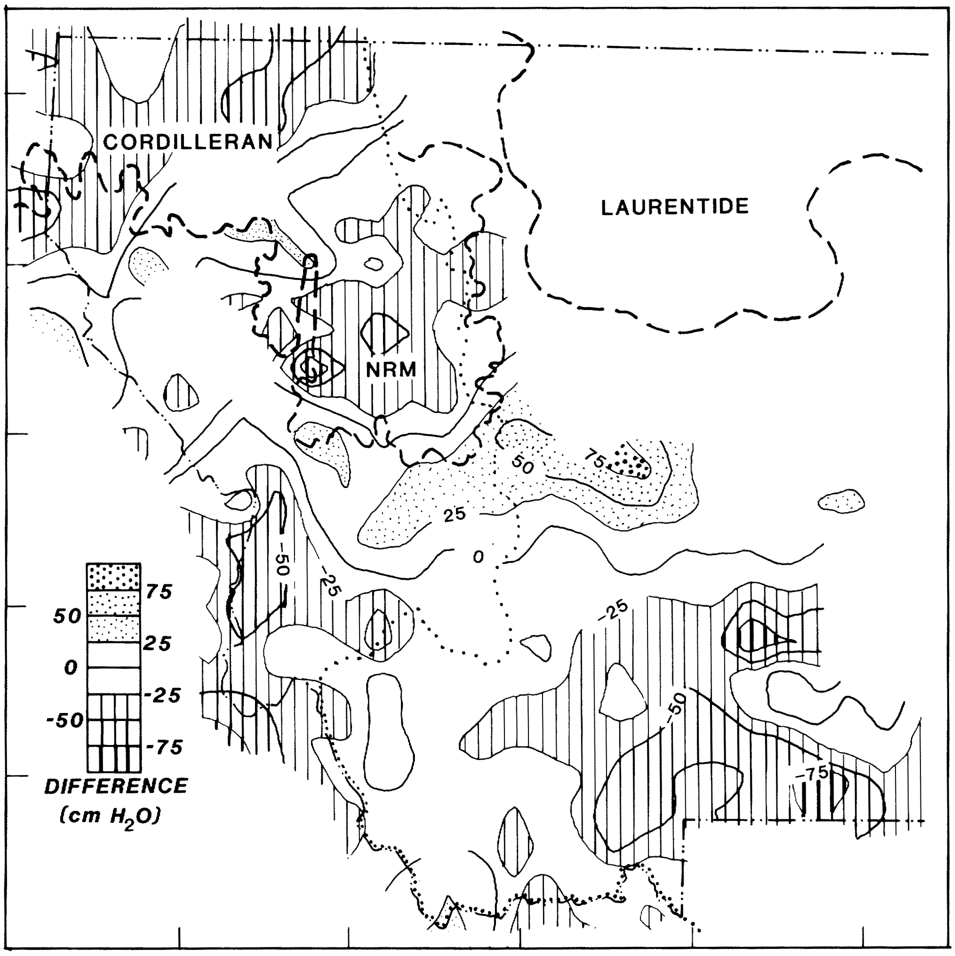

FIGURE 8. Difference between Pleistocene winter accumulation (Figure 6) and modern maximum snowpack (Figure 7) (cm H_2O). Contour interval of 25 cm H_2O may not indicate significant relative increases in precipitation, but almost certainly indicates significant decreases (see text). Symbols as in Figure 3.

using glacier flow theory of peak-glacial precipitation in mountainous regions agree that the last glaciation was drier than present in the central Rocky Mountains (Leonard et al., 1986) and the Alps (Haeberli and Penz, 1985), although neither study is directly comparable to this one because of location and low precision.

CONCLUSIONS

Western Montana is an important locality for paleoclimatic study because of the interaction of Laurentide, Cordilleran, and local ice. Past glacier extents are a useful indicator of paleoclimate in the region because small glaciers were present in many of the mountain ranges. The pattern of paleoequilibrium line altitudes of such former glaciers is a direct indicator of the patterns of climatic variables, chiefly summer temperature and winter precipitation, which are critical to glaciation. Indirectly, combined with an understanding of the present controls on glaciation, former ELAs suggest the distribution of Pleistocene snowfall if several necessary assumptions are valid. Those assumptions include an average regional summer cooling and a Pleistocene relationship among winter precipitation, summer temperature, and continentality which is similar to present.

The distribution of paleoELAs is consistent across the study area, with 80% of the variance explained by latitude and longitude. The gradient of the paleoELA surface is the same as that determined for present glaciers in the region by Locke (in press), but lies 450 m lower. The similarity in the slopes of the surfaces implies only regionally consistent changes in the climatic variables which control glacier behavior. Using the specific assumptions of a regional 10°C depression of summer temperature and the mutual relationshiops among summer temperature, winter precipitation, and continentality of equation (1), the Pleistocene winter snowfall is interpreted as having been significantly higher than modern maximum snowpack only in a small region in the center of the study area of western Montana and lower than modern maximum snowpack in the majority of the region, including all of the higher mountains and along the southern margin of the Cordilleran Ice Sheet.

The relatively low ELAs observed, high summer temperatures assumed, and high winter precipitations calculated for the band across western Montana are consistent with a late Pleistocene storm track from west to east across the center of the state. Higher inferred precipitation in the vicinity of Glacial Lakes Missoula and Great Falls suggest that the storm track was active when the lake surfaces were unfrozen (autumn to mid-winter). The inferred increase in precipitation east of the Rocky Mountains and south of the continental ice sheets, despite an average decrease in precipitation across the region, is interpreted as the result of convergence between prevailing westerly winds and katabatic flow off of the ice sheets. Markedly lower precipitation over the highest mountain ranges of western Montana may reflect dominant moisture transport in the lower atmosphere (<2 km a.g.l.) and the diversion of moist air masses around, rather than over, highland areas.

The results of this detailed study can be compared with the simulation of Northern Hemisphere peak-glacial climates by Kutzbach and Wright (1985). The 10°C summer cooling assumed in this study is similar to that calculated in their model, and the slight decrease in winter precipitation calculated in this model is similar to that which they calculated. The only disagreement between the model results of Kutzbach and Wright and the empirical reconstructions of this study involves their calculation of calm January winds (easterlies to the west of Montana and westerlies to the east) versus the interpretation here of a winter storm track from west to east across Montana (similar to the present). This difference may represent a seasonal variability in windflow or a real difference in the strength of the prevailing westerlies, and may be resolved by future studies of local precipitation through glacial flow models or palynologic studies.

ACKNOWLEDGMENTS

The original data set analyzed here was developed by my students in Glacial Geology, especially T. Scott Kemph. Substantive improvement in the manuscript resulted from comments by Drs. W. D. McCoy and E. M. Leonard and an anonymous reviewer from the *Journal of Glaciology*. Graphics generation capabilities were greatly improved by a gift from Valerie Marsh.

REFERENCES CITED

Alden, W. C., 1953: Physiography and glacial geology of western Montana. *U.S. Geological Survey, Professional Paper,* 231. 200 pp.

Alford, D. and Clark, R., 1968: The 1967 mass balance of the Grasshopper Glacier, Montana. *Northwest Science,* 42: 115–123.

Andrews, J. T., 1975: *Glacial Systems.* North Scituate, Mass.: Duxbury Press. 191 pp.

Andrews, J. T. and Miller, G. H., 1972: Quaternary history of northern Cumberland Peninsula, Baffin Island, N.W.T., Canada: Part IV: Maps of the present glaciation limits and lowest equilibrium line altitude for north and south Baffin Island. *Arctic and Alpine Research,* 4: 45–60.

Atwood, W. W. and Mather, K. F., 1932: Physiography and Quaternary geology of the San Juan Mountains, Colorado. *U.S. Geological Survey, Professional Paper,* 166. 176 pp.

Barry, R. G., 1983: Late Pleistocene climatology. *In* Porter, S. C. (ed.), *Late Quaternary Environments of the United States, Vol. 1: The Late Pleistocene.* Minneapolis: University of Minnesota Press, 390–407.

Barry, R. G. and Chorley, R. J., 1976: *Atmosphere, Weather, and Climate* (3rd ed.). London: Methuen. 432 pp.

Bradley, R. S., 1985: *Quaternary Paleoclimatology: Methods of Paleoclimatic Reconstruction.* Boston: Allen and Unwin. 472 pp.

CLIMAP Project Members, 1981: Seasonal reconstructions of the Earth's surface at the last glacial maximum. Map and Chart Series MC-36, Geological Society of America, Boulder, Colorado.

Colton, R. B., Lemke, R. W., and Linvall, R. M., 1961: Glacial map of Montana east of the Rocky Mountains. *U.S. Geological Survey,* Map MI-327.

Dightman, R. A., 1967: *Historical and Climatological Study of the Grinnell Glacier, Montana.* Western Region Technical Memorandum 24, Salt Lake City: U.S. Department of Commerce. 26 pp.

Flint, R. F., 1971: *Glacial and Quaternary Geology.* New York: Wiley. 892 pp.

Haeberli, W. and Penz, U., 1985: An attempt to reconstruct glaciological and climatological characteristics of 18 ka ice age glaciers in and around the Swiss Alps. *Zeitschrift für Gletscherkunde und Glazialgeologie,* 21: 351–361.

Hawkins, F. F., 1985: Equilibrium-line altitudes and paleo environment in the Merchants Bay area, Baffin Island, N.W.T., Canada. *Journal of Glaciology,* 31(109): 205–213.

Humlum, O., 1985: The glaciation level in west Greenland. *Arctic and Alpine Research,* 17: 311–319.

Kutzbach, J. E. and Wright, H. E., Jr., 1985: Simulation of the climate of 18,000 years BP: Results for the North American/North Atlantic/European sector and comparison with the geologic record of North America. *Quaternary Science Reviews,* 4: 147–187.

Leonard, E. M., 1984: Late Pleistocene equilibrium-line altitudes and modern snow accumulation patterns, San Juan Mountains, Colorado, U.S.A. *Arctic and Alpine Research,* 16: 65–76.

Leonard, E. M., Huston, M. M., and Manley, A. E., 1986: Ice dynamics modelling of Rocky Mountain paleoglaciers — Methods, results, and paleoclimatic inferences. *Geological Society of America Abstracts with Programs,* 18: 671.

Locke, W. W., 1989: Present climate and glaciation of western Montana, U.S.A. *Arctic and Alpine Research,* 21: 234–244.

———, in press: Quantitative approximation of present and former mountain glacial climates. *Annals of Glaciology,* 14.

Loewe, F., 1971: Considerations on the origin of the Quaternary ice sheet of North America. *Arctic and Alpine Research,* 3: 331–344.

Mears, B., Jr., 1981: Periglacial wedges and the late Pleistocene environment of Wyoming's intermontane basins. *Quaternary Research,* 15: 319–321.

Meier, M. F., 1961: Distribution and variations of glaciers in the United States exclusive of Alaska. *In: General Assembly of Helsinki, July 25–August 6, 1960, Snow and Ice Commission,* International Association for Scientific Hydrology, Publication 54, 420–429.

Meierding, T. C., 1982: Late Pleistocene glacial equilibrium-line altitudes in the Colorado Front Range: A comparison of methods. *Quaternary Research,* 18: 289–310.

Mickelson, D. M., Clayton, L., Fullerton, D. S., and Borns, H. W., Jr., 1983: The late Wisconsin glacial record of the Laurentide ice sheet in the United States. *In* Porter, S. C. (ed.), *Late Quaternary Environments of the United States, Vol. 1: The Late Pleistocene.* Minneapolis: University of Minnesota Press, 3–37.

Miller, G. H., Bradley, R. S., and Andrews, J. T., 1975: The glaciation level and lowest equilibrium line altitude in the high Canadian Arctic: Maps and climatic interpretation. *Arctic and Alpine Research,* 7: 155–168.

Montagne, J., 1972: Wisconsin glaciation. *In: Geologic Atlas of the Rocky Mountain Region.* Denver: Rocky Mountain Association of Geologists, 257–260.

Murray, D. R., in preparation: Late Pleistocene glacier dynamics of southwestern Montana and adjacent Idaho and paleoclimatic implications. M.S. thesis, Montana State University.

Murray, D. R. and Locke, W. W., in press: Dynamics of the late Pleistocene Big Timber glacier, Crazy Mountains, Montana, U.S.A. *Journal of Glaciology.*

Østrem, G., 1966: The height of the glaciation limit in southern British Columbia and Alberta. *Geografiska Annaler,* 48A: 126–138.

Pardee, J. T., 1942: Unusual currents in glacial Lake Missoula. *Geological Society of America Bulletin,* 53: 1569–1600.

Peterson, G. M., Webb, T., III, Kutzbach, J. E., van der Hammen, T., Wijmstra, T., and Street, F. A., 1979: The continental record of environmental conditions at 18,000 years B.P.: An initial evaluation. *Quaternary Research,* 12: 47–82.

Péwé, T. L., 1983: The periglacial environment in North America during Wisconsin time. *In* Porter, S. C. (ed.), *Late Quaternary Environments of the United States, Vol. 1: The Late Pleistocene.* Minneapolis: University of Minnesota Press, 157–189.

Pierce, K. L., 1979: History and dynamics of glaciation in the northern Yellowstone National Park area. *U.S. Geological Survey Professional Paper,* 729-F. 90 pp.

Porter, S. C., 1977: Present and past glaciation threshold in the Cascade Range, Washington, U.S.A.: Topographic and climatic controls, and paleoclimatic implications. *Journal of Glaciology,* 18(78): 101–116.

Porter, S. C., Pierce, K. L., and Hamilton, T. D., 1983: Late Wisconsin mountain glaciation in the western United States. *In* Porter, S. C. (ed.), *Late Quaternary Environments of the United States, Vol. 1: The Late Pleistocene.* Minneapolis: University of Minnesota Press, 71–111.

Price, L. W., 1981: *Mountains & Man.* Berkeley: University of California Press. 506 pp.

Richmond, G. M., 1965: Glaciation of the Rocky Mountains. *In* Wright, H. E. and Frey, D. G. (eds.), *The Quaternary of the United States.* Princeton, N.J.: Princeton University Press, 217–230.

Soil Conservation Service, 1988: Montana Annual Data Summary: Water Year 1987. Washington: U.S. Government Printing Office. 42 pp.

Sutherland, D. G., 1984: Modern glacier characteristics as a basis for inferring former climates with particular reference to the Loch Lomond Stadial. *Quaternary Science Reviews,* 3: 291–310.

Taylor, R. F. and Ashley, J. A., undated: Geological Map of Montana and Yellowstone National Park. Bozeman: Montana State University, Department of Earth Sciences.

Waitt, R. B., Jr. and Thorson, R. M., 1983: The Cordilleran ice sheet in Washington, Idaho, and Montana. *In* Porter, S. C. (ed.), *Late Quaternary Environments of the United States, Vol. 1: The Late Pleistocene.* Minneapolis: University of Minnesota Press, 53–70.

Zielinski, G. A. and McCoy, W. D., 1987: Paleoclimatic implications of the relationship between modern snowpack and late Pleistocene equilibrium-line altitudes in the mountains of the Great Basin, U.S.A. *Arctic and Alpine Research,* 19: 127–134.

Zwick, T. T., 1980: A comparison between the modern and composite Pleistocene snow-lines, Absaroka and Beartooth mountains, Montana-Wyoming. *Journal of Glaciology,* 25(92): 347–352.

Ms submitted April 1988
Revised ms submitted June 1989

INTRODUCTION / INTRODUCTION

The Wyoming Province: a distinctive Archean craton in Laurentian North America[1]

P.A. Mueller and C.D. Frost

Abstract: The Wyoming Province is a distinctive Archean craton in the northwestern United States that can be subdivided into three subprovinces, namely, from oldest to youngest, the Montana metasedimentary province, the Beartooth–Bighorn magmatic zone, and the Southern accreted terranes. Archean rocks of the Montana metasedimentary province and the Beartooth–Bighorn magmatic zone are characterized by (1) their antiquity (rock ages to 3.5 Ga, detrital zircon ages up to 4.0 Ga, and Nd model ages exceeding 4.0 Ga); (2) a distinctly enriched $^{207}Pb/^{204}Pb$ isotopic signature, which suggests that this part of the province was not produced by the amalgamation of exotic terranes; and (3) a distinctively thick (15–20 km), mafic lower crust. The Montana metasedimentary province and Beartooth–Bighorn magmatic zone were cratonized by about 3.0–2.8 Ga. Crustal growth occurred via continental-arc magmatism and terrane accretion in the Southern accreted terranes along the southern margin of the province at 2.68–2.50 Ga. By the end of the Archean, the three subprovinces were joined as part of what is now the Wyoming Province. Subsequent to amalgamation of the Wyoming crust to Laurentia at ca. 1.8–1.9 Ga, Paleoproterozoic crust (1.7–2.4 Ga) was juxtaposed along the southern and western boundaries of the province. Subsequent tectonism and magmatism in the Wyoming region are concentrated in the areas underlain by these Proterozoic mobile belts.

Résumé : La Province de Wyoming est un craton archéen distinctif dans le nord-ouest des États-Unis; il peut être subdivisé en trois sous-provinces, lesquelles sont, de la plus ancienne à la plus jeune, la Province métasédimentaire de Montana, la zone magmatique de Beartooth–Bighorn et les terranes accrétés au sud. Les roches archéennes de la Province métasédimentaire de Montana et de la zone magmatique de Beartooth–Bighorn sont caractérisées par (1) leur antiquité (la roche présente des âges atteignant 3,5 Ga, des âges de zircon détritique atteignent 4,0 Ga et des âges modèles pour le Nd dépassent 4,0 Ga), (2) une signature isotopique $^{207}Pb/^{204}Pb$ fortement enrichie, ce qui suggère que cette partie de la province n'a pas été produite par l'amalgamation de terranes exotiques et (3) une croûte mafique inférieure à épaisseur remarquable (15–20 km). La Province métasédimentaire de Montana et la zone magmatique de Beartooth–Bighorn ont subi une cratonisation vers 3,0–2,8 Ga. La croûte s'est agrandie par un magmatisme d'arc continental et l'accrétion de terranes dans les terranes accrétés au sud, le long de la bordure sud de la province, il y a 2,68–2,50 Ga. Vers la fin de l'Archéen, les trois sous-provinces ont été réunies en ce qui forme de nos jours la Province de Wyoming. Après l'amalgamation de la croûte Wyoming à la Laurentia vers 1,8–1,9 Ga, la croûte paléozoïque (1,7–2,4 Ga) a été accolée le long des bordures sud et ouest de la province. Le tectonisme et le magmatisme subséquents dans la région de Wyoming sont concentrés dans les secteurs sus-jacents à ces ceintures protérozoïques mobiles.

[Traduit par la Rédaction]

Location and boundaries of the Wyoming Province

The Wyoming Province consists of Archean crust in Wyoming and parts of adjacent states (Fig. 1) (Condie 1969, 1976) and is bounded on three sides by Proterozoic collisional orogens: Great Falls tectonic zone to the north, Dakota segment of the Trans-Hudson Orogen to the east, and Cheyenne belt to the south. Its western side is composed of Proterozoic and Archean terranes, which probably extend to the rifted Neoproterozoic margin, now marked by the $^{87}Sr/^{86}Sr$ = 0.706 line. The area of the Wyoming Province enclosed by

Received 9 May 2006. Accepted 29 June 2006. Published on the NRC Research Press Web site at http://cjes.nrc.ca on 30 November 2006.

Paper handled by Associate Editor L. Corriveau.

P.A. Mueller. Department of Geological Sciences, University of Florida, Gainesville, FL 32611, USA.
C.D. Frost.[2] Department of Geology and Geophysics, University of Wyoming, Laramie, WY 82071, USA.

[1]This article introduces a selection of papers published in this Special Issue on *The Wyoming Province: a distinctive Archean craton in Laurentian North America*.

[2]Corresponding author (e-mail: frost@uwyo.edu).

Fig. 1. Location map of the Wyoming Province, showing its relationship to surrounding orogens and Precambrian provinces from Foster et al. (2006) and Chamberlain et al. (2003). The only boundary of the province that is exposed lies in the Sierra Madre and Medicine Bow Mountains, where Proterozoic rocks are juxtaposed against the Wyoming Province along the Cheyenne belt. The Montana metasedimentary province (MMP) and Beartooth–Bighorn magmatic zone (BBMZ) represent the portions of the province that were cratonized earliest (ca. 2.80 Ga). To the south lie the Southern accreted terranes (SAT), a collage of terranes that were joined to the southern margin of the Wyoming Province by ca. 2.63 Ga and cratonized by 2.50 Ga. The Sweetwater subprovince is that portion of the BBMZ that was metamorphosed and deformed in the late Archean, and the Hartville uplift – Black Hills block (HU–BH) was affected by Proterozoic west-vergent thrusting (Chamberlain et al. 2003). The area of Precambrian crust between the Wyoming craton and the $^{87}Sr/^{86}Sr = 0.706$ line includes both Archean and Proterozoic rocks. Areas shown in black are Precambrian exposures. AI, Antelope Island; BH, Bighorn Mountains; BT, Beartooth Mountains; LR, Laramie Range; MB, Medicine Bow Mountains; RR-A-GC, Raft River – Albion – Grouse Creek Mountains; SM, Sierra Madre; T, Teton Range; WR, Wind River Mountains.

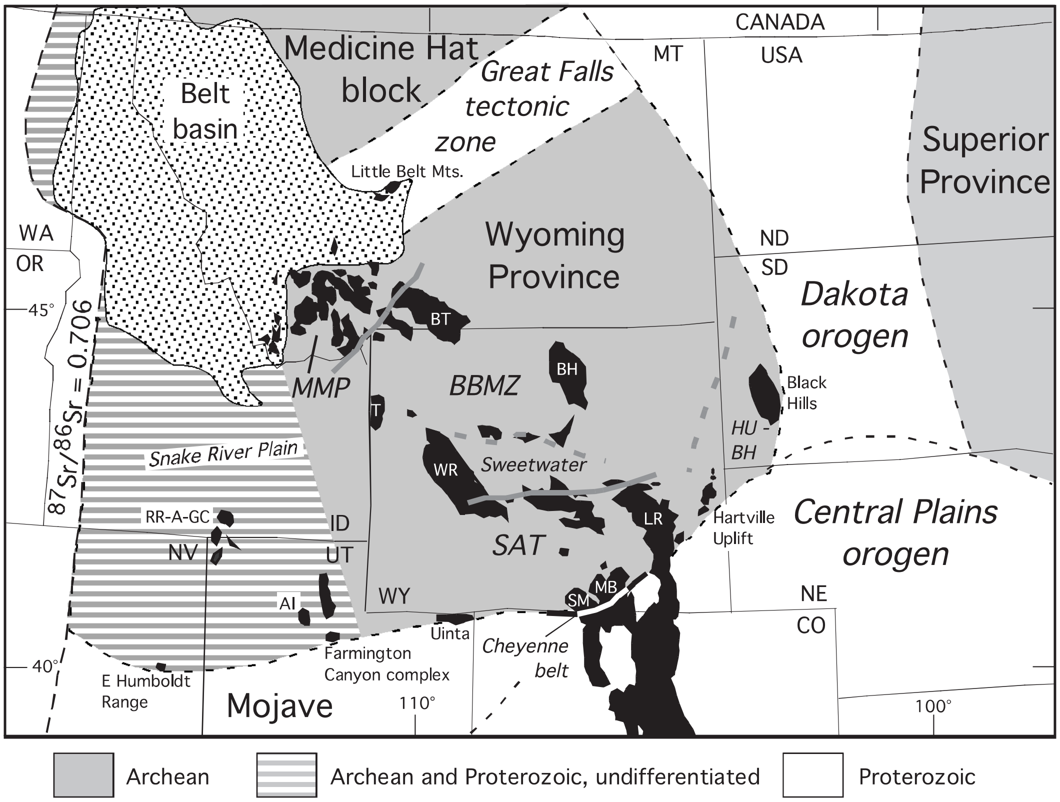

these features is ~500 000 km^2, somewhat larger in area than the Slave Province, but smaller than the Superior and Rae–Hearne provinces of Canada. Precambrian rocks of the province are exposed in the cores of Laramide (Late Cretaceous to early Tertiary) uplifts; outcrops constitute <10% of the area underlain by Archean basement. Houston et al. (1993) described the Precambrian geology exposed in each of these individual Laramie uplifts. This summary focuses on more recent studies, including the 10 in this special issue that provide the basis for our current understanding of the evolution of the Wyoming Province.

The only well-exposed boundary of the province is where shear zones of the Cheyenne belt crop out in the Medicine Bow Mountains and Sierra Madre in southeastern Wyoming. In these uplifts, the boundary is between Archean and Paleoproterozoic rocks on the north juxtaposed against younger Paleoproterozoic volcanogenic rocks on the south (Karlstrom and Houston 1984; Duebendorfer and Houston 1987; Chamberlain 1998; Duebendorfer et al. 2006). The southern margin of the Wyoming Province extends westward from the Cheyenne belt to the Uinta Mountains, which expose the Precambrian Owiyukuts complex and Red Creek quartzite (e.g., Sears et al. 1982; Mueller et al. 2004*a*).

The extent of Archean and Proterozoic rocks along the western margin of the province is poorly constrained. Along this margin, Archean rocks are present in the Raft River – Albion – Grouse Creek Mountains and East Humboldt Range (e.g., Compton et al. 1977; Lush et al. 1988; Wright and Snoke 1993; Egger et al. 2003). U–Pb ages from zircons in crustal xenoliths within Cenozoic volcanic rocks of the Snake River Plain also suggest the presence of Archean basement (Wolf et al. 2005). Archean rocks have not, however, been identified in the Precambrian outcrops of the Farmington Canyon complex of the Wasatch Mountains and Antelope Island in Great Salt Lake (Fig. 1) (Nelson et al. 2002; Mueller et al. 2004*a*; C.D. Frost, unpublished data, 2004). In addition, the oldest rocks exposed north of the Snake River Plain in the Biltmore anticline and Pioneer, Tendoy, and Beaverhead ranges are Paleoproterozoic, although both Archean and Paleoproterozoic rocks are present in the Highland Mountains (Mueller et al. 2005; Foster et al. 2006). These outcrops all occur within the Sevier fold and thrust belt in southwestern Montana. Foster et al. (2006) suggest that the Archean margin of the Wyoming Province may lie near the eastern limit of this fold and thrust belt and that Precambrian rocks (Archean and Proterozoic) to the west are allochthonous with respect to the primary Archean components of the Wyoming Province. Ages of xenocrystic zircons in Cretaceous and younger plutonic rocks support the interpretation that this complex of Proterozoic and Archean rocks extends as far west as the $^{87}Sr/^{86}Sr$ = 0.706 line in western Idaho (e.g., Mueller et al. 1994; Foster and Fanning 1997; Foster et al. 2006). This expanse of Archean and Proterozoic crust west of the most westerly Laramide uplifts has contributed to proposals that this crust should be included as part of the Wyoming Province (e.g., Houston et al. 1993). The exact configuration of the western limit of contiguous Archean crust of the Wyoming Province is not likely to be resolved, however, without additional geophysical data because Precambrian outcrop is sparse.

The Great Falls tectonic zone was interpreted to coincide with the northern boundary of the Wyoming Province (O'Neill and Lopez 1985). This zone, which is marked by pronounced northeast-striking high-angle faults and lineaments and Paleoproterozoic mineral ages in Archean basement, has been interpreted to record the collision between the Wyoming Province and Medicine Hat block and (or) Hearne Province during one or more events between ca. 1.86 and 1.77 Ga (Mueller et al. 2002, 2004*b*, 2005). Evidence for a paleoslab beneath the Medicine Hat block (Gorman et al. 2002) suggests an ocean basin may have closed between these Archean blocks in the Paleoproterozoic.

Along the eastern margin of the Wyoming Province, Archean rocks are present in the Black Hills (McCombs et al. 2004; Dahl and McCombs 2005; Dahl et al. 2006) and Hartville uplift (Krugh 1997). These rocks were deformed along Paleoproterozoic, west-directed thrusts at 1.83–1.72 Ga (Dahl et al. 1999, 2005). This deformation, which has been interpreted to record the collision of the Wyoming Province with the Superior Province, occurred at approximately the same time that Paleoproterozoic terranes were accreted to the southeastern Wyoming Province along the Cheyenne belt (Chamberlain et al. 2003). This temporal coincidence also suggests the possibility that the younger Paleoproterozoic ages (e.g., <1.78 Ga) may represent reactivation of this part of the Trans-Hudson Orogen as a consequence of the multiple arc collisions that occurred along the Cheyenne belt (e.g., Mueller et al. 2005) and that Wyoming–Superior collision may have occurred earlier (e.g., Gosselin et al. 1988).

Cratonization

One important observation concerning the Wyoming craton, and all surviving Archean cratons, is that their structures must extend to mantle depths and be robust enough to survive for billions of years against convective forces in the mantle. These structures (tectosphere; Jordan 1975) apparently form coincident with the last major crust-forming event. In the case of the Wyoming Province, cratonic stabilization apparently occurred in the late Archean (Mueller et al. 2004*b*). Cratonization extends across recognized subprovincial boundaries, despite the fact that these subprovinces have distinctive pre-late Archean histories (e.g., Mogk et al. 1992; Chamberlain et al. 2003). The oldest portions of the craton lie in the northern part of the province and include the Montana metasedimentary province (MMP) and Beartooth–Bighorn magmatic zone (BBMZ) (Fig. 1) (Mogk et al. 1992; Mueller et al. 1996). The MMP is composed of distinctive tracts of younger quartzite, pelite, and carbonate rock associations structurally intercalated with older (3.30–3.50 Ga) Archean quartzofeldspathic gneiss (e.g., Mueller et al. 1993, 2004*b*). The BBMZ is composed predominantly of 2.80–3.00 Ga metaplutonic rocks of the trondhjemite–tonalite–granodiorite (TTG) association, although smaller volumes of high-K granodiorites and granites are also present (Wooden et al. 1988; Frost and Fanning 2006; C.D. Frost et al. 2006*a*). Further evidence of older rocks (>3.00 Ga) in the MMP and BBMZ is suggested by U–Pb dates of 3.30–4.00 Ga on detrital zircon suites and on areas of zircon grains from 2.80–3.00 Ga gneisses interpreted as inherited cores (Mueller et al. 1992, 1998; Frost and Fanning 2006; Grace et al. 2006). Middle and early Archean Nd model ages of metaigneous and metasedimentary rocks also suggest an earlier crustal history (Wooden and Mueller 1988; Frost 1993; Mueller et al. 2004*b*; C.D. Frost et al. 2006*a*; Grace et al. 2006).

The most distinctive and important characteristic that unites these two subprovinces is the enriched $^{207}Pb/^{204}Pb$ isotopic signature shared by tonalitic and more evolved rocks found throughout the MMP and BBMZ (Wooden and Mueller 1988; Mueller et al. 1993; Frost et al. 1998; C.D. Frost et al. 2006*a*). This signature distinguishes the Wyoming Province from all other Archean provinces and is best interpreted as the consequence of an early period of crustal extraction that is recorded in each subprovince (e.g., Mueller and Wooden 1988; Wooden and Mueller 1988; Frost et al. 1998). To generate the observed Pb isotopic ratios, which lie above the model upper continental crust of Zartman and Doe (1981), a Pb reservoir would have to separate from model mantle at ca. 3.60–3.30 Ga and have a high $^{238}U/^{204}Pb$ ratio (higher than average crust); a U/Pb ratio typical of continental crust would require separation of this reservoir at 4.00 Ga or earlier. Alternatively, the mantle reservoir for the Wyoming Province may have had evolved Pb isotopic compositions prior to crustal extraction (C.D. Frost et al. 2006*a*). In either instance, the widely dispersed and enriched $^{207}Pb/^{204}Pb$ isotopic signature of the province suggests the craton is not a collage of exotic terranes in the modern sense, but a single Archean crustal block or group of blocks that formed in close proximity by similar processes early in Earth history (Mogk et al. 1992).

Much of the BBMZ has been undeformed and at high crustal levels for more than 2.70 Ga (e.g., Frost and Fanning 2006). This area also is distinguished by ~50 km thick crust and a 15–20 km thick, high-velocity, dense lower crust interpreted to be composed of mafic rock (Snelson et al. 1998; Gorman et al. 2002). Although the age of this mafic layer is unknown, its coincidence with the oldest parts of the province suggests that it could have formed at 2.80–3.00 Ga, perhaps with additions at 2.71 and 2.68 Ga when the Stillwater complex and mafic dikes were emplaced (Premo et al. 1990; B.R. Frost et al. 2006). Cratonization and subsequent stability of this area may be associated with the formation of this lower crust. Later Archean deformation is limited to the southern and western margin of the BBMZ (Sweetwater subprovince of Chamberlain et al. 2003) (Fig. 1) where the high-velocity lower crust thins and ultimately disappears. Despite these recognizable differences in the geologic evolution of the northern and southern parts of the province, the core of the Wyoming Province has resisted later deformation and intrusion for over 2.50 Ga.

Late Archean magmatism and accretion and the role of plate tectonics

The southernmost part of the province is known as the Southern accreted terranes (SAT; C.D. Frost et al. 2006*b*) and is characterized by slightly younger magmatic and tectonic activity. Late Archean calc-alkalic magmatism and tectonism recorded in the SAT are interpreted to be compatible with a plate tectonic model for crustal growth. Magmatism occurred in three discrete pulses along the southern margin of the Wyoming Province at 2.71–2.67, 2.65–2.62, and 2.55–2.50 Ga (Chamberlain et al. 2003). The spatial, geochemical, and isotopic characteristics of these magmas have been interpreted to result from formation at a long-lived active margin (Frost et al. 1998). The earliest of these periods involved east- or northeast-directed subduction, the formation of a continental magmatic arc now exposed in the Wind River Mountains, and emplacement of a mafic dyke swarm in a back-arc environment. During the climax of this orogenic cycle, high-pressure granulites formed in the Teton Range, an event interpreted to reflect the collision of the Wyoming craton with a continental block to the west (B.R. Frost et al. 2006). These events appear to be distinct in time from the 2.65–2.62 Ga magmatism along the southern Wyoming Province, which appears to have resulted from more north-directed subduction (Frost et al. 1998; Chamberlain et al. 2003; Grace et al. 2006; Keane et al. 2006). The 2.55–2.50 Ga magmatism was widespread (i.e., throughout the entire Wyoming Province) but of relatively small volume and uncertain tectonic significance (e.g., Mogk et al. 1992; Frost et al. 1998; Chamberlain et al. 2003).

Late Archean supracrustal sequences preserved in the central and southern Wyoming Province characterize the southern terranes. They are composed of mafic and sparse ultramafic and felsic metavolcanic rocks, metagraywacke, pelitic schist, and minor quartzite and iron-formation. Following deposition, these metasupracrustal rocks were deformed and metamorphosed and then intruded by granitic plutons (Chamberlain et al. 2003; Bowers and Chamberlain 2006). Nd isotopic data suggest that the sources for several of these metasedimentary successions included older continental detritus, such as would have eroded from the BBMZ and MMP. Other supracrustal sequences preserve radiogenic Nd isotopic signatures suggestive of contributions from more juvenile sources (C.D. Frost et al. 2006*b*; Grace et al. 2006; Souders and Frost 2006). These latter metasedimentary successions compose an area of late Archean, exotic, accreted terranes along the southern margin of the Wyoming Province (Fig. 1). The inferred continental-arc magmatism and presence of accreted terranes along the southern margin of the province indicate that modern plate-tectonic processes were important contributors to magmatic and tectonic crustal growth of the Wyoming Province by 2.70 Ga.

Proterozoic accretion and extension

The post-Archean history began with a period of tectonic and magmatic quiescence that extended into the Paleoproterozoic. This quiet period was followed by a complex series of collisional episodes that ultimately led to the incorporation of the Wyoming Province into Laurentia (e.g., O'Neill and Lopez 1985; Gosselin et al. 1988; Dahl et al. 1999; Mueller et al. 2002, 2004*a*, 2004*b*, 2005). The initial event may have involved the addition of ~2.40 Ga crust along the western boundary of the craton (Kellogg et al. 2003). This was followed at about 1.80–1.90 Ga by the incorporation of the Wyoming Province into Laurentia. Incorporation of the Wyoming Province involved the nearly simultaneous juxtaposition of at least three cratonic blocks: (*i*) Hearne – Medicine Hat terrane with Wyoming along the Great Falls tectonic zone, (*ii*) Wyoming and Superior along the Dakota segment of the Trans-Hudson Orogen, and (*iii*) Hearne – Medicine Hat with the Superior north of the Dakota segment. Production of calc-alkaline 1.86 Ga, arc-related magmatism in the Little Belt Mountains, Montana, and the Trans-Hudson Orogen in Saskatchewan suggests simultaneous ocean closure in at least part of the Great Falls tectonic zone and northern Trans-Hudson Orogen (e.g., Mueller et al. 2002; 2004*b*, 2005). No significant tectonothermal activity is recorded along the Great Falls tectonic zone after 1.77 Ga (Holm and Schneider 2002; Brady et al. 2004; Mueller et al. 2005), which is interpreted as the time of juxtaposition of the Wyoming and Superior provinces along an extension of the Trans-Hudson Orogen.

Subsequent to this welding of Archean cratons, a series of arc and microcontinental accretionary events began at about 1.90 Ga and probably extended to ~1.60 Ga (Mueller et al. 2004*a*). These events involved the addition of Paleoproterozoic (2.40–1.80 Ga) terranes, perhaps with embedded Archean fragments, to the amalgamated Wyoming–Laurentian continent along an open margin that extended from the southeastern to northwestern corners of the craton (i.e., Dakota Orogen to the Cheyenne belt to the western Great Falls tectonic zone; e.g., Chamberlain 1998; Foster et al. 2002; Mueller et al. 2002, 2004*a*, 2004*b*, 2005; Tyson et al. 2002; Resor and Snoke 2005). All phases of this circum-provincial Paleoproterozoic tectonic regime share two important traits: (1) no contemporaneous arc magmatism developed within the Wyoming Province; and (2) except for limited areas of deformation and thermal overprinting, no significant tectonic activity was recorded within the Wyoming Province during the development of these active Paleoproterozoic mobile belts (e.g., Mueller et al. 2005).

Proterozoic mafic dykes, however, are present throughout the province, and at least some appear to reflect periods of craton-wide extension. The earliest of these is marked by mafic dyke intrusion at 2.10–2.00 Ga in both the southeastern and northwestern marginal zones (e.g., Cox et al. 2000; Mueller et al. 2004*b*) and may be related to the formation of a passive margin along the southeastern edge of the province (Houston et al. 1993). Sparse mafic dykes, 1.50–1.40 Ga in age, may be related to rifting in the Belt basin and (or) to extension and "anorogenic" magmatism in the southwest United States and midcontinent region (e.g., Frost et al. 1999; Chamberlain et al. 2003). Younger mafic dykes (0.80–0.70 Ga) along the western margin of the Wyoming–Laurentian continent may be related to rifting, continental breakup, and development of the proto-Pacific Ocean (Harlan et al. 2003). These periods of extension and mafic dyke emplacement may also mark periods of growth of the extensive mafic lower crust that underlies most of the Wyoming Province.

Influence of the Wyoming craton on more recent geologic events

The Wyoming Province appears to have undergone the process of cratonization during extensive magmatism at 2.50–2.90 Ga. The mantle residuum produced as a result of crustal extraction at this time is expected to have higher solidus, effective viscosity, and stiffness than typical upper mantle, thereby forming a long-lived, subcratonic mantle root (e.g., Jordan 1975; Pollack 1986). The Wyoming Province, therefore, likely developed a structurally robust tectosphere contemporaneously with the stabilization of a felsic crust (Mueller et al. 2004*b*, 2005). Heat in the form of convecting mantle and (or) fluids approaching this tectosphere was apparently diverted away from the craton and its mantle root to surrounding areas of oceanic and (or) younger subcontinental lithosphere that developed in response to Paleoproterozoic collisions. These bounding zones of Paleoproterozoic lithosphere appear to be much more fertile for later melting than the adjacent Archean lithosphere, as exemplified by Cretaceous and younger magmatism and mineralization being largely confined to the Great Falls tectonic zone, rather than adjoining Archean lithosphere of either the Medicine Hat block or Wyoming craton (e.g., O'Neill and Lopez 1985; Foster et al. 2006).

This tectosphere appears to be long-lived, i.e., it remains attached to the Wyoming Province crust today, as indicated by isotopic data from young volcanic rocks and xenoliths (e.g., Vollmer et al. 1984; Carlson and Irving 1994; Rudnick et al. 1999; Farmer et al. 2005). The physical and compositional contrasts between this strong, ancient tectosphere and the weaker, younger lithosphere produced as a result of Paleoproterozoic accretion around the southern and western margins of the Wyoming Province have had a substantial impact on the geologic evolution of the northern Rocky Mountain region, including the locus of deposition of the Belt basin, development of the Ancestral Rockies, Sevier–Laramide contraction, and the Yellowstone – Snake River Plain system (Chamberlain et al. 2003; Mueller et al. 2004*b*; Foster et al. 2006).

Summary

This contribution and the other papers in this volume provide a current assessment of our collective understanding of the Archean and Proterozoic evolution of the Wyoming Province. These papers also describe numerous Archean and Proterozoic features that provide an improved framework for making direct comparisons and correlations with other Archean cratons and thereby increase our understanding of Precambrian tectonics in general. In addition, our improved understanding of the architecture and intracratonic relations of the subprovinces of the Wyoming craton and its bounding Proterozoic orogenic belts provides important constraints for the range of processes involved in Archean crustal growth and the assembly of continents.

References

Bowers, N., and Chamberlain, K.R. 2006. Precambrian history of the eastern Ferris Mountains and Bear Mountain, central Wyoming Province. Canadian Journal of Earth Sciences, **43**: this issue.

Brady, J., Kovaric, D., Cheney, J., Jacob, L., and King, J. 2004. $^{40}Ar/^{39}Ar$ ages of metamorphic rocks from the Tobacco Root Mountains, southwest Montana. *In* Precambrian geology of the Tobacco Root Mountains, Montana. *Edited by* J. Brady, H. Burger, J. Cheney, and T. Harms. Geological Society of America, Special Paper 377, pp. 131–149.

Carlson, R.W., and Irving, A.J. 1994. Depletion and enrichment history of subcontinental lithospheric mantle: an Os, Sr, Nd and Pb isotopic study of ultramafic xenoliths from the northwestern Wyoming Craton. Earth and Planetary Science Letters, **126**: 457–472.

Chamberlain, K.R. 1998. Medicine Bow Orogeny: timing of deformation and model of crustal structure produced during continent-arc collision, ca. 1.78 Ga, southeastern Wyoming. Rocky Mountain Geology, **33**(2): 259–277.

Chamberlain, K.R., Frost, C.D., and Frost, B.R. 2003. Early Archean to Mesoproterozoic evolution of the Wyoming Province: Archean origins to modern lithospheric architecture. Canadian Journal of Earth Sciences, **40**(10): 1357–1374.

Compton, R.R., Todd, V.R., Zartman, R.E., and Naeser, C.W. 1977. Oligocene and Miocene metamorphism, folding, and low-angle faulting in northwestern Utah. Geological Society of America Bulletin, **88**: 1237–1250.

Condie, K.C. 1969. Geologic evolution of the Precambrian rocks in northern Utah and adjacent areas. Utah Geological Survey Bulletin, **82**: 71–95.

Condie, K.C. 1976. The Wyoming Archean Province in the western United States. *In* The early history of the Earth. *Edited by* B.F. Windley. Wiley, London, UK., pp. 499–511.

Cox, D.M., Frost, C.D., and Chamberlain, K.R. 2000. 2.01 Ga Kennedy dike swarm, southeastern Wyoming: record of a rifted margin along the southern Wyoming province. Rocky Mountain Geology, **35**: 7–30.

Dahl, P.S., and McCombs, J.A. 2005. "Rosetta grains" of Precambrian accessory minerals, Black Hills, South Dakota: 2900–1700 Ma microprobe ages and implications for regional tectonic history. The Compass, **78**(2): 59–75.

Dahl, P.S., Holm, D.K., Gardner, E.T., Hubacher, F.A., and Foland, K.A. 1999. New constraints on the timing of Early Proterozoic tectonism in the Black Hills (South Dakota), with implications for the docking of the Wyoming province with Laurentia. Geological Society of America Bulletin, **111**: 1335–1349.

Dahl, P.S., Terry, M.P., Jercinovic, M.J., Williams, M.L., Hamilton, M.A., Foland, K.A., Clement, S.M., and Friberg, L.M. 2005. Electron probe (Ultrachron) microchronometry of metamorphic monazite: unraveling the timing of polyphase thermotectonism in the easternmost Wyoming Craton (Black Hills, South Dakota). American Mineralogist, **90**: 1712–1728.

Dahl, P.S., Hamilton, M.A., Wooden, J.L., Foland, K.A., and Frei, R. 2006. Evidence for 2480 Ma mafic magmatism in the easternmost Wyoming craton (Black Hills, S.D.), with implications for the 2900–2500 Ma configuration of supercontinent Kenorland. Canadian Journal of Earth Sciences, **43**: this issue.

Duebendorfer, E.M., and Houston, R.S. 1987, Proterozoic accretionary tectonics at the southern margin of the Archean Wyoming craton: structure and metamorphism of lithotectonic blocks within the Cheyenne Belt, Wyoming. Geological Society of America Bulletin, **98**: 554–568.

Duebendorfer, E.M., Chamberlain, K.R., and Heizler, MT. 2006. Filling the North American Proterozoic tectonic gap: 1.60–1.59 Ga deformation and orogenesis in southern Wyoming, USA. Journal of Geology, **114**: 19–42.

Egger, A.E., Dumitru, T.A., Miller, E.A., and Savage, C.F.I. 2003. Timing and nature of Tertiary plutonism and extension in the Grouse Creek Mountains, Utah. International Geology Review, **45**: 497–532.

Farmer, G.L., Bowring, S.A., Williams, M.L., Christensen, N.I., Matzel, J.P., and Stevens, L. 2005. Contrasting lower crustal evolution across an Archean–Proterozoic suture: physical, chemical and geochronological studies of lower crustal xenoliths in southern Wyoming and northern Colorado. *In* The Rocky Mountain region: an evolving lithosphere. *Edited by* K.E. Karlstrom and G.R. Keller. Geophysical Monograph Series 154, pp. 139–162.

Foster, D., and Fanning, C. 1997. Geochronology of the Idaho–Bitterroot batholith and Bitterroot metamorphic core complex: magmatism preceding and contemporaneous with extension. Geological Society of America Bulletin, **109**: 379–394.

Foster, D., Mueller, P., Heatherington, A., Vogl, J., Meert, J., Lewis, R., and Wooden, J. 2002. Configuration of the 2.0–1.6 Ga accretionary margin of the NW Wyoming province: implications for the Proterozoic continental reconstructions. Geological Society of America, Abstracts with Programs, **34**(6): 559.

Foster, D., Mueller, P.A., Vogl, J., Mogk, D., Wooden, J.L., and Heatherington, A. 2006. Proterozoic evolution of the western margin of the Wyoming craton: implications for the tectonic and magmatic evolution of the northern Rocky Mountains. Canadian Journal of Earth Sciences, **43**: this issue.

Frost, B.R., Frost, C.D., Cornia, M., Chamberlain, K.R., and Kirkwood, R. 2006. The Teton – Wind River domain: a 2.70–2.67 Ga active margin in the western Wyoming Province. Canadian Journal of Earth Sciences, **43**: this issue.

Frost, C.D. 1993. Nd isotopic evidence for the antiquity of the Wyoming province. Geology, **21**: 351–354.

Frost, C.D., and Fanning, C.M. 2006. Archean geochronological framework of the Bighorn Mountains, Wyoming. Canadian Journal of Earth Sciences, **43**: this issue.

Frost, C.D., Frost, B.R., Chamberlain, K.R., and Hulsebosch, T.P. 1998. The Late Archean history of the Wyoming province as recorded by granitic magmatism in the Wind River Range, Wyoming. Precambrian Research, **89**: 145–173.

Frost, C.D., Frost, B.R., Chamberlain, K.R., and Edwards, B.R. 1999. Petrogenesis of the 1.43 Ga Sherman batholith, SE Wyoming, USA: a reduced, rapakivi-type anorogenic granite. Journal of Petrology, **40**: 1771–1802.

Frost, C.D., Frost, B.R., Kirkwood, R., and Chamberlain, K.R. 2006*a*. The tonalite–trondhjemite–grandiorite (TTG) to granodiorite–granite (GG) transition in the late Archean plutonic rocks of the central Wyoming Province. Canadian Journal of Earth Sciences, **43**: this issue.

Frost, C.D., Fruchey, B.L., Chamberlain, K.R., and Frost, B.R. 2006*b*. Archean crustal growth by lateral accretion of juvenile supracrustal belts in the southern Wyoming Province. Canadian Journal of Earth Sciences, **43**: this issue.

Gorman, A.R., Clowes, R.M., Ellis, R.M., Henstock, T.J., Spence, G.D., Keller, G.R., Levander, A., Snelson, C.M., Burianyk, M.J.A., Kanasewich, E.R., Asudeh, I., Hajnal, Z., and Miller, K.C. 2002. Deep Probe: imaging the roots of western North America. Canadian Journal of Earth Sciences, **39**(3): 375–398.

Gosselin, D., Papike, J., Zartman, R., Peterman, Z., and Laul, J. 1988. Archean rocks of the Black Hills, South Dakota: reworked basement from the southern extension of the Trans-Hudson orogen. Geological Society of America Bulletin, **100**: 1244–1259.

Grace, R.L.B., Chamberlain, K.R., Frost, B.R., and Frost, C.D. 2006. Tectonic histories of the Paleoarchean to Mesoarchean Sacawee Block and Neoarchean Oregon Trail structural belt of the south-central Wyoming Province. Canadian Journal of Earth Sciences, **43**: this issue.

Harlan, S.S., Heaman, L., LeCheminant, A.N., and Premo, W.R. 2003. Gunbarrrel mafic magmatic event: a key 780 Ma time marker for Rodinia plate reconstructions. Geology, **31**: 1053–1056.

Holm, D., and Schneider, D. 2002. $^{40}Ar/^{39}Ar$ evidence for ca. 1800 Ma tectonothermal activity along the Great Falls tectonic zone, central Montana. Canadian Journal of Earth Sciences, **39**(12): 1719–1728.

Houston, R.S., Erslev, E.A., Frost, C.D., Karlstrom, K.E., Page, N.J., Zientek, M.L. et al. 1993. The Wyoming province. *In* The Cordilleran orogen: conterminous U.S. *Edited by* J.C. Jr. Reed, M.E. Bickford, R.S. Houston et al. Geological Society of America, Boulder, Colo., The Geology of North America, Vol. C-2, pp. 121–170.

Jordan, T. 1975. The continental tectosphere. Reviews of Geophysics and Space Physics, **13**: 1–12.

Karlstrom, K.E., and Houston, R.S. 1984. The Cheyenne Belt: analysis of a Proterozoic suture in southern Wyoming. Precambrian Research, **25**: 415–446.

Keane, S.D., DeWolf, C.P., Essene, E.J., Halliday, A.N., Hall, C.M., and Cosca, M.A. 2006. Isotopic constraints on the thermal history of the Wind River Range, Wyoming: implications for Archean metamorphism. Canadian Journal of Earth Sciences, **43**: this issue.

Kellogg, K., Snee, L., and Unruh, D. 2003. The Mesoproterozoic Beaverhead impact structure and its tectonic setting, Montana–Idaho — $^{40}Ar/^{39}Ar$ and U–Pb constraints. Journal of Geology, **111**: 639–652.

Krugh, K.A. 1997. U–Pb thermochronologic constraints on the early Proterozoic tectonic evolution of the Hartville Uplift, southeast Wyoming. M.Sc. thesis, University of Wyoming, Laramie, Wyo.

Lush, A.P., McGrew, A.J., Snoke, A.W., and Wright, J.E. 1988. Allochthonous Archean basement in the northern East Humboldt Range, Nevada. Geology, **16**: 349–353.

McCombs, J.A., Dahl, P.S., and Hamilton, M.A. 2004. U–Pb ages of Neoarchean granitoids from the Black Hills, South Dakota, USA: implications for evolution of the Archean Wyoming province. Precambrian Research, **130**: 161–184.

Mogk, D.W., Mueller, P.A., and Wooden, J.L. 1992. The significance of Archean terrane boundaries: evidence from the northern Wyoming Province. Precambrian Research, **55**: 155–168.

Mueller, P.A., and Wooden, J.L. 1988. Evidence for Archean subduction and crustal recycling, Wyoming Province, USA. Geology, **16**: 871–874.

Mueller, P.A., Wooden, J., and Nutman, A. 1992. 3.96 Ga zircons from an Archean quartzite, Beartooth Mountains, Montana. Geology, **20**: 327–330.

Mueller, P.A., Shuster, R., Wooden, J., Erslev, E., and Bowes, D. 1993. Age and composition of Archean crystalline rocks from the southern Madison Range: implications for crustal evolution in the Wyoming craton. Geological Society of America Bulletin, **105**: 437–446.

Mueller, P.A., Heatherington, A.L., Wooden, J.L., Shuster, R., Mogk, D.W., and Nutman, A.P. 1994. Paleoproterozoic evolution of the NW margin of the Wyoming craton: evidence for 1.7 and 2.4 Ga terranes. Geological Society of America, Abstracts with Programs, **26**(7): 340.

Mueller, P.A., Wooden, J.L., Mogk, D.W., Nutman, A.P., and

Williams, I.S. 1996. Extended history of a 3.5 Ga trondhjemitic gneiss, Wyoming province, USA: evidence from U–Pb systematics in zircon. Precambrian Research, **78**: 41–52.

Mueller, P.A., Wooden, J.L., Nutman, A.P., and Mogk, D.W. 1998. Early Archean crust in the northern Wyoming province: evidence from U–Pb ages of detrital zircons. Precambrian Research, **91**: 295–307.

Mueller, P.A., Heatherington, A.L., Kelly, D.M., Wooden, J.L., and Mogk, D.W. 2002. Paleoproterozoic crust within the Great Falls tectonic zone: implications for the assembly of southern Laurentia. Geology, **30**: 127–130.

Mueller, P.A., Foster, D.A., Mogk, D.W., and Wooden, J.L. 2004*a*. New insights into the Proterozoic evolution of the western margin of Laurentia and their tectonic implications. Geological Society of America, Abstracts with Programs, **36**(5): 404.

Mueller, P.A., Burger, H.R., Heatherington, A., Wooden, J., Mogk, D.W., and D'Arcy, K. 2004*b*. Age and evolution of the Precambrian crust, Tobacco Root Mountains, Montana. *In* Precambrian geology of the Tobacco Root Mountains, Montana. *Edited by* J.B. Brady, H.R. Burger, J.T. Cheney, and T.A. Harms. Geological Society of America, Special Paper 377, pp. 179–201.

Mueller, P.A., Burger, R.H., Wooden, J.L., Brady J.B., Cheney, J.T., Harms, T.A., Heatherington, A.L., and Mogk, D.W. 2005. Paleoproterozoic metamorphism in the northern Wyoming province: implications for the assembly of Laurentia. Journal of Geology, **113**: 169–179.

Nelson, S.T., Harris, R.A., Dorais, M.J., Heizler, M., Constenius, K.N., and Barnett, D.E. 2002. Basement complexes in the Wasatch fault, Utah, provide new limits on crustal accretion. Geology, **30**: 831–834.

O'Neill, J., and Lopez, D. 1985. Character and regional significance of Great Falls tectonic zone, east-central Idaho and west-central Montana. American Association of Petroleum Geologists Bulletin, **69**: 437–447.

Pollack, H.N. 1986. Cratonization and thermal evolution of the mantle. Earth and Planetary Science Letters, **80**: 175–182.

Premo, W.R., Helz, R.T., Zientek, M.L., and Langston, R.B. 1990. U–Pb and Sm–Nd ages for the Stillwater complex and its associated sills and dikes, Beartooth Mountains, Montana: identification of a parent magma? Geology, **18**: 1065–1068.

Resor, P.G., and Snoke, A.W. 2005. Laramie Peak shear system, central Laramie Mountains, Wyoming, USA: regeneration of the Archean Wyoming province during Palaeoproterozoic accretion. *In* High-strain zones: structure and physical properties. *Edited by* D. Bruhn and L. Burlini. Geological Society (of London), Special Publication 245, pp. 81–107.

Rudnick, R.L., Ireland, T.R., Gehrels, G., Irving, A.J., Chesley, J.T., and Hanchar, J.M. 1999. Dating mantle metasomatism: U–Pb geochronology of zircons in cratonic mantle xenoliths from Montana and Tanzania. *In* Proceedings of the 7th International Kimberlite Conference, Rondebosch, South Africa. *Edited by* J.J Gurney, J.L. Gurney, M.D. Pascoe, and S.H. Richards. Redroof Design, Cape Town, South Africa, pp. 728–735.

Sears, J., Graff, P., and Holden, G. 1982. Tectonic evolution of lower Proterozoic rocks, Uinta Mountains, Utah and Colorado. Geological Society of America Bulletin, **93**: 990–997.

Snelson, C.M., Henstock, T.J., Keller, G.R., Miller, K.C., and Levander, A. 1998. Crustal and uppermost mantle structure along the Deep Probe seismic profile. Rocky Mountain Geology, **33**(2): 181–198.

Souders, A.K., and Frost, C.D. 2006. In suspect terrane? Provenance of the late Archean Phantom Lake Metamorphic Suite, Sierra Madre, Wyoming. Canadian Journal of Earth Sciences, **43**: this issue.

Tyson, A., Morozova, E., Karlstrom, K., Chamberlain, K.R., Smithson, S.B., Dueker, K., and Foster, C. 2002. Proterozoic Farwell Mountain – Lester Mountain suture zone, northern Colorado: subduction flip and progressive assembly of arcs. Geology, **30**: 943–946.

Vollmer, R., Ogden, P., Schilling, J.-G., Kingsley, R.H., and Waggoner, D.G. 1984. Nd and Sr isotopes in ultrapotassic rocks from the Leucite Hills, Wyoming. Contributions to Mineralogy and Petrology, **87**: 359–368.

Wolf, D.E., Leeman, W.P., and Vervoort, J.D. 2005. U–Pb zircon geochronology of crustal xenoliths confirms presence of Archean basement beneath the central and eastern Snake River Plain. Geological Society of America, Abstracts with Programs, **37**(7): 60.

Wooden, J.L., and Mueller, P.A. 1988. Pb, Sr, and Nd isotopic compositions of a suite of Late Archean, igneous rocks, eastern Beartooth Mountains: implications for crust–mantle evolution. Earth and Planetary Science Letters, **87**: 59–72.

Wooden, J.L., Mueller, P.A., Mogk, D.A., and Bowes, D.R. 1988. A review of the geochemistry and geochronology of Archean rocks of the Beartooth Mountains, Montana–Wyoming. *In* Precambrian and Mesozoic plate margins: Montana, Idaho and Wyoming. *Edited by* S.E. Lewis and R.B. Berg. Montana Bureau of Mines and Geology, Special Publication 96, pp. 23–42.

Wright, J.E., and Snoke, A.W. 1993. Tertiary magmatism and mylonitization in the Ruby – East Humboldt metamorphic core complex, northeastern Nevada: U–Pb geochronology and Sr, Nd, and Pb isotope geochemistry. Geological Society of America Bulletin, **105**: 935–952.

Zartman, R.E., and Doe, B.R. 1981. Plumbotectonics — the model. Tectonophysics, **75**: 135–162.

Precambrian Research, 55 (1992) 155–168
Elsevier Science Publishers B.V., Amsterdam

The nature of Archean terrane boundaries: an example from the northern Wyoming Province

David W. Mogk[a], Paul A. Mueller[b] and Joseph L. Wooden[c]
[a]*Department of Earth Sciences, Montana State University, Bozeman, MT 59717, USA*
[b]*Department of Geology, University of Florida, Gainesville, FL 32611, USA*
[c]*Branch of Isotope Geology MS 937, U.S. Geological Survey, 345 Middlefield Road, Menlo Park, CA 94025, USA*

(Received November 15, 1990; accepted after revision June 24, 1991)

ABSTRACT

Mogk, D.W., Mueller, P.A. and Wooden, J.L., 1992. The nature of Archean terrane boundaries: an example from the northern Wyoming Province. In: D.D. van Reenen, C. Roering, L.D. Ashwal and M.J. de Wit (Editors), The Archaean Limpopo Granulite Belt: Tectonics and Deep Crustal Processes. Precambrian Res., 55: 155–168.

The Archean northern Wyoming Province can be subdivided into two geologically distinct terranes, the Beartooth–Bighorn magmatic terrane (BBMT) and the Montana metasedimentary terrane (MMT). The BBMT is characterized by voluminous Late Archean (2.90–2.74 Ga) magmatic rocks (primarily tonalite, trondhjemite, and granite); metasedimentary rocks are preserved only as small, rare enclaves in this magmatic terrane. The magmatic rocks typically have geochemical and isotopic signatures that suggest petrogenesis in a continental magmatic arc environment. The MMT, as exposed in the northern Gallatin and Madison Ranges, is dominated by Middle Archean trondhjemitic gneisses (3.2–3.0 Ga); metasedimentary rocks, however, are significantly more abundant than in the BBMT. Each terrane has experienced a separate and distinct geologic history since at least 3.6 Ga ago based on differences in metamorphic and structural styles, composition of magmatic and metasupracrustal rocks, and isotopic ages; consequently, these may be described as discrete terranes in the Cordilleran sense. Nonetheless, highly radiogenic and distinctive Pb–Pb isotopic signatures in rocks of all ages in both terranes indicate that the two terranes share a significant aspect of their history. This suggests that these two Early to Middle Archean crustal blocks, that initially evolved as part of a larger crustal province, experienced different geologic histories from at least 3.6 Ga until their juxtaposition in the Late Archean (between 2.75 to 2.55 Ga ago). Consequently, the boundary between the BBMT and MMT appears to separate terranes that are not likely to be exotic in the sense of their Phanerozoic counterparts. Other Archean provinces do appear to contain crustal blocks with different isotopic signatures (e.g. West Greenland, India, South Africa). The use of the term exotic, therefore, must be cautious in situations where geographic indicators such as paleontologic and/or paleomagnetic data are not available. In these cases, isotopic signatures are one of the most useful features for assessing overall genetic relations amongst geologically distinct terranes.

Introduction

One approach that has been used to draw analogies between Archean and modern records of crustal evolution has been that of terrane analysis. Jones et al. (1983) define terranes as "...fault bounded geologic entities of regional extent, each characterized by a geologic history that is different from the histories of contiguous terranes." Metamorphic terranes, for example, are typically distinguished by a regional metamorphism and penetrative deformation that has obscured the original stratigraphic features; contrasts in the protoliths of metamorphic rocks from adjoining terranes must be evident (Jones et al., 1983). Terranes with documentable large-scale displacements have been described as exotic or allochthonous. Archean terranes, in general, must be treated as metamorphic terranes; in the

0301-9268/92/$05.00

absence of reliable paleogeographic indicators it is difficult to ascertain the extent to which they may also be exotic or allochthonous. In Phanerozoic orogens paleomagnetic and/or paleobiogeographic data are generally used for this documentation, but are not available for studies of Archean rocks (e.g. Howell and Jones, 1983). Consequently, integrated petrologic, structural, geochemical, and geochronologic studies constitute the primary components of terrane analysis in Archean settings. For example, index minerals, geothermobarometry, and determination of pressure–temperature–time (*P–T–t*) paths may be used to demonstrate metamorphic histories, relative crustal levels, and possible petrogenetic processes; characterization of mesoscopic lineations and foliations, microfabrics, and kinematic indicators can be used to demonstrate different deformational histories; geochemical tracers may be used as indicators of protolith, provenance, and environment of formation; radiometric ages are mandatory in developing a temporal framework (in the absence of paleontologic or stratigraphic data) to demonstrate differences in geologic histories between adjacent terranes, and isotopic systematics provide important discriminants for distinguishing rocks derived from distinct sources.

In this respect, we discuss the relations between two distinct Archean terranes, the Beartooth–Bighorn magmatic terrane (BBMT) and the Montana metasedimentary terrane (MMT), that are exposed in a series of foreland block uplifts in the northern part of the Archean Wyoming Province of western North America (Foose et al., 1961; Fig. 1). The northeastern part of this province (BBMT) is dominated by Late Archean igneous and meta-igneous rocks, primarily of the tonalite–trondhjemite-granodiorite family, and encompasses the Beartooth Mountains (Mueller et al., 1985, 1988 and references therein), the Bighorn Mountains (Barker et al., 1979; Arth et al., 1980), and adjoining portions of eastern Montana and Wyoming (e.g. Peterman, 1981). The

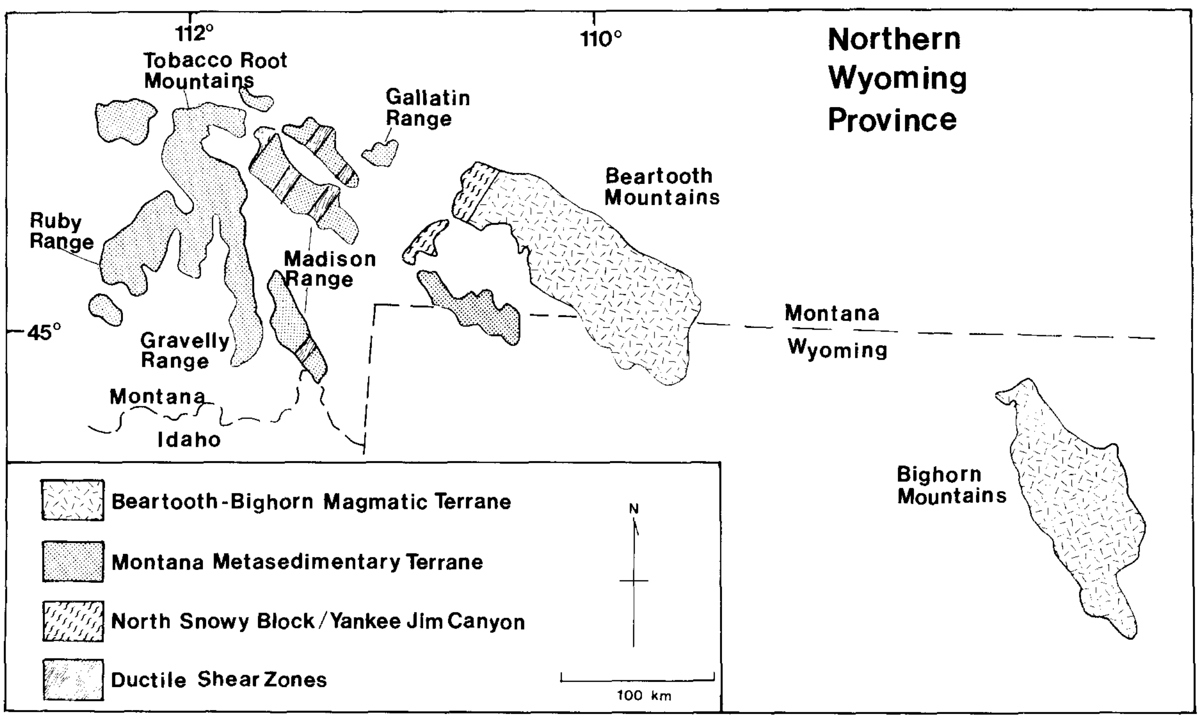

Fig. 1. Index map of the northern Wyoming Province.

northwestern part of the Wyoming Province (MMT) is distinguished by distinctive metasupracrustal sequences within a variety of volumetrically dominant quartzofeldspathic gneisses. Substantial volumes of lower amphibolite- to granulite-facies metasupracrustal rocks are present throughout the MMT (Fig. 1), including the Gallatin, Madison (Spencer and Kozak, 1975; Erslev, 1983; Salt, 1987), Gravelly (Heinrich and Rabbit, 1961), Tobacco Root (Vitaliano et al., 1979), and Ruby Ranges (Garihan, 1979). Though not continuously exposed, the boundary zone between the two terranes appears to be highly faulted and structurally complex as seen in the North Snowy Block, northwestern Beartooth Mountains (Mogk et al., 1988).

Terrane analysis in the northern Wyoming Province appears justified because of obvious differences in lithologic associations, metamorphic grade (Mogk and Henry, 1988), and isotopic ages (Wooden et al., 1988a; Mogk et al., 1992) in the numerous exposures of Archean basement. Although these data clearly show a variety of geologic differences between the two terranes, the geologic histories of the BBMT and MMT in the northern Wyoming Province must be critically evaluated to determine whether their juxtaposition represents a tectonic reorganization of crust formed within a single crustal province or accretion of truly "exotic" terranes. Because of the distinctive isotopic signature of the Wyoming Province (e.g. Wooden and Mueller, 1988; Mueller and D'Arcy, 1990), resolution of this question can rely heavily on a comparison of the isotopic systematics, primarily of the U–Th–Pb system, between the terranes (e.g. Mueller and Wooden, 1988). This type of analysis also has implications for other Archean terranes in which accretionary tectonics have been inferred (e.g. Greenland, Nutman et al., 1989; Superior Province, Card, 1990; India, Krogstad et al., 1989), or where large-scale ductile shear zones separate distinct crustal blocks (e.g. Limpopo Belt, Mason, 1973; Coward, 1976; Barton and Key, 1981; McCourt and Vearncombe, 1987; and references therein).

Geologic relations

The fundamental geologic contrasts and similarities between the BBMT and MMT can readily be seen in two of the most thoroughly studied areas within the two terranes, the Beartooth Mountains (BBMT) and the northern Madison and Gallatin Ranges (MMT). The histories of these two areas are synopsized below and summarized in Table 1.

Geologic history of the Beartooth Mountains

The Beartooth Mountains generally consist of large volumes of Late Archean granitoids with rare inclusions of older metamorphic rocks locally preserved. The petrology, geochemistry, and geochronology of these rocks have been discussed in detail by Mueller et al. (1985, 1988), Wooden et al. (1988a, b), Wooden and Mueller, (1988), and Mogk and Henry (1988, 1992).

The oldest rocks recognized in the Beartooth Mountains are an association of primarily metasupracrustal rocks located in the Quad Creek and Hellroaring Plateau areas of the easternmost Beartooth Mountains (Henry et al., 1982). Included in this association are pelitic schists, quartzites, iron formation, mafic granulites, meta-ultramafites, and granitic, tonalitic, and trondhjemitic gneisses. The provenance of the metasedimentary rocks has been interpreted as evolved crust of dacitic to rhyolitic composition, with a minor contribution from a mafic/ultramafic source (Wooden et al., 1988a). The most distinctive metamorphism of these rocks occurred in the granulite facies [M_1] at a peak metamorphic pressure of 6 kbar and temperatures of 750–800°C (Henry et al., 1982; Mogk and Henry, 1988, 1992). A younger amphibolite facies metamorphism [M_2], with estimated metamorphic conditions of 575–625°C and 5 kbar has partially

TABLE 1

Comparative geologic histories of the Beartooth Mountains (BBMT) and the northern Gallatin and Madison Ranges (MMT)

Age (Ga)	Beartooth Mountains	Northern Gallatin and Madison Ranges
2.55–2.74	Assembly of allochthonous units in the North Snowy Block; U–Pb zircon age of granitic sill and U–Pb sphene cooling age	Granitic unit emplaced in Mirror Lake Shear zone (U–Pb zircon) and U–Pb sphene cooling age
2.75	Emplacement of the Long Lake Granite (U–Pb zircon) Regional amphibolite facies metamorphism	
2.78	Emplacement of the Long Lake Granodiorite (U–Pb zircon)	
2.79	Emplacement of the andesitic amphibolite (U–Pb zircon)	
3.1–3.0		Trondhjemitic gneiss, Gallatin Peak and Jerome Rock Lakes areas (U–Pb zircon)
3.2		Granulite facies metamorphism Monzodiorite–granodiorite sills (U–Pb zircon)
3.35	Granulite facies metamorphism, Quad Creek and Hellroaring Plateau areas	
3.7–3.3	Detrital zircon (U–Pb and Lu–Hf) and Nd–Sm chondritic model ages of metasupracrustal rocks and gneisses in the Quad Creek and Hellroaring Plateau areas.	Detrital zircon (U–Pb and Lu–Hf) and Nd–Sm chondritic model ages from the northern Montana Metasedimentary terrane.

overprinted the granulite facies mineral assemblages (Mogk and Henry, 1988, 1991) (Fig. 2).

The age of the granulite facies metamorphism can only be bracketed. The older limit is based upon detrital zircons from the quartzites of the Quad Creek and Hellroaring Plateau areas that yield U–Pb zircon upper intercept ages of 3.3–3.0 Ga (Mueller et al., 1982) and Lu–Hf chondritic model ages of 3.6 Ga (Stevenson and Patchett, 1990). Nd–Sm chondritic model ages of 3.3 Ga have been obtained on quartzofeldspathic gneisses associated with these metasupracrustal rocks (Wooden et al., 1988a, b). The older ages (3.6 Ga) have been interpreted as the minimum estimate of the provenance age for the metasedimentary rocks (Mueller et al., 1985). The age of metamorphism of these older rocks is difficult to define directly, but a Rb–Sr "scatterchron" age for the entire supracrustal association, assuming an initial Sr isotopic ratio of 0.700, yields an age of 3350 Ma (Henry et al., 1982; Wooden et al., 1988a, b). A similar age is evident in Pb–Pb systematics (Wooden and Mueller, 1988). Though not definitive, an age of ~ 3.35 Ga for the granulite facies metamorphism is compatible with the limits of 3.6 Ga determined for the source of the metasedimentary rocks and the younger limit of 2.79 Ga discussed below. It is possible, however, that other high-grade metamorphic events may have occurred during this interval.

This Early to Middle Archean association was later intruded by Late Archean magmatic rocks that are volumetrically dominant in the Beartooth Mountains. The most completely studied sequence of magmatic rocks occurs in the Long Lake area (Mueller et al., 1985; 1988; Wooden and Mueller, 1988) where amphibolites of andesitic composition (AA unit), a foliated granodiorite (LLGd), and an unfoliated granitic unit (LLG) have been recognized. The compositions of these magmatic rocks are consistent with their formation in a magmatic arc environment (e.g. Mueller et al., 1985, 1988; Wooden et al., 1988a, b). This is best seen in the andesitic amphibolites that occur as both tholeiitic and calc-alkaline varieties. They typ-

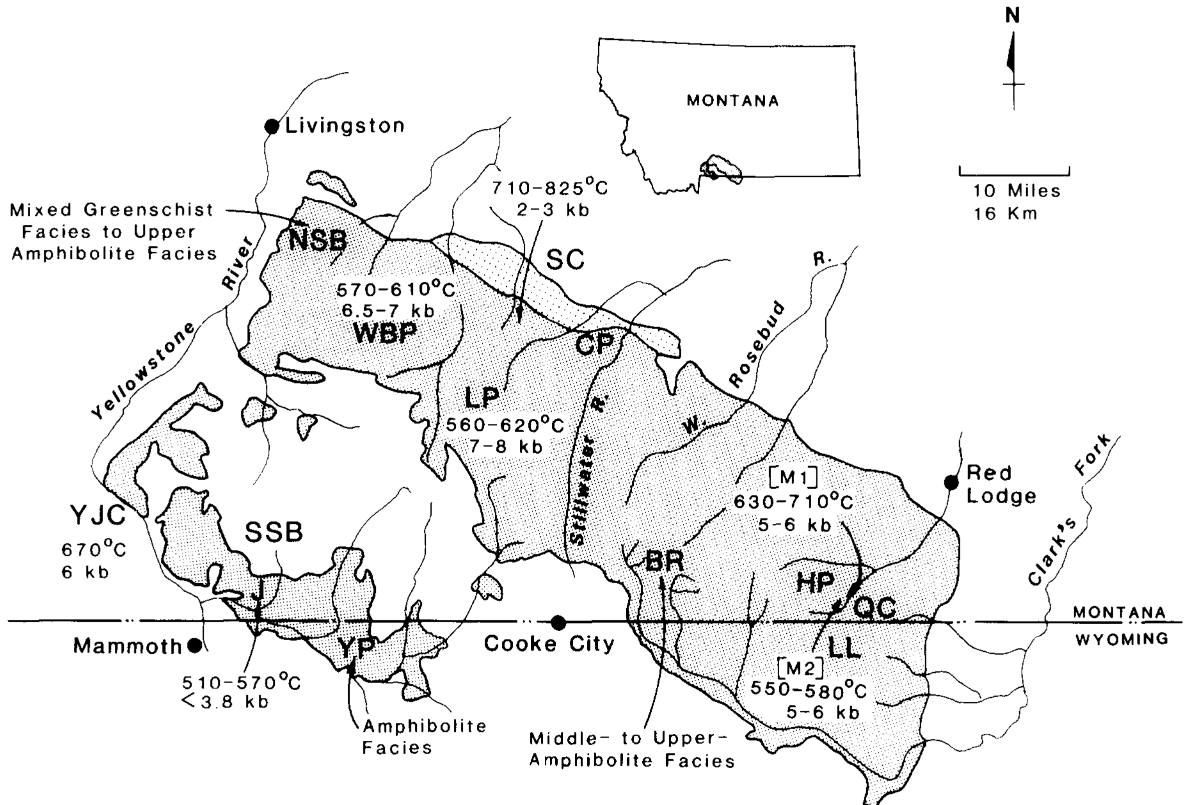

Fig. 2. Index map of the Beartooth Mountains, with calculated metamorphic conditions from Mogk and Henry (1992). The [M_1] metamorphic event is restricted to the granulite facies rocks in the Quad Creek and Hellroaring Plateau areas. Areas designated on the map include: *QC*=Quad Creek; *HP*=Hellroaring Plateau; *LL*=Long Lake; *LP*=Lakes Plateau; *SC*=Stillwater Complex; *NSB*=North Snowy Block; *YJC*=Yankee Jim Canyon; *SSB* =South Snowy Block.

ically have unusually high incompatible element abundances, including strong light rare earth enrichment, and depletion of high field strength elements (Mueller et al., 1983; Wooden and Mueller, 1988; Mueller and Wooden, 1988) which are characteristics of magmas generated in modern arc environments (e.g. Gill, 1981). The LLGd and LLG units have major element compositions typical of sodic to calc-alkaline magmatic suites. Both the LLG and LLGd also exhibit LIL and LREE enrichment and HFSE depletion (Mueller et al., 1985; 1988), although these patterns are not as diagnostic in such evolved rocks.

Ages for the Late Archean magmatic rocks indicate that a major crust-forming event occurred in the Beartooth Mountains between 2.80 and 2.74 Ga. U–Pb zircon ages (upper intercepts) confirm the relative chronology of the magmatic rocks established by field relations which indicate the andesitic magmas formed ~2.79 Ga ago, followed by emplacement of the LLGd at ~2.78 Ga ago, and the LLG ~2.74 Ga ago (Mueller et al., 1985, 1988; Wooden et al., 1988a). A regional amphibolite facies metamorphism [M_2] occurred across the Beartooth Mountains between 2.79 and 2.75 Ga ago because the andesitic amphibolite (AA) and the LLGd are metamorphosed and deformed, whereas the LLG is typically not metamorphosed or foliated.

In summary, the important stages of crustal evolution in the Beartooth Mountains are: (1) Establishment of chemically evolved continental crust in the Early to Middle Archean. Deposition of the protoliths of the metasupracrustal rocks probably occurred in a stable platform environment on, or adjacent to, chemically evolved continental crust. (2) Granulite facies metamorphism(s) of the supracrustal sequences occurred in the Middle Archean, probably at ~3350 Ma ago, and certainly before 2.80 Ga ago. (3) A major crust-forming event was initiated in the Late Archean with the generation of the ~2.80 Ga old andesitic amphibolites and ~2.78 Ga old LLGd, accompanied or followed by amphibolite facies metamorphism, and emplacement of the ~2.74 Ga old LLG. The sodic to calc-alkaline nature of these rocks, trace element abundances (enriched LREE and LIL, depleted HFSE), and arguments based on Sr–Pb–Nd isotope systematics (Wooden and Mueller, 1988), are all consistent with the interpretation that these rocks formed in an environment similar to a modern magmatic arc (e.g. Mueller et al., 1983; 1988; Wooden and Mueller, 1988; Mueller and Wooden, 1988).

Northern Gallatin and Madison Ranges (MMT)

Archean rocks in the MMT include a variety of quartzofeldspathic gneisses with interlayered orthoquartzite, iron formation, marbles and calcareous gneisses, pelitic to mafic schist, mafic amphibolite and granulite, and meta-ultramafic rocks (e.g. Mogk and Henry, 1988, and references therein). Tonalitic to trondhjemitic gneiss, with interlayered metasedimentary rocks and metabasites, are the country rocks in the northern Madison and Gallatin Ranges (Fig. 3). These rocks were intruded by Middle Archean (3.25–3.0 Ga) sill-like bodies of monzodiorite and granodiorite in the Gallatin Peak area, and voluminous bodies of trondhjemites in both the Gallatin Peak and Jerome Rock Lakes areas.

Metamorphism in the northern Gallatin and Madison Ranges is in the upper amphibolite to granulite facies with two distinct regions separated by the Mirror Lake ductile shear zone (Fig. 3). East of the shear zone, in the Gallatin Canyon and Gallatin Peak areas, peak metamorphic temperatures and pressures of 680–770°C and 7–10 kbar have been calculated using numerous independent mineralogic geothermometers and barometers (Mogk, 1990, 1992). West of the shear zone, in the Jerome Rock Lakes area, a kilometer wide selvage of metasupracrustal rocks within trondhjemitic gneisses record peak metamorphic conditions of ~800°C and 6–7 kbar. "Clockwise" P–T–t paths have been interpreted for both regions based on mineral inclusions, corona and symplectite reaction textures, and pressure and temperature estimates based on core and rim mineral compositions (Mogk, 1990, 1992).

Age constraints in the MMT have been determined from detrital and magmatic zircons. Stevenson and Patchett (1990) report Lu–Hf chondritic model ages of 3.4–3.5 Ga for zircons separated from quartzites in the nearby Ruby and Tobacco Root Mountains (in the MMT). These ages are comparable to those obtained by these authors for quartzites from the eastern Beartooth Mountains and probably represent the age of an older crustal component that predated the regional metamorphism. The age of metamorphism is difficult to specify, but some age constraints are available. Rocks that were affected by the granulite facies metamorphism, including tonalitic gneiss and kilometer scale monzodiorite and granodiorite sills, yield maximum U–Pb zircon intercept ages of 3.25 Ga. These magmatic rocks are interpreted as synkinematic to this metamorphic–deformational episode based upon field relations and similar pressure estimates for both the magmatic rocks (Al content of hornblende and the occurrence of magmatic epidote) and the metasupracrustal rocks they intruded (Salt, 1987; Mogk, 1990). The most abundant magmatic rocks in the northern Madison Range have no age or compositional equivalents in the BBMT. These rocks are typically high-Al trondhjemites (Barker, 1979) with U–Pb zircon upper intercept ages between 3.1–3.0 Ga. Juxtaposition of the gneisses and metasupracrustal rocks across the Mirror

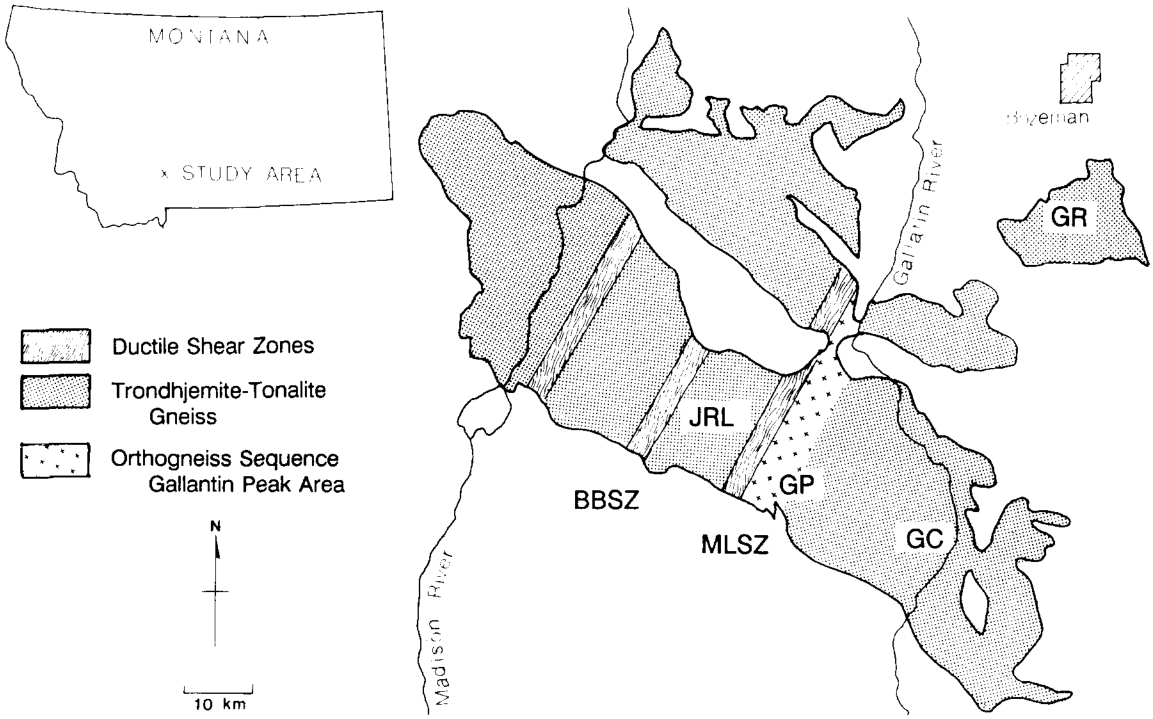

Fig. 3. Index map of the northern Gallatin and Madison Ranges. Areas referred to in the text are: *GR*=Gallatin Range; *GC*=Gallatin Canyon; *GP*=Gallatin Peak; *JRL*=Jerome Rock Lakes; *MLSZ*=Mirror Lake Shear Zone; *BBSZ*=Big Brother Shear Zone. The orthogneiss sequence includes the 3.20 Ga old monzodiorite and granodiorite sills in the Gallatin Peak area and adjacent to the Mirror Lake shear zone.

Lake ductile shear zone must have occurred prior to 2.55 Ga, the U–Pb zircon upper intercept age of an unfoliated granite that was intruded into the shear zone (Weyand, 1989).

In summary, the major geologic events recorded in the northern Madison and Gallatin Ranges of the MMT include: (1) the development of a differentiated crust at least 3.5 Ga, and subsequent deposition of sedimentary cover before 3.2 Ga; (2) concomittant emplacement of granodioritic, tonalitic, and monzodioritic rocks and granulite facies metamorphism ~3.2 Ga; (3) emplacement of substantial volumes of high-Al trondhjemites 3.1–3.0 Ga; and (4) final motion on major shear zones on or before 2.55 Ga. Although the data of Stevenson and Patchett (1990) strongly suggest the presence of continental crust in both the BBMT and MMT by 3.5 Ga, the geologic histories for the two areas diverge significantly after this time.

Discussion

Terrane analysis provides a conceptual framework that can be utilized to integrate geologic, petrologic, structural, geochemical, and geochronologic information into comprehensive models of crustal evolution in Archean as well as Phanerozoic provinces. The criteria for recognizing allochthonous terranes in high-grade metamorphic belts of both eras include: (1) demonstration of different metamorphic and structural histories, as established by geochronologically constrained geothermobarometry and *P–T–t* paths, styles of deformation, and kinematic indicators; ((2) differences in age and composition of magmatic rocks that reflect different environments of formation and/or petrogenetic processes; and (3) recognition of fault or complex structural zones separating otherwise contiguous terranes (e.g. Jones et al., 1983).

A comparison of the geologic history of the BBMT and MMT (Table 1) demonstrates that the first two criteria have been met for these terranes in the northern Wyoming Province. Significant differences in their geologic histories include: (1) prominant granulite facies metamorphism(s) between ~3.35 and 2.79 Ga in the Beartooth Mountains, compared with 3.2 Ga in the northern Madison Range; (2) regional amphibolite facies metamorphism 2.79–2.75 Ga ago throughout the Beartooth Mountains, but not in the northern Madison Range; (3) major magmatic additions to the crust at 2.8–2.74 Ga in the Beartooth Mountains (compositions from andesite to granite with trondhjemitic and granodioritic varieties most prevalent), compared to a 3.25–3.0 Ga event in the northern Madison Range (trondhjemitic gneisses are most abundant, but discrete units of tonalite, monzodiorite, and granodiorite are also present).

The recognition of a major fault or suture zone between the terranes is more problematic because of the lack of lateral continuity of exposures of the Archean basement in the northern Wyoming Province; exposures are limited to widely spaced blocks uplifted by Laramide- and Basin-and-Range-style faults. Earlier studies, however, have recognized zones of structural discontinuity along the western margin of the Beartooth Mountains in the North Snowy Block (Mogk et al., 1988) and in the Yankee Jim Canyon areas (Burnham, 1982; see Fig. 2) that at least partially delineate the two terranes. The North Snowy Block may represent a microcosm of this boundary in that it consists of a series of fault-bounded panels of metasedimentary and metaplutonic rocks that were juxtaposed in the Late Archean (2.75–2.55 Ga ago; Mogk et al., 1988).

Based on these observations, it is valid to consider the BBMT and MMT as terranes in the sense of fault-bounded geologic entities, each with a separate and distinct geologic history. This is an important departure from many earlier studies in the region. Mogk et al. (1988) recognized that the North Snowy Block, and other portions of the MMT (Mogk et al., 1992), consist of numerous fault-bounded panels that were juxtaposed in the Late Archean, in contrast to earlier, more linear chronologic models such as that proposed by Reid et al. (1975). Similar reappraisals have been conducted in other areas. For example, Nutman et al. (1989) have proposed that the Godthabsfjord region, southern West Greenland, is an assembly of gneiss terranes which have experienced separate preassembly histories; this is in contrast to numerous earlier interpretations that this area was part of a single, coherent gneiss complex (e.g. Bridgwater et al., 1976; Chadwick and Nutman, 1979). On a much larger scale, a model for the growth of the Superior Province through accretion of oceanic and continental arcs, accretionary sedimentary wedges, and older microcontinental fragments in a convergent margin setting has been presented by Card (1990).

The recognition that Archean provinces may be collages of terranes leads to a further question: "To what extent are these terranes truly exotic?" In Phanerozoic orogens, exotic or allochthonous terranes include island arcs, oceanic plateaus, and microcontinental fragments that are demonstrably far-travelled based upon stratigraphic, paleontologic, and paleomagnetic studies (e.g. Coney et al., 1980). These data are generally not available for studies of Archean high-grade terranes, and it is unlikely that reliable paleogeographic reconstructions can ever be achieved. Consequently, other tests must be utilized in these older settings. Perhaps the most useful parameters in this regard are determination of the isotopic provenance of igneous rocks as a test of the genetic relationship between adjacent terranes (e.g. Doe and Zartman, 1979; Bennett and De

Paolo, 1987; Wooden et al., 1988c; Wooden and Mueller, 1991). Unless there is a distinct contrast in the signature of the isotopic systematics across terrane boundaries, it is appropriate to question whether adjacent terranes are truly exotic to one another. Other observations commonly used to make these distinctions for high-grade terranes (field relations, igneous and metamorphic petrology, structural relations, geochemistry, and geochronology) may indeed contribute to the compilation of contrasting geologic histories for adjacent crustal blocks, but these contrasts may only reflect differences in the intensity of geologic events as recorded at different crustal levels or in different portions of an otherwise contiguous continental mass. It is unlikely that these geologic discriminants, even in aggregate, have the power of isotopic systematics to distinguish exotic terranes of Archean age.

In the case of the northern Wyoming Province, the BBMT/MMT boundary separates two terranes that have the same distinctive common Pb systematics that require a long-term high U/Pb ratio that is charcteristic of the Wyoming Province in general (Wooden and Mueller, 1988; Mueller and Wooden, 1988; Mueller and D'Arcy, 1990). As shown in Fig. 4, isotopic data strongly suggest that the Late Archean rocks of the BBMT were derived from the same distinctive lithosphere as the older MMT rocks exposed in the northern Gallatin and Madison Ranges. If the Late Archean rocks of the BBMT had formed as a magmatic arc separate from the older rocks of the Wyoming Province, it would probably carry one of the much less radiogenic Pb isotopic signatures associated with most other Archean cratons. For example, it would be particularly easy to distinguish a magmatic arc formed as part of the Late Archean, southern Superior craton that was later juxtaposed against the Wyoming Province. The southern Superior Province has much less radiogenic initial Sr ratios and much more positive initial ϵ_{Nd} values than the Wyoming Province in addition to having some of the least radiogenic initial Pb isotopic compositions observed for Late Archean rocks (Fig. 4). Isotopic data, therefore, constrain the BBMT and MMT to have formed in close proximity to, if not within, what is now distinguished as the Wyoming crustal province. In this context, the significance of the boundary between the BBMT and the MMT is shifted from a boundary separating terranes of entirely different origin to a boundary separating terranes that represent different segments of a single, geochemically distinct crustal province.

Although the isotopic data strongly suggest that the BBMT–MMT boundary is a terrane boundary that did not derive from the accretion of exotic terranes, isotopic contrasts have been reported for other regions that suggest derivation from isotopically distinct crustal provinces. For example, Nutman et al. (1988, 1990) have demonstrated the existence of several separate terranes in southern West Greenland based upon clearly demonstrated differences in geologic history and isotopic (Pb) systematics. Another example of an Archean province that has apparently evolved by accretion of exotic terranes is in the Kolar Schist Belt, southern India. Quartzofeldspathic gneisses and amphibolites on both sides of the schist belt exhibit different geologic histories, as well as distinct Nd and Pb isotopic signatures (Krogstad et al., 1989). These workers have interpreted the Kolar Schist Belt as a suture zone where segments of juvenile continental crust from different source areas and oceanic fragments have been accreted. In the Limpopo Belt, South Africa, there is similar evidence that gneisses in the Central Zone have elevated Pb isotopic compositions which are distinct compared with those of the gneisses in the Southern Marginal Zone (Barton and Key, 1981; Barton, 1983; Barton et al., 1983, 1990).

These occurrences demonstrate the need for integrated field, petrologic, structural, geochemical and isotopic studies to fully characterize the nature of structural boundaries between distinct segments of Archean crust.

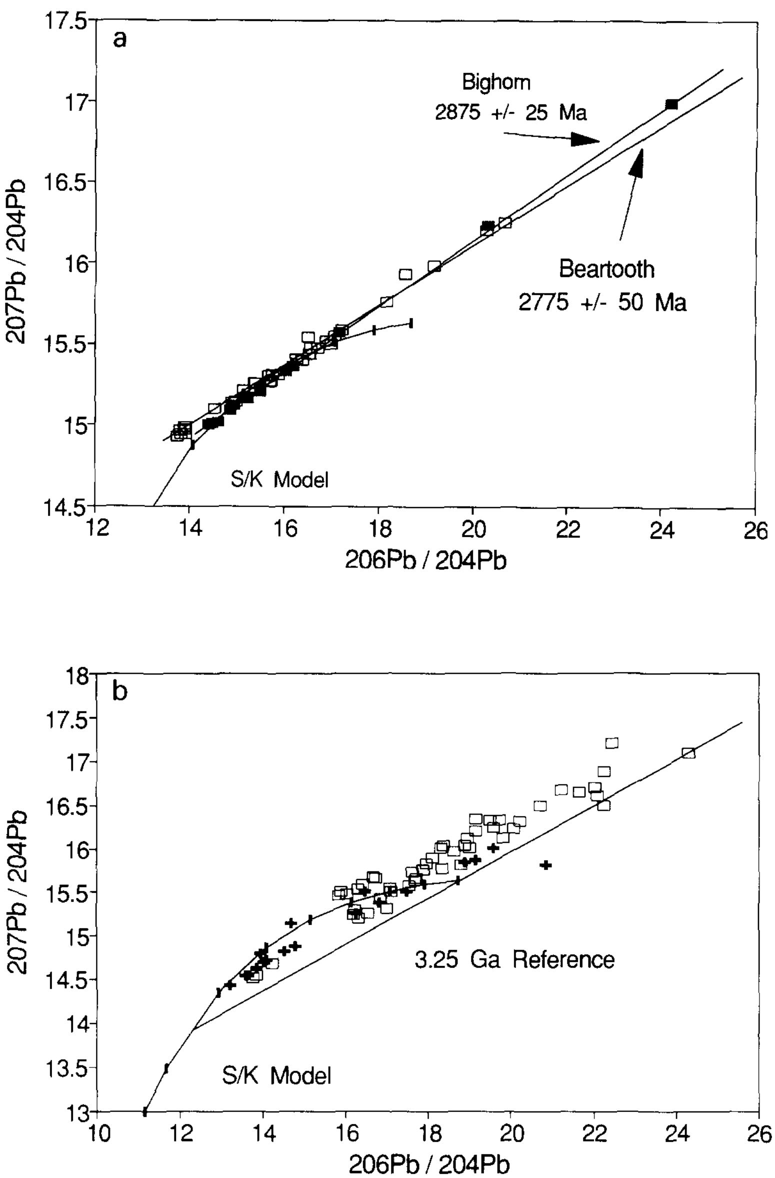

Documentation of different geologic histories in adjacent crustal blocks is not sufficient to allow the interpretation of accretionary tectonics without supporting evidence based on isotopic systematics as discussed above. Characterization of Archean terrane boundaries is particularly important in understanding the degree to which contiguous crustal provinces are reworked and juxtaposed, as is the case across the BBMT–MMT boundary, rather than accreted as distinct, exotic additions to continents, as is apparently the case in some Archean provinces (e.g. Superior Province, Canada; Godthab, Greenland; Kolar Schist Belt, India; Limpopo Belt, South Africa).

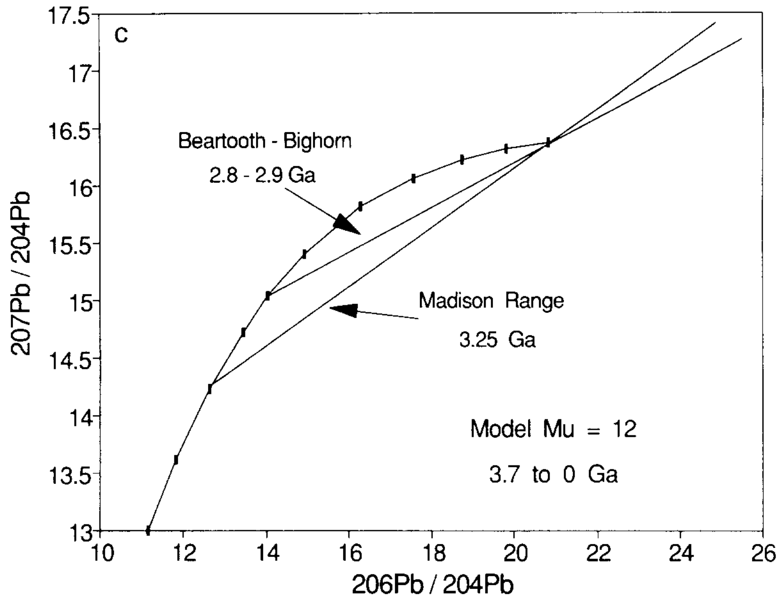

Fig. 4. Plots of $^{206}Pb/^{204}Pb$ versus $^{207}Pb/^{204}Pb$ for plutonic and meta-igneous rocks from (a) the Beartooth (open symbols) and Bighorn Mountains (closed symbols), and (b) the Madison Range (open squares from the northern part of the range, + from the southern part of the range). See Wooden and Mueller (1988) for a full description of the Beartooth Mountain data. Bighorn and Madison Range data are unpublished. Bighorn samples are described by Arth et al. (1980). All Pb isotopic data are shown with respect to the average crust model of Stacey and Kramers (1975), and for all three areas indicate sources more radiogenic than the Stacey and Kramers model. (c) The combined Beartooth–Bighorn array and the Madison Range array are shown schematically. Their more radiogenic initial Pb isotopic compositions are consistent with a reservoir that evolved from 3.7 Ga with $\mu = 12$, significantly higher than the μ value of the Stacey and Kramers model. This is a non-unique model, but is indicative of the general need for a reservoir that had a long-term, higher than the average μ value to explain the Pb isotopic systematics of the Archean rocks of the Wyoming Province.

Conclusion

The concept of terrane analysis has made important contributions to the resolution of geologic histories of orogenic belts, and to a more fundamental understanding of crustal evolution in general. In the northern Wyoming Province two terranes are recognized, the BBMT and MMT, based on differences in their geologic histories as represented by lithologic associations, metamorphic and deformational history, petrology and geochemistry of magmatic rocks, and isotopic ages. Isotopic systematics, however, indicate that these terranes have developed in continental crust that is isotopically indistinguishable on either side of the terrane boundary. We interpret the present configuration of the BBMT and MMT in the northern Wyoming Province, therefore, to be the result of intracratonic reorganization of crustal blocks that were part of a more extensive Early to Middle Archean craton, rather than accretion of exotic terranes. In a non-genetic sense, it is appropriate to represent discrete, fault-bounded crustal blocks as terranes. The extent to which these terranes are exotic, however, is difficult to prove lacking paleontologic or paleomagnetic data. Because isotope systematics can characterize large areas relative to other geologic features (e.g. metamorphic conditions, structural style), isotopic systematics can offer the best opportunity to assess the exotic nature of Archean or younger terranes where more direct geographic assessments are not possible.

Acknowledgments

This research was supported by the National Science Foundation (NSF EAR 82-11828, 86-18885, 89-05076 to PAM; EPSCoR MONTS program and NSF EAR 86-18327, 89-03636 to DWM), USGS DI 14-08-0001-G-651 (PAM), NASA NAG-9-91 (PAM) NRC senior associateship (NASA/JSC to PAM). Discussions with Darrel Henry, Fred Barker, and Emily Weyand helped with the development of this paper. Reviews by Jay Barton, Ken Card and Allen Nutman improved the quality of the mansuscript. Special thanks to Dirk van Reenen and the organizing committee of the 1990 Limpopo Belt Field Conference for providing the opportunity to present these results.

References

Arth, J.G., Barker, F. and Stern, T.W., 1980. Geochronology of Archean gneisses in the Lake Helen area, southwestern Bighorn Mountains, Wyoming. Precambrian Geol., 11: 11–22.

Barker, F., 1979. Trondhjemite: definition, environment and hypothesis of origin. In: F. Barker (Editor), Trondhjemites, Dacites and Related Rocks. Elsevier, Amsterdam, pp. 1–12.

Barker, F., Arth, J.G. and Millard, H.T., Jr., 1979. Archean trondhjemites of the southwestern Bighorn Mountains, Wyoming—a preliminary report.In: F. Barker (Editor), Trondhjemites, Dacites, and Related Rocks. Elsevier, Amsterdam, pp. 401–414.

Barton, J.M., Jr., 1983. Pb-isotopic evidence for the age of the Messina Layered Intrusion, central zone, Limpopo mobile belt. Geol. Soc. S. Afr. Spec. Publ., 8: 39–41.

Barton, J.M., Jr. and Key, R.M., 1981. The tectonic development of the Limpopo mobile belt and the evolution of the Archaean cratons of southern Africa. In: A. Kröner (Editor), Precambrian Plate Tectonics. Elsevier, Amsterdam, pp. 185–212.

Barton, J.M., Jr., Ryan, B. and Fripp, R.E.P., 1983. Rb–Sr and U–Th–Pb isotopic studies of the Sand River Gneisses, central zone, Limpopo mobile belt. Geol. Soc. S. Afr. Spec. Publ, 8: 9–18.

Barton, J.M., Jr., Van Reenen, D.D. and Roering, C., 1990. The significance of 3000 Ma granulite facies mafic dikes in the central zone of the Limpopo belt, southern Africa. Precambrian Res., 48: 299–308.

Bennett, V. and DePaolo, D., 1987. Proterozoic crustal history of the western United States as determined by Nd isotopic mapping. Geol. Soc. Am. Bull., 99: 674–685.

Bridgwater, D., Keto, L., McGregor, V.R. and Muers, J.S., 1976. Archaean gneiss complex of Greenland. In: A. Escher and W.S. Watt (Editors), Geology of Greenland. Geol. Surv. Greenland, Copenhagen, pp. 19–75.

Burnham, R., 1982. Mylonite zones in the crystalline basement rocks of Sixmile Creek and Yankee Jim Canyon, Park County, Montana. MSc Thesis, University of Montana, Missoula, 94 pp.

Card, K.D., 1990. A review of the Superior Province of the Canadian Shield, a product of Archean accretion. Precambrian Res., 48: 99–156.

Chadwick, B. and Nutman, A.P., 1979. Archaean structural evolution in the northwest of the Buksefjorden region, southern West Greenland. Precambrian Res., 9: 199–226.

Coney, P.J., Jones, D.L. and Monger, J.W., 1980. Cordilleran suspect terranes. Nature, 288: 329–333.

Coward, M.P., 1976. Archean deformation patterns in southern Africa. Phil. Trans. R. Soc. Lond., A283: 313–331.

Doe, B. and Zartman, R., 1979. Plumbotectonics I. The Phanerozoic. In: H. Bernes (Editor), Geochemistry of Hydrothermal Ore Deposits. Wiley, New York, pp. 22–70.

Erslev, E.A., 1983. Pre-Beltian geology of the southern Madison Range, southwestern Montana. Mont. Bur. Min. Geol. Mem., 55: 1–26.

Foose, R.M., Wise, D.U. and Garbarini, G.S., 1961. Structural geology of the Beartooth Mountains, Montana and Wyoming. Geol. Soc. Am. Bull., 72: 1143–1172.

Garihan, J.M., 1979. Geology and structure of the central Ruby Range, Madison County, Montana. Geol. Soc. Am. Bull., , 90 (Pt. II): 695–788.

Gill, J.B., 1981. Orogenic Andesites and Plate Tectonics. Springer, New York, 390 pp.

Heinrich, E.W. and Rabbit, J.C., 1961. Pre-Beltian geology of the Cherry Creek and Ruby Mountains Areas, southwestern Montana. Mont. Bur. Min. Geol. Mem., 38: 40 pp.

Henry, D.J., Mueller, P.A., Wooden, J.L., Warner, J.L. and Lee-Berman, R., 1982. Granulite grade supracrustal assemblages of the Quad Creek area, eastern Beartooth Mountains, Montana, In: P.A. Mueller and J.L. Wooden (Editors), Precambrian Geology of the Beartooth Mountains, Montana and Wyoming. Mont. Bur. Min. Geol. Spec. Publ., 84: 147–159.

Howell, D.G. and Jones, D.L., 1983. Tectonostratigraphic terrane analysis and some terrane vernacular. In: D.G. Howell, D.L. Jones, A. Cox and A. Nur (Editors), Proc. Circum-Pacific Terrane Conf. Stanford University, Stanford, CA, pp. 6–8.

Jones, D.L., Howell, D.G., Coney, P.J. and Monger J.W.H., 1983. Recognition, character and analysis of tectonostratigraphic terranes in western North America, In: M. Hashimoto and S. Uyeda (Editors), Accretion Tectonics in the Circum-Pacific Regions. Terra Scientific, Tokyo, pp. 21–35.

Krogstad, E.J., Balakrishnan, S., Mukhopadhyay, D.K., Rajamani, V. and Hanson, G.N., 1989. Plate tectonics 2.5 billion years ago: evidence at Kolar, south India. Science, 243: 1337–1340.

Mason, R., 1973. The Limpopo mobile belt—southern Africa. Phil. Trans. Geol. Soc. Lond., A273: 463–485.

McCourt, S. and Vearncombe, J.R., 1987. Shear zones bounding the central zone of the Limpopo mobile belt, southern Africa. J. Struct. Geol., 9: 127–137.

Mogk, D.W., 1990. A model for granulite–migmatite associations in the Archean basement of SW Montana: geochemical and tectonic implications. In: D. Vielzeuf and Ph. Vidal (Editors), Granulites and Crustal Evolution. NATO ASI Series C, 311. Kluwer, Dordrecht, pp. 133–156.

Mogk, D.W., 1992. Ductile shearing and migmatization at mid- crustal levels in an Archean high-grade gneiss belt, northern Gallatin Range, Montana, USA. J. Metamorph. Geol., in press.

Mogk, D.W. and Henry, D.J., 1988. Metamorphic petrology of the northern Archean Wyoming Province, southwestern Montana: evidence for Archean collisional tectonics. In: W.G. Ernst (Editor), Metamorphism and Crustal Evolution in the Western United States. Prentice-Hall, New York, pp. 363–382.

Mogk, D.W. and Henry, D.J., 1992. Metamorphic petrology of the Beartooth Mountains: evidence for crustal evolution. J. Petrol., in review.

Mogk, D.W., Mueller, P.A. and Wooden, J.L., 1988. Archean tectonics of the North Snowy Block, Beartooth Mountains, Montana. J. Geol., 96: 125–141.

Mogk, D.W., Mueller, P.A. and Wooden, J.L., 1991. The northern Archean Wyoming Province: contrasts in crustal evolution. Proc. VIIIth Int. Basement Tectonics Conf., in press.

Mueller, P.A. and D'Arcy, K., 1990. Sm–Nd systematics of the Late Archean Wyoming greenstone terrane. EOS, 71: 662.

Mueller, P.A. and Wooden, J.L., 1988. Evidence for Archean subduction and crustal recyling, Wyoming province. Geology, 16: 871–874.

Mueller, P.A., Wooden, J.L., Odom, A.L. and Bowes, D.R., 1982. Geochemistry of the Archean rocks of the Quad Creek and Hellroaring Plateau areas of the eastern Beartooth Mountains. Mont. Bur. Min. Geol. Spec. Publ., 84, 69–82.

Mueller, P.A., Wooden, J.L., Schulz, K. and Bowes, D., 1983. Incompatible element rich andesitic amphibolites from the Archean of Montana and Wyoming: evidence for mantle metasomatism. Geology, 11: 203–206.

Mueller, P.A., Wooden, J.L., Henry, D.J. and Bowes, D.R., 1985. Archean crustal evolution of the eastern Beartooth Mountains, Montana and Wyoming. In: G.K. Czamanske and M.L. Zientek (Editors), The Stillwater Complex, Montana—Geology and Guide. Mont. Bur. Min. Geol. Spec. Publ., 92: 9–20.

Mueller, P.A., Shuster, R.D., Graves, M.A., Wooden, J.L. and Bowes, D.R., 1988. Age and composition of a Late Archean magmatic complex, Beartooth Mountains, Montana–Wyoming. Mont. Bur. Min. Geol. Spec. Publ., 96: 7–22.

Nutman, A.P., Taylor, P., Moorbath, S., Friend, C., Duke, M., Baadsgaard, H. and McGregor, V., 1988. The Pb isotopic signatures of Archean terranes, Godthab region, southern West Greenland, 143 pp.

Nutman, A.P., Friend, C.R.L., Baadsgaard, H. and McGregor, V.R., 1989. Evolution and assembly of Archean gneiss terranes in the Godthabsfjord region, southern West Greenland: structural, metamorphic and isotopic evidence. Tectonics, 8: 573–589.

Peterman, Z., 1981. Dating of Archean basement in northeastern Wyoming and southern Montana. Geol. Soc. Am. Bull. 92 (Pt. 1): 139–146.

Reid, R.R., McMannis, W.J. and Palmquist, J.C., 1975. Precambrian geology of the North Snowy Block, Beartooth Mountains, Montana. Geol. Soc. Am. Spec. Pap., 157: 135 pp.

Salt, K., 1987. Archean geology of the Spanish Peaks area, southwestern Montana. MSc Thesis, Montana State University, Bozeman, MT, 81 pp.

Spencer, E. and Kozak, S.V., 1975. Precambrian evolution of the Spanish Peaks, Montana. Geol. Soc. Am. Bull., 86: 785–792.

Stacey, J.S. and Kramers, J.D., 1975. Approximation of terrestrial lead isotope evolution by a two-stage model. Earth Planet. Sci. Lett., 26: 207–221.

Stevenson, R.K. and Patchett, P.J., 1990. Implications for the evolution of continental crust from Hf isotope systematics of Archean detrital zircons. Geochim. Cosmochim. Acta, 54: 1683–1698.

Vitaliano, C.J., Cordua, W.S., Hess, D.F., Burger, H.R., Hanley, T.B. and Root, F.K., 1979. Explanatory text to accompany geologic map of southern Tobacco Root Mountains, Madison County, Montana. Geol. Soc. Am. Map and Chart Series MC-31.

Weyand, E., 1989. U–Pb zircon geochronology of Archean rocks from the Spanish Peaks area, Madison Range, Montana. MSc Thesis, Univ. Florida, Gainesville, FL, 113 pp.

Wooden, J.L. and Mueller, P.A., 1988. Pb, Sr and Nd isotopic compositions of a suite of Late Archean igneous rocks, eastern Beartooth Mountains: implications for crust–mantle evolution. Earth Planet. Sci. Lett., 87: 59–72.

Wooden, J.L. and Mueller, P.A., 1991. Evidence that the Wyoming Province represents crustal growth from an Early Archean enriched crust–mantle system. EOS Abs. Suppl., 72: 296.

Wooden, J.L., Mueller, P.A. and Mogk, D.W., 1988a. A review of the geochemistry and geochronology of the Archean rocks of the northern part of the Wyoming Province. In: W.G.Ernst (Editor), Metamorphism and Crustal Evolution of the Western United States. Prentice-Hall, New York, pp. 383–410.

Wooden, J.L., Mueller, P.A. and Mogk, D.W., 1988b. A review of the Archean rocks of the Beartooth Mountains, Montana and Wyoming. Mont. Bur. Min. Geol. Spec. Publ., 96: 23–42.

Wooden, J., Stacey, J., Doe, B., Hovack, K., Miller, D., 1988c. Pb isotopic evidence for the formation of Proterozoic Crust. In: W.G. Ernst (Editor), Metamorphism and Crustal Evolution of the Western United States. Rubey Vol. VII. Prentice Hall, Englewood Cliffs, NJ, pp. 69–86.

Economic Geology
Vol. 85, 1990, pp. 585–600

Petrogenesis and Timing of Talc Formation in the Ruby Range, Southwestern Montana

DALE L. ANDERSON,* DAVID W. MOGK, AND JOHN F. CHILDS**

Department of Earth Sciences, Montana State University, Bozeman, Montana 59717

Abstract

Talc deposits in the Ruby Range, southwestern Montana, have formed in Archean dolomitic marbles that were mineralized during retrograde talcification in the Proterozoic. Calcite-rich marbles contain the assemblage calcite-olivine-phlogopite ± tremolite, indicating that metamorphism occurred in the upper amphibolite to granulite facies (M_1); crystallization of serpentine and chlorite, and dolomitization of the marbles in the greenschist facies overprinted the high-grade calc-silicate assemblages (M_2); and talc has replaced dolomite and the other greenschist-grade silicate minerals in the latest stage of recrystallization which resulted in the formation of the main talc bodies (M_3). Structural control of the talc formation is suggested by discontinuous occurrences of talc bodies along layer-parallel fractures. Preservation of relict textures indicates that the talc formed during constant volume replacement. Geochemical analyses and mass balance calculations demonstrate that introduction of large quantities of Si and Mg and removal of Ca is required to maintain constant volume. Model reactions indicate that infiltration of a minimum of 4.8×10^5 l of water is needed to convert a cubic meter of the average high-grade marble to talc (volumetric water/rock ratio > 600). The infiltration mechanism is consistent with the observation that no isobaric univariant mineral assemblages were present to buffer the composition of the metamorphic fluids. Estimates of the maximum conditions of talc formation of 2 kbars and 400°C are based on field observations and heterogeneous phase equilibria; it is probable that the talc actually formed at much lower temperatures and pressures, possibly in a near-surface hot spring deposit. Regional geologic relations indicate that the talc mineralization occurred during the middle Proterozoic.

Introduction

INDUSTRIAL minerals such as talc are of great economic significance but are relatively poorly understood with respect to their occurrence, petrogenesis, and timing of formation compared to precious and base metal deposits. The field relations, petrography, and whole-rock chemistry of six talc prospects in the Ruby Range, southwestern Montana, have been studied in detail to develop a model for the mechanism(s) of formation of these talc deposits and to determine the timing of their formation.

Talc (and chlorite) deposits have been reported in Archean rocks that have been exposed in foreland block uplifts in the Ruby Range, Tobacco Root Mountains, Highland Mountains, Gravelly Range, and Greenhorn Range across southwestern Montana (Fig. 1; Berg, 1979; and references therein). In the Ruby Range two talc mines are currently in production: the Beaverhead mine, operated by Cyprus Industrial Minerals Company, and the Treasure Chest mine, operated by Pfizer, Inc. The talc occurrences described in this report are satellitic to these major talc-producing mines. The talc deposits of the Ruby Range are the principal source of steatite-grade talc in the United States and ore reserves for the district are estimated on the order of 10^6 tons (Chidester et al., 1964). Talc from the Ruby Range varies in color from light green, high-purity material, to impure gray-brown and maroon talc.

Formation of economically viable talc deposits is generally restricted to two geologic environments: metamorphosed siliceous dolomitic carbonate rocks; and altered ultramafic bodies (e.g., Brown, 1973). High-purity talc deposits in the Ruby Range occur as bodies of pure talc which have replaced Archean dolomitic marble (Okuma, 1971; Garihan, 1973; Berg, 1979); alteration of ultramafic bodies in the range has not been recognized as a mechanism for formation of mineable talc bodies (Desmarais, 1981).

Geologic Setting

Archean basement rocks in southwestern Montana are exposed in Laramide-style foreland block uplifts which have been modified by subsequent basin-and-range extension (Fig. 1; Schmidt and Garihan, 1983). The Archean rocks in the Ruby Range are dominated by quartzofeldspathic gneiss (the Dillon Gneiss), with intercalated schists, quartzites, amphibolites, and marbles. These rocks have undergone amphibolite- to granulite-grade, dynamothermal metamorphism (M_1), dated at approximately 2,750 Ma using the Rb-

* Present address: R. L. Stollar and Associates, Inc., 143 Union Boulevard, Suite 640, Lakewood, Colorado 80228.

** Present address: Consulting Geologist, 705 South 5th Avenue, Bozeman, Montana 59715.

0361-0128/90/1058/585-16$3.00

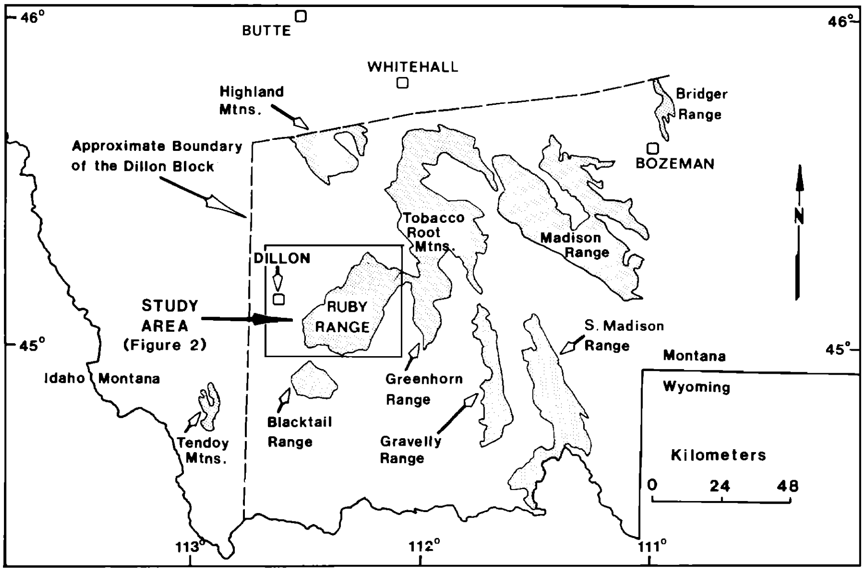

FIG. 1. Regional location map showing the study area and Archean basement exposures (stippled pattern) in southwestern Montana (modified from Bergantino and Clark, 1985).

Sr whole-rock method (James and Hedge, 1980). The peak metamorphic conditions are 700° to 750°C and 6 to 8 kbars (Dahl, 1979). M_1 metamorphism produced the dominant foliation within the central and southern Ruby Range, which strikes northeast and dips to the northwest (Karasevich et al., 1981). Megascopic and macroscopic folds associated with M_1 are isoclinal to tight with axial surfaces that strike northeast and dip to the northwest.

A Proterozoic retrograde regional thermal event (M_2) resulted in overprinting of the granulite-amphibolite-grade assemblages by greenschist-grade assemblages; no penetrative deformational features are associated with this thermal event (Okuma, 1971; Garihan, 1973; Dahl, 1979; Desmarais, 1981). Giletti (1966) reported K-Ar dates for biotite and muscovite and Rb-Sr whole-rock dates of 1.6 ± 0.1 Ga for the Dillon Gneiss. The major faults in the Ruby Range strike northwest (Fig. 2), offset the northeast-trending Archean structures, and have undergone recurrent movement since Proterozoic time (Schmidt and Garihan, 1983, 1986). Previous workers have suggested that talc formation is the result of fluid movement along these structures during the Proterozoic greenschist thermal event (Okuma, 1971; Garihan, 1973; Olson, 1976; Berg, 1979).

Contemporaneous with, and possibly prior to, incipient rifting of the Belt basin, two distinct sets of northwest-trending mafic dikes intruded the area, at 1,455 Ma and 1,120 to 1,130 Ma, probably along preexisting fracture zones (Wooden et al., 1978). It has been postulated that these dikes may also have been the source of heat and fluids for talc formation (Wooden et al., 1978). However, no apparent spatial association between mafic dikes and talc-bearing marble was documented during the present study.

The Ruby Range and surrounding area (Fig. 1) has been interpreted as a positive tectonic feature (termed

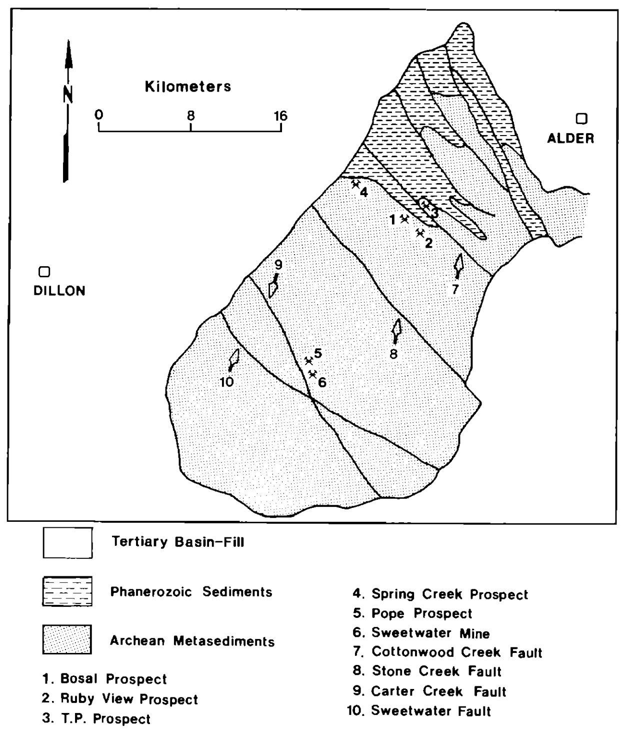

FIG. 2. Location map showing the Ruby Range, with locations of prospects examined, and major northwest-trending faults (modified from Schmidt and Garihan, 1986).

the Dillon block by Harrison et al., 1974) during middle to late Proterozoic time. The Archean rocks in the Dillon block are the most probable source for clasts of marble, gneiss, and amphibolite in the LaHood Formation, which was deposited along the southern margin of the Belt basin (McMannis, 1963; Boyce, 1975). Deposition of the LaHood Formation has been interpreted as marking incipient rifting of the Belt basin (McMannis, 1963). This observation is significant because it places the Archean rocks in a near-surface environment at roughly the same time as the thermal metamorphism in the middle Proterozoic.

The northernmost portion of the Ruby Range is covered by Phanerozoic sediments which have been subjected to Laramide-style deformation (Tysdal, 1976; Schmidt and Garihan, 1983); this area has subsequently been overprinted by basin-and-range-style extension. There are a number of Cambrian and younger dolomitic units (Pilgrim Formation, Meagher Formation, Madison Group) which unconformably overlie or are in fault contact with the Archean basement; none of these carbonate rocks have been subjected to thermal metamorphism or talc mineralization.

Field Relationships and Petrography

Six talc prospects (Fig. 2) from different parts of the Ruby Range were mapped in detail on a scale of 1″ = 5′ or 1″ = 10′ (e.g., Fig. 3). The detailed maps illustrate the nature of lithologic layering of marbles within the gneiss and schist; distribution of massive talc bodies; and the dominant structural features including folds, shear zones, fault surfaces, and joints. Within each prospect, high-grade marbles, talc-bearing marbles, and altered country rock were sampled for petrologic and whole-rock geochemical analysis. All prospects examined exhibit similar mineralogic, textural, and structural relationships (Anderson, 1987). One prospect, the Sweetwater mine, exhibits additional unique mineralogic and textural relations which will be documented below. In aggregate, the mineralogic, petrologic, and structural relationships observed in these six occurrences provide a basis for interpreting the petrogenesis and timing of talc formation in the Ruby Range.

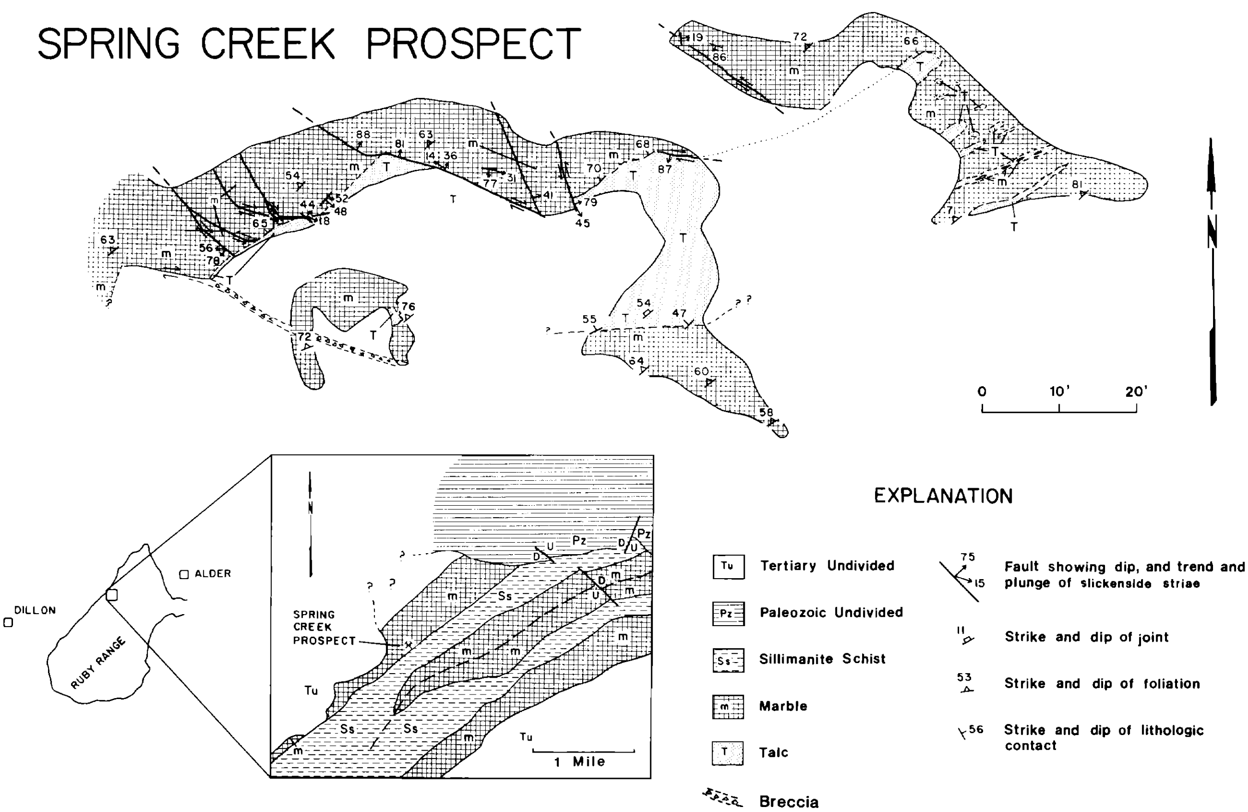

FIG. 3. Geologic map of the Spring Creek talc prospect. The solid outline delineates the extent of development on the deposit. The talc bodies have developed as local replacements of the Archean marbles; the distribution of these bodies is structurally controlled by foliation and compositional layering within the marbles. The inset map shows the regional geologic setting of this deposit (after Garihan, 1973).

High-grade marble (HGM)

Marbles containing high-grade mineral assemblages are present within tens of meters of talc-bearing zones in all prospects and are typically more calcitic than talc-bearing marbles. High-grade marbles contain the M_1 assemblage calcite-olivine-phlogopite ± dolomite ± garnet. Tremolite occurs as a replacement of olivine, in a fibrous form in shear zones, and as randomly oriented prisms in the carbonate matrix. It has not been possible, based on textural criteria, to determine if tremolite is part of the peak M_1 mineral assemblage, if it has grown in a late retrograde stage of the M_1 event, or if it is associated with the overprinting M_2 greenschist facies event. It is probable that tremolite formation was not restricted to any one of these possibilities. High-grade assemblages have been overprinted by retrograde (M_2) serpentine and chlorite. Retrograde serpentine occurs dominantly as pseudomorphs replacing olivine in a characteristic mesh texture. Accessory minerals include graphite, pyrite, and hematite.

The carbonate matrix of the high-grade marbles varies from fine to coarse grained (2–10 mm). A complex polymetamorphic recrystallization history for the carbonate matrix, similar to the metamorphic history recorded by the silicate parageneses, has been observed by transmitted light, cathodoluminescence (CL), and ultraviolet (UV) microscopy. Calcite grains in the high-grade marbles commonly contain exsolution lamellae of dolomite, indicating unmixing from a higher grade mineral assemblage (Fig. 4). These grains also exhibit zones of patchy extinction in transmitted light and anomolous fluorescence when viewed by CL and UV, suggesting that they have incompletely reequilibrated during the overprinted M_2 greenschist facies metamorphism. Many of the calcite grains that have experienced the earlier amphibolite facies metamorphism (M_1) are rimmed by homogeneous recrystallized calcite; the abrupt boundary between cores of these grains, which exhibit exsolution lamellae and patchy zoning, and the homogeneous rims suggests that the rims formed as overgrowths during a separate metamorphic event. Calcite is also present in late-stage veins which crosscut serpentine mats. These mats are characteristic of the M_2 greenschist facies event. Dolomite is rare or absent in the high-grade marbles; presumably it has been consumed during prograde reactions that formed the Mg-bearing silicate minerals.

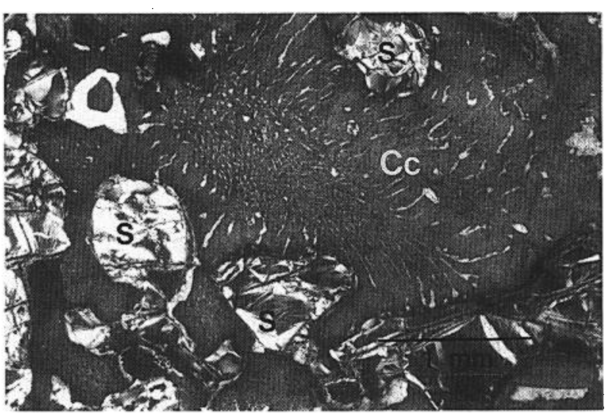

FIG. 4. Photomicrograph of a high-grade marble showing exsolution lamellae of dolomite in calcite (Cc) and an overgrowth of homogeneous calcite over the high-grade calcite core (crossed nichols). The ovoid areas with low birefringence are pseudomorphs of olivine by serpentine (S); these exhibit mesh texture.

Quartz is rare as a primary phase and is dominantly present as late-stage filling of vugs and fractures (during M_2). Centimeter-scale siliceous layers occur locally as boudins and detached fold hinges in the carbonate matrix; these may have been primary cherty layers in the carbonate protoliths of the marble. Individual disseminated quartz grains have not been observed in the marbles, and if originally present, were probably consumed in the prograde amphibolite facies metamorphism M_1. Some quartz was mobilized, and possibly introduced into the marbles, during high-grade metamorphism, as evidenced in outcrop by disharmonically folded quartz veins and stringers.

Talc-bearing marble (TBM)

Talc-bearing marbles have selectively replaced the high-grade marbles with greenschist facies silicate minerals and the carbonate matrix has been dolomitized during a second distinct metamorphic event (M_2). The textural evidence for the petrogenetic history of the talc-bearing marbles is described below and is summarized in Table 1. The contacts between the two marbles are abrupt and are marked by changes in dolomite content, grain size, and Mg silicate mineralogy. Talc-bearing marbles occur as isolated pods within larger marble bodies or at the contacts of the marbles with the surrounding quartzofeldspathic gneiss. The talc bodies are typically conformable with compositional layering in the surrounding marbles; they range from 1.5 to 4 m in thickness. In most cases larger talc bodies appear to pinch out along strike rather than being terminated by faults. It is important to note that the talc bodies occur as replacements of the high-grade marbles and that there is no field evidence for significant changes in volume accompanying talc formation. The dominant mineral assemblage in the talc-bearing marbles is talc-dolomite-chlorite ± calcite with accessory graphite, pyrite, manganese oxide, and quartz. Serpentine, tremolite, and phlogopite may be present as relics but are almost always seen in a reaction texture if talc is present.

The carbonate matrix of the talc-bearing marbles is dominantly composed of dolomite. It is the direct replacement of dolomite by talc that is volumetrically

TABLE 1. Summary of Replacement Reactions and Intergrowths Observed during Petrographic Analysis

Prospect		Bosal	Ruby View	T.P.	Spring Creek	Pope	Sweetwater
	Observed Replacement						
1	Do → Tc	X	X	X	X		
2	S → Tc	X	X	X	X	X	
3	Ph → Tc	X	X	X	X		
4	Tr → Tc	X	X		X	X	
5	Qtz → Tc				X		X
6	M → Tc						X
7	Ph → Ch	X			X		
8	Qtz → S		X				
9	Ol → S	X		X		X	
10	Tr → S					X	
11	Feld → Ch						X
	Intergrowths						
1	Ch—Tc	X	X	X	X	X	
2	Do—Ch		X		X	X	
3	Do—S	X					
4	Ch—S		X	X	X		
5	Cc—Tc					X	

Abbreviations: Cc = calcite, Ch = chlorite, Do = dolomite, Feld = feldspar, M = magnesite, Ol = olivine, Qtz = quartz, Ph = phlogopite, S = serpentine, Tr = tremolite

the most important mineralization process. Dolomite exhibits several distinct textures which suggest that it has formed as a replacement mineral after the dynamothermal amphibolite facies metamorphism and prior to the crystallization of talc. Incomplete alteration of high-grade marbles to talc is indicated by inclusion of relict high-grade marble blocks within the talc-bearing marbles and massive talc bodies. On a microscopic scale, dolomite of the talc-bearing marbles has developed serrate boundaries convex to the calcite of the high-grade marbles, with small apophyses of dolomite growing into the calcite matrix along grain boundaries. The overall morphology of the ovoid talc-bearing marble bodies, with the wedge-shaped terminations, may be interpreted as a dolomitic front that has migrated along the M_1 structural fabric in the marble.

Within the talc-bearing marble bodies, dolomite typically occurs as discrete 1-mm to 1-cm, homogeneous hypidiomorphic to idiomorphic grains (Fig. 5). These are quite unlike the carbonate matrix of the high-grade marbles in which fine-grained calcite grains are highly strained and typically exhibit exsolution features, patchy zoning, and numerous carbonate overgrowths (as observed by CL and UV microscopy). Dolomite also occurs as rims on earlier formed calcite grains, as thin replacement zones along cleavage traces in calcite, in fracture fillings which crosscut calcite grains, and as terminated, rhombohedral crystals filling cavities. Exsolution textures are not observed in dolomite and patchy and undulose extinction in dolomite are present but not common.

The most important occurrence of talc is as the direct replacement of dolomite. Evidence for this mechanism of talc formation is present in discrete laths or cryptocrystalline masses of talc disseminated in a dolomite matrix, as well as in massive bodies of pure talc meters across. Talc which occurs disseminated in the marble is not of economic importance. However, this talc does preserve textural relationships that allow interpretation of the talc-forming processes, as well as the timing of talc formation. The most important talc-forming reaction is:

$$3CaMg(CO_3) + 4SiO_2 + 2H_2O = Mg_3Si_4O_{10}(OH)_4 + 3CaCO_3 + 3CO_2. \quad (1)$$

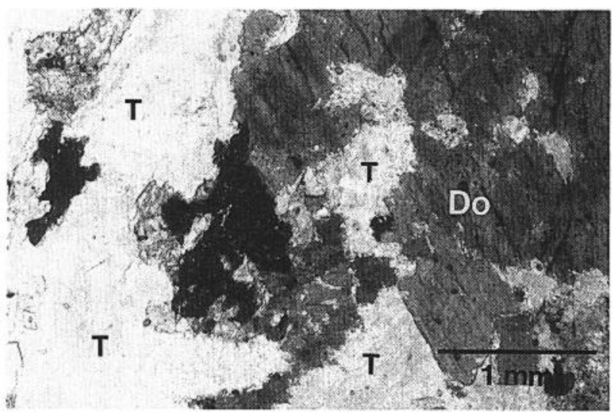

FIG. 5. Photomicrograph showing rhombohedral dolomite (Do) being replaced by talc (T). This is the dominant mechanism for talc formation in the Ruby Range. The dolomite formed during M_2 and is characteristically coarse-grained, eu- to subhedral, undeformed, and devoid of patchy zoning or exsolution lamellae.

The outlines of relict rhombohedral dolomite crystals are clearly preserved in monomineralic masses of talc (Fig. 6), and fine-grained masses of talc are observed growing at the expense of dolomite in the carbonate matrix (Fig. 5). The multivariant assemblage dolomite-talc is characteristic of large volumes of the talc-bearing marble, and there are few relict textures of earlier silicate phases in this occurrence. Quartz in the matrix was very rarely identified as a reactant mineral in the talc-bearing marbles, except for local occurrences where talc selvages may have formed adjacent to cherty layers in the dolomitic marbles. Similarly, secondary calcite, which should be a product of this reaction, is only locally present in small quantities within and adjacent to the talc-bearing marbles.

The replacement of silicate porphyroblasts by talc is common in the talc-bearing marbles, although this occurrence is volumetrically insignificant. In terms of their petrogenetic history, the most important observation is that olivine porphyroblasts are replaced by serpentine (in a characteristic mesh texture) and that the mats of serpentine, in turn, are replaced by talc (Fig. 7). Tremolite is replaced by talc, although all of the mineral reactants and products are not directly observed if one of the following reactions was operative:

$$\text{tremolite} + \text{dolomite} + H_2O + CO_2 = 2\ \text{talc} + 3\ \text{calcite}, \quad (2)$$

$$3\ \text{tremolite} + 6CO_2 + 2H_2O = 5\ \text{talc} + 6\ \text{calcite} + 4\ \text{quartz}, \quad (3)$$

and

$$\text{tremolite} + 4CO_2 = 2\ \text{dolomite} + \text{talc} + 4\ \text{quartz}. \quad (4)$$

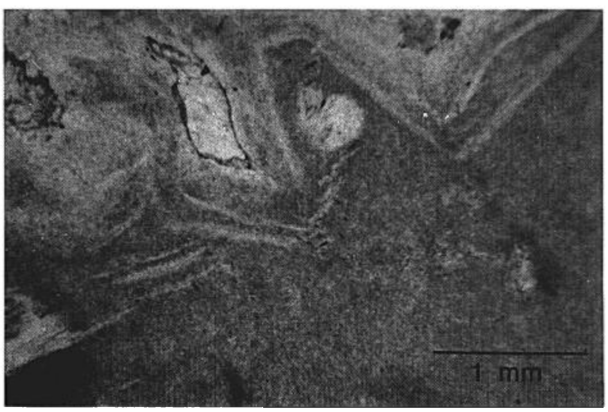

FIG. 6. Photomicrograph of massive fine-grained talc which has completely replaced dolomite. A single larger talc grain has formed in the fine-grained matrix. The outline of rhombohedral dolomite is preserved by the color bands in the talc matrix.

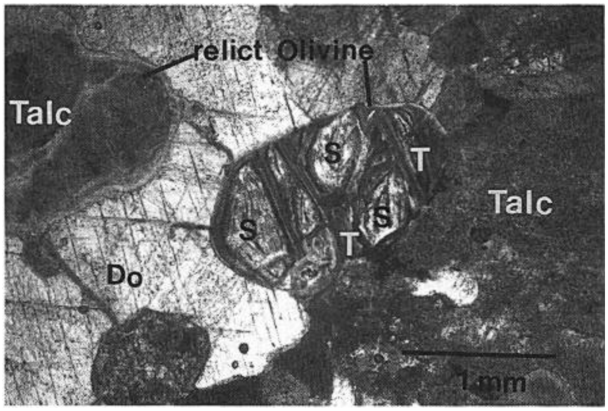

FIG. 7. Photomicrograph showing talc (T) pseudomorphs after serpentine (S) (which has previously replaced olivine). Talc occupies the ovoid mass in the upper left and the matrix on the right margin. The ovoid mass in the center is a pseudomorph of an olivine grain which has been replaced by serpentine; talc veins in this mass have subsequently replaced the serpentine. The carbonate matrix is dolomite (Do).

Puhan (1988) described the replacement of tremolite by talc and interpreted this occurrence as the result of reequilibration during the late decompressive stage of the clockwise P-T-t path of the Damara orogen. This mechanism of talc formation is not applicable in the Ruby Range because the characteristic jacket texture (quartz grains armored by dolomite as a result of the breakdown of tremolite + calcite to dolomite + quartz; Puhan, 1988) is not present. More important, the observation that serpentine precedes talc in the petrogenetic sequence provides the key evidence that talc formation occurred during a separate and distinct metamorphic cycle rather than at the retrograde stage of the earlier M_1 regional metamorphism. Phlogopite is also replaced by talc, but it is usually intergrown with chlorite that contains sagenitic rutile needles oriented at 60° to each other in pseudohexagonal symmetry.

In addition, talc occurs as botryoidal blebs which occur as open-space fillings within vugs lined by coarsely crystalline dolomite. Talc which occurs in this habit is interpreted to be a direct precipitate from hydrothermal solutions. Late-stage talc is also observed in scattered veinlets parallel to compositional layering, as small lenses in hinge zones of meter-scale open folds in marble (rare), and on joint and fracture surfaces.

The Sweetwater mine is similar to the other prospects studied in that it shows evidence of high-grade marbles being replaced by talc-bearing marbles, and in the geometry and distribution of the talc. However, it is unique because magnesite (detected by XRD analysis) is the dominant carbonate mineral. The mineral assemblage at the Sweetwater mine is magnesite-talc-chlorite. Also present are dolomite; relict phlogopite, serpentine, and tremolite; and accessory graphite and pyrite. Where magnesite is in contact with talc, grain boundaries are irregular and jagged, indicating formation of talc from magnesite. Quartz and calcite are present but occur in late-stage veins.

Quartz occurs as a secondary mineral in all of the talc-bearing marbles. Terminated crystals of quartz and rhombohedral dolomite occur in partially to completely filled vugs and in late-stage fractures which crosscut the foliation in the marbles. Quartz also occurs as thin layers along growth zones in the dolomite. The association of dolomite and quartz requires either lower temperature or lower $X_{(H_2O)}$ than that required for talc stability. This vug- and fracture-filling quartz indicates that SiO_2 must have been mobile at least in the latest stages of metamorphism. The numerous textural varieties of talc, such as wholesale talcification of dolomite and the occurrence of talc in vugs and in fractures, indicate that mobilization of silica also occurred at an earlier stage of the greenschist facies metamorphism when the system was within the talc stability field.

The talc-forming event is designated M_3 because talc formation occurred after dolomitization of the carbonate matrix and after serpentinization of olivine porphyroblasts. It is not possible, based on regional geologic relations, textural analysis, or ambiguous geochronologic studies, to determine if this is merely a late stage of the greenschist event (M_2) or yet another overprinted thermal metamorphism.

A summary of the petrogenetic history of the talc-bearing marbles is presented in Figure 8 based on field and petrographic observations. The protolith of the marbles can only be inferred but is most reasonably a siliceous dolomitic limestone. Primary quartz and dolomite were probably subordinate to calcite and were most likely consumed during prograde metamorphism at amphibolite to granulite conditions during M_1 (e.g., Garihan, 1973; Dahl, 1979; Karesevich et al., 1981). The high-grade marbles typically have a calcite-rich matrix and contain the silicate paragenesis olivine-phlogopite ± tremolite. Tremolite most likely has formed at different stages of M_1 as evidenced by its occurrence as porphyroblasts in the high-grade marble matrix, as well as in a fibrous habit in late-stage shears. Quartz is locally present in the high-grade marbles as relict cherty layers or as disharmonically folded quartz veins.

The talc-bearing marbles have formed as a result of a regional greenschist grade metamorphism that is only locally expressed as the selective replacement of the high-grade marbles. Dolomitization of the carbonate matrix occurred during M_2 and was accompanied by the replacement of olivine by serpentine and phlogopite by chlorite. The dominant occurrence of talc is as the replacement of dolomite. The replacement of serpentine by talc is of particular importance to the petrogenetic history because it precludes the possibility that talc simply formed during the retrograde path of M_1 and raises the possibility that some of the talc formed either at the latest stage of M_2 or perhaps even during another metamorphic event (M_3). Magnesite is only present at the Sweetwater mine. The Mg-rich bulk composition required for magnesite formation suggests that magnesite and dolomite formed as a result of extensive metasomatism of the original carbonates at the Sweetwater mine. Calcite and quartz occurrences are restricted to vein relationships, and the filling of vuggy cavities, during and after the major talc-forming events.

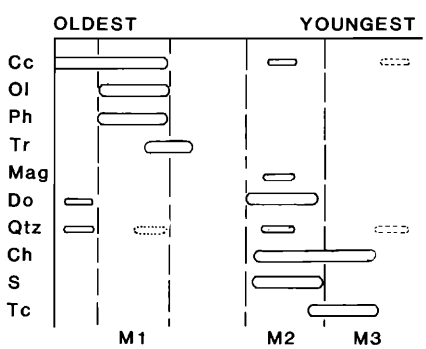

FIG. 8. Generalized paragenetic sequence representative of all six prospects examined. The larger symbols represent dominant minerals, smaller symbols are subordinate minerals, dashed symbols are minerals present in veins. Mineral abbreviations are: Cc = calcite, Ch = chlorite, Do = dolomite, Mag = magnesite, (Sweetwater mine only) Ol = olivine, Ph = phlogopite, Qtz = quartz, S = serpentine, Tc = talc, Tr = tremolite. M_1 is the regional amphibolite-granulite facies metamorphism, M_2 is the localized retrograde greenschist facies metamorphism, and M_3 is the latest stage talc-forming event. See text for full discussion.

Dillon Granite Gneiss and interlayered schists

The Dillon Granite Gneiss conformably surrounds marble bands throughout the Ruby Range. Bands of pelitic schist are conformably interlayered within the gneiss and marble layers. Schistose layers within talc-bearing marbles have locally been isoclinally folded. Centimeter- to meter-scale boudins of schist and gneiss occur in the marbles. The amphibolite- to granulite-grade assemblage plagioclase (An_{14-54})-amphibole (cummingtonite)-biotite-quartz is dominant in the gneisses and the assemblage oligoclase-K feldspar-quartz-biotite-garnet-sillimanite is characteristic of the schists.

Both the schist and gneiss have undergone varying degrees of retrogression. The most intense alteration is characteristically developed at the contacts between marble and gneiss (or schist) layers or boudins. The degree of alteration decreases with distance from marble-gneiss contacts. In almost all cases the alteration front separating amphibolite facies and greenschist facies assemblages is abrupt.

The most obvious effect of retrogression in the schists and gneisses is chloritization of garnet and biotite and sericitization of the feldspars. Chlorite formed by alteration of biotite commonly includes sagenitic rutile needles oriented at 60°. Serpentine, minor talc stringers, rare secondary quartz, and fine-grained sericite and calcite are also present in the alteration assemblage of the schist and gneiss. Carbonate occurs in the altered gneiss both as disseminated grains with sericite and in very fine veinlets, suggesting influx of carbonate-bearing fluids. Retrogression of the schists is recognized as either pervasive chloritization of schist lenses, or as 6- to 10-cm-thick chloritic selvages in schists where the schist is in contact with marble. Boudins of schist and gneiss within talc-bearing marbles commonly exhibit crenulated, chloritized rims. Centimeter-scale talc halos are common in marble immediately adjacent to schistose boudins.

The gneiss in and adjacent to the Sweetwater mine has excellently preserved textural relations which document the development of the chloritic alteration. Chloritic alteration of gneiss involves a chemical system different from alteration of dolomitic marble to talc. However, this process is analogous to that responsible for talc formation. Chloritization varies in intensity within the gneisses at the Sweetwater mine and is probably cogenetic with formation of magnesite and talc in intercalated marbles. Even the most intensely altered gneisses have a well-preserved relict (M_1) tectonite fabric, exhibiting foliation defined by changes in grain size, quartz ribbons, and ovoid plagioclase porphyroblasts (Fig. 9). However, the quartz ribbons have been completely replaced by talc and the plagioclase porphyroblasts have been completely replaced by magnesian chlorite (Fig. 10; chlorite analysis by Bernard Evans, pers. commun.). In these cases the talc- and chlorite-forming reactions have clearly occurred as a result of constant volume replacement processes.

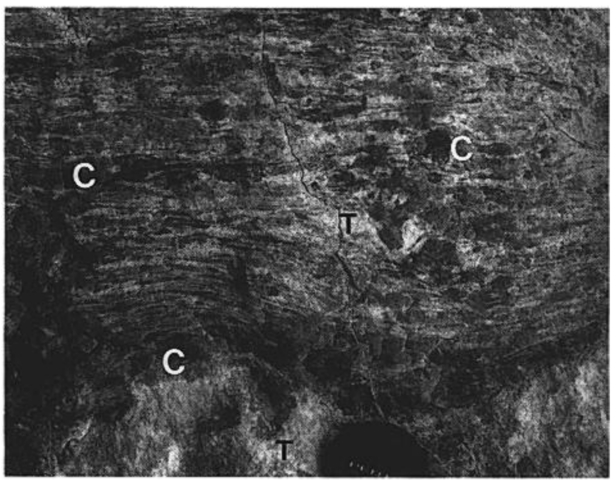

FIG. 9. Photograph of an outcrop at the Sweetwater mine showing complete replacement of the Dillon Granite Gneiss by M_2 greenschist facies minerals. The dark areas are chlorite rich (C) and the light bands are talc rich (T). Relict gneissic texture is preserved, and the larger chlorite-rich areas were once pegmatitic feldspar-rich patches. Preservation of these primary textures by talc and chlorite indicates constant volume replacement of the gneisses. The lens cap is 55 mm across.

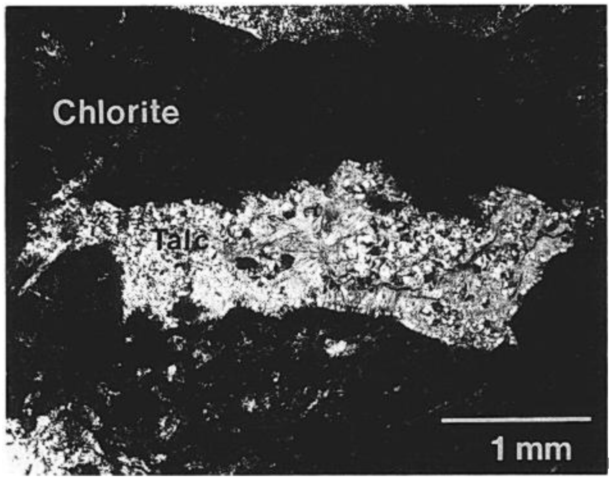

FIG. 10. Photomicrograph of talc bands (high birefringence) and chlorite (anomolous low-order birefringence) from the Dillon Granite Gneiss adjacent to the Sweetwater mine. The talc bands selectively replace quartz ribbons and the chlorite replaces feldspar-rich layers, mimicking the tectonite fabric of the gneiss.

Structure

Faults within the prospects examined are dominantly northwest striking, and steeply dipping. The latest movement on these faults postdates talc mineralization. Measurable offset of lithologic contacts ranges from 2 cm to 7 m. Structures which crosscut marble bands at high angles and predate talc formation have not been recognized in those areas examined. The dominant joint sets strike northwest and dip to the southwest. Joint and layering surfaces are typically coated by thin selvages of talc, chlorite, and iron oxide.

Deformation resulting from talc formation, in the form of faulting or distortion of layering, has not been noted on an outcrop scale. Also, structures which may have provided large-volume conduits for fluid movement are no longer recognizable. However, it is obvious that talc-forming fluids migrated at least in part along joints, compositional layering, fault surfaces, and lithologic contacts, as evidenced by thin selvages of talc and chlorite along these surfaces.

Structural control of talc formation is indicated by the localized and discontinuous nature of talc bodies parallel to the foliation in the marbles. The structures which controlled fluid movement during talc formation are inferred to have been parallel or subparallel to layering in the marbles. This conclusion is based upon the lack of crosscutting fractures which can be visually related to talc formation.

Whole-Rock Geochemistry

Twenty-seven samples of high-grade marble, talc-bearing marble, and talc were collected for whole-rock geochemical analysis using X-ray fluorescence (XRF). Where appropriate, samples of altered gneiss immediately adjacent to marbles and/or talc were also analyzed to determine how the nature of the alteration within the gneisses relates to that seen in the marbles. Chemical analyses are presented in Table 2.

Analyses for high-grade marble, talc-bearing marble, and talc are shown on a ternary CaO-MgO-SiO_2 diagram in Figure 11A. As shown in Figure 11B, the two marbles and monomineralic talc bodies occupy distinct fields with little, if any, compositional overlap. It is unlikely that differences in bulk composition between the two marbles are due to compositional variation between the protoliths of these rocks, and a protolith composition equivalent to that of pure end-member talc would be highly unusual and fortuitous. Compositions on the Mg-rich side of the diagram (Fig. 11A) are unusual in nature and are generally restricted to special environments of formation (e.g., evaporite deposits). In addition, the forsterite- and talc-bearing parageneses are dependent on the physical conditions of formation rather than being compositionally dependent (Fig. 11 C and D). These considerations, coupled with the textural evidence of selective retrogression of the high-grade marbles to form the talc-bearing marbles, support the argument of metasomatic processes during talc formation.

The compositional changes that have accompanied the replacement of high-grade marbles by talc-bearing marbles and massive talc bodies are indicated by two distinct trends indicated by arrows in Figure 11B. The first trend (Fig. 11B) marks the transition from high-grade to talc-bearing marble. This transition involves an increase in MgO, marked by increased MgO/CaO ratios, with little apparent introduction of SiO_2. Increased MgO values in talc-bearing marble are interpreted to be the result of dolomitization which post-dates amphibolite-grade metamorphism. This interpretation is in agreement with microscopic carbonate textures which indicate that calcite in the high-grade marbles has been replaced by dolomite in the talc-bearing marbles.

The second trend shown in Figure 11B marks the transition from talc-bearing marble to massive talc bodies. Many of the talc-bearing marbles which exhibit only incipient talc formation have inherited an initial low SiO_2 content from the high-grade marbles, and their bulk compositions lie close to the composition of dolomite due to the pervasive nature of the dolomitization of the matrix. Talc-bearing marbles that exhibit higher degrees of talcification lie on a linear chord that originates near the composition of dolomite and trends toward the composition of talc. The analyses of the massive talc bodies are slightly more siliceous than the composition of end-member talc; the higher silica values can be accounted for by the presence of small amounts of chalcedony and quartz veins in the massive talc bodies. The SiO_2/MgO ratio increases systematically along this chord in the talc-bearing marble field, suggesting introduction of large quantities of SiO_2 to form talc. This interpretation suggests that the fluid phase controlled the mineralogy of the system during talc formation by the process of infiltration (Rice and Ferry, 1982), with the amount of introduced SiO_2 acting as one of the limiting components of talc formation from precursor dolomitic marble. This interpretation is similar to conclusions drawn during previous studies (Okuma, 1971; Garihan, 1973; Olson, 1976; Berg, 1979; Walton, 1981; Piniazkiewicz, 1984).

It is interesting to note that the slope of the trend from talc-bearing marbles to talc crosses MgO/SiO_2 isopleths at a relatively high angle, in contrast to the approximately parallel trend line-isopleth relationship noted for the high-grade to talc-bearing transition. These relationships suggest the possibility that two periods of fluid flux occurred. Alternatively, differing MgO/SiO_2 ratios may have resulted from compositional changes in the fluid phase during a single prolonged period of fluid flux, which could have caused this transition, followed by the transformation of talc-bearing marble to form massive talc. In either case, textural evidence cited above indicates that dolomitization occurred, in part, prior to the formation of talc. A third possible trend, the direct transition of high-grade marble to talc, is not considered likely due to lack of macroscopic and microscopic evidence supporting such an interpretation.

Geochemistry of gneiss

The whole-rock geochemistry of the gneiss in the Sweetwater mine is particularly useful for deciphering metasomatic processes associated with talc formation. Efforts were made to ensure that samples were taken from the same compositional layer to minimize variations caused by primary chemical heterogeneity between layers. Changes in the chemistry of the gneiss from the Sweetwater mine (Table 2) indicate that approximately one-half of the total SiO_2 present in the least altered gneiss was removed during transformation to intensely chloritized gneiss, and that substantial quantities of Mg^{+2} were added. These changes result in an end product of gneiss with a bulk composition similar to that of magnesian chlorite (X_{Mg} = 0.99; analysis by B. Evans, pers. commun.).

TABLE 2. Whole-Rock Geochemical Analyses (XRF) of High-Grade Marble

A. High-grade marble

	AB-71	AP-36	AS-68	ASW-18	AT-28	AT-31	AR-49
SiO_2	13.30	7.88	1.03	3.78	3.48	5.81	14.20
Al_2O_3	0.32	0.18	0.13	0.14	0.52	0.19	<0.01
CaO	34.20	50.50	30.00	29.00	29.40	34.00	36.50
MgO	16.60	2.61	21.20	21.30	20.40	17.30	14.10
Na_2O	<0.01	<0.01	<0.01	<0.01	<0.01	<0.01	<0.01
K_2O	0.13	0.06	0.03	0.03	0.04	0.04	0.03
Fe_2O_3	0.63	0.44	1.50	0.86	1.11	0.70	0.95
MnO	0.74	0.63	0.84	0.75	1.00	0.73	0.77
TiO_2	0.03	<0.01	0.02	0.02	0.04	0.01	<0.01
P_2O_5	0.02	0.02	0.04	0.02	0.02	0.02	0.02
Cr_2O_3	<0.01	<0.01	<0.01	<0.01	<0.01	<0.01	<0.01
L.O.I.	34.00	37.50	45.20	44.60	44.50	41.70	33.40
Sum	98.97	99.82	99.99	100.50	100.51	100.50	99.97

B. Talc-bearing marble

	AB-65	AB-70	AP-37	AS-69	AS-70	ASW-19	AT-23
SiO_2	14.00	17.70	6.64	8.33	4.88	4.97	5.15
Al_2O_3	0.25	0.41	0.52	0.22	0.48	0.15	0.49
CaO	23.40	24.10	27.40	26.60	28.00	0.55	27.40
MgO	24.00	21.40	22.90	23.00	22.30	49.00	21.20
Na_2O	<0.01	<0.01	<0.01	<0.01	<0.01	<0.01	<0.01
K_2O	0.04	0.04	0.03	0.03	0.04	0.03	0.04
Fe_2O_3	1.20	1.40	0.92	1.44	1.08	1.96	3.18
MnO	0.10	0.28	0.27	0.45	0.56	0.22	0.88
TiO_2	0.03	0.02	0.04	0.01	0.04	0.03	0.03
P_2O_5	0.02	0.02	0.02	0.02	0.03	0.03	0.02
Cr_2O_3	<0.01	<0.01	<0.01	<0.01	<0.01	<0.01	<0.01
L.O.I.	37.40	35.00	41.80	40.50	42.80	43.30	42.20
Sum	100.44	100.37	100.31	100.24	100.54	100.60	100.59

	AT-24	AT-25	AT-26	AR-30	AR-33	AR-34	AR-37
SiO_2	2.63	5.35	8.13	3.04	14.50	22.30	11.60
Al_2O_3	0.14	0.42	0.24	0.04	<0.01	0.01	0.62
CaO	29.50	27.60	26.30	25.50	23.80	19.30	18.70
MgO	21.40	22.00	21.30	25.40	24.00	25.50	28.30
Na_2O	<0.01	<0.01	<0.01	<0.01	<0.01	<0.01	<0.01
K_2O	0.03	0.04	0.04	0.03	0.04	0.04	0.04
Fe_2O_3	1.64	1.51	3.20	0.95	1.00	1.54	1.46
MnO	0.91	0.88	0.84	0.12	0.60	0.17	0.15
TiO_2	0.01	0.03	0.02	0.02	0.01	0.02	0.05
P_2O_5	0.02	0.02	0.02	0.02	0.02	0.02	0.02
Cr_2O_3	<0.01	<0.01	<0.01	<0.01	<0.01	<0.01	<0.01
L.O.I.	44.20	42.40	40.20	45.20	36.50	31.50	39.50
Sum	100.48	100.25	100.29	100.32	100.47	100.40	100.44

Chloritization of gneiss is interpreted to have resulted from addition of Mg^{+2} to the system under greenschist-grade conditions. This Mg^{+2} enrichment may explain coeval magnesite formation in the adjacent marbles, which is unique to this prospect. Chloritization of the gneisses resulted in SiO_2 depletion. This SiO_2, once removed from the gneisses, would then be available for talc formation or quartz veining in adjacent marbles by the process of mass transfer across lithologic boundaries. If MgO is present in excess, as suggested by the presence of magnesian chlorite and magnesite, it would appear that SiO_2 is the limiting component of talc formation in this prospect.

Physical Conditions of Talc Formation

The talc stability field is fairly well defined in terms of pressure (P), temperature (T), and mole fraction CO_2 (X_{CO_2}) of the fluid phase based on the experi-

TABLE 2. (*Cont.*)

C. Massive talc bodies

	AB-67	AP-39	AS-71	ASW-21	AT-21	AR-35
SiO_2	60.00	59.00	58.50	60.10	59.90	60.50
Al_2O_3	0.46	1.20	1.02	0.55	0.09	0.03
CaO	0.15	0.17	0.08	0.30	0.01	0.13
MgO	32.20	32.10	31.80	32.50	27.80	31.70
Na_2O	<0.01	<0.01	<0.01	0.05	<0.01	<0.01
K_2O	0.03	0.03	0.04	0.01	0.03	0.04
Fe_2O_3	0.44	0.78	0.83	0.27	6.80	1.02
MnO	0.01	0.01	0.01	0.01	0.01	0.05
TiO_2	0.04	0.07	0.07	0.04	0.02	0.02
P_2O_5	0.02	0.09	0.01	0.17	0.02	0.02
Cr_2O_3	<0.01	<0.01	<0.01	<0.01	<0.01	<0.01
L.O.I.	6.08	6.31	6.08	5.70	4.93	5.47
Sum	99.43	99.76	98.44	99.71	99.61	98.98

D. Gneisses from a single gneissic layer at the Sweetwater mine

	ASW-16	ASW-15	ASW-17
SiO_2	33.00	71.40	74.10
Al_2O_3	18.10	13.60	14.40
CaO	0.24	0.38	0.53
MgO	35.00	6.13	0.13
Na_2O	<0.01	<0.01	3.75
K_2O	0.05	3.14	5.00
Fe_2O_3	0.71	0.33	1.05
MnO	0.02	0.02	0.02
TiO_2	0.03	0.03	0.05
P_2O_5	0.02	0.01	0.10
Cr_2O_3	0.01	<0.01	0.01
L.O.I.	13.20	4.16	0.39
Sum	99.30	100.37	99.53

Sample ASW-17 is a relatively unaltered gneiss, ASW-15 is partially altered, and ASW-16 has been completely altered to talc and chlorite

Area designators are: AB = Bosal prospect, AP = Pope prospect, AR = Ruby View prospect, AS = Spring Creek prospect, AS = Spring Creek prospect, ASW = Sweetwater mine, AT = T.P. prospect

mental studies of Gordon and Greenwood (1970), Skippen (1971, 1974), Slaughter et al. (1975), and Eggert and Kerrick (1981). Talc phase relations are represented on the isobaric T-X_{CO_2} diagram in Figure 12 (after Evans and Guggenheim, 1988, calculated from the thermochemical data of Berman, 1988 and applying the modified Redlich-Kwong expression for nonideal mixing of H_2O-CO_2 of Kerrick and Jacobs, 1981).

There is no mineralogic geobarometer presently applicable for the M_3 talc-forming metamorphism, but two observations place a maximum limit on pressure estimates. Regional geologic relationships suggest that the crystalline rocks of the Ruby Range were exposed at the surface during the middle Proterozoic (Harrison et al., 1974); this is the most probable time of talc formation (presented below). In addition, the interpretation that talc formed by constant volume processes suggests that the reaction took place in host rocks which provided a rigid framework; again, this suggests that talc formation occurred at relatively shallow crustal levels, and certainly above the brittle-ductile transition in the crust. A maximum pressure of 2 kbars (corresponding to a crustal level of 6 km or less) is estimated for this system. There is some dispute about the effect of pressure on the talc stability field. Recent experimental studies by Eggert and Kerrick (1981) suggest that the talc stability field contracts at higher pressures, so the isobaric T-X_{CO_2} relations calculated at 2 kbars should nearly encompass the widest range of physical conditions for talc formation.

Direct temperature estimates, based on calcite-dolomite geothermometry, are suspect because of the complex history of recrystallization, exsolution, and replacement in the carbonate rocks (e.g., M_2 dolomite is not in equilibrium with M_1 calcite, nor with calcite in later stage veins). A maximum temperature limit

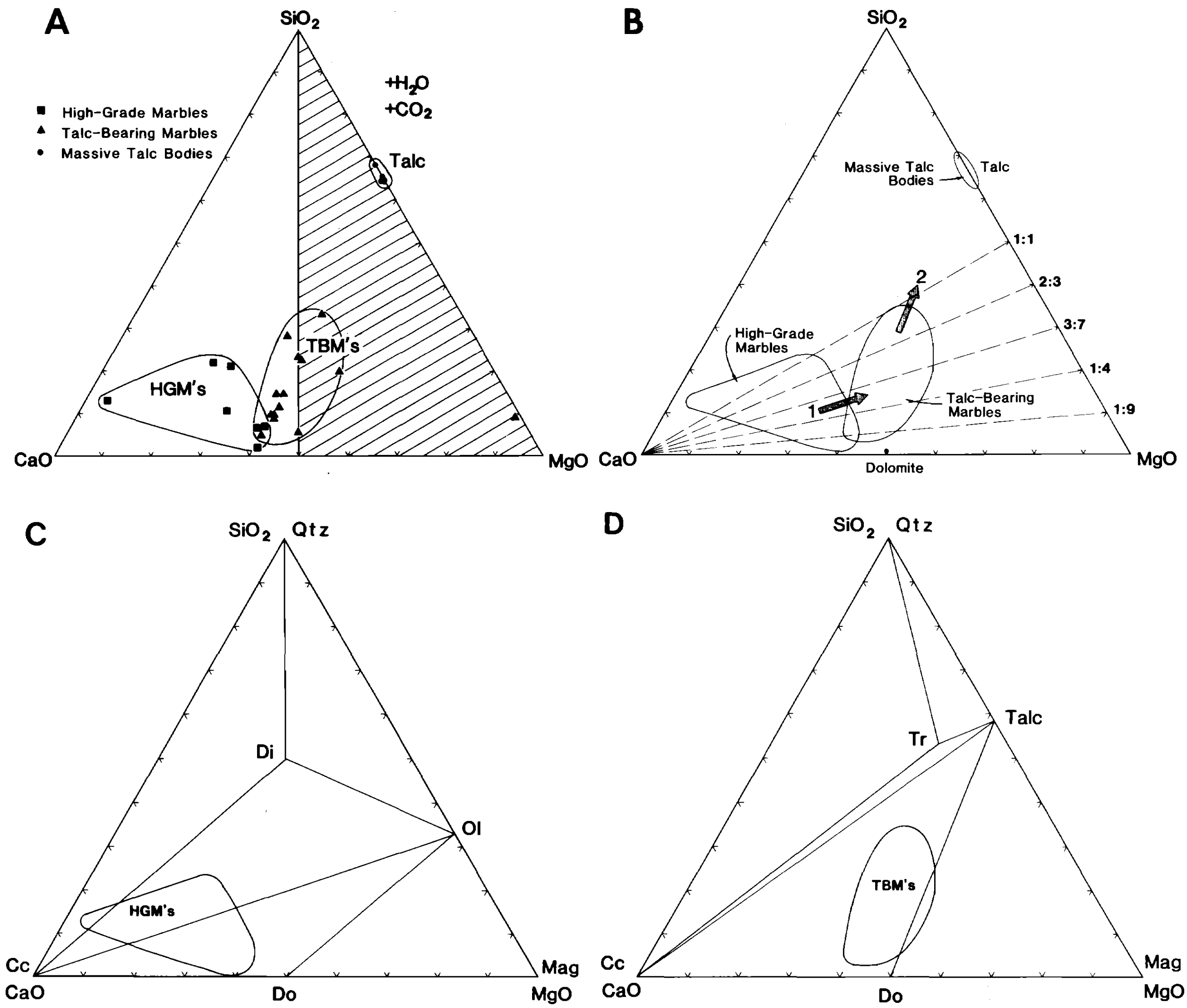

FIG. 11. CaO-MgO-SiO_2 ternary diagram showing the composition of high-grade marbles (squares), talc-bearing marbles (triangles), and massive talc bodies (circles). A. Primary compositions on the Mg-rich side of the diagram (stippled area). These are unusual in nature. B. Compositional fields occupied by high-grade marbles, talc-bearing marbles and massive talc bodies. Arrow 1 denotes the trend from high-grade to talc-bearing marble during the dolomitization stage; note the increase in MgO content without a large increase in SiO_2. Arrow 2 denotes the trend from dolomite-rich talc-bearing marbles to massive talc bodies; these marbles generally lie on a linear trend from dolomite to talc, indicating progressive increase in the amount of SiO_2 in them. The dashed lines are isopleths that define constant SiO_2/MgO ratios. C and D. Chemographies showing phase relations for the high-grade marbles, talc-bearing marbles; differences in their parageneses are due to changes in physical conditions rather than bulk compositional effects.

can be determined by examination of the stability of talc on the T-X_{CO_2} diagram. Assuming a binary mixture of H_2O-CO_2 the maximum temperature at which talc can form is approximately 460°C with X_{CO_2} = 0.45 at 2-kbar fluid pressure.

Isobaric univariant reactions, such as those represented in Figure 12 are mineralogic fluid buffers that can be used to determine the T-X_{CO_2} relations during prograde metamorphism (Skippen, 1971, 1974; Greenwood, 1975; Rice, 1977a and b; Ferry and Burt, 1982; Rice and Ferry, 1982; Flowers and Helgeson, 1983). However, the talc deposits of the Ruby Range characteristically exhibit high variance mineral assemblages; indeed, no talc-forming, fluid-buffering assemblages have been documented in any of the prospects studied. The lack of buffering assemblages has two important implications. First, the composition of the fluid phase is externally controlled by an infiltration mechanism. The large influx of water required to introduce SiO_2 and Mg^{+2} in the constant-volume

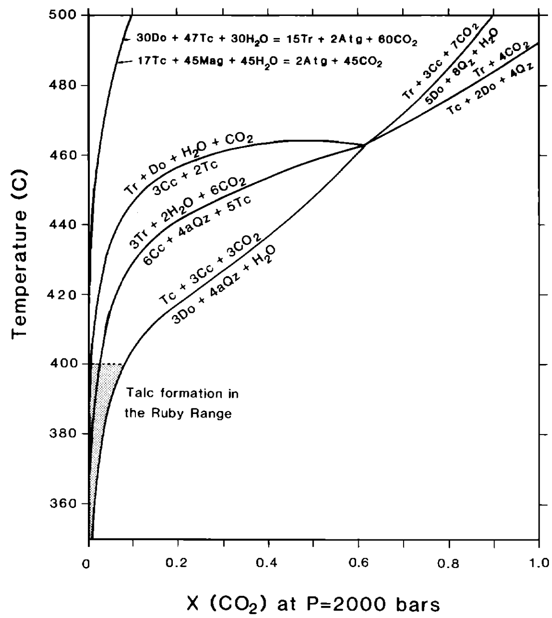

FIG. 12. Isobaric temperature-X_{CO_2} diagram showing the stability field of talc (stippled area) at P_{fluid} = 2 kbars (from Evans and Guggenheim, 1988). The bundle of curves can represent the talc stability for most of the deposits in the Ruby Range; the talc-magnesite and talc-dolomite curves (superposed) in the upper left part of the diagram represent phase relations for the Sweetwater mine. The interpreted conditions of talc formation in the Ruby Range is stippled. See text for further discussion. Mineral abbreviations are: aQz—alpha quartz, Atg—antigorite, Cc—calcite, Do—dolomite, Mag—magnesite, Tc—talc, Tr—tremolite.

talc-forming reaction would effectively dilute any liberated CO_2 so that X_{CO_2} approaches 0. For the case of pure dolomite being completely replaced by talc according to reaction (1), and using the minimum calculated fluid flux (see below), X_{CO_2} = 0.0008. Second, the limiting reactions involving talc and dolomite are assymptotic to the ordinate of the T-X_{CO_2} diagram at low temperatures. Therefore, at sufficiently low values of X_{CO_2} talc formation can occur at much lower temperatures.

The stability field of talc may be affected by other factors such as changes in pressure (e.g., Skippen, 1971, 1974; Slaughter et al., 1975; Eggert and Kerrick, 1981), the composition of talc (specifically X_{Mg} and X_F; e.g., Valley et al., 1982; Abercrombie et al., 1987), and nonideal behavior of H_2O-CO_2-NaCl solutions (Bowers and Helgeson, 1983). We expect that changes in the talc stability field due to the pressure effect will be minimal at pressures of less than 2 kbars. The composition of the talc at the Sweetwater mine is very near the pure end member with respect to Mg (X_{Mg} = 0.994; analysis by B. Evans, pers. commun.); analyses of F in the talc of the Ruby Range are currently not available. We have no direct evidence for the presence of NaCl or other dissolved components in this system (e.g., freezing point depression of fluid inclusions, presence of NaCl daughter salts). There are no fluid inclusions in the talc (phyllosilicates typically are devoid of inclusions) and the fluid inclusions in the carbonates are difficult to interpret due to multiple generations, potential for leakage along cleavage planes, or reequilibration during recrystallization of the host carbonates.

The inferred conditions for talc formation in the Ruby Range are shaded in Figure 12. Most of the talc prospects of the Ruby Range can be represented by the talc-calcite curves in this figure, and the talc-magnesite relations are added to represent the unique occurrence at the Sweetwater mine. Our best estimates for the physical conditions of talc formation in the Ruby Range are P < 2 kbars, T < 400°C and probably much lower, and $X_{CO_2} = 10^{-4}$.

Mass Balance and Fluid Flux Calculations

The results of mass balance and fluid flux calculations are presented in Table 3. These calculations are based on the assumptions that reaction (1) is the dominant talc-forming reaction; talc formation is a constant volume process in this system; and Mg^{+2}, SiO_2, and H_2O must be introduced and Ca^{+2} removed from the system. These assumptions are in accord with field and petrographic observations presented above. The conversion of 1 m^3 of the average high-grade marble composition to talc requires the addition of 1,170 kg of SiO_2 and 194 kg of Mg^{+2} and the removal of 2,083 kg of calcite. These compositional changes are integrated over the entire talc-forming process, from high-grade marbles (which probably underwent near-isochemical metamorphism during M_1), through dolomitization, development of talc-bearing marbles, and finally, formation of massive talc bodies.

The minimum fluid flux through the system can be estimated based on the experimentally determined solubilities of SiO_2 (Walther and Orville, 1983) and $CaCO_3$ (Fein and Walther, 1987). Given the total mass of silica required to transform the average high-grade marble to talc (1,170 kg/m^3, from above) and the solubility of SiO_2 at the temperature and pressure of interest (400°C and 2 kbars), the minimum fluid flux is 4.80×10^5 l of water/m^3. At 400°C and 2 kbars this volume of water corresponds to a volumetric water/rock ratio of 600 (data from Burnham et al., 1969).

The solubility of calcite at the specified conditions is considerably lower than the solubility of quartz. The removal of 2,083 kg of calcite (for the average high-grade marble composition) from the system requires 1.47×10^8 l/m^3 of pure water, corresponding to a volumetric water/rock ratio of 1.86×10^5. The water-rock ratios determined from calcite solubility data are extremely high and may be moderated if the solubility is increased by some other factor such as the presence of CO_2 in solution or changes in pH. If X_{CO_2} = 0.02 the solubility of calcite increases (Fein and Walther, 1987); the replacement of the average

TABLE 3. Results of Mass Balance and Fluid Flux Calculations

Mass balance—conversion of 1 m^3 dolomite or average high-grade marble to talc

	Mg^{+2} (kg)	SiO_2 (kg)	Calcite (kg)	Talc (m^3)	Volume (%)
Mg conserved					
model reaction (1)		(+)1,245	(−)1,556	0.706	(−)29
Constant volume					
Model reaction (1)	(+)157	(+)1,764	(−)1,556	1	
High-grade marble average	(+)194	(+)1,170	(−)2,083	1	

Minimum fluid flux in l/m^3 and volumetric water/rock ratio (W/R), (calculated at 400°C, 2 kbar)[1]

	SiO_2	W/R	Calcite	W/R	Calcite ($a_{CO_2} = 0.02$)	W/R
Model reaction (1)	7.0×10^5	890	1.1×10^8	1.4×10^5	4.0×10^7	5.0×10^5
High-grade marble average	4.8×10^5	607	1.5×10^8	1.9×10^5	5.4×10^7	6.8×10^5

[1] These conditions should provide a limit for the maximum solubility of SiO_2 in this system, and therefore, a minimum fluid flux; solubility data are from Walther and Orville (1983) for SiO_2, from Fein and Walther (1987) for calcite, volume data for water are from Burnham et al. (1969), and mineral volume data are from Robie et al. (1979)

high-grade marble by talc will require 5.35×10^7 l/m^3 (or 6.76×10^4 W/R ratio). We have no independent estimate of the pH of these solutions, but some qualitative evidence is available. Sulfur may be a component in the solutions because accessory pyrite is found in some of the talc bodies. It is not likely that the solutions were extremely acidic due to the presence of accessory graphite. It is possible that dilute sulfuric, hydrochloric, or carbonic acids were present in the system. Even a minor decrease in the pH of the fluids would significantly decrease the calculated water/rock ratios. In the absence of hard constraints on calcite solubility in this system, we suggest that the minimum fluid flux in the system is best estimated by the SiO_2 solubility data and that a minimum estimate of the volumetric water/rock ratio is 600.

Timing of Talc Formation

Talc mineralization in the Ruby Range occurred during the middle Proterozoic, as interpreted from the overprinting of high-grade assemblages in Archean marbles (ca. 2,750 Ma, James and Hedge, 1980), and the lack of talc deposits in spatially related Phanerozoic siliceous carbonate rocks (e.g., Garihan, 1973; Tysdal, 1976). A regional retrograde thermal metamorphism dated at 1,600 Ma (Giletti, 1966) and emplacement of mafic dikes at 1,455 Ma and 1,130-1,120 Ma (Wooden et al., 1978) are the most likely thermal events that could be responsible for talc formation. These thermal events can be related to continent-scale orogenic events: accretion of arc-type terranes (1,780-1,630 Ma), extension associated with granite-rhyolite terranes (1,500-1,340 Ma), and extension associated with the Grenville orogeny (1,100 Ma; Bickford et al., 1986). In addition, a higher geothermal gradient may have developed during extensional tectonics associated with the opening of the Belt basin (Schmidt and Garihan, 1986). The age of talc mineralization is middle Proterozoic, but the absolute age is only poorly bracketed by the age limits of 1,600 to 1,100 Ma.

Summary and Conclusions

The petrogenesis and timing of talc formation in the Ruby Range, southwestern Montana, have been determined using field relations, detailed mapping and petrography, and geochemical considerations. These studies have resulted in the following conclusions:

1. The occurrence of the talc deposits is restricted to Archean high-grade calcitic marbles that have been overprinted by dolomitization and a greenschist facies metamorphic event. Talc was formed in a constant volume process by replacement of dolomite and all earlier greenschist facies silicate minerals.
2. Talcification of the dolomitic marbles requires the metasomatic introduction of SiO_2, Mg^{+2}, and H_2O, and the removal of large amounts of $CaCO_3$. This is the dominant talc-forming process in the Ruby Range and may be a common mechanism in other carbonate-replacement deposits (e.g., Waterboro, Alabama; Blount and Vassiliou, 1980).
3. The composition of the metasomatic fluids is externally controlled due to the absence of mineralogic fluid buffer assemblages. To mobilize sufficient SiO_2 to form talc from the high-grade marbles, a minimum of 4.80×10^5 l of water/m^3 of dolomite must be flushed through the system (a volumetric water/rock ratio of 600). This fluid flow is localized in layer-parallel fractures in the marble. The tremendous volumes of water passing through the system are sufficient to dilute X_{CO_2} to the point where it is effectively equal to zero.

4. Talc formation is interpreted as a near-surface process. This interpretation is based, in part, on the requirement of constant volume during talc formation. A maximum temperature of 450°C and maximum pressure of 2 kbars are considered likely for the formation of talc in this system. However, low X_{CO_2} values would permit talc-forming reactions to occur at much lower temperatures. Calcite as a product of talc-forming reactions has not been observed and was most likely removed from the system. The constriction of the talc stability field as a function of increasing pressure suggests that talc bodies large enough to be orebodies will be favored by a low-pressure environment of formation. Extremely water-rich solutions, formation of talc at relatively low temperatures, and removal of $CaCO_3$ from the talc-forming environment may indicate a relationship between talc mineralization and formation of surficial hot spring deposits.

5. The source of the large volumes of water and Mg^{+2} remains problematic, although numerous Mg-rich talc and chlorite deposits occur in the Archean rocks throughout southwest Montana (Berg, 1979). Harrison et al. (1974) have postulated an open seaway just to the west of the Dillon block during the opening of the Belt basin. It is possible that locally Mg-rich seawater, driven by thermal anomolies, could have penetrated the Archean basement along structurally controlled pathways to replace marble and gneiss with talc and chlorite deposits.

6. Talc formation clearly postdates the regional dynamothermal metamorphism that occurred in the Archean and predates the deposition of Phanerozoic sedimentary cover. A protracted period of thermal events is recorded between 1,600 and 1,100 Ma as determined by the resetting of K-Ar isotope ages and the emplacement of mafic dikes. These thermal pulses may be related to regional extension in the middle Proterozoic during opening of the Belt basin.

Acknowledgments

Funding for this study was provided by the Cyprus Industrial Minerals Company. Special thanks are extended to Howard M. Harlan II for support and encouragement throughout the project and to Robert J. Piniazkiewicz for his review of an early version of this manuscript. This article is a condensation of an M.S. thesis completed at Montana State University. We wish to thank Bernard Evans for providing preliminary microprobe analyses of talc and chlorite and for a critical review of this paper. Discussions with Mark Ghiorso helped with the mass balance calculations. Two anonymous *Economic Geology* reviews greatly improved the quality of the text. Any persisting errors are the responsibility of the authors. Preparation of this manuscript was supported by National Science Foundation grant EAR-86-18327.

March 15, 1988; November 2, 1989

REFERENCES

Abercrombie, H. J., Skippen, G. B., and Marshall, D. D., 1987, F-OH substitution in natural tremolite, talc, and phlogopite: Contr. Mineralogy Petrology, v. 97, p. 305–312.

Anderson, D. L., 1987, Timing and mechanism of formation of selected talc deposits in the Ruby Range, southwestern Montana: Unpub. M.S. thesis, Bozeman, Montana State University, 90 p.

Berg, R. B., 1979, Talc and chlorite deposits in Montana: Montana Bur. Mines Geology Mem. 45, 66 p.

Bergantino, R. N., and Clark, M. C., 1985, Structure contour map on the top of Precambrian crystalline rocks, Montana: Montana Bur. Mines Geology Open-File Rept. 158.

Berman, R. B., 1988, Internally consistent thermodynamic data for minerals in the system Na_2O-K_2O-CaO-MgO-FeO-Fe_2O_3-Al_2O_3-SiO_2-TiO_2-H_2O-CO_2: Jour. Petrology, v. 29, p. 445–522.

Bickford, M. E., Van Schmus, W. R., and Zietz, I., 1986, Proterozoic history of the midcontinent region of North America: Geology, v. 14, p. 492–496.

Blount, A. M., and Vassiliou, A. H., 1980, The mineralogy and origin of the talc deposits near Winterboro, Alabama: ECON. GEOL., v. 75, p. 107–116.

Bowers, T. S., and Helgeson, H. C., 1983, Calculation of the thermodynamic and geochemical consequences of nonideal mixing in the system H_2O-CO_2-NaCl on phase relations in geological systems. Metamorphic equilibria at high pressures and temperatures: Am. Mineralogist, v. 68, p. 1059–1075.

Boyce, R. L., 1975, Depositional systems in the LaHood Formation, Belt Supergroup, Precambrian, southwestern Montana: Unpub. Ph.D. dissert., Univ. Texas at Austin, 247 p.

Brown, C. E., 1973, Talc: U. S. Geol. Survey Prof. Paper 820, p. 619–626.

Burnham, C. W., Holloway, J. R., and Davis, N. F., 1969, Thermodynamic properties of water to 1000°C and 10,000 bars: Geol. Soc. America Spec. Paper 132, 96 p.

Chidester, A. H., Engel, A. E. J., and Wright, L. A., 1964, Talc resources of the United States: U. S. Geol. Survey Bull. 1167, 61p.

Dahl, P., 1979, Comparative geothermometry based on major element and oxygen isotope distributions in Precambrian metamorphic rocks from southwestern Montana: Am. Mineralogist, v. 64, p. 1280–1293.

Desmarais, N. R., 1981, Metamorphosed Precambrian ultramafic rocks in the Ruby Range, Montana: Precambrian Research, v. 16, p. 67–101.

Eggert, R. G., and Kerrick, D. M., 1981, Metamorphic equilibria in the siliceous dolomite system: 6 kbar experimental data and geologic implications: Geochim. et Cosmochim. Acta, v. 45, p. 1039–1049.

Evans, B. W., and Guggenheim, S., 1988, Talc, pyrophyllite, and related minerals: Reviews Mineralogy, v. 19, p. 225–294.

Fein, J. B., and Walther, J. V., 1987, Calcite solubility in supercritical CO_2-H_2O fluids: Geochim. et Cosmochim. Acta, v. 51, p. 1665–1673.

Ferry, J. M., and Burt, J. M., 1982, Characterization of metamorphic fluid composition through mineral equilibria: Reviews Mineralogy, v. 10, p. 207–262.

Flowers, G. C., and Helgeson, H. C., 1983, Equilibrium and mass transfer during progressive metamorphism of siliceous dolomites: Am. Jour. Sci., v. 283, p. 230–286.

Garihan, J. M., 1973, Geology and talc deposits of the central Ruby Range, Madison County, Montana: Unpub. Ph.D. dissert., Pennsylvania State Univ., 209 p.

Giletti, B., 1966, Isotopic ages from southwestern Montana: Jour. Geophysical Research, v. 71, p. 4029–4036.

Gordon, T. M., and Greenwood, H. J., 1970, The reaction: Dolomite + quartz + water = talc + calcite + carbon dioxide: Am. Jour. Sci., v. 268, p. 225–242.

Greenwood, H. J., 1975, Buffering of pore fluids by metamorphic reactions: Am. Jour. Sci., v. 275, p. 573–593.

Harrison, J. E., Griggs, A. B., and Wells, J. D., 1974, Tectonic features of the Precambrian Belt basin and their influence on post-Belt structures: U. S. Geol. Survey Prof. Paper 866, 15 p.

James, H. L., and Hedge, C. E., 1980, Age of the basement rocks of southwest Montana: Geol. Soc. America Bull., v. 91, p. 11–15.

Karasevich, L. P., Garihan, J. M., Dahl, P. S., and Okuma, A. F., 1981, Summary of Precambrian metamorphic and structural history, Ruby Range, southwest Montana: Geol. Soc. Montana 1981 Field Conf. Guidebook, p. 225–237.

Kerrick, D. M., and Jacobs, G. K., 1981, A modified Redlich-Kwong equation for H_2O, CO_2 and H_2O-CO_2 mixtures at elevated pressures and temperatures: Am. Jour. Sci., v. 281, p. 735–767.

McMannis, W. J., 1963, LaHood Formation—a coarse facies of the Belt Series in southwestern Montana: Geol. Soc. America Bull., v. 74, p. 407–436.

Okuma, A. F., 1971, Structure of the southwestern Ruby Range near Dillon, Montana: Unpub. Ph.D. dissert., Pennsylvania State Univ., 122 p.

Olson, R. H., 1976, The geology of Montana talc deposits: Montana Bur. Mines Geology Spec. Pub. 74, p. 99–143.

Piniazkiewicz, R. J., 1984, Geology and exploration techniques for pre-Beltian talc on the Malesich Ranch, Ruby Range, Madison County, Montana: Unpub. M.S. thesis, Univ. Arizona, 101 p.

Puhan, D., 1988, Reverse age relations of talc and tremolite deduced from reaction textures in metamorphosed siliceous dolomites of the southern Damara orogen (Namibia): Contr. Mineralogy Petrology, v. 98, p. 24–27.

Rice, J. M., 1977a, Progressive metamorphism of impure dolomitic limestone in the Marysville aureole, Montana: Am. Jour. Sci., v. 277, p. 1–24.

—— 1977b, Contact metamorphism of impure dolomitic limestone in the Boulder aureole, Montana: Contr. Mineralogy Petrology, v. 59, p. 237–259.

Rice, J. M., and Ferry, J. M., 1982, Buffering, infiltration, and the control of intensive variables during metamorphism: Rev. Mineralogy, v. 10, p. 263–326.

Robie, R. A., Hemingway, B. S., and Fisher, J. R., 1979, Thermodynamic properties of minerals and related substances at 298.15 K and 1 bar pressure and at higher temperatures: U. S. Geol. Survey Bull. 1452, 456 p.

Schmidt, C. J., and Garihan, J. M., 1983, Laramide tectonic development of the Rocky Mountain foreland of southwestern Montana, *in* Lowell, J. D., ed., Rocky Mountain foreland basins and uplifts: Denver, Rocky Mountain Assoc. Geologists, p. 271–294.

—— 1986, Middle Proterozoic and Laramide tectonic activity along the southern margin of the Belt basin: Montana Bur. Mines Geology Spec. Pub. 94, p. 217–235.

Skippen, G., 1971, Experimental data for reactions in siliceous marbles. Jour. Geology, v. 79, p. 457–481.

—— 1974, An experimental model for low pressure metamorphism of siliceous dolomitic marble: Am. Jour. Sci., v. 274, p. 487–509.

Slaughter, J., Kerrick, D. M., and Wall, V. J., 1975, Experimental study of equilibria in the system CaO-MgO-SiO_2-H_2O-CO_2: Am. Jour. Sci., v. 275, p. 143–162.

Tysdal, R. G., 1976, Geologic map of northern part of Ruby Range, Madison County, Montana: U. S. Geol. Survey Misc. Inv. Ser., map I-951.

Valley, J. W., Petersen, E. U., Essene, E. J., and Bowman, J. R., 1982, Fluorphlogopite and fluortremolite in Adirondack marbles and calculated C-O-H-F fluid compositions: Am. Mineralogist, v. 67, p. 545–557.

Walther, J. V., and Orville, P. M., 1983, The extraction-quench technique for determination of the thermodynamic properties of solute complexes: Application to quartz solubility in fluid mixtures: Am. Mineralogist, v. 68, p. 731–741.

Walton, K., 1981, A study of the Treasure Chest talc mine and other talc deposits in southwestern Montana: Unpub. senior thesis, Smith College, Northhampton, Massachusetts, 30 p.

Wooden, J. L., Vitaliano, C. J., Koehler, S. W., and Ragland, P. C., 1978, The late Precambrian mafic dikes of the southern Tobacco Root Mountains, Montana: Geochemistry, Rb-Sr geochronology and relationship to Belt tectonics: Canadian Jour. Earth Sci., v. 15, p. 467–479.

REFERENCE MATERIAL

1. Composition comparison chart
2. Charts for use with sedimentary rocks
3. Charts for use with igneous rocks
4. Charts for use with metamorphic rocks
5. Magnetic declination map
6. Geologic Framework of Montana
7. Geologic time scale
8. Stratigraphic Columns for SW Montana

AGI DATA SHEET 15.1

Comparison Chart for Estimating Percentage Composition

Prepared by Richard D. Terry and George V. Chilingar, Allen Hancock Foundation, Los Angeles. Reprinted from *Journal of Sedimentary Petrography*, v. 25, n. 3, p. 229–234, Sept. 1955.

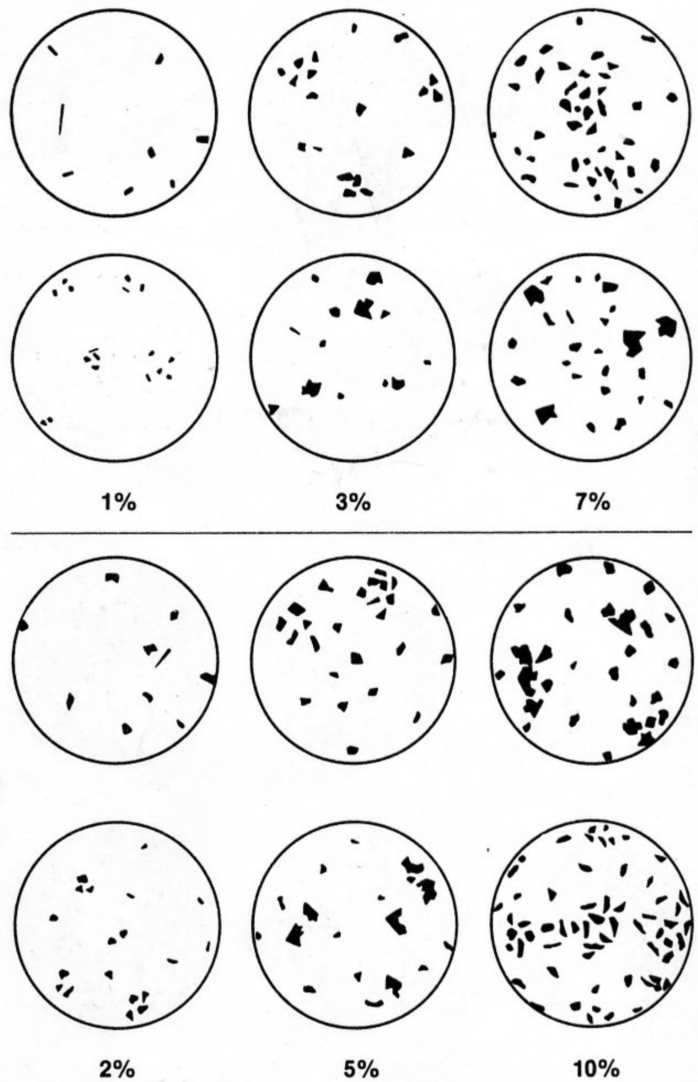

AGI-DS-65

AGI DATA SHEET 15.2

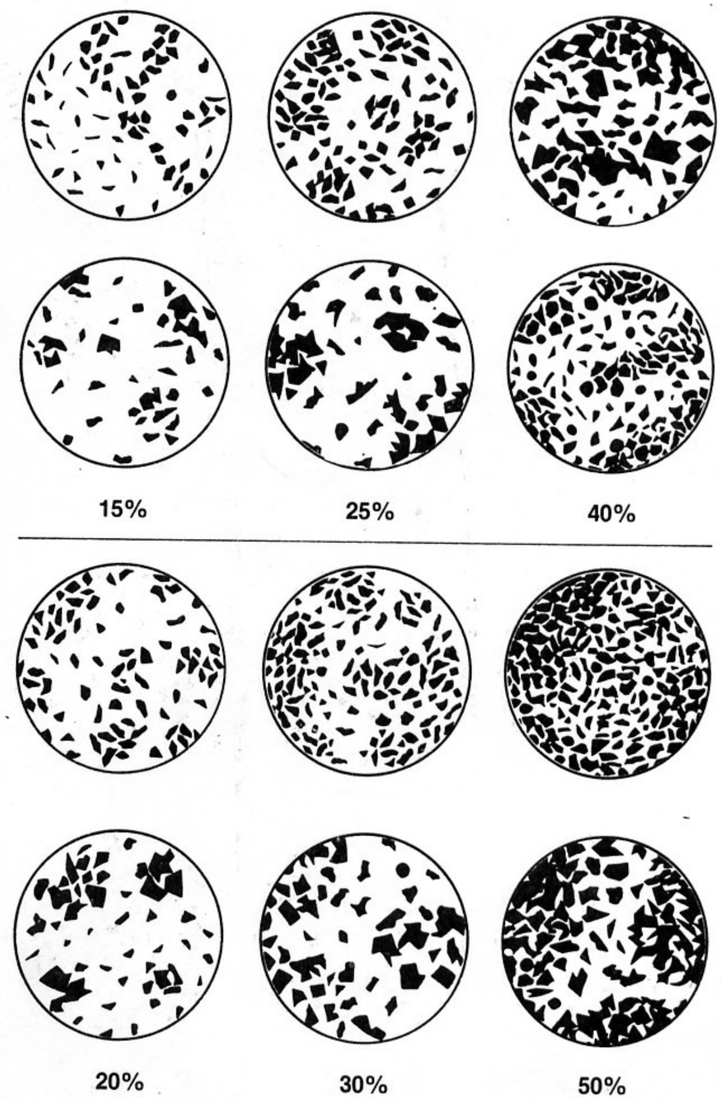

Clastic Sediment & Sedimentary Rock Classification - Texture & Composition

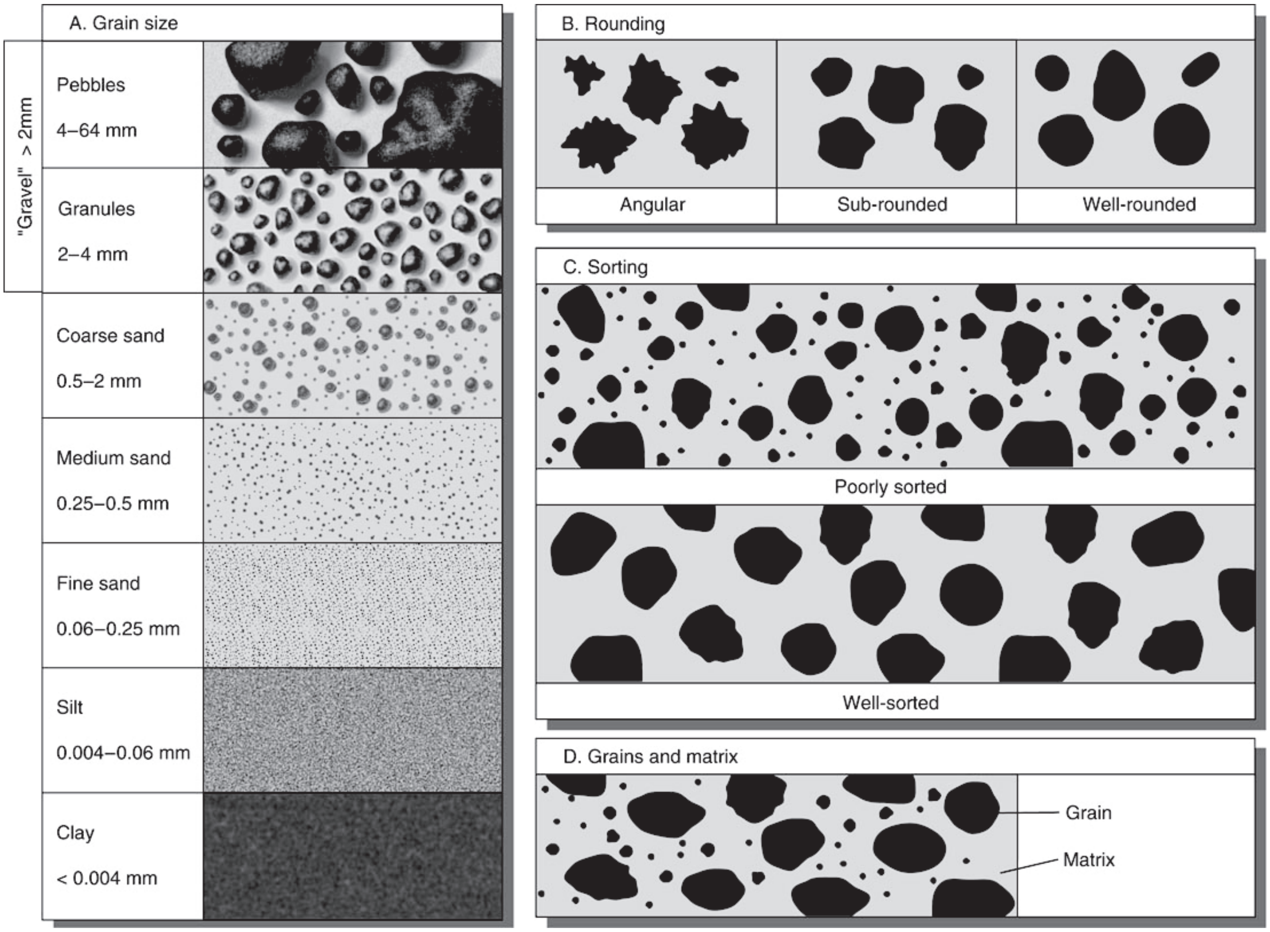

Silicate-rich clastic sediments & rocks

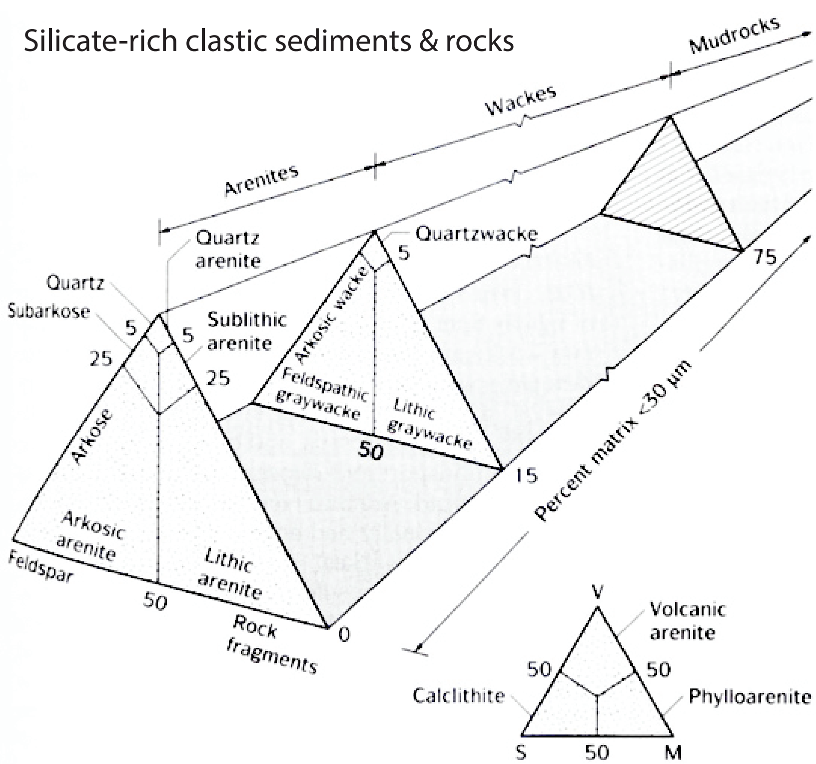

Silicate-rich Sandstone
- arenite: well-sorted s.s.
- wacke: poorly sorted s.s.
- graywacke: dark/well-indurated wacke

Silicate-rich Rudite
- conglomerate: subangular-rounded
- breccia: angular clasts

Silicate-rich Luttites
- claystone: clay-sized particles
- siltstone: silt-zized particles
- mudstone: silt+ clay sized particles
- shale: fissile mudstone
- argillite

Wentworth Sediment Size Chart

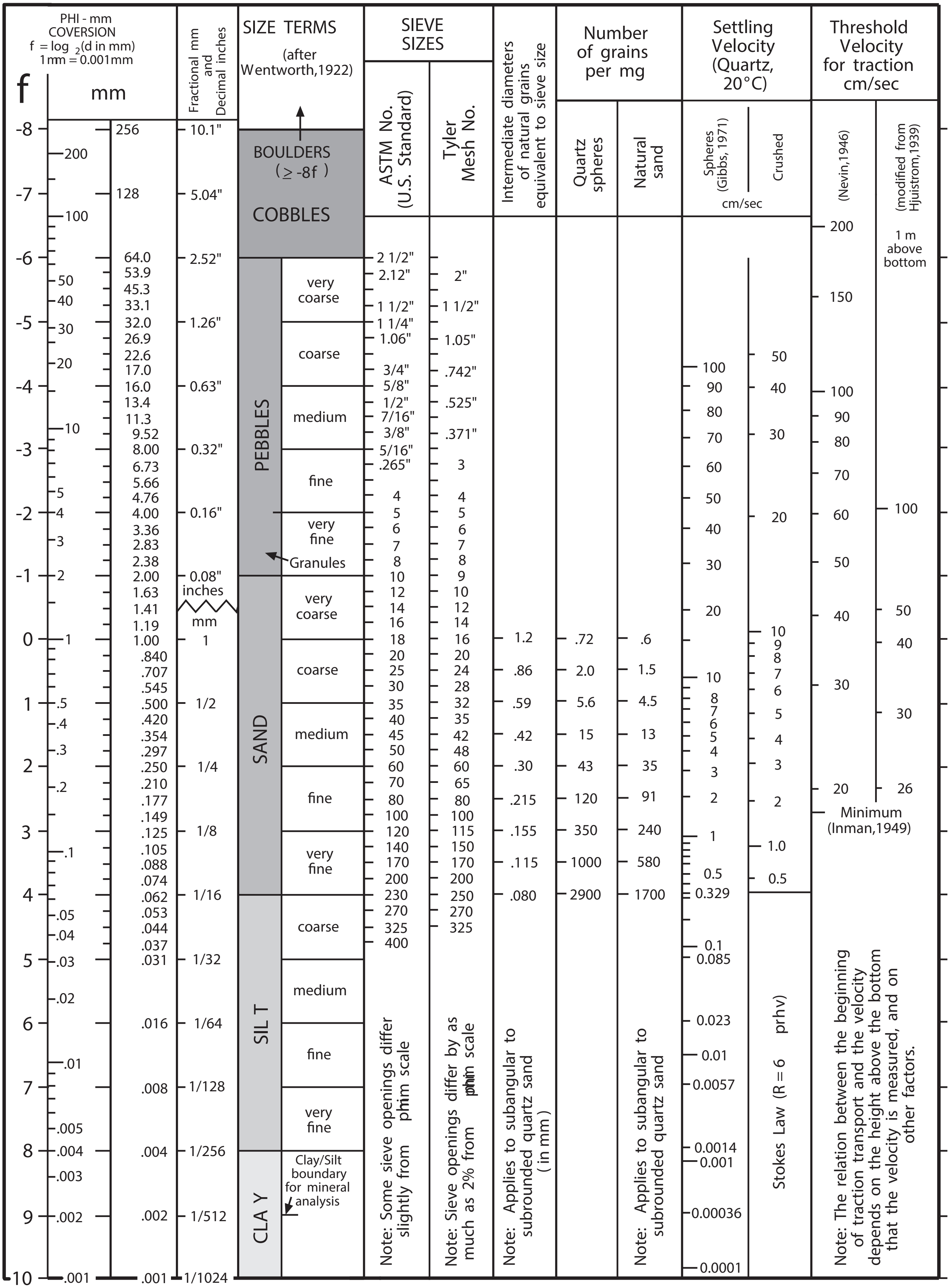

Classification of Carbonate Rocks

Two classification schemes for carbonate rocks are in wide use. The Dunham classification is best for outcrop and hand-samples. It is based on depositional texture including: (1) presence/absence of carbonate mud (<20μm), (2) abundance of carbonate grains (>20μm), (3) mud-supported vs. grain supported, (4) evidence of organic binding during deposition (i.e. reef-forming). The Folk classification is used mainly in thin section study. Lithologic designations are formed by concatenating a prefix indicating the type of allochem (large particle) that dominates the rock and a suffix indicating the matirx type. Allochems (and associated prefixes) include ooids (oo-), pellets (pel-), fossil fragments (bio-) and intraclasts (intra-). Matrix types (and suffixes) are micrite (-micrite) and crytalline (-spartite).

Folk (1959, 1962)

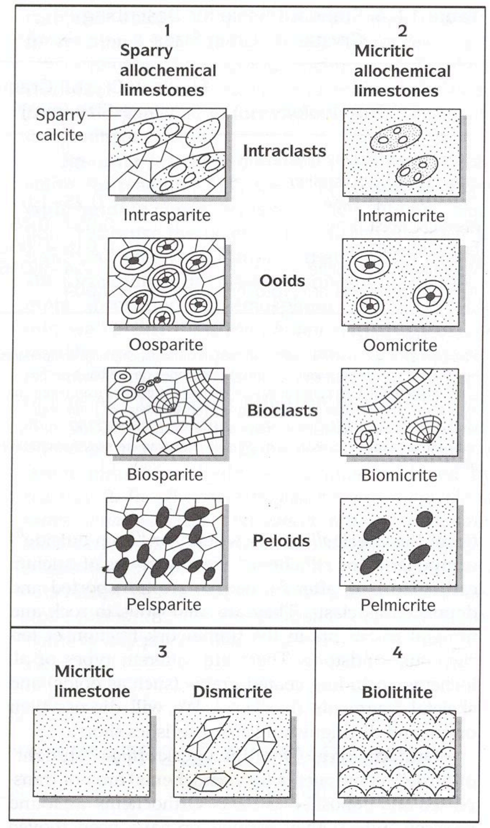

Dunham (1962), modified by Embry & Klovan (1972)

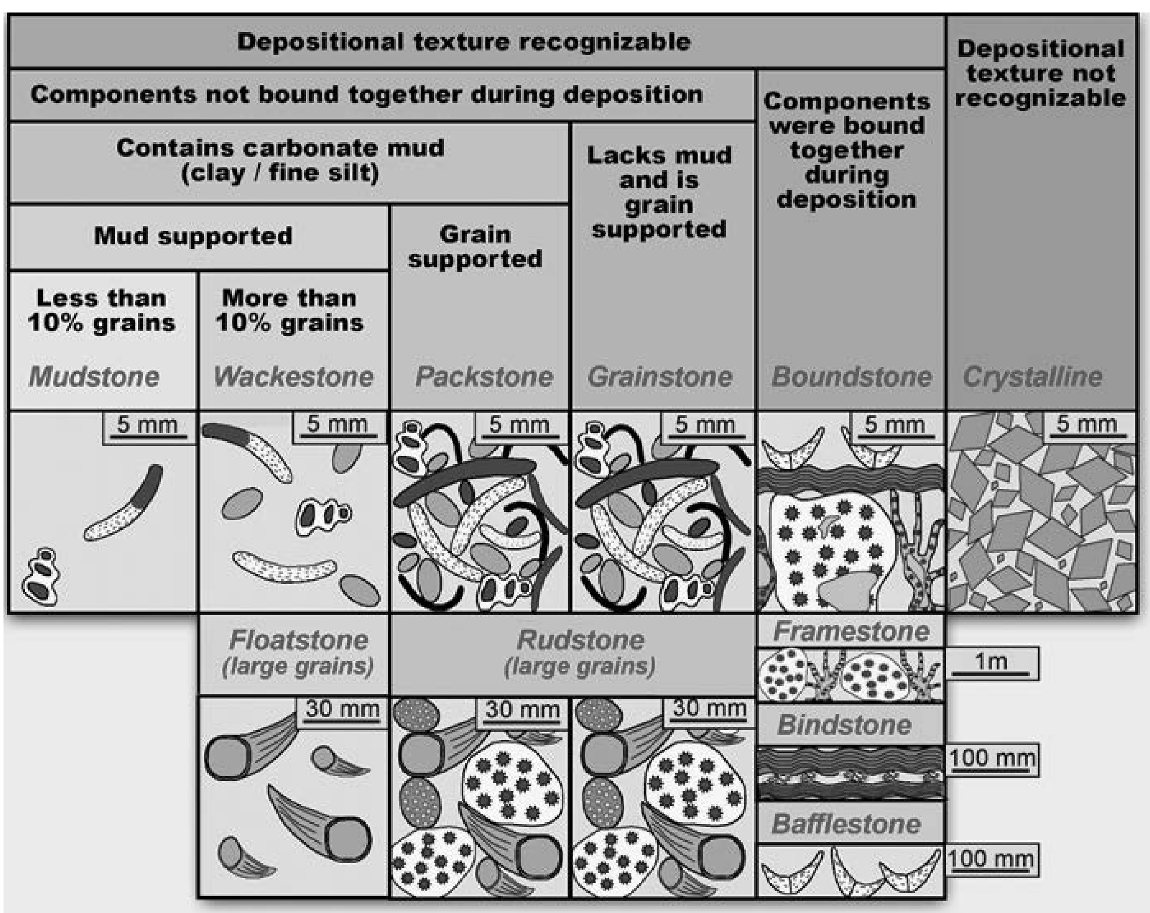

Mineralogic Classification of Igneous Rocks

Classification of Igneous Rocks by Mineral Abundance

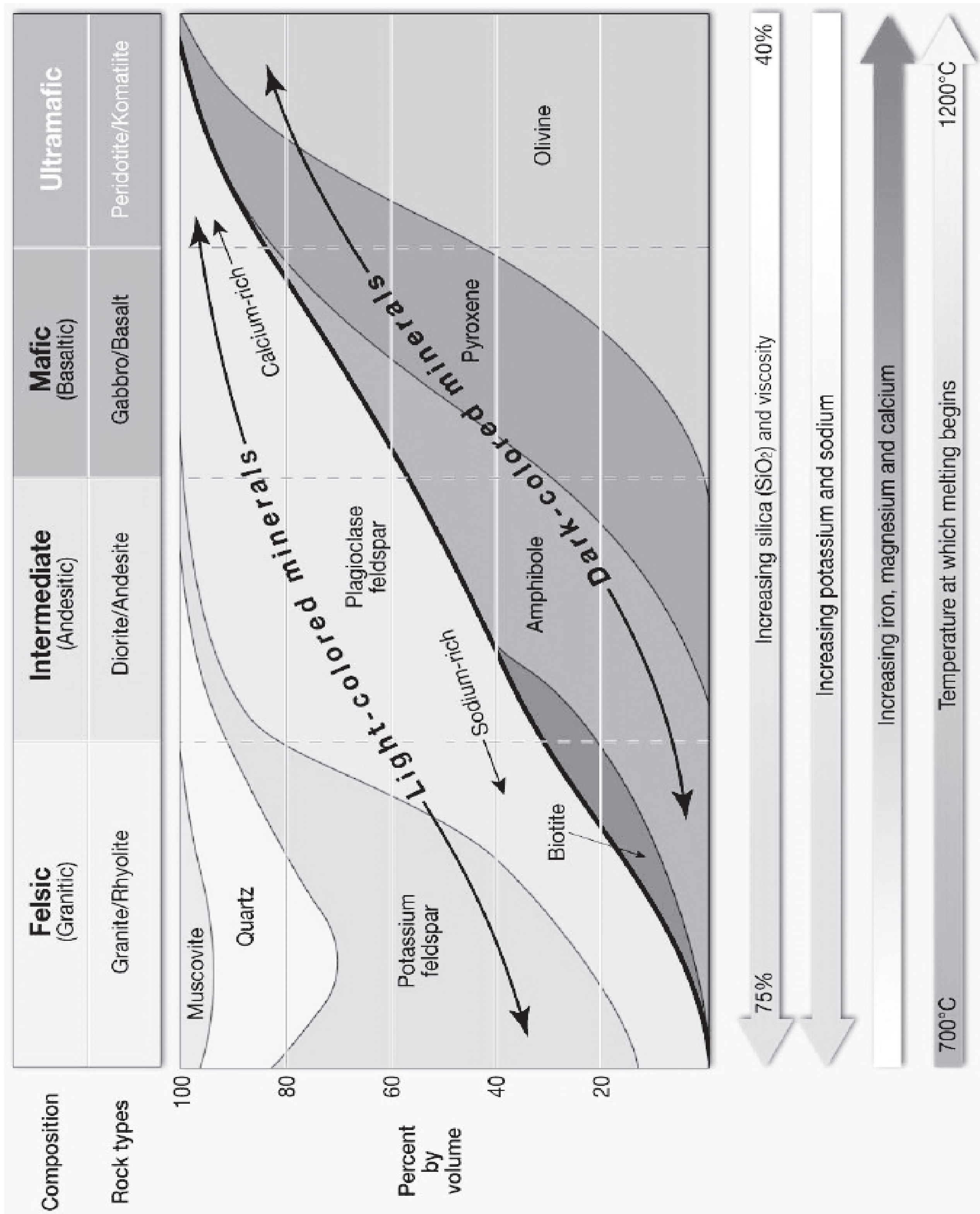

IUGS Classification of Igneous Rocks - Grainitoids & Volcanic Equivalents

Phaneritic Rocks ((Plutonic)

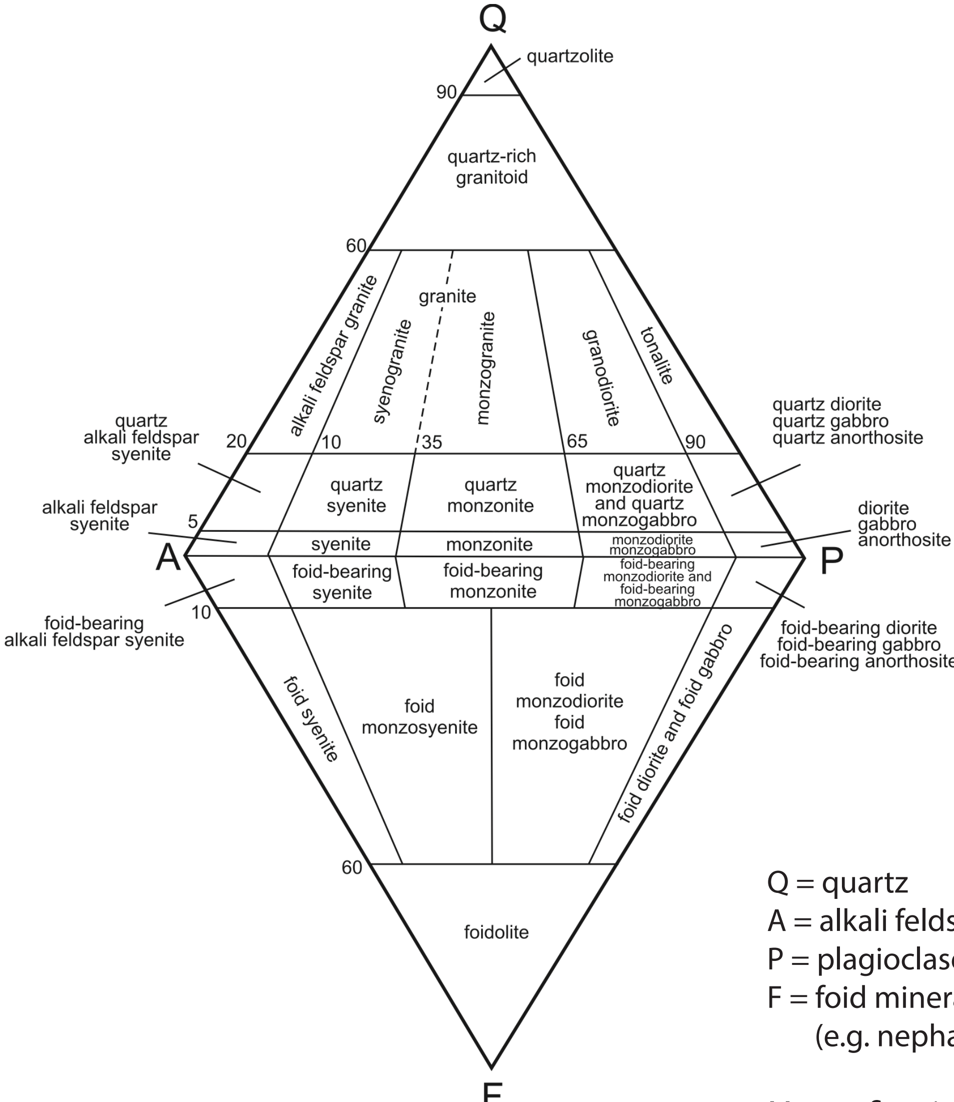

Aphanitic Rocks ((Volcanic)

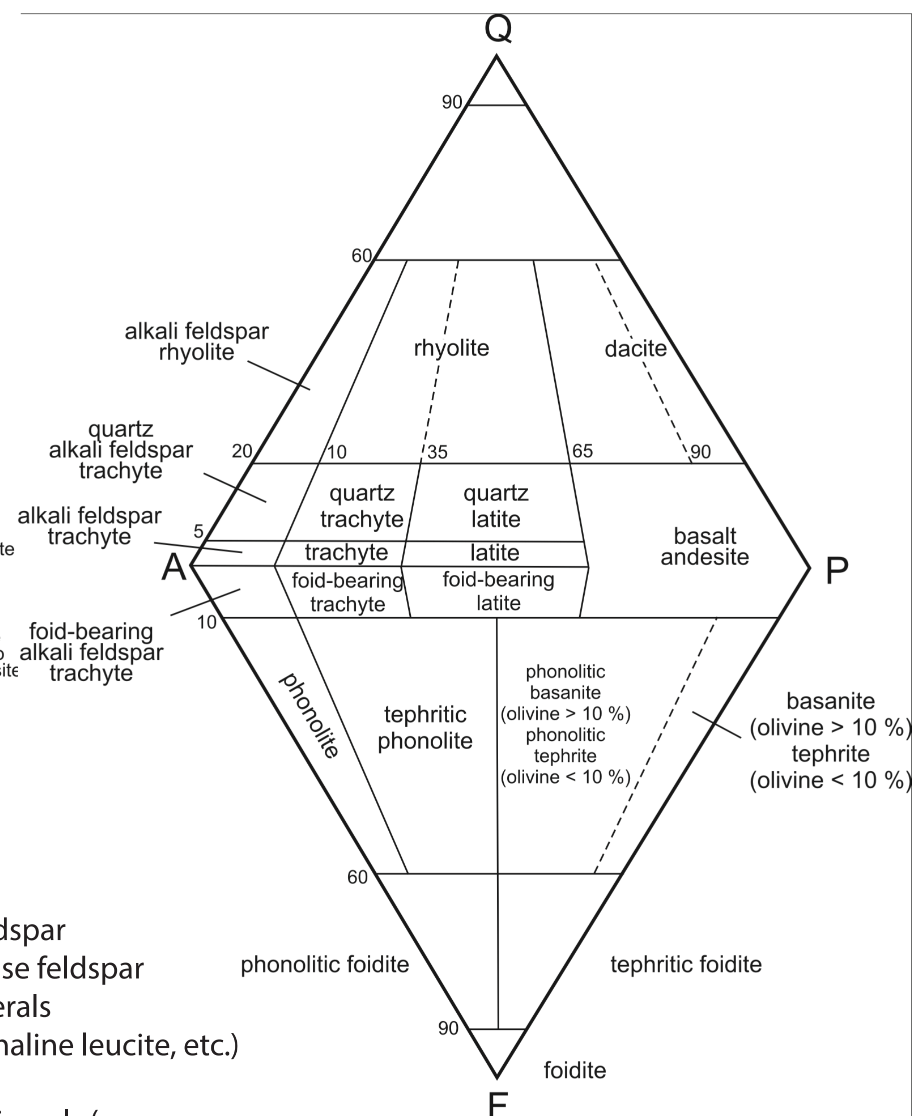

Q = quartz
A = alkali feldspar
P = plagioclase feldspar
F = foid minerals
(e.g. nephaline leucite, etc.)

M = mafic minerals (e.g. pyroxene, olivine, biotite, amphibole, etc.)

These charts are for use with rocks with M < 90

Table 4.6 Mineral properties in igneous rock hand specimens

Mineral	Typical chemical formula	Colour	Cleavage	Lustre	Habit	Hardness
Felsic minerals						
Quartz	SiO_2	Colourless to pale grey when surrounded by dark minerals; transparent	None; irregular, or curved fracture surfaces	Glassy, shiny	Rare trigonal pyramids but usually irregular, anhedral 	7
Alkali feldspar	$(K,Na)AlSi_3O_8$	White or pink, sometimes orange or yellow	2 sets at 90°, poorly visible	Usually dull, sometimes silky or vitreous	Tabular crystals; shiny cleavage surfaces 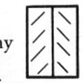 may show simple twins. Elongate rectangular 'laths', lamellae, or irregular masses of plagioclase may be noted: perthite	6
Plagioclase feldspar	$NaAlSi_3O_8$ to $CaAl_2Si_2O_8$	White or green, rarely pink or black	2 sets almost at 90°, poorly visible	Usually dull, sometimes silky or vitreous	Lath-shaped crystals; shiny cleavage surfaces  may show multiple, parallel twins	6–6.5
Nepheline	$NaAlSiO_4$	White to pale grey	2 poor cleavages, 1 occasionally distinct	Greasy, vitreous	Usually occurs in microcrystalline groundmass; occasional aggregates of crystals	5.5–6
Muscovite (mica)	$KAl_2(AlSi_3O_{10})(OH)_2$	Colourless to pale brown or green	1 excellent cleavage, cleaves into thin flexible sheets	Shiny, silver and pearly	Tabular crystals sometimes 6-sided, especially in pegmatites	2–2.5
Mafic minerals						
Olivine	$(Mg,Fe)_2SiO_4$	Olive green, yellow-green, sometimes brown	Very poor, usually fractures	Glassy when fresh, vitreous when altered	Usually rounded anhedral crystals, occasionally equidimensional tabular forms	6–7
Pyroxene	(i) $(Mg,Fe,Ca)_2Si_2O_6$ (augite, etc.) (ii) $NaFeSi_2O_6$ (aegirine)	Black to dark green or brown } Yellowish-green	2 good sets meeting at nearly 90°	Vitreous when fresh, dull when altered	4- or 8-sided prismatic crystals occasionally showing cleavage 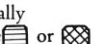 Aegirine more acicular	6
Amphibole	(i) $Ca_2(Mg,Fe)_5Si_8O_{22}(OH)_2$ (e.g. tremolite) (ii) $Na_2Fe_3^{2+}Fe_2^{3+}Si_8O_{22}(OH)_2$ (riebeckite)	Black to brownish black or dark green } Dark blue	2 good sets meeting at 120°	Vitreous when fresh, dull when altered	Prismatic or lozenge-shaped crystals often showing cleavage 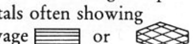 Riebeckite more acicular	5–6
Biotite (mica)	$K(Mg,Fe)_3(AlSi_3O_{10})(OH)_2$	Black to dark brown or green	1 excellent cleavage; cleaves into thin flexible sheets	Very shiny	Thin tabular crystals, occasionally 6-sided, especially in ignimbrites and acid lavas	2.5–3
Tourmaline	$Na(Mg,Fe)_3Al_6B_3Si_6O_{22}(OH,F)_4$	Black, but varieties may be blue, red or green	Very poor	Vitreous shiny	Long thin prismatic needle-shaped crystals, sometimes longitudinally striated and often in clusters; occasionally striated curved surfaces 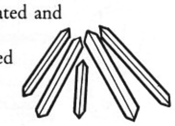	7
Frequent accessory minerals						
Apatite	$Ca_5(PO_4)_3(OH)$	Pale green to yellow green	Very poor	Vitreous	Often euhedral, sub-hexagonal crystals; sometimes fibrous	5
Sphene	$CaTiSiO_4(OH)_2$	Colourless to yellow, green or brown	1 good cleavage	Vitreous	Characteristic 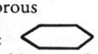 euhedral rhombic crystals	5

Textural & Mineralogic Classification of Volcanic Rocks

Textural Classification

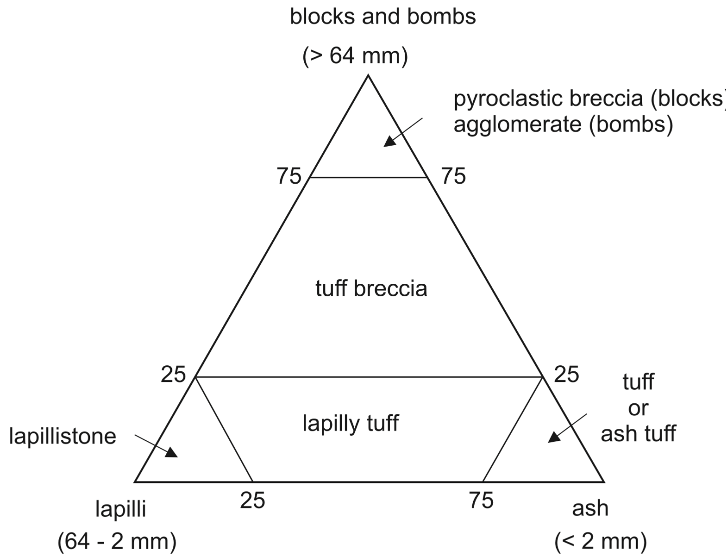

TAS - Total Alkali/Silica Diagram

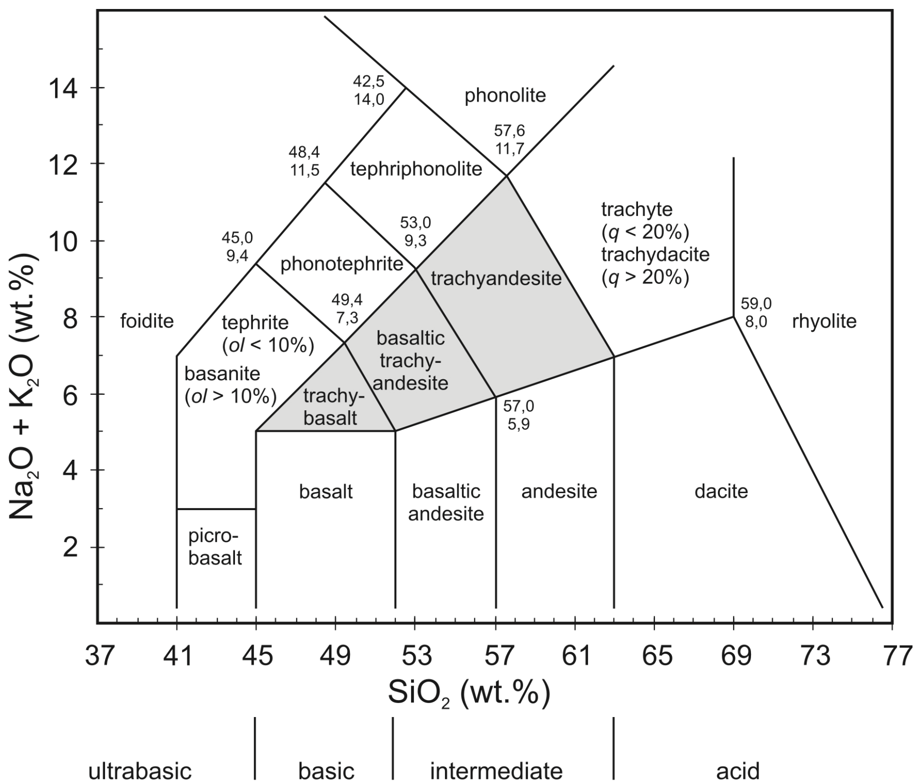

Further subdivisions of shaded fields	trachybasalt	basaltic trachyandesite	trachyandesite
$Na_2O - 2.0 \geq K_2O$	hawaiite	mugearite	benmoreite
$Na_2O - 2.0 \leq K_2O$	potassic trachybasalt	shoshonite	latite

AFM Diagrams for Metamorphic Rocks, Spear, 1995

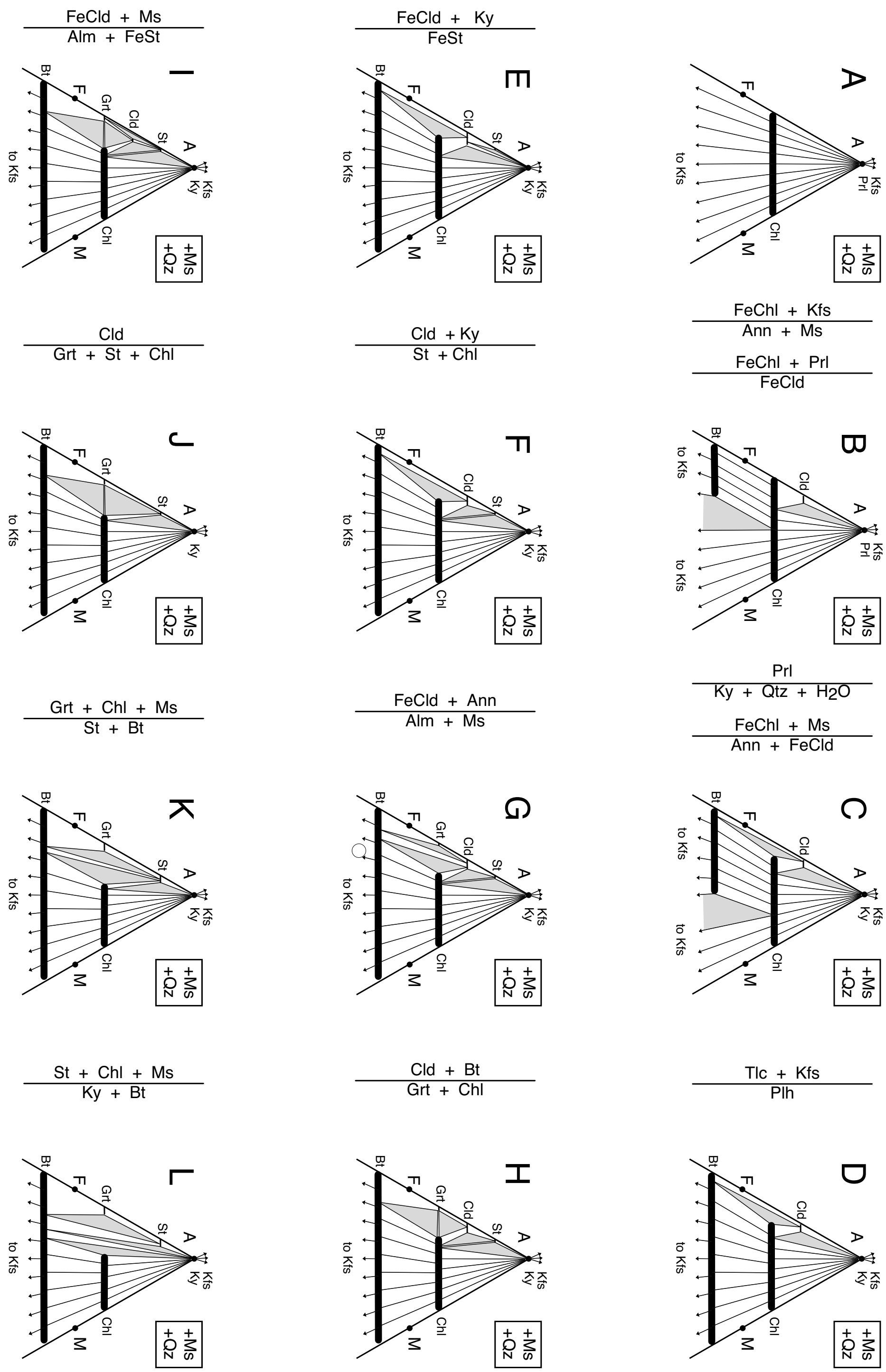

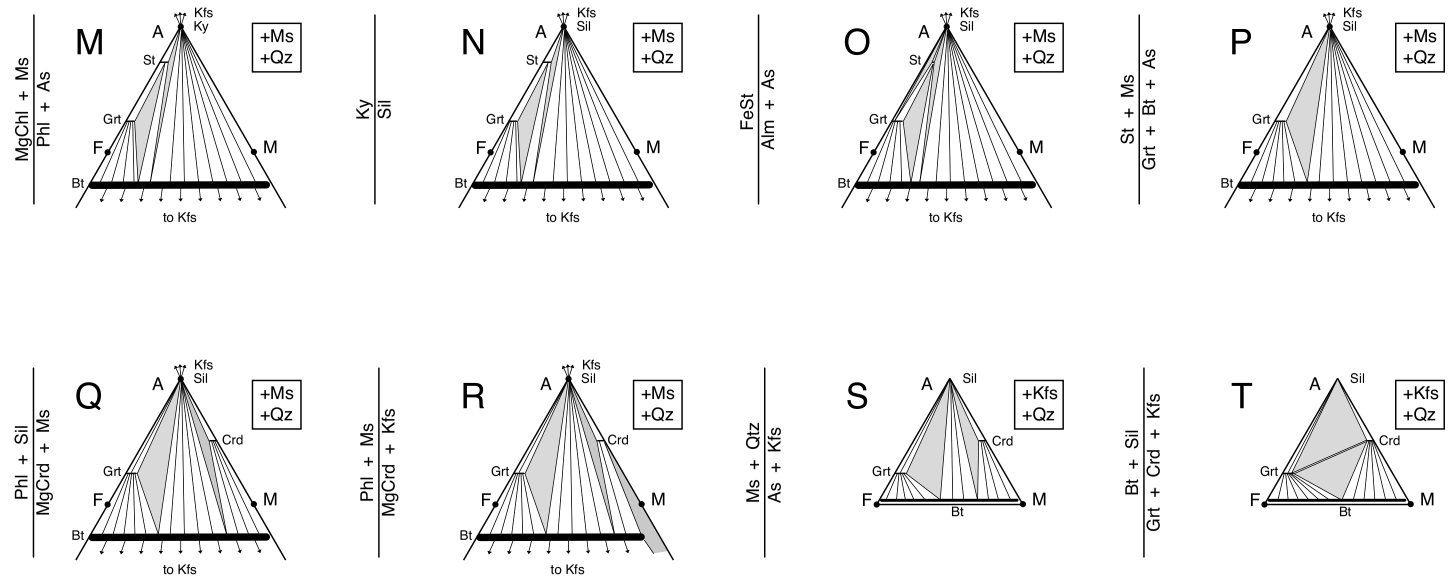

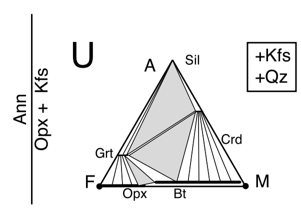

AFM sequence for medium-pressure metapelitic rocks. Remember always to look for quartz and either muscovite or K-feldspar!!

modified from Spear, 1993

Petrogenetic Grid (P-T Diagram) for Metamorphic Rocks

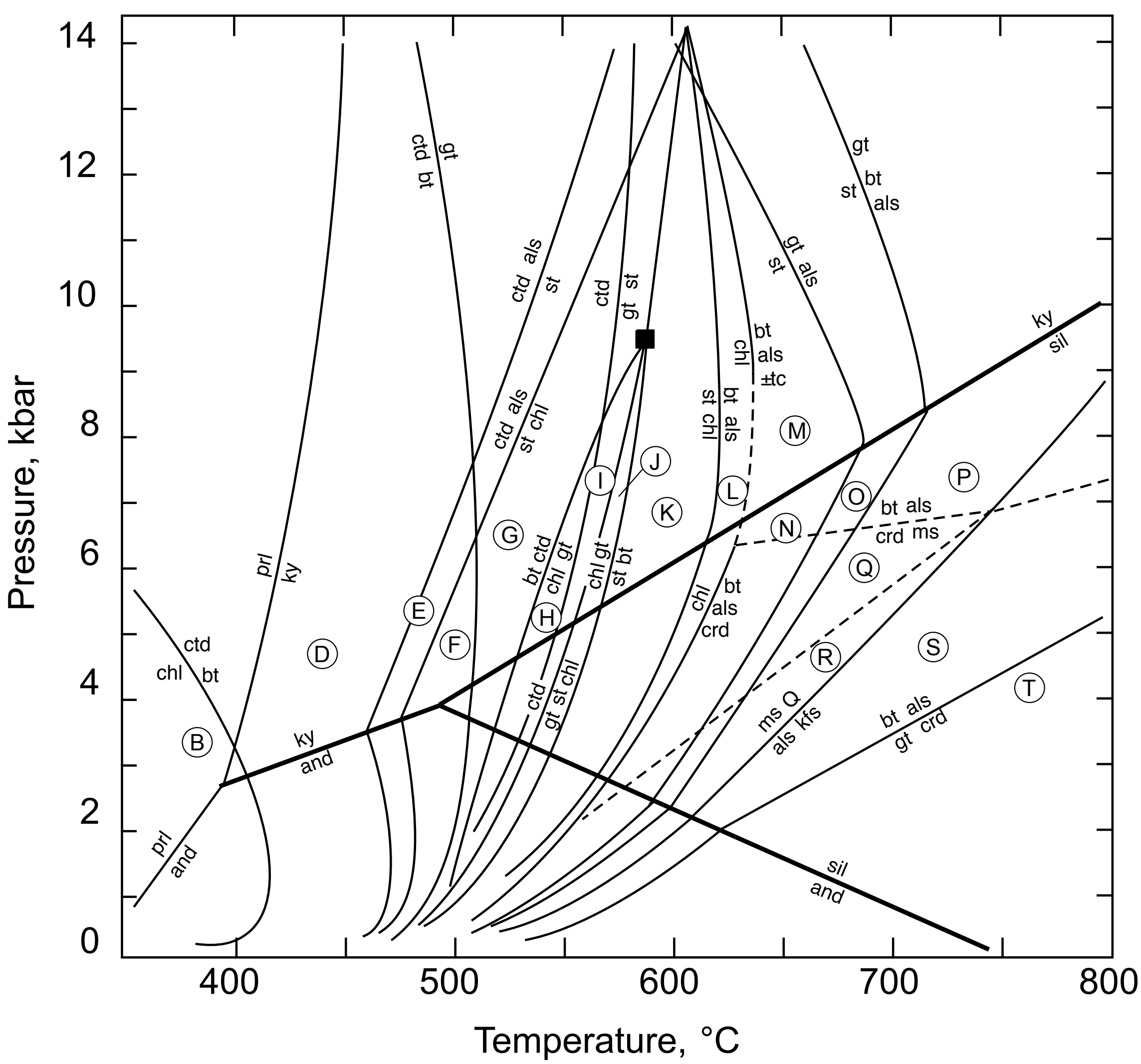

Labeled fields represent divariant regions; the labels correspond to the specific AFM topologies shown on the attached page. Solid lines are for rocks that lie within the AFM diagram. Dashed lines are for Mg endmember system.

als = and, ky, or sil	ctd = chloritoid	prl = pyrophyllite
and = andalusite	gt = garnet	Q = quartz
bt = biotite	kfs = K-feldspar	sil = sillimanite
chl = chlorite	ky = kyanite	st = staurolite
crd = cordierite	ms = muscovite	tc = talc

Modified from Spear (1993)

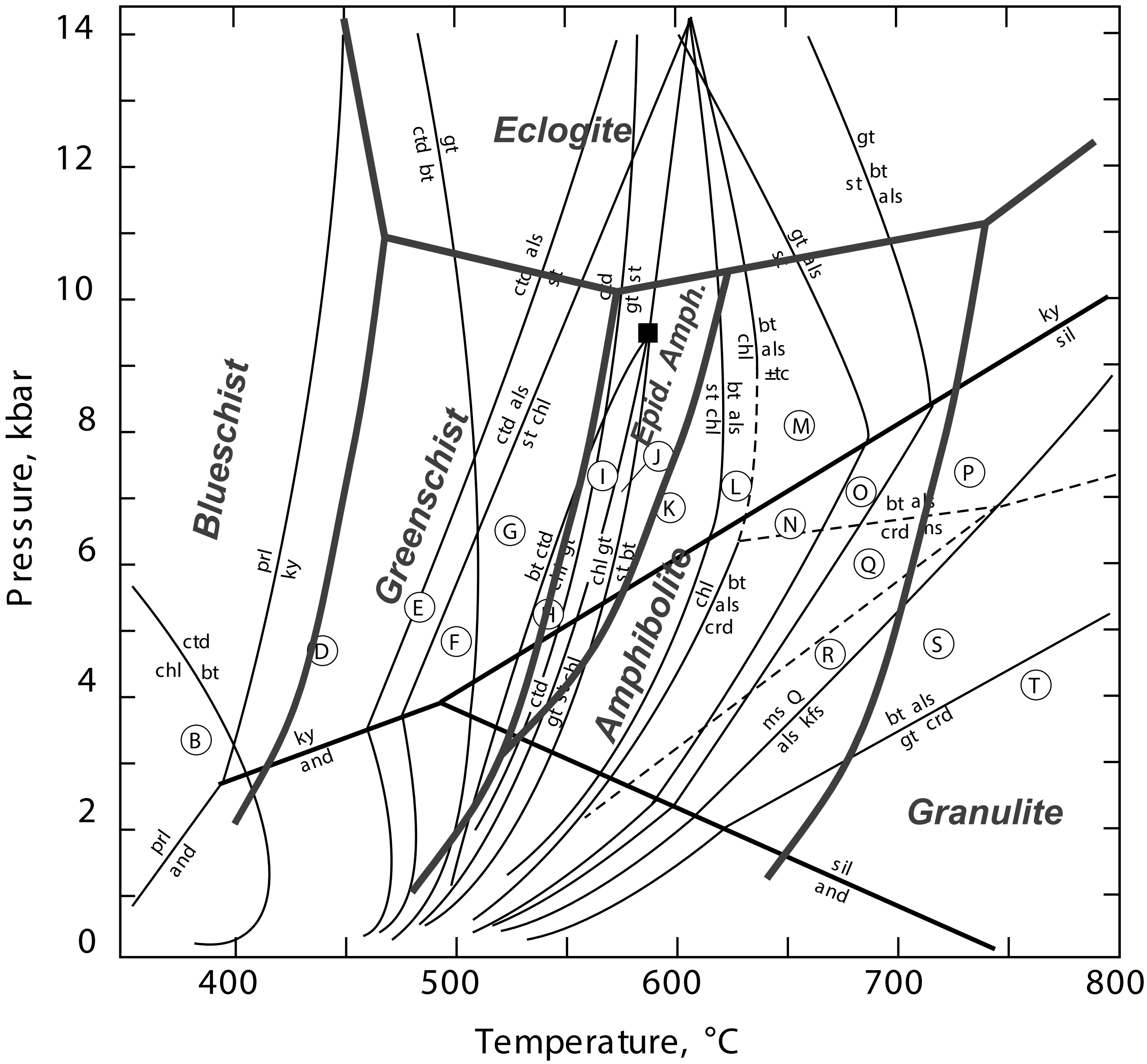

Labeled fields represent divariant regions; the labels correspond to the specific AFM topologies shown on the attached page. Solid lines are for rocks that lie within the AFM diagram. Dashed lines are for Mg endmember system.

als = and, ky, or sil	ctd = chloritoid	prl = pyrophyllite
and = andalusite	gt = garnet	Q = quartz
bt = biotite	kfs = K-feldspar	sil = sillimanite
chl = chlorite	ky = kyanite	st = staurolite
crd = cordierite	ms = muscovite	tc = talc

Modified from Spear (1993)

Typical Metamoprhic Facies Indicator Parageneses for Different Protolith Compositions

FACIES – PROTOLITH—MINERAL ASSEMBLAGE TABLE:

Facies	Pelitic	Calcareous	Mafic
Zeolite 100-200° C	interlayered smectite/chlorite calcite	calcite	Laumonite, thompsonite, calcite, interlayered smectite/chlorite
Prehnite-Pumpellyite 150-300° C	Prehnite, pumpellyite, calcite, chlorite, albite	calcite	Prehnite, pumpellyite, calcite, chlorite, albite
Greenschist 300-450° C	muscovite, chlorite, quartz, albite, biotite, garnet	calcite, dolomite, quartz, epidote, tremolite	albite, chlorite, quartz, epidote, actinolite, sphene
Epidote Amphibolite 450-550° C	muscovite, biotite, garnet, albite, quartz	calcite, quartz, tremolite, epidote,diopside	albite, epidote, hornblende, quartz
Amphibolite 500-700° C	garnet, biotite, muscovite, quartz, plagioclase, staurolite, kyanite or sillimanite	calcite, diopside quartz, wollastonite	hornblende, plagioclase, garnet, quartz, sphene, biotite
Granulite 700-900° C	garnet, Kspar, sillimanite or kyanite, quartz, plagioclase, hypersthene	calcite, quartz, plagioclase, diopside, hypersthene	plagioclase, augite, hypersthene, hornblende, garnet, olivine
Blueschist 150-350° C P > 5-8 Kb	Jadeite, albite, quartz, lawsonite, aragonite, paragonite	aragonite, white mica	Glaucophane, albite, lawsonite, sphene, ± garnet
Eclogite 350-750° C P > 8-10 Kb	coesite, Kspar, sillimanite, plagioclase	aragonite, quartz, plagioclase, diopside, hypersthene	omphacite (px), pyrope garnet

Magnetic Declination Map of North America for the year 2010

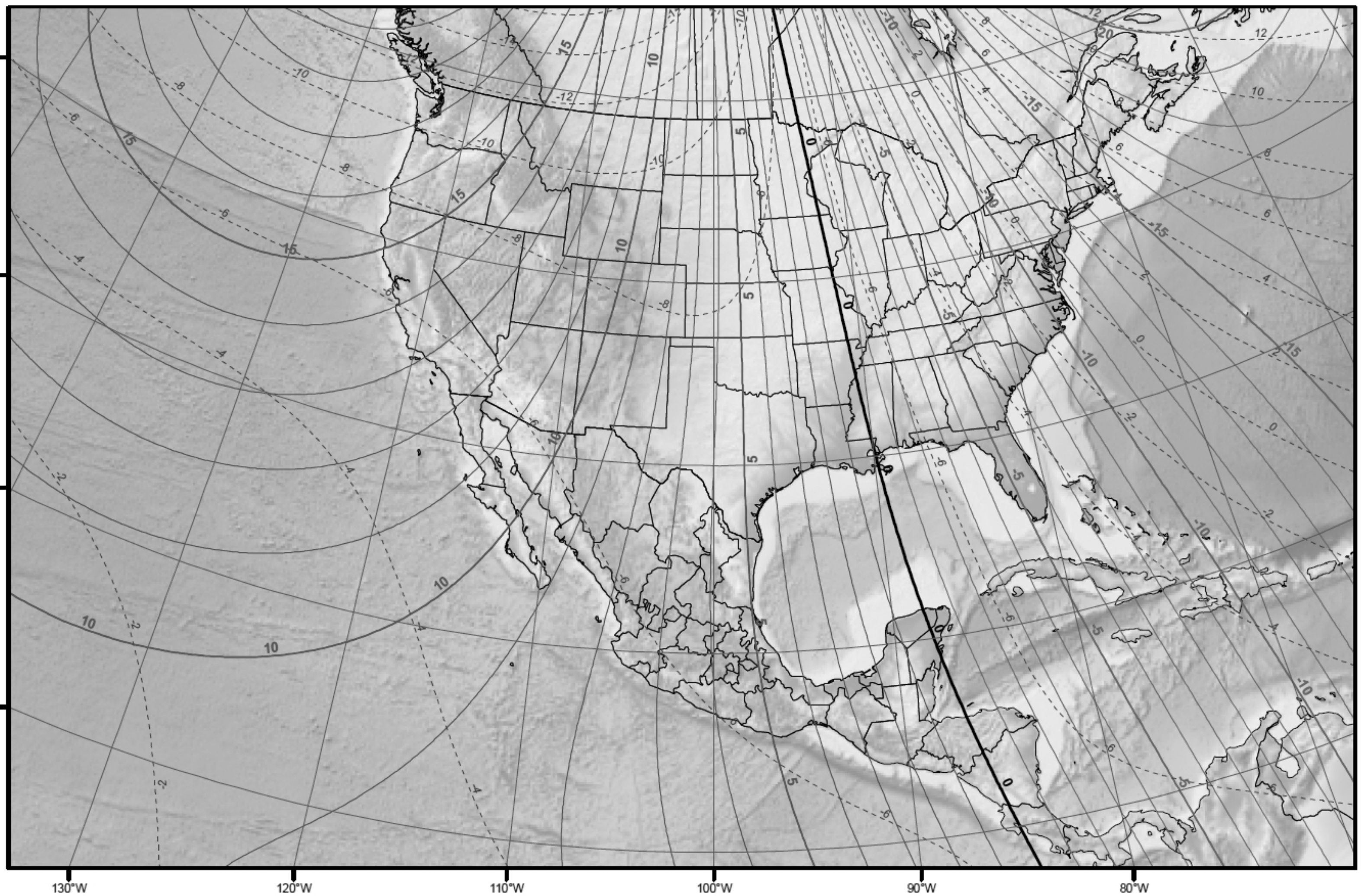

The term magnetic declination (also known as magnetic variation) refers to the angle between the magnetic north (MN - compass north) and true north (TN - true north) at any given latitude / longitude. The black contour line shows the imaginary line along which the declination is zero (MN and TN converges). The magnetic declination increases as one moves east or west from this line. The red line shows the negative (west) declination contours and the blue line shows the positive (east) declination contours. The degrees of declination required in order to orient the compass with the map is added east of this line and subtracted west of this line. (e.g., 10 degrees east would indicate that MN lies 10 degrees clockwise from the TN). Magnetic declination gradually changes with time and location. The dotted grey lines show the expected annual change in the magnetic declination in arc minutes. The above map is produced from the World Magnetic Model (WMM 2010) for the year 2010.

Structural Framework of Montana

Major faults. Base map from Geologic Map of Montana.
Quaternary faults from Stickney and others (2000).

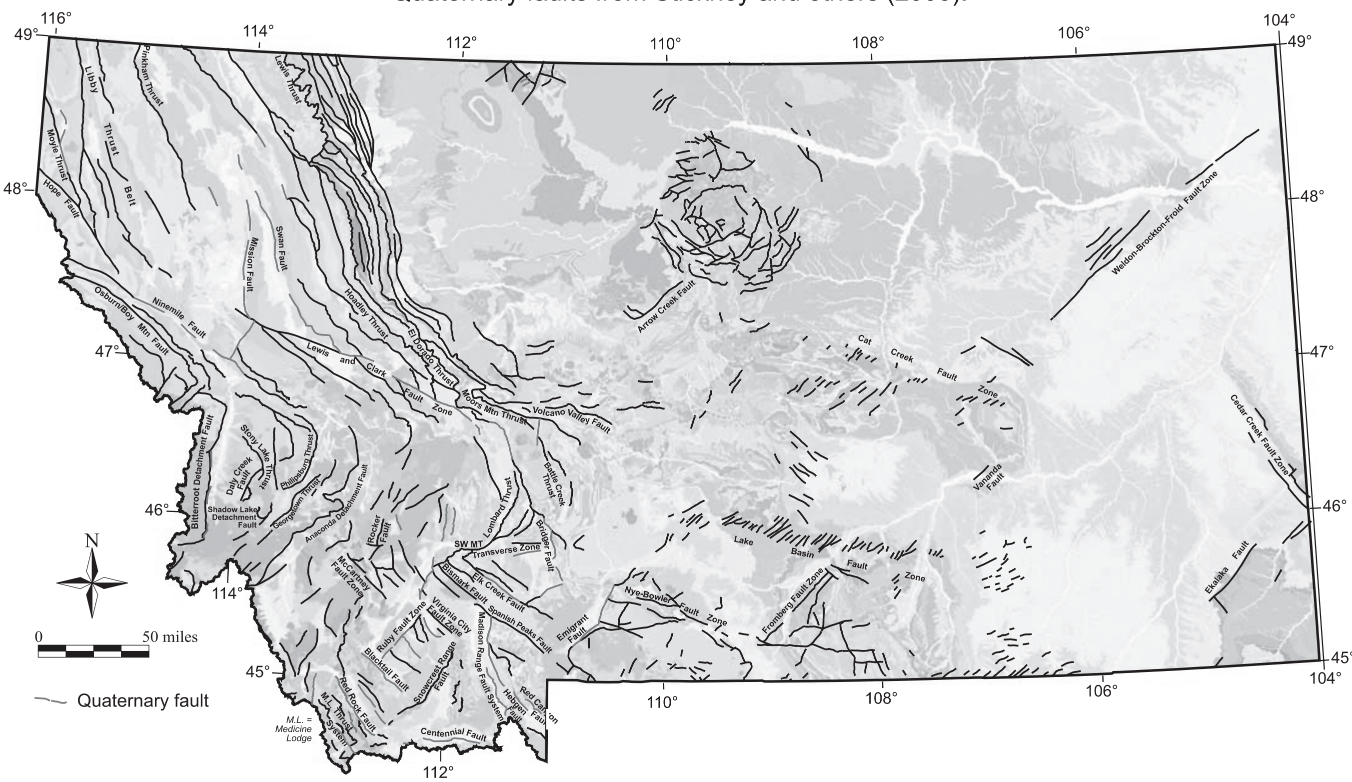

Precambrian Provinces. Modifed and compiled from Lisenbee and DeWitt (1993),
Nelson (1993), Sears (2006), and Sims and others (2004).

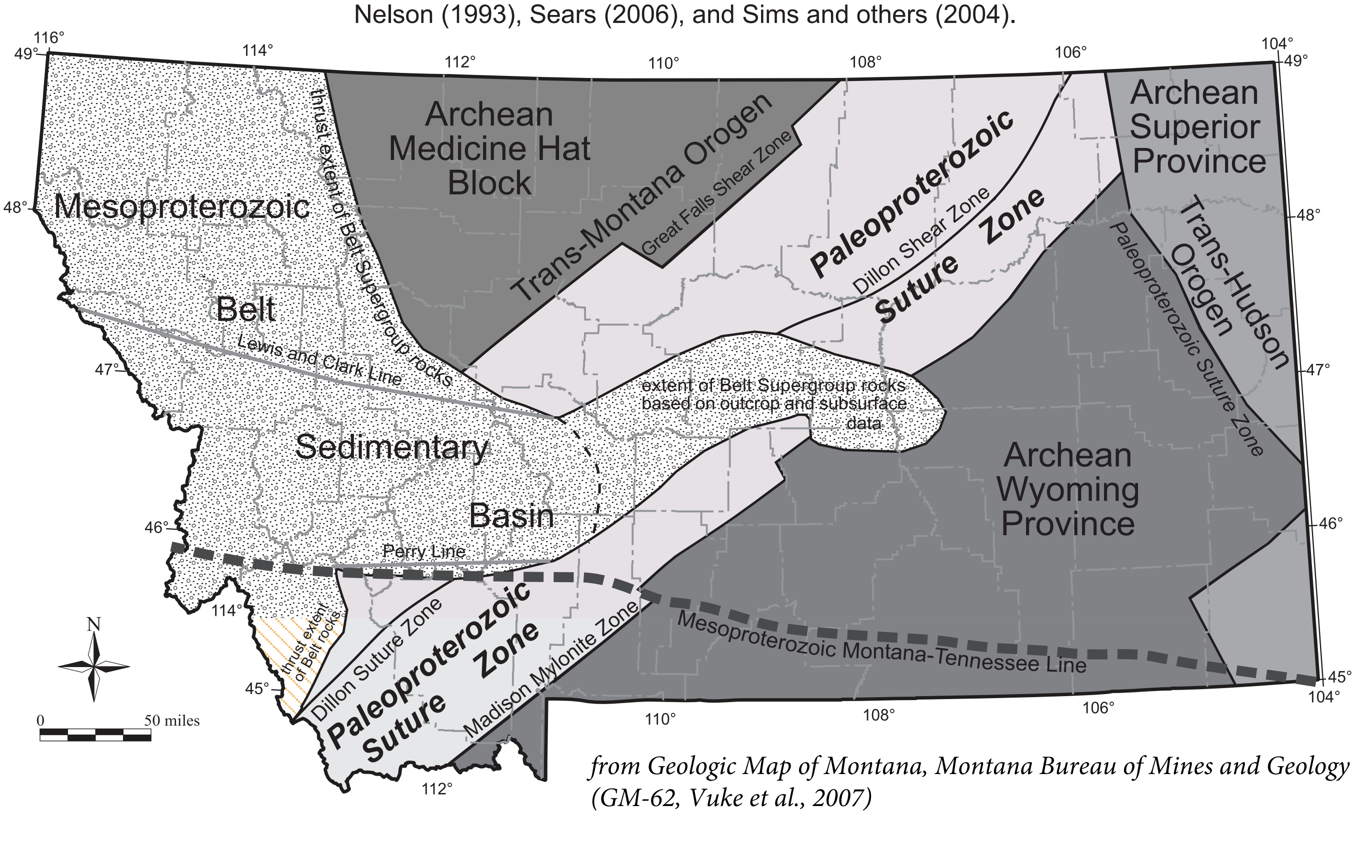

from Geologic Map of Montana, Montana Bureau of Mines and Geology (GM-62, Vuke et al., 2007)

Igneous Rocks of Montana

Plutons, diatremes, and other intrusive rock.
Compiled from Geologic Map of Montana and Hearn and others (1989).

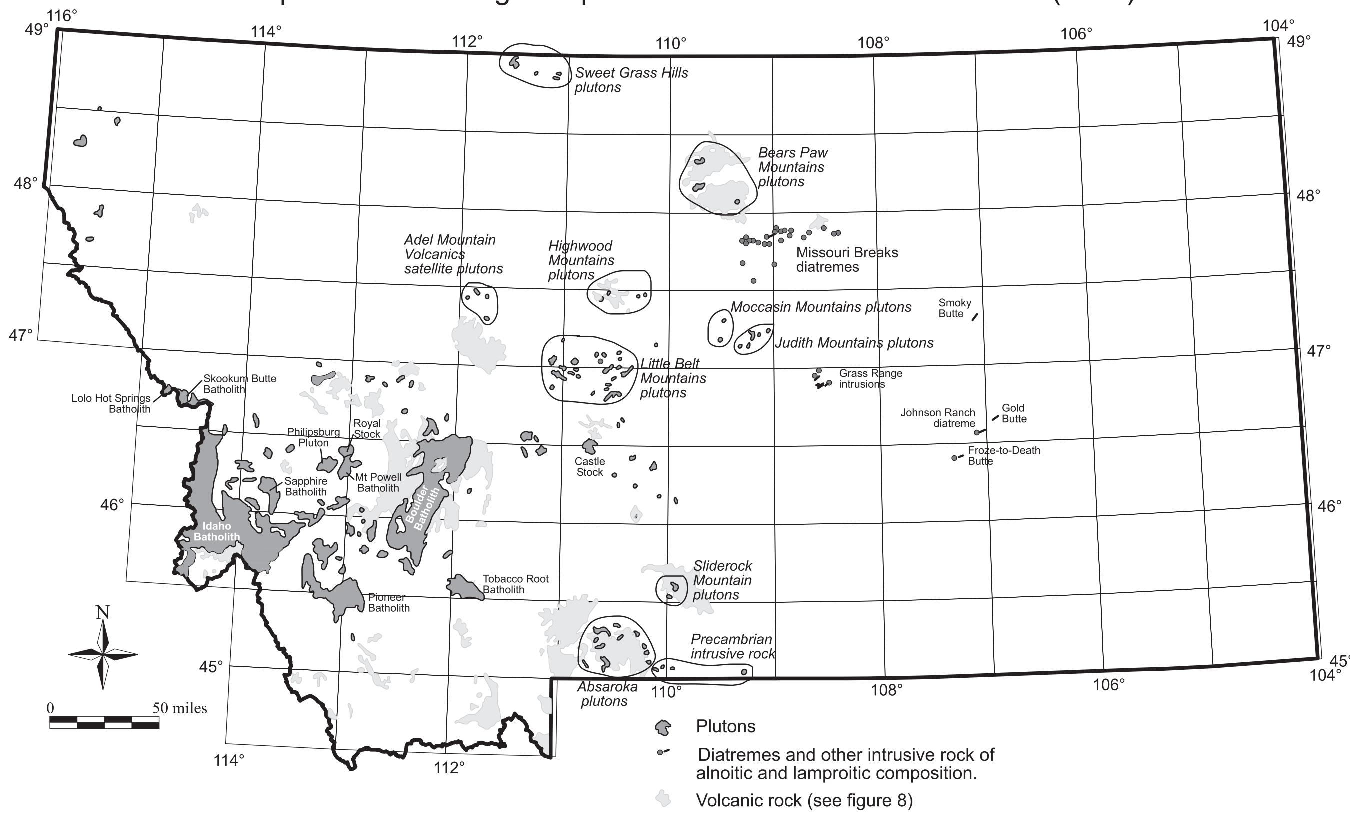

Volcanic rock. Compiled from Geologic map of Montana.

from Geologic Map of Montana, Montana Bureau of Mines and Geology (GM-62, Vuke et al., 2007)

1999 GEOLOGIC TIME SCALE

CENOZOIC

Period		Epoch		Age	Picks (Ma)
QUATERNARY		HOLOCENE			0.01
QUATERNARY		PLEISTOCENE		CALABRIAN	1.8
TERTIARY	NEOGENE	PLIOCENE	L	PIACENZIAN	3.6
TERTIARY	NEOGENE	PLIOCENE	E	ZANCLEAN	5.3
TERTIARY	NEOGENE	MIOCENE	L	MESSINIAN	7.1
TERTIARY	NEOGENE	MIOCENE	L	TORTONIAN	11.2
TERTIARY	NEOGENE	MIOCENE	M	SERRAVALLIAN	14.8
TERTIARY	NEOGENE	MIOCENE	M	LANGHIAN	16.4
TERTIARY	NEOGENE	MIOCENE	E	BURDIGALIAN	20.5
TERTIARY	NEOGENE	MIOCENE	E	AQUITANIAN	23.8
TERTIARY	PALEOGENE	OLIGOCENE	L	CHATTIAN	28.5
TERTIARY	PALEOGENE	OLIGOCENE	E	RUPELIAN	33.7
TERTIARY	PALEOGENE	EOCENE	L	PRIABONIAN	37.0
TERTIARY	PALEOGENE	EOCENE	M	BARTONIAN	41.3
TERTIARY	PALEOGENE	EOCENE	M	LUTETIAN	49.0
TERTIARY	PALEOGENE	EOCENE	E	YPRESIAN	54.8
TERTIARY	PALEOGENE	PALEOCENE	L	THANETIAN	57.9
TERTIARY	PALEOGENE	PALEOCENE	L	SELANDIAN	61.0
TERTIARY	PALEOGENE	PALEOCENE	E	DANIAN	65.0

Magnetic polarity (Anom. / Chron): 1 C1, 2 C2, 2A C2A, 3 C3, 3A C3A, 4 C4, 4A C4A, 5 C5, 5A C5A, 5B C5B, 5C C5C, 5D C5D, 5E C5E, 6 C6, 6A C6A, 6B C6B, 6C C6C, 7 C7, 7A C7A, 8 C8, 9 C9, 10 C10, 11 C11, 12 C12, 13 C13, 15 C15, 16 C16, 17 C17, 18 C18, 19 C19, 20 C20, 21 C21, 22 C22, 23 C23, 24 C24, 25 C25, 26 C26, 27 C27, 28 C28, 29 C29, 30 C30

Age (Ma): 5, 10, 15, 20, 25, 30, 35, 40, 45, 50, 55, 60, 65

MESOZOIC

Period	Epoch		Age	Picks (Ma)	Uncert. (m.y.)
CRETACEOUS	LATE			65	.2
CRETACEOUS	LATE		MAASTRICHTIAN	71.3	1
CRETACEOUS	LATE		CAMPANIAN	83.5	1
CRETACEOUS	LATE		SANTONIAN	85.8	1
CRETACEOUS	LATE		CONIACIAN	89.0	1
CRETACEOUS	LATE		TURONIAN	93.5	4
CRETACEOUS	LATE		CENOMANIAN	99.0	1
CRETACEOUS	EARLY		ALBIAN	112	2
CRETACEOUS	EARLY		APTIAN	121	3
CRETACEOUS	EARLY	NEOCOMIAN	BARREMIAN	127	3
CRETACEOUS	EARLY	NEOCOMIAN	HAUTERIVIAN	132	4
CRETACEOUS	EARLY	NEOCOMIAN	VALANGINIAN	137	4
CRETACEOUS	EARLY	NEOCOMIAN	BERRIASIAN	144	5
JURASSIC	LATE		TITHONIAN	151	6
JURASSIC	LATE		KIMMERIDGIAN	154	7
JURASSIC	LATE		OXFORDIAN	159	7
JURASSIC	MIDDLE		CALLOVIAN	164	8
JURASSIC	MIDDLE		BATHONIAN	169	8
JURASSIC	MIDDLE		BAJOCIAN	176	8
JURASSIC	MIDDLE		AALENIAN	180	8
JURASSIC	EARLY		TOARCIAN	190	8
JURASSIC	EARLY		PLIENSBACHIAN	195	8
JURASSIC	EARLY		SINEMURIAN	202	8
JURASSIC	EARLY		HETTANGIAN	206	8
TRIASSIC	LATE		RHAETIAN	210	8
TRIASSIC	LATE		NORIAN	221	9
TRIASSIC	LATE		CARNIAN	227	9
TRIASSIC	MIDDLE		LADINIAN	234	9
TRIASSIC	MIDDLE		ANISIAN	242	9
TRIASSIC	EARLY		OLENEKIAN	245	9
TRIASSIC	EARLY		INDUAN	248	10

Magnetic polarity (Anom. / Chron): 30 C30, 31 C31, 32 C32, 33 C33, 34 C34, M0, M1, M3, M5, M10, M12, M14, M16, M18, M20, M22, M25, M29; RAPID POLARITY CHANGES

Age (Ma): 70, 80, 90, 100, 110, 120, 130, 140, 150, 160, 170, 180, 190, 200, 210, 220, 230, 240

PALEOZOIC

Period		Epoch	Age		Picks (Ma)
PERMIAN		L			248
PERMIAN		L	TATARIAN		252
PERMIAN		L	UFIMIAN-KAZANIAN		256
PERMIAN		L	KUNGURIAN		260
PERMIAN		E	ARTINSKIAN		269
PERMIAN		E	SAKMARIAN		282
PERMIAN		E	ASSELIAN		290
CARBONIFEROUS	PENNSYLVANIAN	L	GZELIAN	S.	296
CARBONIFEROUS	PENNSYLVANIAN	L	KASIMOVIAN	S.	303
CARBONIFEROUS	PENNSYLVANIAN	L	MOSCOVIAN	W.	311
CARBONIFEROUS	PENNSYLVANIAN	L	BASHKIRIAN	N.	323
CARBONIFEROUS	MISSISSIPPIAN	E	SERPUKHOVIAN	N.	327
CARBONIFEROUS	MISSISSIPPIAN	E	VISEAN		342
CARBONIFEROUS	MISSISSIPPIAN	E	TOURNAISIAN		354
DEVONIAN		L	FAMENNIAN		364
DEVONIAN		L	FRASNIAN		370
DEVONIAN		M	GIVETIAN		380
DEVONIAN		M	EIFELIAN		391
DEVONIAN			EMSIAN		400
DEVONIAN			PRAGHIAN		412
DEVONIAN			LOCKHOVIAN		417
SILURIAN		L	PRIDOLIAN		419
SILURIAN		L	LUDLOVIAN		423
SILURIAN		E	WENLOCKIAN		428
SILURIAN		E	LLANDOVERIAN		443
ORDOVICIAN		L	ASHGILLIAN		449
ORDOVICIAN		L	CARADOCIAN		458
ORDOVICIAN		M	LLANDEILIAN		464
ORDOVICIAN		M	LLANVIRNIAN		470
ORDOVICIAN		E	ARENIGIAN		485
ORDOVICIAN		E	TREMADOCIAN		490
CAMBRIAN*		D	SUNWAPTAN*		495
CAMBRIAN*		D	STEPTOEAN*		500
CAMBRIAN*		C	MARJUMAN*		506
CAMBRIAN*		C	DELAMARAN*		512
CAMBRIAN*		B	DYERAN*		516
CAMBRIAN*		B	MONTEZUMAN*		520
CAMBRIAN*		A			543

Age (Ma): 260, 280, 300, 320, 340, 360, 380, 400, 420, 440, 460, 480, 500, 520, 540

PRECAMBRIAN

Eon	Era	Bdy. Ages (Ma)
		543
PROTEROZOIC	LATE	900
PROTEROZOIC	MIDDLE	1600
PROTEROZOIC	EARLY	2500
ARCHEAN	LATE	3000
ARCHEAN	MIDDLE	3400
ARCHEAN	EARLY	3800?

Age (Ma): 750, 1000, 1250, 1500, 1750, 2000, 2250, 2500, 2750, 3000, 3250, 3500, 3750

GEOLOGICAL SOCIETY OF AMERICA

 Compilers: A. R. Palmer, John Geissman

*International ages have not been established. These are regional (Laurentian) only. Boundary Picks were based on dating techniques and fossil records as of 1999. Paleomagnetic attributions have errors, Please ignore the paleomagnetic scale.

Sources for nomenclature and ages: Primarily from Gradstein, F., and Ogg, J., 1996, *Episodes*, v. 19, nos. 1 & 2; Gradstein, F., et al., 1995, SEPM Special Pub. 54, p. 95–128; Berggren, W. A., et al., 1995, SEPM Special Pub. 54, p. 129–212; Cambrian and basal Ordovician ages adapted from Landing, E., 1998, *Canadian Journal of Earth Sciences*, v. 35, p. 329–338; and Davidek, K., et al., 1998, *Geological Magazine*, v. 135, p. 305–309. Cambrian age names from Palmer, A. R., 1998, *Canadian Journal of Earth Sciences*, v. 35, p. 323–328.

THREE FORKS BASIN STRATIGRAPHIC COLUMN

W. McManus. MSU

ERA	PERIOD	EPOCH	UNIT NAME	LITHOLOGY	DESCRIPTION
CENOZOIC		HOLOCENE	ALLUVIUM COLLUVIUM NEOGLACIATION		Immature silt, sand and gravel; chaotic debris, till in cirques (0-100').
		PLEISTOCENE	PINEDALE, BULL LAKE & PRE-BULL LAKE GLACIATION		Lacustrine silt; fresh, weathered, and deeply weathered till (0-200').
			HUCKLEBERRY RIDGE		Welded phenocryst-rich rhyolitic ash-flow tuff (2 my B.P.) (0-200').
		PLIOCENE	UNNAMED GRAVEL		Unconsolidated stream gravel (0-100').
		MIOCENE	BOZEMAN GROUP		Light-colored alternating biosparite, tuffaceous biomicrite, tuffaceous silty shale, vitric ash, and conglomerate, with cross-bedded sandstone in upper part (0-5,000').
		OLIGOCENE			
		EOCENE	GALLATIN ABSAROKA VOLCANICS		Light to dark grayish-brown andesite and basalt flows, breccia, agglomerate, and tuff (0-6,000').
			CONGLOMERATE & SILTSTONE		Conglomerate consisting of Precambrian and later boulders and cobbles (0-50').
		PALEOCENE	FORT UNION		Light brown to dark gray sandstone and basal conglomerate (0-600').
MESOZOIC	CRETACEOUS	UPPER	LIVINGSTON GROUP		Light and dark grayish-green andesitic or tuffaceous siltstone, sandstone, and conglomerate with some fresh-water limestone lenses in the lower part (0-7,000').
			EAGLE		Light gray, thin- to thick-bedded, locally cross-bedded, fine to medium grained, salt and pepper sandstone with some intercalated carbonaceous shale and thin coal beds (0-600').
			COLORADO GROUP: TELEGRAPH CREEK		Medium gray, thin-bedded siltstone containing calcareous concretions and some resistant sandstone beds (0-250').
			COLORADO GROUP: CODY SHALE		Medium to dark gray and brown thin-bedded shale with some beds of siltstone and sandstone, especially in middle part. Locally fossiliferous (50-600').
			COLORADO GROUP: FRONTIER		Buff to medium gray thin- to medium-bedded, fine- to coarse-grained arkosic sandstone, locally silty (50-200').
		LOWER	COLORADO GROUP: MOWRY		Grayish-brown and green shale and siltsone with some sandstone beds. Locally carbonaceous (25-400').
			COLORADO GROUP: THERMOPOLIS SHALE		Medium gray to black shale with numerous fine- to medium-grained gray sandstone beds. Locally arkosic, glauconitic, or carbonaceous. Lower resistant sandstone.
			KOOTENAI		Buff to light gray, medium- to thick-bedded shale and sandstone with cross-bedded basal conglomerate. Locally contains fresh-water limestone nodules and beds near top (100-490').
		DISCONF			
	JURASSIC		MORRISON		Variegated red and green, thin- to medium-bedded shale and siltstone with intercalated yellowish-brown calcareous siltstone and sandstone. Upper part locally contains carbonaceous shale (110-444').
			SWIFT		Yellowish-brown, medium-bedded, fine-grained, calcareous sandstone. Basal chert conglomerate (100').
			RIERDON-SAWTOOTH		Upper massive gray, resistant oolitic limestone. Lower variegated and mostly dark gray limestone with interbedded siltstone and shale. Chert pebbles in lower part (200').
		DISCONF			
PALEOZOIC	PERM		PHOSPHORIA		Pale yellowish-brown, calcareous sandstone with chert nodules & breccias (0-26').
	PENNSYLVANIAN		QUADRANT		White to pinkish-gray, medium- to thick-bedded (locally cross-bedded), subrounded, fine- to medium-grained orthoquartzite; dolomitic in lower part (135-250').
			AMSDEN		Pale yellow to reddish-brown, medium- to thick-bedded siltstone with some dolomite and impure fossiliferous limestone beds (11-189').
		DISCONF			

continued on next page...

...continued from previous page

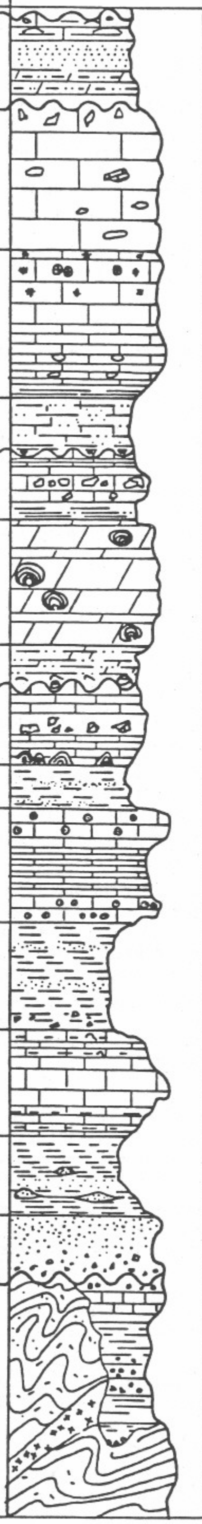

ERA	PERIOD	EPOCH	UNIT NAME	DESCRIPTION
PALEOZOIC	MISSISSIPPIAN	DISCONF	BIG SNOWY GROUP	Upper dark-gray to black, cherty, fossiliferous shale and limestone. Middle, pink-buff, platy- to massive-bedded sandstone and siltstone. Lower pink- to buff dolomite and siltstone (0-263').
		DISCONF	MISSION CANYON	Light gray, massive or poorly bedded, resistant limestone with solution breccias at top. Locally contains chert nodules (430-950').
			LODGEPOLE	Dark gray thin- to medium-bedded fossiliferous, limestone. Lower medium to dark gray, thin-bedded, sparsely fossiliferous limestone with occasional chert nodules. Black shale at base (600-810').
	DEVONIAN		SAPPINGTON	Buff-brown, thin- to medium-bedded, fine-grained, calcareous siltstone and sandstone. Basal, black, conodont-bearing shale (46-100').
		DISCONF	THREE FORKS	Upper gray, thin-bedded silty limestone. Middle buff, medium to thick bedded, brecciated limestone. Basal, red-orange limonite-nodule shale, and siltstone (100-150').
			JEFFERSON	Light and dark-brown, medium- to thick-bedded, fine- to medium-grained, dolomite and limestone. Often petroliferous and containing stromatoporoids. Intercalated yellow-pale pink, dolomitic siltstone beds (400-620').
			MAYWOOD	Yellow to brown, thin-bedded calcareous siltstone with some dolomite. Trilobite-brachiopod fossil hash in lower part (39-92').
	CAMBRIAN	DISCONF UPPER	SAGE PEBBLE	Yellow-brown to olive, thin- to medium-bedded, fine- to course-grained, commonly glauconitic and fossiliferous limestone and limestone-pebble conglomerate (121-204').
			DRY CREEK SHALE	Gray-green shale with intercalated pale-orange to buff calcareous siltstone and sandstone (50-76').
			PILGRIM	Dark and light-gray mottled, medium-thick bedded, ledge-forming, oolitic limestone. Gray to yellow-brown, thin- to medium-bedded limestone with limestone-pebble conglomerate and interbedded green shale. Gray, massive oolitic, limestone (363-433').
		MIDDLE	PARK	Gray-green and maroon shale with interbedded brown, very fine-grained quartz sandstone, arkosic limestone, and arkosic conglomerate (100-200').
			MEAGHER	Light to dark-gray, thin-bedded, fine-grained, fossiliferous mottled limestone with some interbedded green shale. Dark-gray, massive, resistant limestone. Gray, thin-bedded, fine-grained limestone with interbedded green shale. Blue & gold mottled (350-450').
			WOLSEY	Green and maroon, micaceous shale with interbedded micaceous sandstone and siltstone. Locally contains glauconitic, arkosic limestone (152-210').
			FLATHEAD	White, buff, and orange, thin- to medium-bedded, fine-to coarse-grained quartz sandstone. Locally highly feldspatic, some glauconite and conglomerate (119-142').
	PRECAMBRIAN	UNCONF	LAHOOD (BELT) AND CRYSTALLINE METAMORPHICS (PRE-BELT)	Dark grayish-green, coarse- to very coarse-grained, poorly bedded arkose and conglomeratic arkose. Interbedded dark-gray argillite and siliceous limestone beds in northern part of area. Thickens to north (0-10,000'). Gneiss, schist, metaquartzite, marble, injection gneiss, amphibolite, numerous pegmitite dikes and veins.

IDEALIZED STRATIGRAPHIC COLUMN
Northern Gallatin and Madison Ranges
Montana

Compiled by

John Montagne
Professor of Geology, Department of Earth Sciences
Montana State University

Assisted by John Goering
Drafting by Cecilia Vaniman

After: Hall, 1961 ; McMannis and Chadwick, 1964 ; Witkind, 1969 ; Kehew, 1971 ; Montagne, C., 1972 ; Montagne, J., 1975

TIME UNITS: ERA	PER.	EPOCH	THICK. (AVG.)	FORMATION
CENOZOIC	QUATERNARY	HOLOCENE (RECENT)	0-100'	ALLUVIUM COLLUVIUM MASSWASTING AEOLIAN DEP. NEOGLACIATION
		PLEISTOCENE	0-200'	PINEDALE GLACIATION; BULL LAKE GLACIATION; PRE BULL LAKE GLACIATION
		2 M.Y.B.P. (Million Years Before Present)		HUCKLEBERRY RIDGE TUFF
	TERTIARY	PLIOCENE	0-100'	GRAVEL
		MIOCENE	0-?	BOZEMAN GROUP
		OLIGOCENE		
		EOCENE (MIDDLE)	3000'-6000'	GALLATIN - ABSAROKA VOLCANICS
		(EARLY)	0-50'	CONGLOMERATE and SILTSTONE
		PALEOCENE 70 M.Y.B.P.	100'+	LIVINGSTON GROUP ?
MESOZOIC	CRETACEOUS	UPPER	1000'+	
		LOWER	440'	ALBINO FORMATION
			70'	MUDDY SS
			150'	THERMOPOLIS SHALE
		135 M.Y.B.P.	400'	KOOTENAI FORMATION

LITHOGRAPHIC COLUMN

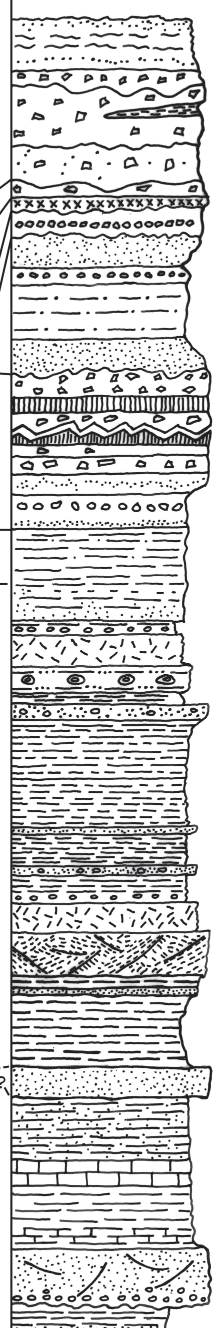

ABBREVIATED LITHOLOGY

- Chaotic debris
- Loess and sand
- Till restricted to cirques
- Lacustrine silts from ice dammed lakes
- Fresh till
- Partly weathered till
- Deeply weathered till
- Welded rhyolite tuff
- Streamgravel, unconsolidated
- Assorted conglomerate sandstone, siltstone and shale, mostly light colored, calcareous and tuffaceous
- Andesite lava flows, flow breccias and stratified volcanic breccia
- Conglomerate consisting of Precambrian and later boulders and cobbles
- Siltstone, shale, some andesitic sandstone
- Sandstone and chert pebble conglomerate
- Latite or monzonite porphyry sill
- Gray siliceous shale with interbedded hard, white tuff
- Well cemented salt and pepper sandstone
- Black shale with interbedded bentonite seams
- Pastel colored claystone, mudstone, and shale with interbedded sandstone
- ? Andesite porphyry sill (local only)
- Grayish - green to buff cross - bedded salt and pepper sandstone
- Medium to dark gray, fissile carbonaceous shale
- Well sorted white to hematite stained quartz sandstone
- Fresh water limestone with overlying variegated red, yellow - brown, and gray mudstone
- Yellow - brown to maroon mudstone and shale, limy siltstone, and fresh water limestone
- Gray, thick bedded, cross - bedded coarse grained sandstone. Conglomeratic at base (chert pebble cgl)

*see next page for Jurassic & older rocks

*see previous page for Cretaceous & younger rocks